



# MONASH University

## **Computed Tomography Coronary Angiography derived quantitative and qualitative plaque assessment and determination of functional significance of coronary stenosis**

Ravi Kiran Munnur

MBBS, FRACP

A thesis submitted for the degree of *Doctor of Philosophy* at  
Monash University in 2018

Monash Cardiovascular Research Centre, Department of Medicine, School of Clinical  
Sciences at Monash, Faculty of Medicine, Nursing & Health Science

## **Copyright notice**

### ***Notice 1***

© Ravi Kiran Munnur (2018).

# Table of Contents

1. Addendum: Response to reviewers.....	4
2. Abstract .....	14
3. Declaration.....	16
4. Publications during enrolment.....	17
5. Presentations and Awards .....	18
6. Thesis including published works declaration .....	19
7. Acknowledgements .....	22
8. Introduction to thesis .....	23
9. Chapter 1: Imaging of coronary atherosclerosis in various susceptible groups.....	27
10. Chapter 2: Cardiac CT: atherosclerosis to acute coronary syndrome.....	57
11. Chapter 3: Quantitative and Qualitative Coronary Plaque Assessment Using Computed Tomography Coronary Angiography: A comparison with Intravascular Ultrasound.....	99
12. Chapter 4: Longitudinal assessment of coronary Plaque using Computed Tomography Coronary Angiography (CTCA) and Intravascular Ultrasound (IVUS).....	126
13. Chapter 5: Quantitative plaque characterisation and association with acute coronary syndrome on medium to long term follow up: Insights from computed tomography coronary angiography .....	153
14. Chapter 6: Diagnostic Accuracy of ASLA Score (A Novel CT Angiographic Index) and Aggregate Plaque Volume in the Assessment of Functional Significance of Coronary Stenosis.....	187
15. Chapter 7: Novel Non-Invasive CT-Derived Fractional Flow Reserve Based on Structural and Fluid Analysis (CT-FFR) for Detection of Functionally Significant Stenoses: a Comparison with Invasive Fractional flow reserve.....	214
16. Chapter 8: Conclusion .....	245

---

## ***Response to Reviewers***

I would like to thank the reviewers for their assessment. The response to the reviewers' comments is below.

### **Reviewer 1**

Chapter 3: *Quantitative and Qualitative Coronary Plaque Assessment Using Computed Tomography Coronary Angiography: A Comparison with Intravascular Ultrasound*

**Comment 1.** Methods: AF, obesity and renal impairment, for differing reasons, may impair CT image quality. Were these sorts of patients excluded? If not, what means were used to optimize image quality in such patients?

**Response:** This was retrospective study and the patients were included in the final analysis based on image quality. The images with severe calcification that precluded accurate interpretation were excluded. Although AF, obese patients and those with renal impairment were not excluded, image quality was improved in such patients by either widening the window if heart rate was an issue or the KV was increased to ensure adequate tissue penetration in obese patients. No specific precautions were taken for patients with renal failure.

**Comment 2.** Methods: Both the rotational 40 MHz and steady-state 20 MHz IVUS systems were used. These are fundamentally different to each other in terms of the type of image resolution produced, and in phantom testing, confer different biases. It is known that the 20 MHz systems tends to overestimate lumen dimensions relative to the 40 MHz rotational system, with the difference being exaggerated in smaller vessels. Perhaps this is less of an issue here given the inherent comparisons with CT, however the investigators should consider this as a source of bias-

error.

**Response:** We agree that the use of different IVUS catheters could have been a source of bias – error. We acknowledge this limitation and we have now included a statement in the limitation section. Page 112, paragraph 2.

**3. Comments:** Methods - Why wasn't percent atheroma volume (PAV) (or plaque area as a function of vessel area) measured? TAV was used here to measure plaque volume, yet in IVUS progression-regression studies, PAV (due to its lower coefficient of variation and association with MACE) tends to figure as the primary endpoint, with TAV as a secondary endpoint.

**Response:** We have described in the discussion section, the inherent differences between CTCA and IVUS, which lead to inter method variability. Our aim was to establish the comparability of IVUS and CTCA in the measurement of plaque volume. Whilst the CT overestimates the lumen due to blooming from the contrast, it also overestimates the vessel volume as it does not track external elastic membrane the way IVUS does. Hence, for comparison purpose, TAV was better than PAV. In the past, studies that compared CT vs IVUS have also used TAV and not PAV. The next chapter dealt with the longitudinal plaque assessment where PAV and TAV changes were calculated and compared between the imaging modalities.

**4. Comment:** Methods - It seems that there are 24 segments per patient, translating to 8 segments per artery. A simple pictorial representation of arterial segmentation might help the reader to understand how the vessels were segmented and what rules were followed.

**Response:** We acknowledge that the usage of terminology of segments and slices is confusing. We examined only the proximal and the mid segments of coronary arteries. We divided the coronary artery on CTCA into slices of 0.5mm thickness from the ostium of the artery proximally to the distal point from where IVUS pull back was commenced. These slices were then matched to the

IVUS images based on fiduciary points. The slices that could not be matched were excluded. Page 105, paragraph 2.

**5. Comment:** Results - In the automated CT section, there are some typos/missing words. What units of plaque are used, presumably mm<sup>3</sup>? The results weave from a per vessel analysis to a per slice analysis. How/where/which were slices were chosen and why?

**Response:** Thank you for pointing this out. The measurements are in mm<sup>3</sup> and the typos have been rectified. The vessels on CTCA were divided into slices of 0.5 mm thickness and were matched with the images on IVUS based on fiduciary points. The slices that were not matched with IVUS were excluded. Per vessel analysis included all the matched slices in a vessel. Page 107, paragraph 4

**6. Comment:** Results - The Bland-Altman plots are missing

**Response:** Thank you for bringing this to our attention. Bland Altmans plot are inserted. Page 124 and 125

**7. Comment:** Results - Tables 3 and 4 are missing, Fig 2 is missing

**Response:** Thank you for bringing this to our attention. Table 3 and 4 and fig 2 have been included. Page 119, 120 and 122

*Chapter 4: Longitudinal Assessment of Coronary Plaque Using Computed Tomography Angiography and Intravascular Ultrasound*

**1. Comment:** Methods - the sample size is very small, thus limiting any major conclusions drawn from this analysis

**Response:** We agree that the sample size was small and it was a hypothesis generating study

**2. Comment:** Methods - The 0.5 mm stepping interval appears fine for image tracing, however given the limited sample size, consideration could have been given for a smaller stepping interval (i.e. 0.25 mm) in order to increase the sampling given the relative paucity of slices analyzed

**Response:** Although 0.25 slices would increase the no. of slices available for assessment, technically it is not possible to analyse slices less than 0.5mm in thickness on CTCA due to software limitations. Cardiac CT is also limited by temporal and spatial resolution.

**3. Comment:** Methods - The PAV and TAV calculation equations are repeated in the Methods section

**Response:** The repeated PAV and TAV equations have been deleted.

**4. Comment:** Results - In the 2nd paragraph, 'plaque volume' is mentioned. Does this refer to PAV or TAV?

**Response:** Plaque volume refers to TAV. TAV refers to the normalised TAV. We apologise for this confusion and we now have appropriately labelled them as TAV, nTAV and PAV.

**5. Comment:** Results - What is essentially demonstrated is that there was a concordance rate of 70% in terms of each modality (CT and IVUS) measuring either plaque progression or regression. Thus a 30% discordance rate seems quite high.

**Response:** Concordance was 70% for PAV and 100 % for TAV. Due to the intermethod variability, in our experience, PAV may not be the ideal measurement to compare CT with IVUS due to the differences in the lumen and the vessel volume between CTCA and IVUS. A similar observation was made in a prospective study that compared CT to IVUS where normalised TAV was found to be the best tool to study the difference in plaque measurement between the imaging modalities. We discussed these aspects in the discussion section.

**6. Comment:** Results - Furthermore, the main issue appears to be that on CT, the EEM is much harder to define, which is why PAV measurements track less well on CT compared with IVUS. TAV, on the other hand, appears more consistent. What we see therefore is a disparity in the 2 imaging modalities for measuring these 2 plaque volumetric endpoints used in clinical trials of disease progression-regression. IVUS trials have shown a correlation between PAV (but not TAV) with MACE, and a much lower coefficient of variation in Core Lab analyses. This is important when powering for clinical trials and attempting to show a difference in disease progression (which may be subtle, yet significant) between 2 potential therapeutic strategies. Hence the results of the present analysis, albeit in a very limited sample size, could have important implications for the CT world moving forwards in terms of its utility for assessing disease progression-regression, and choice of endpoints.

**Response:** We completely agree with the comments which are very valid. Larger studies are required to study this difference between PAV and TAV between CTCA and IVUS.

The first step would be to establish the feasibility of using CTCA to measure plaque change over time. We agree that moving forward, it would be important to establish the choice of end points for CTCA by comparing the performance of normalised TAV and PAV change in CTCA in a larger study.

**7. Comment:** Results -What is PV? You've measured TAV, PAV, so what is PV?

**Response:** PV was plaque volume (TAV) and TAV was normalised TAV. We apologise for the confusing terminology. We have now labelled them as TAV, nTAV and PAV

**8. Comment:** Discussion - I would suggest to greatly temper the discussion in terms of the utility of CT giving us IVUS-like results for measuring plaque progression-regression. The results here do not reflect that, and much work needs to be undertaken to standardize the process for CT moving

forwards in this space. If I was a potential academic investigator or drug-developer, I'm not sure I'd be hugely confident of using CTCA for demonstrating potentially subtle yet meaningful and significant differences in plaque progression rates based on these data! That being said, this argument is contingent upon how much delta plaque volume change one would anticipate from the therapies being tested.

**Response:** The results of the study are encouraging that CTCA could be developed further for serial plaque measurements. We do not believe that it is ready for commercial use and further refinements are required as rightly pointed out. Larger studies are needed to replicate the findings of this study

*Chapter 5: Quantitative Plaque Characterization and Association with Acute Coronary Syndrome on Medium- to Long-Term Follow-Up: Insights from Computed Tomography Coronary Angiography*

**1. Comment:** Methods - Perhaps the authors should make it clearer if subsequent ACS events, and corresponding culprit lesion characteristics, geographically match the precise location in the coronary vasculature that were analyzed on CT. This is the crux of this paper and should be reinforced.

**Response:** Thank you making the suggestion. This point has been reinforced in the article. Page 159, paragraph 1

**2. Comment:** Results - Figure 2: Perhaps better to change the Y-axis scale such that you can show the differences in MACE more clearly

**Response:** Thank you for your comment. We will aim to change the Y axis scale for the final manuscript.

**3. Comment:** Results - Figure 5: HRP is described in figure legend yet in the figure there is 'VP.'

Please be consistent with terminology

**Response:** The terminology has been amended. Page 171

**4. Comment:** Results - Perhaps ROC curves may be better in demonstrating the incremental value of HRP and OS (with net reclassification index)?

**Response:** We agree with the comments. However, on multi-variate analysis we were able to show the incremental diagnostic value of HRP over OS.

**General comments:** The limitations section is very important as it clearly spells out the biases in sample population. Also, 'ACS' is lumped together as a term and endpoint, yet we know that the plaque substrate and phenotype for NSTEMI and STEMI may differ. Plaque erosion plays an important, and likely underestimated role in NSTEMI. The underlying composition and burden of plaques with erosion will thus vary. I also wonder if some sort of time-point analysis is worthwhile relative to CT scan date to the date of ACS, relative to plaque burden/OS. The longer time frame, the more likely that underlying plaque burden in the culprit lesion at time of baseline imaging would be lower. This is important, as true stenosis severity in STEMI patients is likely to be much higher/greater than previously published and perpetuated. Many patients, if specifically questioned, to admit to angina/chest discomfort prior to their sentinel STEMI event. Whilst these plaques may have been 30-40% obstructive on baseline imaging in the remote past, the time period leading to the STEMI usually shows a much more stenotic plaque that rapidly progressed likely due to repeat plaque rupture/healing in the time preceding the STEMI.

**Response:** We agree that pathophysiology of STEMI and NSTEMI differs. As far as time point analysis is concerned we have observed that HRP with obstructive stenosis presented early with ACS compared to the HRP without obstructive stenosis. This illustrates the point that true stenosis is likely to be more severe close to an event.

*Chapter 6: Diagnostic Accuracy of ASLA Score (A Novel CT Angiographic Index) and Aggregate Plaque Volume in the Assessment of Functional Significance of Coronary Stenosis*

**Comment:** How are we able to be relatively certain, before we subject our patient to radiation and IV contrast, that we will obtain images relatively unaffected by calcium blooming? Is it protocol to perform a low-dose scan just to look for Ca<sup>2+</sup>, and if

Agatson score is > a specific threshold (i.e. 300), then better not to move forwards with the full protocol as accuracy may be limited due to blooming? Surely in the presence of calcified arteries, a CTCA would be less accurate than invasive coronary angiography?

**Response:** Calcium can cause blooming artefact and can potentially make CTCA uninterpretable. Currently we do not have a protocol to assess calcium score prior to a CTCA. We think it is a very good suggestion to perform calcium score prior to performing CTCA in select patients. However, the current generation CTCA involves very low radiation and with appropriate patient selection avoiding very elderly, those with renal impairment and long standing diabetes may mitigate the problem to some extent.

*Chapter 7: Novel Non-invasive CT-derived Fractional Flow Reserve Based on Structural and Fluid Analysis (CT-FFR) for Detection of Functionally Significant Stenosis: A Comparison with Invasive Fractional Flow Reserve*

**General comment:** Is correlation the correct means of ascertaining novel indices against a known gold standard or reference? One could be systematically 2-fold more than the reference/goldstandard yet have an R-value close to 1 (i.e. perfect correlation!). I think Bland-Altman curves is what counts most, especially around the grey-zones, and how the re-classification results. Also, it'd be interesting to compare your novel CT-FFR method with QFR

**Response:** This was a novel study where we used correlation to compare against the gold standard test. Further studies utilising CT FFR are underway at our institution and will employ Bland-Altman analysis. We agree that it would be interesting to compare CT FFR to QFR and we thank you for the suggestion.

### *Chapter 8: Conclusions*

**Comment:** This is generally appropriate – however I feel the conclusions pertaining to the utility of CT for assessing serial plaque volume, especially PAV. Pharma studies show often-subtle yet significant between-group differences in plaque volume changes over much larger study populations. Delta PAV correlates with MACE, as it inherently considers the remodeling process in addition to simply the flux in plaque. We need a much more rigorous and standardized validation of CTCA derived approaches for serial plaque evaluation/quantification before this imaging modality is to provide equivalent sensitivity and accuracy as IVUS. This however is inevitable as imaging technologies move forward.

**Response:** We completely agree with the reviewer comments. With improving technology and with improvement in spatial and temporal resolution of CTCA, accuracy of plaque measurement will inevitably improve. Further refinements are required before CTCA could be used for serial plaque measurements. At present it appears that normalised TAV is best suited to detect plaque change on CTCA.

## **Reviewer 2**

**Comment:** Other concerns include the authorship of the candidate in the list of published papers; In five out of eight published papers, the candidate was not the first author.

**Response:** I would like to clarify that I am the first author in six of the seven papers.

**Comment:** The usefulness ASLA score has been previously published before by one of the candidate's co-researchers. Hence, the study of ASLA score appears to be the extension from its previous study and it is no longer a novel study.

**Response:** ASLA score was developed by my colleagues and was tested in only vessels with discrete lesion of intermediate severity. We explored the utility of the score in vessels with varying stenosis severity and multiple stenoses, which was never done before.

**Comment:** The conclusion chapter was a bit short; I would expect much more detailed discussion about what have been done in the studies covered by this thesis

**Response:** The limitations and future potential of the research undertaken was explained in the individual papers separately. The final conclusion was more of an overview.

## **Abstract**

We undertook comprehensive plaque assessment in this thesis with the purpose of expanding the clinical utility of computed tomography coronary angiography (CTCA) beyond the diagnosis of luminal stenosis.

### *1) Quantitative plaque assessment*

Although CTCA has been shown to be comparable to IVUS with small mean differences in plaque volumes, the limits of agreement have been generally wide. To improve plaque quantification, we developed novel methods that were accurate and reproducible and demonstrated excellent correlation and agreement with narrow limits for plaque measurements between CTCA and IVUS. Subsequently, in a prospective study that involved serial imaging with CTCA and IVUS, we demonstrated no significant differences in plaque volume measurements at baseline and follow up and there was excellent correlation for normalised total atheroma volume change between CTCA and IVUS. These results suggest that CTCA can be used in an individual patient to monitor plaque changes in response to various anti atherosclerotic therapies. In addition, we also confirmed that CT derived high-risk plaques correlate to the presence of echo attenuated and echo lucent plaques on IVUS, which have been shown to be associated with future events.

### *2) Qualitative plaque assessment*

In a study of 1254 patient with follow up date for 7 years, we demonstrated that CTCA derived high-risk plaques (HRP) characterised by positive-remodelling, low-attenuation-plaque and spotty-calcification) are an independent predictor of future ACS beyond traditional cardiovascular risk factors. HRP with obstructive stenosis (>50%) had more frequent ACS and presented early. Cross sectional single slice LAP volume at the site of maximum stenosis added further prognostic value and identified the plaques that were at greatest risk of future ACS. Stenosis severity alone without HRP was not predictive. Identification of at-risk patient may pave way for individualised therapies.

### 3) *Determination of functional significance of coronary stenosis*

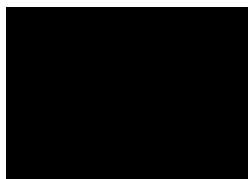
We compared the performance of %aggregate plaque volume (APV) and ASLA score (area stenosis, lesion length and area of myocardium subtended), a novel CT index in the identification of functionally significant lesions on CTCA. Both these techniques were previously described in vessels with discrete lesion of intermediate stenosis. We applied these techniques in vessels with multiple lesions and with varying degree of stenosis. The novel plaque quantification techniques that we derived allowed accurate plaque quantification needed for calculating %aggregate plaque volume. We observed that only ASLA score, which take five minutes to apply, predicted ischaemia specific lesions but %APV did not. The extremes of ASLA score can accurately rule out or confirm ischemia help in further streamlining patient management.

FFR<sub>CT</sub> has been shown to be most accurate in detecting ischaemia. However, the existing model is complex involving super computer based calculations and requires offshore processing and cost. We demonstrated a highly reproducible alternative non-invasive CT-FFR technique based on structural and fluid analysis using a reduced-order flow model, which improved the accuracy of CTCA to detect FFR significant lesion compared to CTCA alone This technique can be applied readily at point of care and takes less than 30 minutes.

## **Declaration**

This thesis contains no material which has been accepted for the award of any other degree or diploma at any university or equivalent institution and that, to the best of my knowledge and belief, this thesis contains no material previously published or written by another person, except where due reference is made in the text of the thesis.

Signature:



Print Name: Ravi Kiran Munnur

Date: 28/6/2018

## **Publications during enrolment**

*Munnur RK, Cameron JD, Ko BS, Meredith IT, Wong DT.*

Cardiac CT: atherosclerosis to acute coronary syndrome

Cardiovasc Diagn Ther. 2014 Dec;4 (6):430-48.

*Psaltis PJ, Talman AH, Munnur K, Cameron JD, Ko BS, Meredith IT, Seneviratne SK, Wong DT.*

Relationship between epicardial fat and quantitative coronary artery plaque progression: insights from computed tomography coronary angiography

Int J Cardiovasc Imaging. 2016 Feb;32(2):317-28

*Ko BS, Seneviratne S, Cameron JD, Gutman S, Crossett M, Munnur K, Meredith IT, Wong DT.*

Rest and stress transluminal attenuation gradient and contrast opacification difference for detection of haemodynamically significant stenosis in patients with suspected coronary artery disease.

Int J Cardiovasc Imaging. 2016 Jul;32(7):1131-41

*Munnur RK, Nerlekar N, Wong DT.*

Imaging of coronary atherosclerosis in various susceptible groups.

Cardiovasc Diagn Ther. 2016 Aug;6(4):382-95

*Adams DB, Narayan O, Munnur RK, Cameron JD, Wong DT, Talman AH, Harper RW, Seneviratne SK, Meredith IT, Ko BS.*

Ethnic differences in coronary plaque and epicardial fat volume quantified using computed tomography.

Int J Cardiovasc Imaging. 2017 Feb;33(2):241-249.

*Ko BS, Cameron JD, Munnur RK, Wong DTL, Fujisawa Y, Sakaguchi T, Hirohata K, Hislop-Jambrich J, Fujimoto S, Takamura K, Crossett M, Leung M, Kuganesan A, Malaiapan Y, Nasis A, Troupis J, Meredith IT, Seneviratne SK.*

Noninvasive CT-Derived FFR Based on Structural and Fluid Analysis: A Comparison With Invasive FFR for Detection of Functionally Significant Stenosis.

JACC Cardiovasc Imaging. 2017 Jun;10(6):663-673

*Potter EL, Machado C, Malaiapan Y, Narayan O, Ko BS, Psaltis PJ, Munnur K, Cameron JD, Meredith IT, Wong DT.*

Stenotic flow reserve derived from quantitative coronary angiography has modest but incremental value in predicting functionally significant coronary stenosis as evaluated by fractional flow reserve.

Cardiovasc Diagn Ther. 2017 Feb;7(1):52-59.

*Ko B, Cameron J, Wong D, Munnur R, Seneviratne S.*

The Authors Reply

JACC Cardiovasc Imaging. 2017 Apr;10(4):498-499.

*Munnur RK, Cameron JD, McCormick LM, Psaltis PJ, Nerlekar N, Ko BSH, Meredith IT, Seneviratne S, Wong DTL.*

Diagnostic accuracy of ASLA score (a novel CT angiographic index) and aggregate plaque volume in the assessment of functional significance of coronary stenosis.

Int J Cardiol. 2018 Jun 8. pii: S0167-5273(18)30781-2

## **Presentations and Awards**

### **Oral presentations at Conferences**

Diagnostic Accuracy Of ASLA Score (A Novel CT Angiographic Index) and Aggregate Plaque Volume in the Assessment of Functional Significance of Coronary Stenosis.

*Ravi Kiran Munnur, James Cameron, Brian Ko, Peter Psaltis, Ian Meredith, Sujith Seneviratne, Dennis Wong. CSANZ 2016, Adelaide, USA*

Computed Tomography Coronary Angiography Can Accurately Quantify Coronary Luminal area and Plaque Volume Compared to Invasive Intravascular Ultrasound

*Ravi Kiran Munnur, Jordan Andrews, Stephen Nicholls, Yuvaraj Malaiapan, Brian Ko, James Cameron, Ian Meredith, Sujith Seneviratne, Dennis Wong. Society of cardiovascular computed tomography, Las Vegas, USA, July 2015*

### **Poster Presentation at Conferences**

Diagnostic Accuracy Of ASLA Score (A Novel CT Angiographic Index) and Aggregate Plaque Volume in the Assessment of Functional Significance of Coronary Stenosis.

*Ravi Kiran Munnur, James Cameron, Brian Ko, Peter Psaltis, Ian Meredith, Sujith Seneviratne, Dennis Wong. American College of Cardiology, 2016, Chicago, USA*

Epicardial Fat Volume measured by Computed Tomography Coronary Angiography Is Associated With Significant Coronary Stenosis Independent of Traditional Risk Factors

*Ravi Kiran Munnur, Liz Potter, Rahul Muthalaly, Brian Ko, James Cameron, Ian Meredith, Sujith Seneviratne, Dennis Wong. Society of cardiovascular computed tomography, Las Vegas, USA, July 2015 and CSANZ 2015*

Vulnerable Plaque Features On Computed Tomography Coronary Angiography Are Associated With Long Term Acute Coronary Syndrome Events

*Ravi Kiran Munnur, Rahul Muthalaly, Brian Ko, Liz Potter, Andrew Talman, Yi-Wei Baey, Sarah Qian, HueMun Au-Yeung, Damien Tharmaratnam, Jason Nogie, Jason Moghadas, James Cameron, Ian Meredith, Sujith Seneviratne, Dennis Wong. Cardiac Society of Australia and New Zealand, Melbourne, 2015*

Computed Tomography Coronary Angiography Can Accurately Quantify Coronary Luminal area and Plaque Volume Compared to Invasive Intravascular Ultrasound

*Ravi Kiran Munnur, Jordan Andrews, Stephen Nicholls, Yuvaraj Malaiapan, Brian Ko, James Cameron, Ian Meredith, Sujith Seneviratne, Dennis Wong. Cardiac Society of Australia and New Zealand, Melbourne, 2015*

Relationship between epicardial fat and quantitative coronary artery plaque progression: Insights from cardiac computed tomography angiography

*Peter J. Psaltis MBBS, Andrew H. Talman, Kiran Munnur, James D. Cameron, Brian SH Ko, Ian T. Meredith, Sujith K Seneviratne, Dennis T. L. Wong. Society of cardiovascular computed tomography, Las Vegas, USA, July 2015*

Australian Post graduate Scholarship 2016

Cardiac Society of Australia and New Zealand Post Graduate Research Scholarship 2014

Monash Health Clinical Academic Scholarship 2014 -2016

Young Investigator Award – Finalist (Monash Health research week)

Monash Health research week (cardiovascular division) 2<sup>nd</sup> prize for poster presentation

Best poster – Asia Pacific region: SCCT, 2015

## Thesis including published works declaration

I hereby declare that this thesis contains no material which has been accepted for the award of any other degree or diploma at any university or equivalent institution and that, to the best of my knowledge and belief, this thesis contains no material previously published or written by another person, except where due reference is made in the text of the thesis.

This thesis includes 4 original papers published in peer reviewed journals and 1 submitted publication. The core theme of the thesis is comprehensive *coronary plaque assessment on computed tomography coronary angiography*. The ideas, development and writing up of all the papers in the thesis were the principal responsibility of myself, the student, working within the *Monash cardiovascular research centre* under the supervision of A/Prof Dennis Wong.

The inclusion of co-authors reflects the fact that the work came from active collaboration between researchers and acknowledges input into team-based research.

In the case of 5 manuscripts my contribution to the work involved the following:

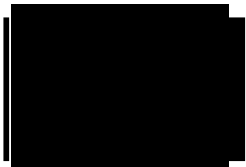
Thesis Chapter	Publication Title	Status (published, in press, accepted or returned for revision, submitted)	Nature and % of student contribution	Co-author name(s) Nature and % of Co-author's contribution*	Co-author (s), Monash student Y/N*
1	Imaging of coronary atherosclerosis in various susceptible groups	Published	70% concept and collecting data and writing first draft	1) Nitesh Nerlekar Input into manuscript 30% 2) Dennis TL Wong Supervision and reviewing manuscript	Yes  No
2	Cardiac CT: atherosclerosis to acute coronary syndrome	Published	80% concept and collecting data and writing first draft	All authors provided input to manuscript through either abstract review and editing, totalling to 20% contributions 1) James D Cameron 2) Brian S.Ko 3) Ian T Meredith 4) Dennis TL Wong	No
3	Quantitative and Qualitative Coronary Plaque Assessment Using Computed Tomography Coronary Angiography: A comparison with Intravascular Ultrasound	Submitted	70% concept and collecting data and writing first draft	All authors provided input to manuscript through either abstract review, editing, data analysis and statistical analysis expertise totalling to 30% contributions  1) Jordan Andrews 2) Yu Kataoka 3) Nitesh Nerlekar 4) Peter J Psaltis 5 5) Stephen J Nicholls	Yes

				6) Yuvaraj Malaiapan, 7) James D Cameron 8) Ian T Meredith 9) Sujith Seneviratne 10) Dennis TL Wong	
4	Diagnostic Accuracy of ASLA Score (A Novel CT Angiographic Index) and Aggregate Plaque Volume in the Assessment of Functional Significance of Coronary Stenosis	Published	80% concept and collecting data and writing first draft	All authors provided input to manuscript through either abstract review, editing, data analysis and statistical analysis expertise totalling to 20% contributions 1) James D Cameron, 2) Liam M McCormick 3) Peter J Psaltis 4) Nitesh Nerlekar 5) Brian SH Ko 6) Ian T Meredith 7) Sujith Seneviratne 8) Dennis TL Wong	Yes
5	Novel Non-Invasive CT-Derived Fractional Flow Reserve Based on Structural and Fluid Analysis (CT-FFR) for Detection of Functionally Significant Stenoses: a Comparison with Invasive Fractional Flow Reserve	Published	50% Concept, Design, Data collection and manuscript contribution	All authors provided input to concept, design, data analysis, technical expertise and statistical analysis, manuscript review through either abstract review, editing, expertise totalling to 30% contributions  1) Brian S Ko Writing first draft 2) James D Cameron 3) Dennis TL Wong 4) Yasuko Fujisawa 5) Takuya Sakaguchi 6) Kenji Hirohata 7) JacquieHislopJambrich 8) Shinichiro Fujimoto 9) Kazuhisa Takamura 10) Marcus Crossett 11) Michael Leung 12) Ahilan Kuganesan 13) Yuvaraj Malaiapan 14) Arthur Nasis 15) John Troupis 16) Ian T Meredith	No

*\*If no co-authors, leave fields blank*

I have renumbered sections of submitted or published papers in order to generate a consistent presentation within the thesis.

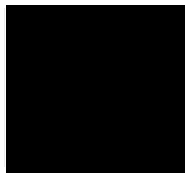
**Student signature:**



**Date:** 28/6/2018

The undersigned hereby certify that the above declaration correctly reflects the nature and extent of the student's and co-authors' contributions to this work. In instances where I am not the responsible author I have consulted with the responsible author to agree on the respective contributions of the authors.

**Main Supervisor signature:**



**Date:** 28/6/2018

## **Acknowledgements**

I would like to express my gratitude to my supervisor A/Prof Dennis Wong for giving me the opportunity to pursue PhD under his guidance. His unwavering support, approachability and encouragement have made this thesis possible. I would like to thank him sincerely for the time and effort he has invested in mentoring me.

I thank Prof James Cameron and Prof Ian Meredith for their guidance and A/Prof Brian Ko for his supervision and support. Dr. Yuvaraj Malaiapan has been a mentor and I thank him for his guidance and support. I would like to thank the senior staff members, my colleagues, junior doctors, nurses, and research team members at Monash Heart who have helped me at various stages of my thesis.

I would like to acknowledge Cardiac Society for Australia and New Zealand, Monash Health and the Australian Government for their assistance with scholarships.

This PhD journey would not have been possible without the sacrifices made by my wife, Pavithra and family. My children Shreyas and Saanvi are my treasure. I would like to sincerely thank them all.

## **INTRODUCTION TO THESIS**

Computed tomography coronary angiography (CTCA) is an established, safe first line investigation for patients presenting with chest pain. In addition, it also provides valuable information on the atherosclerotic burden and composition. As the technology advances with reduction in radiation doses and with improvement in temporal and spatial resolution, we foresee a pivotal role for CTCA in future in the prevention, diagnosis and management of coronary artery.

The focus of the thesis was to address some of the gaps in our knowledge and expand the clinical utility of CTCA beyond the diagnosis of luminal stenosis. We undertook comprehensive coronary plaque assessment using CTCA and our aims were threefold: i) To develop techniques for accurate plaque quantification on CTCA; ii) To determine the predictors in CTCA derived high-risk plaques that are at high risk of causing future cardiac events based on quantitative and qualitative plaque assessment; iii) To derive physiological information from anatomy in determining functional significance of coronary stenosis;

The first chapter is an in depth review on coronary atherosclerosis, its characteristics and composition in various susceptible groups. Atherosclerosis is a complex multifactorial disease and we now appreciate the varying influence of different cardiovascular risk factors on disease onset, plaque composition and progression, and future events. Understanding these differences was vital as we sought to use CTCA derived plaque characteristics to identify the patients who are at risk of future cardiac events.

The second chapter is a comprehensive review article summarising the diagnostic capability and utility of CTCA, its emerging role in plaque quantification, predictive ability of future cardiovascular events based on CTCA derived high risk plaque features and its evolving role in determining function significance of coronary stenosis. This chapter highlights the important

advancement made over the years in the application of CTCA and helped understand the gaps in the knowledge that still exist.

## Results section

### *i) Quantification of coronary plaque on CTCA*

#### Chapter 3

In our first results section, we compared plaque quantification and the presence of high-risk plaques on CTCA to IVUS. This was an important chapter that laid the foundation for plaque quantification techniques that were used throughout this thesis and forms the basis for ongoing and future plaque quantification studies at our institution. Multiple studies in the past have shown that although the mean plaque volume differences between CTCA and IVUS were small, the limits of agreement have generally been wide. This implies that CTCA can be used at a population level but not in an individual patient. We developed novel methods for plaque measurement that best suited our scan protocols. In this retrospective study, we demonstrated excellent agreement for plaque volume between CTCA and IVUS with good correlation and narrow limits of agreement. In addition, we also confirmed that CT derived high-risk plaques correlate to the presence of echo attenuated and echo lucent plaques on IVUS, which have been shown to be associated with future events. This chapter also laid the foundation for qualitative plaque analysis and an important result of the study was in defining the Hounsfield unit (HU) threshold for low attenuation plaque (LAP). We observed that  $< 56$  HU cut off was more accurate for our CT images compared to the LAP definition of  $< 30$  HU in the literature, which was based on old CT scanners that used higher radiation dose.

#### Chapter 4

In this results chapter we compared the serial plaque change measurements between CTCA and IVUS in a prospective study. We found good agreement and correlation between CTCA and IVUS for total atheroma volume change and percent atheroma volume change. The results of the chapter

confirmed that CTCA could reliably detect plaque volume change in an individual patient. It was important to demonstrate CTCA's ability to detect plaque progression / regression that was comparable to IVUS if CTCA was to become an alternative investigative tool to test the efficacy of various anti atherosclerotic therapies.

ii) To determine the predictors in CTCA derived high-risk plaques that are at high risk of causing future cardiac events based on quantitative and qualitative plaque assessment.

## Chapter 5

In this results chapter we studied the association between CT derived high-risk plaques (HRP) and acute coronary syndrome (ACS) or cardiac death and the results were in agreement with the previous studies that have established an unequivocal relationship beyond cardiovascular risk factors. Despite knowing this relationship, the management of these high-risk plaques is not well understood, partly due to the low event rates. In this chapter we further analysed the high-risk plaques using quantitative techniques developed in chapter one to differentiate and identify those that were more likely to cause events. Patients with obstructive high-risk plaques appear to be at greatest risk and plaque volume (PV) and low attenuation plaque (LAP) are important determinants of future risk. Quantitative plaque measurement is time consuming but we have shown that it is feasible to derive the prognostic information by measuring LAP volume just at a single cross section at the site of maximum stenosis to identify the patients who are at the greatest risk of future events.

iii) *Determination of functional significance of coronary stenosis*

## Chapter 6

We compared the performance of percent aggregate plaque volume and ASLA score (area stenosis, lesion length and area of myocardium subtended), a novel CT index conceptualised previously by co-authors, in determining functional significance of coronary stenosis. Both these techniques were

previously described in vessels with discrete lesion of intermediate stenosis. We applied these techniques in vessels with multiple lesions and with varying degree of stenosis. The plaque quantification techniques developed in the first chapter allowed accurate plaque quantification needed for calculating percent aggregate plaque volume. The results demonstrated that only ASLA score predicted functionally significant lesions. This score can be readily applied at the time of reporting CTCA and may help in further streamlining patient management. At low ASLA score 4 or less provided 100% sensitivity negative predictive value ruling out ischemia specific lesions and at high score of  $> 15$  had  $>94\%$  specificity and positive predictive value for identifying functionally significant lesions. ASLA score can be applied in  $< 5$  minutes and has the potential to streamline patient management.

## Chapter 7

In this results chapter, we explored novel CT fractional flow reserve (FFR) technique based on alternative boundary conditions. Amongst the emerging techniques for the assessment of functional significance of coronary stenosis,  $FFR_{CT}$  has been shown to be most accurate. The existing model is complex involving super computer based calculations and requires offshore processing and cost. We demonstrated a highly reproducible non-invasive FFR technique based on structural and fluid analysis using a reduced-order flow model, which improved the accuracy of CTCA to detect FFR significant lesion compared to CTCA alone. This technique can be applied readily at point of care and takes less than 30 minutes. Further refinements of technique and studies are underway at our institution.

# Chapter 1: Imaging of coronary atherosclerosis in various susceptible groups

Ravi Kiran Munnur<sup>1</sup>MBBS<sup>1</sup>, Nitesh Nerlekar<sup>1</sup>MBBS<sup>1</sup> Dennis TL Wong, MBBS PhD<sup>1</sup>

*1 Monash Cardiovascular Research Centre, Department of Medicine (Monash Medical Centre) Monash University and Monash Heart, Monash Health, 246 Clayton Road, Clayton, 3168 VIC, Australia*

**Accepted and Published: Cardiovasc Diagn Ther. 2016 Aug;6(4):382-95**

## Introduction

Coronary artery disease (CAD) is the leading cause of death and disability worldwide(1, 2). Atherosclerosis, which is the primary pathophysiologic mechanism for the development of plaque leading to CAD, is a multifactorial process resulting from a complex interplay between genetic susceptibility and various risk factors such as hypertension, dyslipidaemia, diabetes mellitus and smoking(3). In addition, influences from other disease states such as chronic kidney disease, obesity and the metabolic syndrome as well as gender and ethnic diversity also contribute to the disease process. Insights from pathological observations and advances in cellular and molecular biology have helped us understand the process of plaque formation, progression and rupture leading to events. Several intravascular imaging techniques such as intravascular ultrasound (IVUS), Virtual histology IVUS (VH-IVUS) and optical coherence tomography (OCT) allow in vivo assessment of plaque burden, plaque morphology and response to therapy. In addition, non invasive assessment using coronary artery calcium (CAC) score allows risk stratification and plaque burden assessment whilst computed tomography coronary angiography (CTCA) allows evaluation of luminal stenosis, plaque characterisation and quantification.

This review aims to summarise the results of invasive and non-invasive imaging studies of coronary atherosclerosis seen in various high-risk populations including diabetes mellitus, metabolic syndrome, obesity, chronic kidney disease and, gender differences and ethnicity. Understanding the phenotype of plaques in various susceptible groups may allow potential development of personalised therapies.

## **Background: Atherosclerosis - Pathophysiology**

Atherosclerosis is a result of deranged lipids, inflammation and endothelial dysfunction(4). Dyslipidemia is the most important risk factor in the pathogenesis of atherosclerosis, which is evident in patients with genetic hyperlipidemia who have increased incidence of coronary artery disease even in the absence of other risk factors. Conversely, lower levels of lipids are sufficient to cause atherosclerosis in the presence of other cardiovascular risk factors. The mechanism of this interaction and the role of individual cardiovascular risk factors in the pathogenesis of atherosclerosis are not well understood. Atherosclerotic plaques have a predilection to develop in regions of an artery with low or oscillatory endothelial shear stress. Binding of low density lipoprotein – Cholesterol (LDL-C) to intimal proteoglycans is an important initial step (5) followed by LDL modification by oxidation and aggregation resulting in foam cells (6). This leads to endothelial dysfunction, smooth muscle cell migration and stimulation of innate and adaptive immune responses. Higher levels of LDLs are required to initiate the disease than to sustain the lesions once they have formed (7, 8). Foam cells, macrophages and smooth muscle cells undergo apoptosis, and along with intraplaque haemorrhage lead to formation of necrotic core. The lesion is then described as a fibroatheroma. Smooth muscles cells undergo modulation and migration, and are a source of fibrous cap made of type I collagen that replaces the arterial intima and separates the necrotic core from the lumen (9). Some plaques undergo fibrosis whilst in some, apoptotic cells, extracellular matrix and necrotic core material act as nidus for microscopic calcium granules which can expand subsequently to forms plates or large lumps of calcium deposits (10). During

atherogenesis, the vessel segment undergoes positive remodelling, expanding outward in such a way that the lumen is not compromised. This is often seen in fibroatheromas and is positively correlated to the size of necrotic core and inflammation (11, 12). Constrictive remodelling is seen in plaques that are rich in fibrous tissue (12). The development of atherosclerosis may lead to either obstruction of lumen limiting blood flow or may lead to acute coronary syndrome (ACS) due to plaque rupture, and less often due to plaque erosion and calcified nodule.

## **Diabetes Mellitus**

Diabetes mellitus (DM) is a growing epidemic worldwide and is highly atherogenic with contributing factors being hyperglycaemia, advanced glycation end products along with inflammation and oxidative stress(13). Amongst the traditional cardiovascular risk factors, it is the strongest predictor of future myocardial infarction, and is associated with significantly higher mortality as well as poorer outcome after percutaneous coronary intervention when compared to non-diabetic counterparts. (14), (15) (16). Necropsy studies have suggested that DM is associated with a greater and more diffuse disease burden particularly in the distal vessels(17) and numerous imaging studies have allowed us to understand the disease in vivo.

In a systematic analysis of 2,237 subjects from randomised controlled studies evaluating plaque progression in response to various pharmacological therapies using serial IVUS, the extent of coronary atherosclerosis, pattern of arterial remodelling and disease progression was compared between DM and non-DM patients. It was observed that DM subjects had more extensive atherosclerosis and total atheroma volume (TAV) when compared to non-DM subjects. Despite the presence of more extensive disease, DM subjects had smaller lumen and similar external elastic membrane (EEM) accounting for greater percent atheroma volume (PAV). It was also observed that insulin-requiring diabetics had even smaller EEM and lumen volumes resulting in even larger

PAV. Although the prevalence of hypertension (HT) and dyslipidaemia was higher in DM group, DM was an independent predictor of increased plaque burden. Surprisingly, in this systematic analysis the number of segments affected was not different in DM and non-DM subjects raising the possibility that DM could lead to a more aggressive localised disease and not necessarily a generalised disease as previously thought. DM patients were more likely to have plaque PAV progression and were less likely to undergo plaque regression despite the use of established medical therapies (18). Plaque regression rates achieved with an intensive lowering regimen of low-density lipoprotein cholesterol (LDL-C) in DM, achieves the same regression rates as non-DM subjects with non-intensive lowering regimens. Of note, the achieved LDL-C level in this pooled study was 80mg/dL. However, target LDL levels of 61 mg/dL were achieved in the SATURN trial, where the response rate to high intensity statin therapy demonstrated equivalent degrees of PAV and TAV regression in DM and non-DM subjects when an LDL-C <70 mg/dL was achieved (19). Although there was comparable TAV regression in both groups when post-therapy LDL-C was >70 mg/dL, PAV regression was greater in the non-DM group. These observations suggest that abnormalities of arterial remodelling also influence the clinical expression of atherosclerotic disease in DM. (Fig1)

To examine the natural history of vascular remodelling and predictors of vessel shrinkage, 237 DM patients were examined using IVUS(20). Significant lumen shrinkage was associated with vessel shrinkage and was identified in 37.1% of segments. Independent predictors were insulin requirement, glycosylated haemoglobin, Apolipoprotein B, HT, the number of diseased vessels and prior revascularisation. It was observed in another study that even at angiographically normal sites, mild atherosclerosis was detected by IVUS in both DM and non-DM patients. Despite both the groups having similar plaque area and vessel area, lumen area was smaller in DM group, again suggesting a constrictive mechanism even in early stages of atherosclerosis (21). Furthermore, it has been noted that in pre-DM patients there is evidence of smaller coronary size and diffuse luminal narrowing particularly in the distal left anterior descending artery (22). The mechanisms that

promote impaired arterial remodelling in diabetic subjects is not fully understood and it has been postulated that impaired endothelial-dependent relaxation (23), increased deposition of calcium (24) and fibrous tissue (25) deposition in arterial wall may limit vessel expansion from plaque accumulation. This is particularly more pronounced in insulin-treated patients leading to speculation that smooth muscle proliferation and fibrous tissue deposition in response to insulin may impair arterial wall expansion (26).

The use of VH-IVUS and OCT imaging has allowed us to determine plaque composition in addition to the assessment of plaque burden. In a study of stable angina pectoris patients using VH-IVUS, the percentage area of necrotic core and dense calcium was found to be significantly higher in DM group compared to non-DM group. It was also observed that the frequency of VH-IVUS derived thin cap fibro-atheroma (TCFA) and fibro calcific plaques were higher in DM group (27). Although the incidence of ruptured plaques and TCFA at culprit lesion sites were similar, non-culprit lesion (NCL) TCFA were observed more frequently in DM patients than in non-DM patients, in a three-vessel OCT study of patients presenting with acute coronary syndrome(28). DM patients demonstrate a larger lipid index ( $LI = \text{averaged lipid arc} \times \text{lipid length}$ ) and higher prevalence of calcification and thrombus, and those with HbA1C of  $\geq 8\%$  have larger LI and the highest prevalence of TCFA and macrophage infiltration (29). In addition, among DM subjects, those with higher insulin resistance were observed to have more frequent TCFA's with significantly thinner cap thickness compared to DM subjects with lower insulin resistance (30). These observations suggest that poorly controlled DM and insulin resistance is associated with high-risk plaque features.

Another study evaluated angiographic and OCT parameters in DM and non-DM patients with an index acute coronary syndrome (ACS) (31). Angiographically, although DM was associated with

higher stenosis score and extent index, these patients surprisingly had more collateral vessels directed towards the culprit artery. On OCT examination, minimum lumen area (MLA) of the culprit segment was similar in both the groups. In DM patients, less lipid quadrants, smaller lipid arcs, more frequent superficial calcified nodules, greater number of calcified quadrants and a wider calcified arc were noted (Fig 1). Despite accelerated atherosclerosis seen in diabetic patients, they do not present early with ACS and it has been speculated that there may be an unknown protective mechanism might delay the onset of a first event (32).

In a sub-analysis of the TRUTH study, the effect of statin therapy on plaque composition was studied in DM and non-DM groups using serial VH-IVUS (33). Although there was reduction in the fibro fatty component in both groups, the DM group had less reduction at follow up. In an IVUS study that examined the relationship between glycaemic status and CAD, fasting blood sugars, HbA1C and DM were associated with severity and progression of atherosclerosis (34). A similar observation was made in the COSMOS study, where despite similar improvements in lipid levels, plaque regression was less pronounced in patients with high HbA1C.

DM is often associated with HT and dyslipidaemia and it is not surprising that greatest clinical benefit of medical management in diabetes is seen with optimisation of blood pressure (35) and lipids (36). In an IVUS study, disease progression was compared in patients who were stratified according to the achievement of treatment goals of individual risk factors: HbA1C < 7 %, LDL-C < 2.5 mmol/L, Triglycerides < 1.7 mmol/L, systolic blood pressure (SBP) < 130 mmHg, high sensitivity CRP (hsCRP) < 2 mg/L). It was observed that slowing of progression of PAV correlated with the greater number of risk factors that achieved treatment goals (37).

DM is a significant CV risk factor that causes accelerated coronary atherosclerosis, vessel shrinkage and increased events. It is further complicated by attenuated plaque regression in response to

conventional treatment modalities. Optimisation of all other associated risk factors apart from intense management of sugars and lipids appears to be the best strategy.

## **METABOLIC SYNDROME**

Metabolic syndrome as defined by National Cholesterol Education Program Adult Treatment Panel III criteria (38) consists of  $\geq 3$  of the following criteria: Body mass index (BMI)  $\geq 30\text{kg/m}^2$ , triglyceride level  $\geq 150\text{ mg/dl}$ , HDL-C ( $<40\text{ mg /dL}$  in men and,  $<50\text{ mg/dl}$  in women), impaired fasting glucose (100 to 125 mg/dL), and high systolic or diastolic blood pressure ( $\geq 130\text{mmHg}$  or  $\geq 85\text{mmHg}$  respectively). It is not clearly understood if the metabolic syndrome is truly a syndrome or just a cluster of risk factors. Although the metabolic syndrome is associated with higher clinical events, it has been suggested that the risk is equal to the sum of individual risk factors (39).

The extent and progression of atherosclerosis was compared between DM, metabolic syndrome and those with neither diagnosis from data pooled from 7 clinical trials involving 3,459 patients who were studied with serial IVUS (40). In keeping with previous observations, DM was associated with more extensive disease, greater lumen constriction and greater plaque progression. Despite the metabolic syndrome group having the most risk factors, the extent of atherosclerosis and progression rate was no greater than those with neither diagnosis. Another observation was that EEM and lumen were larger in metabolic syndrome group for the same amount of PAV and TAV. Interestingly, the IVUS findings in sole DM patients vs. DM patients with concomitant metabolic syndrome were no different. In a Korean study involving 2,869 symptomatic subjects who underwent CTCA, metabolic syndrome was independently associated with the presence and severity of CAD only in the non-DM group but not in the DM group (41). These observations highlight the significant risk of coronary atherosclerotic disease progression when metabolic syndrome leads to DM.

It has been observed that although metabolic syndrome was an independent predictor of plaque progression, when its individual components were used it was no longer significant. Whilst hypertriglyceridemia and BMI were independent predictors in one study (42), abdominal obesity and high blood pressure were found to be significantly associated in another study where asymptomatic subjects were assessed using CTCA (43). The impact of metabolic syndrome and its components on coronary plaque progression in response to intensive statin therapy was studied in the JAPAN-ACS trial (44). Although percent change in PAV was no different between metabolic syndrome and non-metabolic syndrome group, in the former, response to therapy was attenuated with increasing number of metabolic syndrome components, especially  $\geq 4$  risk factors. In addition, it was observed that percent BMI change was an independent predictor of plaque regression. It has also been demonstrated that prognostic information is added to the diagnosis of metabolic syndrome if stratification is performed by hsCRP (45).

Although a previous VH-IVUS study showed a higher prevalence of TCFA in patients with DM and metabolic syndrome (46) (Fig 2 & 3), no such association was seen in PROSPECT trial and other VH-IVUS studies (47, 48). DM, metabolic syndrome and a control group were compared where OCT was used to characterize coronary plaque. It was observed that Lipid Index was higher in DM and metabolic syndrome group compared to those with neither diagnosis while calcification was more frequent in DM group. Of note, frequency of TCFA, macrophage accumulation and micro vessels did not differ among the 3 groups and ACS was the only independent predictor of TCFA (28). Yet in another study, when clinical predictors of culprit plaque rupture were assessed on IVUS in ACS patients who were divided into two groups based on the presence or absence of plaque rupture (49), the prevalence of metabolic syndrome was higher in the plaque rupture group. The waist circumference in these patients was greater and they had lower HDL-C levels.

Metabolic syndrome as a syndrome or due to individual risk factor components appears to be associated with atherosclerotic disease progression. The presence of high-risk plaque features such as high lipid content and positive remodelling, and the association of metabolic syndrome with plaque rupture suggests that this is a high-risk group. In addition, as metabolic syndrome is regarded as a prediabetic state (50), aggressive risk factor management, especially central adiposity, is essential to prevent cardiovascular disease progression from the development of frank DM.

## **GENDER**

IVUS analysis has demonstrated that women have less extent of CAD compared to men, which has also been confirmed by pathologic studies. (51, 52) (53, 54). It has also been proposed that women take longer to develop significant atherosclerosis, which may relate to differences in the influence of risk factors between the sexes. It has been hypothesised that oestrogen has an anti-inflammatory effect that might stabilise existing plaque and slow plaque progression with postmenopausal women (>65 years) having the same risk of CAD as men. However, oestrogen has shown no protective effect against plaque erosion which is more common in women (55).

In patients presenting with ACS, no significant sex difference was seen in culprit plaque characteristics as determined by OCT and IVUS (56, 57). In a follow-up VH-IVUS analysis of culprit lesions in ACS patients, (58) it was noted that women had a greater prevalence of TCFA. However, women were also more likely to be diabetic and have higher high sensitivity C-reactive protein (hsCRP) levels, which when adjusted for on multivariate analysis, negated the differences seen in the presence of TCFA.

In the PROSPECT study, it was demonstrated that majority of future MACE arose from plaques that caused only mild stenosis angiographically (diameter stenosis < 50%) but were characterised by high risk plaque features such as large plaque burden  $\geq 70\%$ , small MLA  $\leq 4 \text{ mm}^2$ , and / or are

TCFA's as assessed by VH-IVUS (59). A sex-based analysis of patients from the PROSPECT trial revealed that women had fewer vessels with NCL and more focal NCL, with, less calcium, necrotic core and fibrous volume. Whilst women were more likely to have at least one high risk plaque feature, the attributable risk of MACE appears to be highly associated with TCFA in women and PB > 70% in men. Despite these differences, the NCL MACE between men and women at 3 years was similar (6.1% Vs. 7.5%, p=0.49)(60). The authors postulate that these observed differences in NCL plaque characteristics might balance out to explain the similar event rates. It is important to note that most of these sex differences are usually seen in patients <65 years of age and that plaque characteristics become increasingly similar between men and women with increasing age (56).

In a meta-analysis of 170,000 participants women demonstrated the greatest proportional benefit in terms of reduction of plaque and MACE events (61), however the factors that contribute to these effects are poorly understood. . In the SATURN trial of intensive lipid-lowering therapy (62), female sex female sex was independently associated with coronary atheroma plaque regression to statin treatment (Fig 4). Women achieved greater PAV reduction only if LDL-C levels reached  $\leq 70$  mg/dL despite fewer women reaching target levels compared to men and it was suggested that women may derive greater benefit from rosuvastatin compared to atorvastatin. Interestingly, plaque regression was more likely to occur in women with diabetes mellitus, stable angina pectoris, and higher baseline LDL-C and CRP levels. The reduction was irrespective of HDL-C levels, which is in contrast to the findings in the REVERSAL trial where HDL-C levels above the collective mean were significantly associated with plaque regression (63). Of note, it was observed that on treatment CRP levels and not the absolute LDL-C change was shown to be associated with plaque reduction and MACE in a sub study of SATURN (64).

These findings highlight the complex interaction between female sex, cardiovascular risk factors, CRP and HDL-C and their association with plaque regression, response to therapy and events.

## **ETHNICITY**

Differences in atherosclerotic disease patterns have been identified in various ethnic groups. It is not well understood as to whether this is attributable to genetic differences or due to the differences in prevalent risk factors. In seven clinical trials that utilized serial IVUS, African American patients were compared to Caucasians, and were more likely to be female with a greater number of co-morbidities. Despite a higher use of anti-atherosclerotic therapies, African American patients had higher LDL-C, CRP and SBP at baseline and follow up. Although baseline atheroma volume did not differ, at follow up there was greater atheroma progression in the African American group despite adjustment for the differences in risk factor control (65).

Ethnic differences were assessed in an IVUS comparison of left main artery disease between white and Asian patients (Japanese and South Korean) with matching parameters of age, gender and prevalence of DM. Asian patients had lower BMI and lipid levels, and were observed to have smaller lumen, larger vessel area and larger plaque burden, while white patients had greater calcification despite having less plaque volume. On the contrary, when coronary angiography was used to compare coronary lesions between Mainland Chinese and Australians, the incidence of left main artery and left anterior descending artery lesions in Australians were higher than that for Chinese of the same gender. It was observed that Australians typically have artery lesions 10 years earlier (66).

South Asians from Mediator of Atherosclerosis in South Asians living in America (MASALA) study were compared to the ethnic groups in Multi-Ethnic Study of Atherosclerosis (MESA)

consisting of whites, African Americans, Latinos and Chinese (67). CAC score was used for comparison and it was observed that South Asian men had similar CAC burden as white men but higher scores than other ethnic groups. South Asian women  $\geq 70$  years were found to have higher CAC than most other groups (Fig 5). Additionally, in a study that used CTCA and CAC to compare symptomatic South Asians and Caucasians with similar risk factors, it was observed that in patients aged  $\geq 50$  years, South Asians had a greater mean number of arterial segments with both obstructive and non obstructive plaque, and higher CAC scores. Interestingly, in patients  $\leq 50$  years, Caucasians showed a higher mean number of diseased segments with non obstructive plaques with similar CAC scores suggesting that Caucasians are likely to have more diffuse atherosclerosis at an earlier age although South Asians had higher prevalence and severity of disease (68).

In a quantitative coronary angiography study, symptomatic South Asians were observed to have a higher percentage multivessel disease, higher mean percent stenosis per vessel and smaller proximal LAD luminal diameters when compared to Caucasians (69). These findings are important as South Asians form 20% of the world's population and are among the fastest growing ethnic groups in various countries. It is estimated that by 2020, South Asians will contribute to 40% of the global cardiovascular burden (70).

These observations highlight the differences in coronary plaque burden and prevalence that is seen in various ethnic groups. The effects of ethnicity may contribute to cardiovascular disease burden beyond traditional risk factors and further studies are needed to confirm these findings.

## **Chronic Kidney Disease**

Studies of coronary atherosclerosis in chronic kidney disease (CKD) patients are limited and heterogeneous. Studies differ significantly in methodology and patient inclusion with some

dedicated to patients requiring renal replacement therapy (RRT), and others involving those with progressively declining glomerular filtration rate (GFR) not yet on dialysis. Therefore there is marked variation in results from these studies. What is of certainty however is that there is a very high prevalence of obstructive CAD in these patients (96) and the primary cause of death is due to cardiovascular events (95).

The pathophysiology of vascular disease in CKD patients differs to the general population (97). In addition to traditional risk factors, there is a complex and poorly understood interplay between malnutrition, inflammation, atherosclerosis and calcification that play a role in the development of vascular disease (106). Autopsy studies have confirmed that CKD patients have an extensive atherosclerotic burden. Schwarz et al performed a post-mortem analysis of 27 end stage renal disease (ESRD) patients comparing epicardial artery plaque characteristics with age and sex matched normal renal function patients. The authors demonstrated that ESRD patients had a greater proportion of calcified plaques, greater media thickness and reduced lumen area with a trend to higher intima thickness but no overall difference in plaque area(71). Further pathologic analysis has confirmed this greater proportion of dense coronary calcific disease and media thickness, amongst all groups of renal dysfunction compared to normal controls, independent of other cardiovascular risk factors(72).

There is a limited literature with respect to non-invasive techniques; CACS has been widely investigated in patients with CKD with clear evidence of increasing CACS burden as GFR decreases (73, 74). As calcification in ESRD tends to be within the media as described pathologically, this partly explains the probably reduced specificity for obstructive disease(75). CTCA is an ideal non-invasive tool for coronary luminal plaque assessment. However the large degree of coronary calcification may impact upon interpretation and the rates of unevaluable segments or patients' ranges from 10-27%(76-78). Despite this, the sensitivity and negative

predictive value for obstructive disease remains high (93% and 97%) at the expense of reduced specificity and positive predictive value (63% and 41%) as was seen in a study of 138 CKD patients undergoing both CTA and invasive coronary angiogram(76). No CT study has yet imitated invasive studies to evaluate high-risk plaque features between normal, CKD and ESRD patients.

There have been several small in-vivo analyses of coronary plaques to investigate the impact of renal function, predominantly with the use of IVUS. Several studies have demonstrated that plaque characteristics worsen significantly with declining GFR. Miyagi and colleagues evaluated two groups (GFR <60mL/min and >60mL/min) of patients undergoing percutaneous intervention (PCI) with IVUS guidance and found that impaired renal function related to a higher percentage of lipid volume and reduced percentage of fibrous volume; however there were no dialysis patients included in this analysis nor was calcific plaque assessed(79). A study of 136 ACS patients who underwent culprit artery angioscopy revealed a greater proportion of “yellow plaques” with CKD being an independent predictor of multiple yellow plaques per vessel(80). Furthermore, in a study of 310 ACS patients that had culprit artery IVUS interrogation, progressively declining GFR was an independent predictor of plaque rupture, with patients in the lowest creatinine clearance group having a greater degree of lesion site plaque burden and plaque length(81).

In a substudy of the PROSPECT trial that included only ACS patients, CKD patients had a higher prevalence of necrotic core, dense calcium and lower fibrous tissue in non-culprit artery plaques (82). Similarly, an OCT study of non-culprit plaques in a group of patients by Kato et al observed higher lipid index and higher calcium prevalence and plaque disruption in patients with GFR <60 (83). Ogita et al established that in a study of stable angina patients, diabetics with CKD, had a greater proportion of dense calcium and necrotic core compared to non-diabetics, with a progressive increase in necrotic core associated with declining renal function; in particular the highest values

were seen in RRT patients (84). Kono et al evaluated both stable angina and ACS patients and clearly demonstrated on IVUS that as GFR reduced there was a significantly increased volume of dense calcification and necrotic core with the highest values in ACS patients on RRT(85). Finally, A meta-analysis of 989 patients from plaque progression studies stratified patients by GFR >60 and <60 (including RRT patients) and concluded that there was no difference in progression rates of atheroma volume despite preventive therapies(86).

## **Obesity**

The worldwide prevalence of obesity is reaching pandemic status and there are strong links between obesity and CAD, which makes imaging of these plaques all the more relevant. There is compelling evidence to support an association between obesity and CACS as was seen in over 6000 patients analysed in the MESA study(87). Furthermore, in a cross-sectional study of 14,828 metabolically healthy adults without CAD, individuals with a higher BMI had a greater CACS prevalence compared to their normal weight counterparts (88). The question of progression of plaque burden in obese patients was evaluated by Cassidy et al in a study that reviewed baseline CACS and follow up at a median of 8.9 years. This demonstrated that waist circumference; waist-to-hip ratio and BMI were all strongly associated with an increased progression of CACS in those initially deemed to be of low risk(89). Additionally, Imai et al studied 553 patients who underwent serial CT coronary angiography and noted that the risk of non-calcified plaques increased as visceral adipose tissue increased regardless of underlying CAD risk factors.

Few invasive studies have been performed with the specific aim of evaluation of obesity and coronary plaque with most studies utilising IVUS to assess the effects of pharmacologic therapy on plaque progression. A large systematic review of 7 serial IVUS studies comprising 3459 patients to

monitor atheroma progression in patients with the metabolic syndrome demonstrated that a BMI  $\geq 30$  independently predicted plaque progression (42).

Plaque vulnerability and its association with obesity have also been reviewed by multi-modality assessment. Ohashi et al showed that visceral adiposity independently predicted the presence and extent of noncalcified coronary plaque that also contained multiple features of plaque vulnerability (positive remodelling, spotty calcification and low attenuation plaque) – however BMI itself was not found to be a significant predictor(90). Similarly, another prospectively performed CTCA study demonstrated that visceral abdominal fat predicted the progression of noncalcified but not calcified plaque after a mean of 38 month follow up independent of other risk factors(91). In a large retrospective database of 3158 patients to evaluate plaque characteristics, 32% of patients with BMI  $>25\text{kg/m}^2$  demonstrated evidence of high-risk plaque features and BMI itself was an independent predictor of future ACS events (92).

Regarding invasive methods to assess plaque vulnerability, Kang et al reviewed 780 patients undergoing PCI with IVUS also performed, and noted that increasing BMI was associated with a greater plaque burden and plaque area compared to lower BMI controls(93). Tani et al demonstrated that increasing BMI attenuated statin induced atherosclerotic regression and BMI was well correlated with present plaque volume and an independent predictor of plaque volume change(94). Finally Yonetsu et al studied patients undergoing 3-vessel OCT in patients with and without diabetes and the metabolic syndrome. Those with the metabolic syndrome had higher BMIs and longer lipid plaque length and index compared to control patients(28).

Obesity is not only linked with increased atherosclerotic plaque burden and progression, but is also associated with attenuated response to therapies, increased plaque vulnerability and events. Its association with metabolic syndrome and DM further complicates the management of obesity.

## CONCLUSION

Intravascular imaging techniques give unparalleled information about atherosclerotic plaques and CTCA allows assessment of plaque extent and morphology non-invasively. These imaging techniques allows us to appreciate in vivo the various stages of plaque development, determine plaque burden, identify high risk plaque features, monitor response to therapy and appreciate the differences in disease pattern in various “at risk” groups. Understanding the differences in phenotype and response to therapy in various susceptible groups is vital in our endeavours to develop personalised medicine.

### References:

1. Murray CJ, Lopez AD. Measuring the global burden of disease. *N Engl J Med*. 2013;369(5):448-57.
2. Fuster V, Mearns BM. The CVD paradox: mortality vs prevalence. *Nat Rev Cardiol*. 2009;6(11):669.
3. Lim SS, Vos T, Flaxman AD, Danaei G, Shibuya K, Adair-Rohani H, et al. A comparative risk assessment of burden of disease and injury attributable to 67 risk factors and risk factor clusters in 21 regions, 1990-2010: a systematic analysis for the Global Burden of Disease Study 2010. *Lancet*. 2012;380(9859):2224-60.
4. Wentzel JJ, Chatzizisis YS, Gijzen FJ, Giannoglou GD, Feldman CL, Stone PH. Endothelial shear stress in the evolution of coronary atherosclerotic plaque and vascular remodelling: current understanding and remaining questions. *Cardiovasc Res*. 2012;96(2):234-43.
5. Skalen K, Gustafsson M, Rydberg EK, Hulten LM, Wiklund O, Innerarity TL, et al. Subendothelial retention of atherogenic lipoproteins in early atherosclerosis. *Nature*. 2002;417(6890):750-4.
6. Steinberg D, Witztum JL. Oxidized low-density lipoprotein and atherosclerosis. *Arterioscler Thromb Vasc Biol*. 2010;30(12):2311-6.
7. Tabas I, Williams KJ, Boren J. Subendothelial lipoprotein retention as the initiating process in atherosclerosis: update and therapeutic implications. *Circulation*. 2007;116(16):1832-44.
8. Stamler J, Davignus ML, Garside DB, Dyer AR, Greenland P, Neaton JD. Relationship of baseline serum cholesterol levels in 3 large cohorts of younger men to long-term coronary, cardiovascular, and all-cause mortality and to longevity. *JAMA*. 2000;284(3):311-8.
9. Kragel AH, Reddy SG, Wittes JT, Roberts WC. Morphometric analysis of the composition of atherosclerotic plaques in the four major epicardial coronary arteries in acute myocardial infarction and in sudden coronary death. *Circulation*. 1989;80(6):1747-56.
10. Otsuka F, Sakakura K, Yahagi K, Joner M, Virmani R. Has our understanding of calcification in human coronary atherosclerosis progressed? *Arterioscler Thromb Vasc Biol*. 2014;34(4):724-36.
11. Glagov S, Weisenberg E, Zarins CK, Stankunavicius R, Kolettis GJ. Compensatory enlargement of human atherosclerotic coronary arteries. *N Engl J Med*. 1987;316(22):1371-5.

12. Burke AP, Kolodgie FD, Farb A, Weber D, Virmani R. Morphological predictors of arterial remodeling in coronary atherosclerosis. *Circulation*. 2002;105(3):297-303.
13. Stancoven A, McGuire DK. Preventing macrovascular complications in type 2 diabetes mellitus: glucose control and beyond. *Am J Cardiol*. 2007;99(11A):5H-11H.
14. Huxley R, Barzi F, Woodward M. Excess risk of fatal coronary heart disease associated with diabetes in men and women: meta-analysis of 37 prospective cohort studies. *BMJ*. 2006;332(7533):73-8.
15. Donnan PT, Boyle DI, Broomhall J, Hunter K, MacDonald TM, Newton RW, et al. Prognosis following first acute myocardial infarction in Type 2 diabetes: a comparative population study. *Diabet Med*. 2002;19(6):448-55.
16. Ashfaq S, Ghazzal Z, Douglas JS, Morris DC, Veledar E, Weintraub WS. Impact of diabetes on five-year outcomes after vein graft interventions performed prior to the drug-eluting stent era. *J Invasive Cardiol*. 2006;18(3):100-5.
17. Burchfiel CM, Reed DM, Marcus EB, Strong JP, Hayashi T. Association of diabetes mellitus with coronary atherosclerosis and myocardial lesions. An autopsy study from the Honolulu Heart Program. *Am J Epidemiol*. 1993;137(12):1328-40.
18. Nicholls SJ, Tuzcu EM, Kalidindi S, Wolski K, Moon KW, Sipahi I, et al. Effect of diabetes on progression of coronary atherosclerosis and arterial remodeling: a pooled analysis of 5 intravascular ultrasound trials. *J Am Coll Cardiol*. 2008;52(4):255-62.
19. Stegman B, Puri R, Cho L, Shao M, Ballantyne CM, Barter PJ, et al. High-intensity statin therapy alters the natural history of diabetic coronary atherosclerosis: insights from SATURN. *Diabetes Care*. 2014;37(11):3114-20.
20. Jimenez-Quevedo P, Suzuki N, Corros C, Ferrer C, Angiolillo DJ, Alfonso F, et al. Vessel shrinkage as a sign of atherosclerosis progression in type 2 diabetes: a serial intravascular ultrasound analysis. *Diabetes*. 2009;58(1):209-14.
21. Tamada H, Nishikawa H, Mukai S, Setsuda M, Nakamura M, Suzuki H, et al. Impact of diabetes mellitus on angiographically silent coronary atherosclerosis. *Circ J*. 2003;67(5):423-6.
22. Ertan C, Ozeke O, Gul M, Aras D, Topaloglu S, Kisacik HL, et al. Association of prediabetes with diffuse coronary narrowing and small-vessel disease. *J Cardiol*. 2014;63(1):29-34.
23. Cersosimo E, DeFronzo RA. Insulin resistance and endothelial dysfunction: the road map to cardiovascular diseases. *Diabetes Metab Res Rev*. 2006;22(6):423-36.
24. Anand DV, Lim E, Darko D, Bassett P, Hopkins D, Lipkin D, et al. Determinants of progression of coronary artery calcification in type 2 diabetes: role of glycemic control and inflammatory/vascular calcification markers. *J Am Coll Cardiol*. 2007;50(23):2218-25.
25. Portik-Dobos V, Anstadt MP, Hutchinson J, Bannan M, Ergul A. Evidence for a matrix metalloproteinase induction/activation system in arterial vasculature and decreased synthesis and activity in diabetes. *Diabetes*. 2002;51(10):3063-8.
26. Nigro J, Osman N, Dart AM, Little PJ. Insulin resistance and atherosclerosis. *Endocr Rev*. 2006;27(3):242-59.
27. Nasu K, Tsuchikane E, Katoh O, Fujita H, Surmely JF, Ehara M, et al. Plaque characterisation by Virtual Histology intravascular ultrasound analysis in patients with type 2 diabetes. *Heart*. 2008;94(4):429-33.

28. Yonetsu T, Kato K, Uemura S, Kim BK, Jang Y, Kang SJ, et al. Features of coronary plaque in patients with metabolic syndrome and diabetes mellitus assessed by 3-vessel optical coherence tomography. *Circulation Cardiovascular imaging*. 2013;6(5):665-73.
29. Kato K, Yonetsu T, Kim SJ, Xing L, Lee H, McNulty I, et al. Comparison of nonculprit coronary plaque characteristics between patients with and without diabetes: a 3-vessel optical coherence tomography study. *JACC Cardiovasc Interv*. 2012;5(11):1150-8.
30. Iguchi T, Hasegawa T, Otsuka K, Matsumoto K, Yamazaki T, Nishimura S, et al. Insulin resistance is associated with coronary plaque vulnerability: insight from optical coherence tomography analysis. *Eur Heart J Cardiovasc Imaging*. 2014;15(3):284-91.
31. Niccoli G, Giubilato S, Di Vito L, Leo A, Cosentino N, Pitocco D, et al. Severity of coronary atherosclerosis in patients with a first acute coronary event: a diabetes paradox. *Eur Heart J*. 2013;34(10):729-41.
32. Hess K, Grant PJ. Inflammation and thrombosis in diabetes. *Thromb Haemost*. 2011;105 Suppl 1:S43-54.
33. Nozue T, Yamamoto S, Tohyama S, Fukui K, Umezawa S, Onishi Y, et al. Impact of diabetes mellitus on coronary atherosclerosis and plaque composition under statin therapy - subanalysis of the TRUTH study. *Circ J*. 2012;76(9):2188-96.
34. Berry C, Noble S, Gregoire JC, Ibrahim R, Levesque S, Lavoie MA, et al. Glycaemic status influences the nature and severity of coronary artery disease. *Diabetologia*. 2010;53(4):652-8.
35. Turnbull F, Neal B, Algert C, Chalmers J, Chapman N, Cutler J, et al. Effects of different blood pressure-lowering regimens on major cardiovascular events in individuals with and without diabetes mellitus: results of prospectively designed overviews of randomized trials. *Arch Intern Med*. 2005;165(12):1410-9.
36. Colhoun HM, Betteridge DJ, Durrington PN, Hitman GA, Neil HA, Livingstone SJ, et al. Primary prevention of cardiovascular disease with atorvastatin in type 2 diabetes in the Collaborative Atorvastatin Diabetes Study (CARDS): multicentre randomised placebo-controlled trial. *Lancet*. 2004;364(9435):685-96.
37. Kataoka Y, Shao M, Wolski K, Uno K, Puri R, Tuzcu EM, et al. Multiple risk factor intervention and progression of coronary atherosclerosis in patients with type 2 diabetes mellitus. *Eur J Prev Cardiol*. 2013;20(2):209-17.
38. Grundy SM, Cleeman JI, Merz CN, Brewer HB, Jr., Clark LT, Hunninghake DB, et al. Implications of recent clinical trials for the National Cholesterol Education Program Adult Treatment Panel III guidelines. *Circulation*. 2004;110(2):227-39.
39. Stern MP, Williams K, Hunt KJ. Impact of diabetes/metabolic syndrome in patients with established cardiovascular disease. *Atheroscler Suppl*. 2005;6(2):3-6.
40. Bayturan O, Tuzcu EM, Uno K, Lavoie AJ, Hu T, Shreevatsa A, et al. Comparison of rates of progression of coronary atherosclerosis in patients with diabetes mellitus versus those with the metabolic syndrome. *Am J Cardiol*. 2010;105(12):1735-9.
41. Won KB, Chang HJ, Sung J, Shin S, Cho IJ, Shim CY, et al. Differential association between metabolic syndrome and coronary artery disease evaluated with cardiac computed tomography according to the presence of diabetes in a symptomatic Korean population. *BMC Cardiovasc Disord*. 2014;14:105.
42. Bayturan O, Tuzcu EM, Lavoie A, Hu T, Wolski K, Schoenhagen P, et al. The metabolic syndrome, its component risk factors, and progression of coronary atherosclerosis. *Archives of internal medicine*. 2010;170(5):478-84.

43. Ryu J, Yong HS, Huh S, Kang EY, Woo OH. Relation of coronary atherosclerosis and metabolic syndrome in asymptomatic subjects: evaluation with coronary CT angiography. *Int J Cardiovasc Imaging*. 2013;29 Suppl 2:101-7.
44. Takashima H, Ozaki Y, Morimoto T, Kimura T, Hiro T, Miyauchi K, et al. Clustering of metabolic syndrome components attenuates coronary plaque regression during intensive statin therapy in patients with acute coronary syndrome: the JAPAN-ACS subanalysis study. *Circ J*. 2012;76(12):2840-7.
45. Sattar N, Gaw A, Scherbakova O, Ford I, O'Reilly DS, Haffner SM, et al. Metabolic syndrome with and without C-reactive protein as a predictor of coronary heart disease and diabetes in the West of Scotland Coronary Prevention Study. *Circulation*. 2003;108(4):414-9.
46. Zheng M, Choi SY, Tahk SJ, Lim HS, Yang HM, Choi BJ, et al. The relationship between volumetric plaque components and classical cardiovascular risk factors and the metabolic syndrome a 3-vessel coronary artery virtual histology-intravascular ultrasound analysis. *JACC Cardiovasc Interv*. 2011;4(5):503-10.
47. Marso SP, Mercado N, Maehara A, Weisz G, Mintz GS, McPherson J, et al. Plaque composition and clinical outcomes in acute coronary syndrome patients with metabolic syndrome or diabetes. *JACC Cardiovasc Imaging*. 2012;5(3 Suppl):S42-52.
48. Lee MG, Jeong MH, Kim DH, Lee KH, Park KH, Sim DS, et al. Can metabolic syndrome predict the vulnerable plaque in patients with stable angina pectoris? Virtual histology-intravascular ultrasound analysis. *J Cardiol*. 2012;59(3):266-74.
49. Kato M, Dote K, Naganuma T, Sasaki S, Ueda K, Okita M, et al. Clinical predictors of culprit plaque rupture assessed on intravascular ultrasound in acute coronary syndrome. *Circ J*. 2010;74(9):1936-42.
50. Laaksonen DE, Lakka HM, Niskanen LK, Kaplan GA, Salonen JT, Lakka TA. Metabolic syndrome and development of diabetes mellitus: application and validation of recently suggested definitions of the metabolic syndrome in a prospective cohort study. *Am J Epidemiol*. 2002;156(11):1070-7.
51. Virmani R, Burke AP, Kolodgie FD, Farb A. Pathology of the thin-cap fibroatheroma: a type of vulnerable plaque. *J Interv Cardiol*. 2003;16(3):267-72.
52. Mautner SL, Lin F, Mautner GC, Roberts WC. Comparison in women versus men of composition of atherosclerotic plaques in native coronary arteries and in saphenous veins used as aortocoronary conduits. *J Am Coll Cardiol*. 1993;21(6):1312-8.
53. Nicholls SJ, Wolski K, Sipahi I, Schoenhagen P, Crowe T, Kapadia SR, et al. Rate of progression of coronary atherosclerotic plaque in women. *J Am Coll Cardiol*. 2007;49(14):1546-51.
54. Kornowski R, Lansky AJ, Mintz GS, Kent KM, Pichard AD, Satler LF, et al. Comparison of men versus women in cross-sectional area luminal narrowing, quantity of plaque, presence of calcium in plaque, and lumen location in coronary arteries by intravascular ultrasound in patients with stable angina pectoris. *Am J Cardiol*. 1997;79(12):1601-5.
55. Burke AP, Farb A, Malcom G, Virmani R. Effect of menopause on plaque morphologic characteristics in coronary atherosclerosis. *Am Heart J*. 2001;141(2 Suppl):S58-62.
56. Schoenenberger AW, Urbanek N, Toggweiler S, Stuck AE, Resink TJ, Erne P. Ultrasound-assessed non-culprit and culprit coronary vessels differ by age and gender. *World J Cardiol*. 2013;5(3):42-8.
57. Chia S, Christopher Raffel O, Takano M, Tearney GJ, Bouma BE, Jang IK. In-vivo comparison of coronary plaque characteristics using optical coherence tomography in women vs. men with acute coronary syndrome. *Coron Artery Dis*. 2007;18(6):423-7.

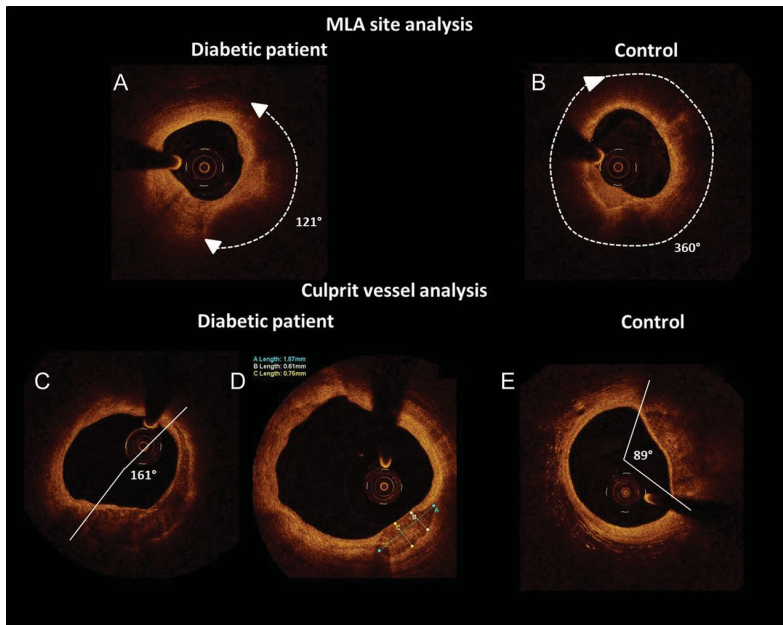
58. Hong YJ, Jeong MH, Choi YH, Ma EH, Cho SH, Ko JS, et al. Gender differences in coronary plaque components in patients with acute coronary syndrome: virtual histology-intravascular ultrasound analysis. *J Cardiol*. 2010;56(2):211-9.
59. Stone GW, Maehara A, Lansky AJ, de Bruyne B, Cristea E, Mintz GS, et al. A prospective natural-history study of coronary atherosclerosis. *The New England journal of medicine*. 2011;364(3):226-35.
60. Lansky AJ, Ng VG, Maehara A, Weisz G, Lerman A, Mintz GS, et al. Gender and the extent of coronary atherosclerosis, plaque composition, and clinical outcomes in acute coronary syndromes. *JACC Cardiovasc Imaging*. 2012;5(3 Suppl):S62-72.
61. Cholesterol Treatment Trialists C, Baigent C, Blackwell L, Emberson J, Holland LE, Reith C, et al. Efficacy and safety of more intensive lowering of LDL cholesterol: a meta-analysis of data from 170,000 participants in 26 randomised trials. *Lancet*. 2010;376(9753):1670-81.
62. Puri R, Nissen SE, Shao M, Ballantyne CM, Barter PJ, Chapman MJ, et al. Sex-related differences of coronary atherosclerosis regression following maximally intensive statin therapy: insights from SATURN. *JACC Cardiovasc Imaging*. 2014;7(10):1013-22.
63. Nissen SE, Tuzcu EM, Schoenhagen P, Brown BG, Ganz P, Vogel RA, et al. Effect of intensive compared with moderate lipid-lowering therapy on progression of coronary atherosclerosis: a randomized controlled trial. *JAMA : the journal of the American Medical Association*. 2004;291(9):1071-80.
64. Puri R, Nissen SE, Libby P, Shao M, Ballantyne CM, Barter PJ, et al. C-reactive protein, but not low-density lipoprotein cholesterol levels, associate with coronary atheroma regression and cardiovascular events after maximally intensive statin therapy. *Circulation*. 2013;128(22):2395-403.
65. Kataoka Y, Hsu A, Wolski K, Uno K, Puri R, Tuzcu EM, et al. Progression of coronary atherosclerosis in African-American patients. *Cardiovasc Diagn Ther*. 2013;3(3):161-9.
66. Jang IK, Tearney GJ, MacNeill B, Takano M, Moselewski F, Iftima N, et al. In vivo characterization of coronary atherosclerotic plaque by use of optical coherence tomography. *Circulation*. 2005;111(12):1551-5.
67. Kanaya AM, Kandula NR, Ewing SK, Herrington D, Liu K, Blaha MJ, et al. Comparing coronary artery calcium among U.S. South Asians with four racial/ethnic groups: the MASALA and MESA studies. *Atherosclerosis*. 2014;234(1):102-7.
68. Koulaouzidis G, Nicoll R, Charisopoulou D, McArthur T, Jenkins PJ, Henein MY. Aggressive and diffuse coronary calcification in South Asian angina patients compared to Caucasians with similar risk factors. *Int J Cardiol*. 2013;167(6):2472-6.
69. Hasan RK, Ginwala NT, Shah RY, Kumbhani DJ, Wilensky RL, Mehta NN. Quantitative angiography in South Asians reveals differences in vessel size and coronary artery disease severity compared to Caucasians. *Am J Cardiovasc Dis*. 2011;1(1):31-7.
70. Gholap N, Davies M, Patel K, Sattar N, Khunti K. Type 2 diabetes and cardiovascular disease in South Asians. *Prim Care Diabetes*. 2011;5(1):45-56.
71. Schwarz U, Buzello M, Ritz E, Stein G, Raabe G, Wiest G, et al. Morphology of coronary atherosclerotic lesions in patients with end-stage renal failure. *Nephrology, dialysis, transplantation : official publication of the European Dialysis and Transplant Association - European Renal Association*. 2000;15(2):218-23.
72. Nakano T, Ninomiya T, Sumiyoshi S, Fujii H, Doi Y, Hirakata H, et al. Association of kidney function with coronary atherosclerosis and calcification in autopsy samples from Japanese elders: the Hisayama study. *American journal of kidney diseases : the official journal of the National Kidney Foundation*. 2010;55(1):21-30.

73. Kramer H, Toto R, Peshock R, Cooper R, Victor R. Association between chronic kidney disease and coronary artery calcification: the Dallas Heart Study. *Journal of the American Society of Nephrology : JASN*. 2005;16(2):507-13.
74. Raggi P, Boulay A, Chasan-Taber S, Amin N, Dillon M, Burke SK, et al. Cardiac calcification in adult hemodialysis patients. A link between end-stage renal disease and cardiovascular disease? *Journal of the American College of Cardiology*. 2002;39(4):695-701.
75. Sharples EJ, Pereira D, Summers S, Cunningham J, Rubens M, Goldsmith D, et al. Coronary artery calcification measured with electron-beam computerized tomography correlates poorly with coronary artery angiography in dialysis patients. *American journal of kidney diseases : the official journal of the National Kidney Foundation*. 2004;43(2):313-9.
76. Winther S, Svensson M, Jorgensen HS, Bouchelouche K, Gormsen LC, Pedersen BB, et al. Diagnostic Performance of Coronary CT Angiography and Myocardial Perfusion Imaging in Kidney Transplantation Candidates. *JACC Cardiovascular imaging*. 2015;8(5):553-62.
77. de Bie MK, Buiten MS, Gaasbeek A, Boogers MJ, Roos CJ, Schuijf JD, et al. CT coronary angiography is feasible for the assessment of coronary artery disease in chronic dialysis patients, despite high average calcium scores. *PLoS one*. 2013;8(7):e67936.
78. Mao J, Karthikeyan V, Poopat C, Song T, Pantelic M, Chattahi J, et al. Coronary computed tomography angiography in dialysis patients undergoing pre-renal transplantation cardiac risk stratification. *Cardiology journal*. 2010;17(4):349-61.
79. Miyagi M, Ishii H, Murakami R, Isobe S, Hayashi M, Amano T, et al. Impact of renal function on coronary plaque composition. *Nephrology, dialysis, transplantation : official publication of the European Dialysis and Transplant Association - European Renal Association*. 2010;25(1):175-81.
80. Wada M, Ueda Y, Higo T, Matsuo K, Nishio M, Hirata A, et al. Chronic kidney disease and coronary artery vulnerable plaques. *Clinical journal of the American Society of Nephrology : CJASN*. 2011;6(12):2792-8.
81. Hong YJ, Jeong MH, Choi YH, Ma EH, Ko JS, Lee MG, et al. Effect of renal function on ultrasonic coronary plaque characteristics in patients with acute myocardial infarction. *The American journal of cardiology*. 2010;105(7):936-42.
82. Baber U, Stone GW, Weisz G, Moreno P, Dangas G, Maehara A, et al. Coronary plaque composition, morphology, and outcomes in patients with and without chronic kidney disease presenting with acute coronary syndromes. *JACC Cardiovascular imaging*. 2012;5(3 Suppl):S53-61.
83. Kato K, Yonetsu T, Jia H, Abtahian F, Vergallo R, Hu S, et al. Nonculprit coronary plaque characteristics of chronic kidney disease. *Circulation Cardiovascular imaging*. 2013;6(3):448-56.
84. Ogita M, Funayama H, Nakamura T, Sakakura K, Sugawara Y, Kubo N, et al. Plaque characterization of non-culprit lesions by virtual histology intravascular ultrasound in diabetic patients: impact of renal function. *Journal of cardiology*. 2009;54(1):59-65.
85. Kono K, Fujii H, Nakai K, Goto S, Shite J, Hirata K, et al. Composition and plaque patterns of coronary culprit lesions and clinical characteristics of patients with chronic kidney disease. *Kidney international*. 2012;82(3):344-51.
86. Nicholls SJ, Tuzcu EM, Hsu A, Wolski K, Sipahi I, Schoenhagen P, et al. Comparison of coronary atherosclerotic volume in patients with glomerular filtration rates < or = 60 versus > 60 ml/min/1.73 m(2): a meta-analysis of intravascular ultrasound studies. *The American journal of cardiology*. 2007;99(6):813-6.

87. Blaha MJ, Rivera JJ, Budoff MJ, Blankstein R, Agatston A, O'Leary DH, et al. Association between obesity, high-sensitivity C-reactive protein  $\geq 2$  mg/L, and subclinical atherosclerosis: implications of JUPITER from the Multi-Ethnic Study of Atherosclerosis. *Arteriosclerosis, thrombosis, and vascular biology*. 2011;31(6):1430-8.
88. Chang Y, Kim BK, Yun KE, Cho J, Zhang Y, Rampal S, et al. Metabolically-healthy obesity and coronary artery calcification. *Journal of the American College of Cardiology*. 2014;63(24):2679-86.
89. Cassidy AE, Bielak LF, Zhou Y, Sheedy PF, 2nd, Turner ST, Breen JF, et al. Progression of subclinical coronary atherosclerosis: does obesity make a difference? *Circulation*. 2005;111(15):1877-82.
90. Ohashi N, Yamamoto H, Horiguchi J, Kitagawa T, Kunita E, Utsunomiya H, et al. Association between visceral adipose tissue area and coronary plaque morphology assessed by CT angiography. *JACC Cardiovascular imaging*. 2010;3(9):908-17.
91. Imai A, Komatsu S, Ohara T, Kamata T, Yoshida J, Miyaji K, et al. Visceral abdominal fat accumulation predicts the progression of noncalcified coronary plaque. *Atherosclerosis*. 2012;222(2):524-9.
92. Motoyama S, Ito H, Sarai M, Kondo T, Kawai H, Nagahara Y, et al. Plaque Characterization by Coronary Computed Tomography Angiography and the Likelihood of Acute Coronary Events in Mid-Term Follow-Up. *Journal of the American College of Cardiology*. 2015;66(4):337-46.
93. Kang SJ, Mintz GS, Witzendichler B, Metzger DC, Rinaldi MJ, Duffy PL, et al. Effect of obesity on coronary atherosclerosis and outcomes of percutaneous coronary intervention: grayscale and virtual histology intravascular ultrasound substudy of assessment of dual antiplatelet therapy with drug-eluting stents. *Circulation Cardiovascular interventions*. 2015;8(1).
94. Tani S, Nagao K, Anazawa T, Kawamata H, Furuya S, Takahashi H, et al. Association of body mass index with coronary plaque regression: 6-month prospective study. *Journal of atherosclerosis and thrombosis*. 2009;16(3):275-82.
95. Schwarz U, Buzello M, Ritz E, Stein G, Raabe G, Wiest G, et al. Morphology of coronary atherosclerotic lesions in patients with end-stage renal failure. *Nephrology, dialysis, transplantation : official publication of the European Dialysis and Transplant Association - European Renal Association*. 2000 Feb;15(2):218-23. PubMed PMID: 10648668.
96. Nakamura S, Ishibashi-Ueda H, Niizuma S, Yoshihara F, Horio T, Kawano Y. Coronary calcification in patients with chronic kidney disease and coronary artery disease. *Clinical journal of the American Society of Nephrology : CJASN*. 2009 Dec;4(12):1892-900. PubMed PMID: 19833908. Pubmed Central PMCID: 2798876.
97. Nicholls SJ, Tuzcu EM, Hsu A, Wolski K, Sipahi I, Schoenhagen P, et al. Comparison of coronary atherosclerotic volume in patients with glomerular filtration rates  $\leq 60$  versus  $> 60$  ml/min/1.73 m<sup>2</sup>: a meta-analysis of intravascular ultrasound studies. *The American journal of cardiology*. 2007 Mar 15;99(6):813-6. PubMed PMID: 17350372.

## FIGURES

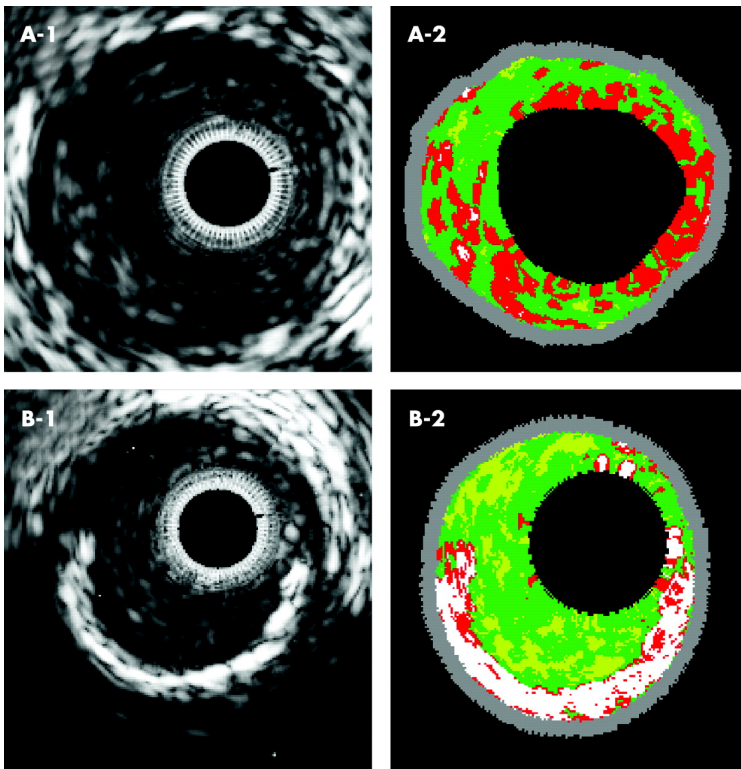
Fig 1



Optical coherence tomography findings at the minimal lumen area (MLA) site (*A* and *B*) and along the culprit vessel (*C–E*) in diabetic and non-diabetic patients. (*A*) Lipid plaque with a lipid arc of 121° was imaged at the MLA site in a diabetic patient. (*B*) Lipid plaque with a wider lipid arc (360°) was imaged at the MLA site in a non-diabetic patients. (*C*) Calcified plaque with a large calcified arc (161°) was imaged along the culprit vessel in a diabetic patient. (*D*) A typical superficial calcified nodule in a diabetic patient. The nodule has a length of 1.87 mm and a mean depth of 0.68 mm. (*E*) Calcified plaque with a small calcified arc (89°) was imaged along the culprit vessel in a non-diabetic patients.

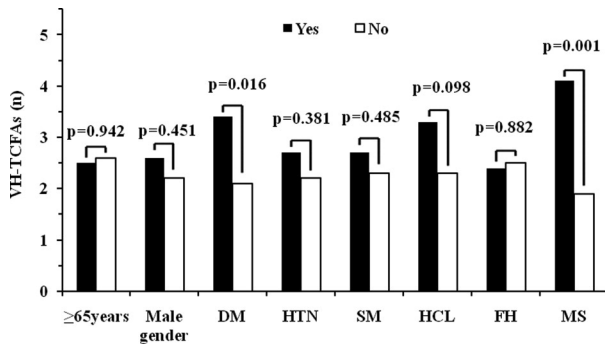
(Adapted from Niccoli G et al, Eur Heart J. 2013;34(10):729-41.)

Fig 2



Intravascular ultrasound and typical Virtual Histology (VH) intravascular ultrasound (IVUS) images of VH IVUS-derived thin-cap fibroatheroma (VHD-TCFA) and VH IVUS-derived fibrocalcific atheroma (VHD-FCA). VHD-TCFA: (A-1) greyscale IVUS image of target lesion. Note the heterogeneity of the plaque. (A-2) Colour-coded map of A-1 reconstructed by VH IVUS. Note a necrotic core rich plaque without evidence of fibrous cap. VHD-FCA: (B-1) greyscale intravascular ultrasound image at target lesion. Note the significant deep calcium plate with acoustic shadow. (B-2) Colour-coded map of B-1. Note the confluent dense calcium at bottom of the plaque. (Adapted from Nasu K et al, Heart. 2008;94(4):429-33.)

Fig 3

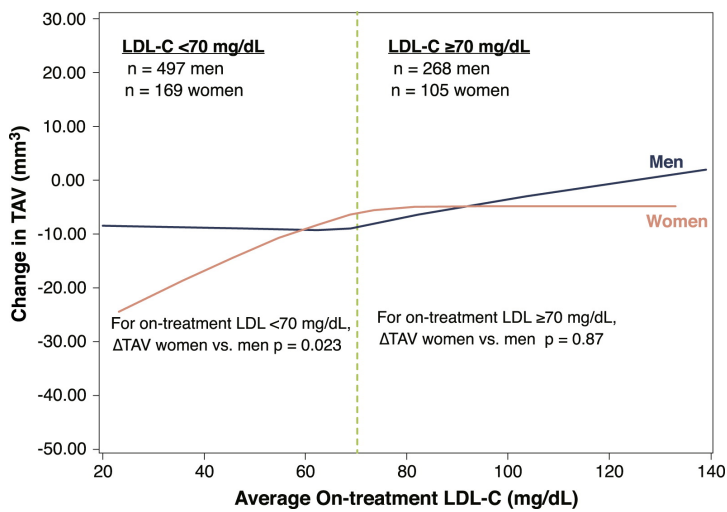


#### VH-TCFAs in Regard to Being With or Without Risk Factors

The virtual histology–intravascular ultrasound–derived thin-cap fibroatheroma (VH-TCFA) was significantly more frequent in diabetes mellitus (DM) patients or metabolic syndrome (MS) patients than in the patients without DM or MS. FH = family history of coronary artery disease; HCL = high cholesterol level; HTN = hypertension; SM = smoking.

(Adapted from Zheng M et al, JACC Cardiovasc Interv. 2011;4(5):503-10.)

Fig 4

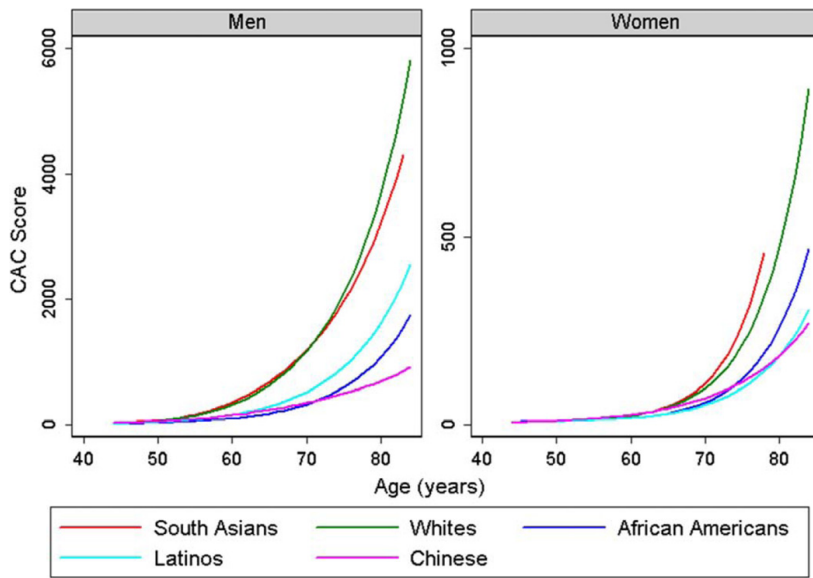


#### Sex-Related Variations of Changes in TAV Versus Average On-Treatment LDL-C Levels

Locally weighted (moving average) plot outlining the relationship between predicted changes in total atheroma volume (TAV) from baseline versus average on-treatment LDL-C levels stratified according to sex. The average on-treatment LDL-C values on the x-axis reflect the first to 99th percentile LDL-C values in the SATURN (Study of Coronary Atheroma by Intravascular Ultrasound: Effect of Rosuvastatin Versus Atorvastatin) study; **blue** represents men, **pink** represents women. The **dotted green line** represents an on-treatment LDL-C value of 70 mg/dl. For on-treatment LDL-C <70 mg/dl, the least squares mean (LSM) changes in TAV for women versus men are  $-10.1 \pm 1.13 \text{ mm}^3$  vs.  $-7.16 \pm 0.65 \text{ mm}^3$  ( $p = 0.023$ ). For on-treatment LDL-C  $\geq 70 \text{ mg/dl}$ , the LSM changes in PAV for women versus men are  $-5.26 \pm 1.43 \text{ mm}^3$  versus  $-5.55 \pm 0.89 \text{ mm}^3$  ( $p = 0.87$ ).

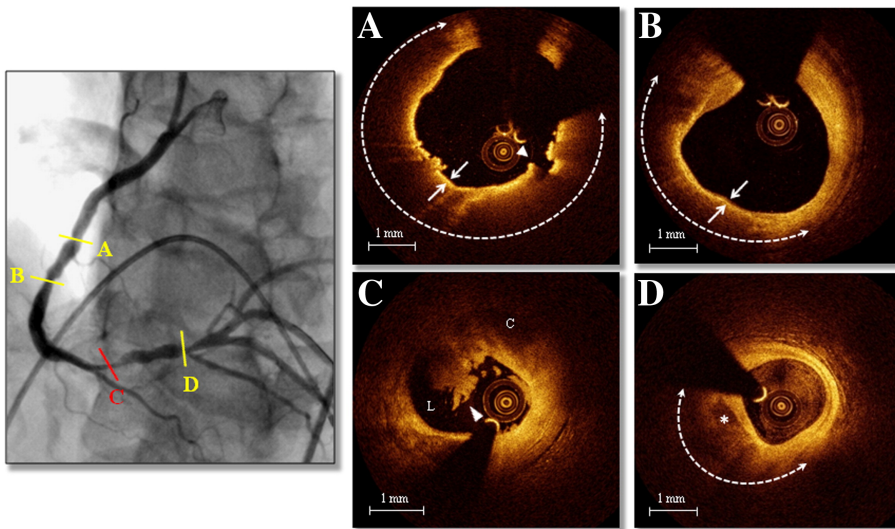
(Adapted from Puri R et al, JACC Cardiovasc Imaging. 2014;7(10):1013-22.)

Fig 5



Mean coronary artery calcium score by age for five ethnic groups by sex, the MASALA and MESA studies (Adapted from Kanaya AM et al, Atherosclerosis. 2014;234(1):102-7.)

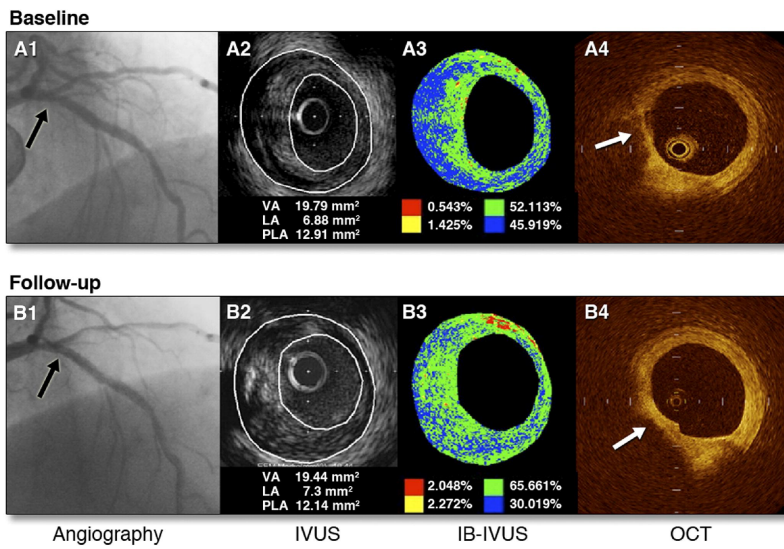
Fig 6



**A**, Nonculprit lesion showing TCFA (large lipid arc [dashed line] and fibrous cap  $<65 \mu\text{m}$  [arrows]) with disruption of the fibrous cap (arrowhead). **B**, Nonculprit plaque showing TCFA (large lipid arc [dashed line] and fibrous cap  $<65 \mu\text{m}$  [arrows]). **C**, Culprit lesion with plaque rupture: massive thrombus (arrowhead) overlying a ruptured plaque (C, cavity; L, lumen). **D**, Nonculprit lesion showing lipid-rich plaque with spotty calcification (asterisk) inside the lipid core (dashed line).

(Adapted from Vergalo R et al *Am Heart J.* 2014;167(1):59-67).

Fig 7



Images of Coronary Angiographic, Grayscale IVUS, IB-IVUS, and OCT at baseline and follow up after statin therapy. (Adapted from Hattori K et al, JACC Cardiovasc Imaging. 2012;5(2):169-77.)

## Chapter 2: Cardiac CT: atherosclerosis to acute coronary syndrome

Ravi Kiran Munnur<sup>1</sup>, James D Cameron<sup>1</sup>, Brian S Ko<sup>1</sup>, Ian T Meredith<sup>1</sup>, Dennis T Wong<sup>1</sup>

*1 Monash Cardiovascular Research Centre, Department of Medicine (Monash Medical Centre) Monash University and Monash Heart, Monash Health, 246 Clayton Road, Clayton, 3168 VIC, Australia*

**Accepted and Published: Cardiovasc Diagn Ther. 2014 Dec;4 (6):430-48.**

### Institution

Monash Heart, Monash Medical Centre

[REDACTED]

### Correspondence

Dr. Dennis Wong

[REDACTED]

[REDACTED]

Address: MonashHeart, Monash Medical Centre

[REDACTED]

**Abstract:** Cardiac computed tomographic angiography (CCTA) is a robust non-invasive method to assess coronary artery disease (CAD). Qualitative and quantitative assessment of atherosclerotic coronary stenosis with CCTA has been favourably compared with invasive coronary angiography (ICA) and intravascular ultrasound (IVUS). Importantly, it allows the study of preclinical stages of atherosclerotic disease, may help improve risk stratification and monitor the progressive course of the disease. The diagnostic accuracy of CCTA in the assessment of coronary artery bypass grafts (CABG) is excellent and the constantly improving technology is making the evaluation of stents feasible. Novel techniques are being developed to assess the functional significance of coronary stenosis. The excellent negative predictive value of CCTA in ruling out disease enables early and

safe discharge of patients with suspected acute coronary syndromes in the emergency department. In addition, CCTA is useful in predicting clinical outcomes based on the extent of coronary atherosclerosis and also based on individual plaque characteristics such as low attenuation plaque, positive remodelling and spotty calcification. In this article, we review the role of CCTA in the detection of coronary atherosclerosis in native vessels, stented vessels, calcified arteries and grafts; the assessment of plaque progression, evaluation of chest pain in the emergency department, assessment of functional significance of stenosis and the prognostic significance of CCTA.

#### Key Words

CCTA = Computed Coronary Tomographic Angiography

ACS = Acute coronary Syndrome

CAD = Coronary Artery Disease

Vulnerable plaques

Atherosclerosis

#### **Introduction**

Coronary artery disease (CAD) is the leading cause of morbidity and mortality worldwide and makes up for more than half of all cardiovascular events in men and women < 75 years of age in United States (1). Atherosclerosis is a chronic disease characterised by plaque formation inside the arteries as a result of complex interaction between lipoproteins, endothelium and inflammatory cells. All the cardiovascular risk factors contribute to the pathogenesis by aggravating the underlying inflammation (2). The development and progression of atherosclerosis is likely determined, in part, by other still unidentified risk factors and genetic host susceptibility. It initially begins as fatty streak and grows over many years to become advanced atherosclerotic plaque. In majority of men and women with coronary atherosclerosis, the initial presentation is with acute myocardial infarction or sudden cardiac death and two thirds of acute coronary syndromes (ACS) are due to disruption of atherosclerotic plaque. The features of ruptured plaques on histopathology include large plaque volumes and large necrotic cores that are covered by thin fibrous cap (<65µm), and typically infiltrated with monocytes and macrophages (3). Plaques vulnerable to rupture are termed thin cap fibroatheroma (TCFA) which share similar histopathological characteristics as

ruptured plaques except that the fibrous caps are still intact. The term “vulnerable plaque” has therefore been used to describe rupture prone plaques before an event occurs (4). Studies of disrupted plaques with invasive intravascular imaging such as intravascular ultrasound (IVUS) have identified imaging characteristics of plaque vulnerability. These features include positive remodelling, large lipid core and spotty calcification (5, 6). Intravascular techniques are however limited by high cost and invasive nature of the test. It is therefore desirable to have a non-invasive imaging technique which can assess plaque burden and detect vulnerable plaque. Coronary computed tomographic angiography (CCTA) has established itself as a non-invasive modality with high sensitivity and high negative predictive value for detecting coronary artery stenosis (7). In addition, CCTA permits the assessment of coronary atherosclerotic plaque morphology and composition in good agreement with IVUS (8).

### **Coronary Plaque Imaging of Atherosclerotic Plaques by CCTA**

CCTA is performed on multidetector CT (MDCT) systems after the injection of iodine contrast media for opacification of lumen. Current generation scanners range from 64-320 detector rows with spatial resolution of approximately 230 to 625 $\mu$ m and temporal resolution of approximately 75 to 175ms. The spatial resolution of latest generation CT scanners is marginally lower than the 100 $\mu$ m and 200 $\mu$ m afforded by IVUS and invasive coronary angiography (ICA) respectively. The improved temporal resolution of new generation scanners permit scan acquisition for patients with atrial fibrillation and higher heart rates with preserved image quality. Plaques are identified on CCTA as any discernible structure outside the lumen that is either calcified or has attenuation value less than the lumen. They are usually classified into 3 categories: non-calcified, mixed or calcified.

### **Qualitative assessment of Coronary Plaque and Stenosis Assessment - Comparison with Invasive Coronary Angiography**

Invasive coronary angiography (ICA) is established in the assessment of coronary arteries and in the measurement of severity of luminal stenosis. There are several studies that have compared the diagnostic accuracy of CCTA to ICA, based on visual assessment using a binary approach in classifying lumen stenosis as  $< 50$  or  $\geq 50\%$ . 64 detector CCTA identified significant coronary artery stenosis with a sensitivity of 85-99%, specificity of 64–90% and a negative predictive value of 83–99% when compared to ICA in three large multicentre studies (9-11). These patients had low to intermediate risk of CAD. In a meta-analysis comprising 7,516 patients with suspected and known CAD in 89 studies, the per-patient sensitivity and specificity for  $>16$  slice CCTA was 98% and 89%, respectively (12). Furthermore, there was excellent interobserver and intraobserver agreement for stenosis ratings in high quality images (13, 14). These studies demonstrate that among all other non-invasive imaging modalities, CCTA most closely resembles ICA in terms of providing coronary assessment. Accordingly current European and US guidelines advocate the use of CT in patients with low to intermediate risk of CAD with a Class IIa and Class IIb indication (15, 16). In addition, since 2010, the ACC/ AHA appropriate use criterion has recommended that it is appropriate to use CCTA as an upfront investigation in this population (17).

## **Quantitative assessment of atherosclerotic plaques**

### **Comparison with IVUS**

CCTA provides vessel lumen geometry and volumetric assessment of plaque which had previously been obtained only on IVUS. Geometric parameters including minimal lumen area, minimal luminal diameter, diameter stenosis and area stenosis can be quantified using dedicated computed software (Fig 1). Furthermore, the total volume of plaque in a coronary segment, defined as the volume between the vessel lumen and outer wall, can be determined using a semi-automated method based on software detection of the lumen and outer vessel walls (Fig 1). Plaque area or burden, defined as  $(\text{vessel area} - \text{lumen area}) / \text{vessel area}$ , can be quantified and volume of calcified and non-calcified plaque based on relative CT densities can also be derived.

In a recent meta-analysis by Voros et al. (18), including a cohort of 946 patients from 33 studies that compared the accuracy of 64-detector CCTA to IVUS (18), CCTA was demonstrated to have an excellent sensitivity (94%) and specificity (92%) to qualitatively detect atherosclerotic plaque (Fig. 2). Compared to IVUS, CCTA was found to slightly overestimate luminal area ( $0.46\text{mm}^2$  or by 6.7%;  $p = 0.005$ ), while there was no significant differences in plaque area ( $0.09\text{mm}^2$ ;  $p = 0.88$ ), volume ( $5.3\text{mm}^3$ ;  $p = 0.21$ ) and percent area stenosis ( $-1.81\%$ ;  $p = 0.12$ ) (Fig. 3). In addition, two separate studies showed that CCTA underestimated plaque volume in non-calcified plaques and overestimated plaque volume in mixed / calcified plaque (19, 20). The overestimation in calcified plaque is typically related to blooming artefact.

Albeit the high diagnostic accuracy of CCTA to qualitatively assess plaque, its accuracy and reproducibility to quantify plaque is important, as this may determine the potential use of CCTA to non-invasively monitor plaque progression. Two studies have demonstrated that the mean difference in quantifying minimal luminal diameter and minimal luminal area between two experienced observers was small (13, 21). There was excellent interobserver correlation for quantification of plaque volume with  $r$  values ranging between 0.83 and 0.99, although the limits of agreement were wide ranging from 87 to 226% (22). High quality images were used in these studies and were found to significantly improve reproducibility. The reported mean interobserver difference in calcified and non-calcified plaque volume was  $-0.74\%$  and  $-0.76\%$  with corresponding limits of agreement of  $\pm 23.5\%$  and  $\pm 11.5\%$ , respectively in high quality coronary CCTA datasets (13). Otzuka and colleagues demonstrated that interobserver and intraobserver reproducibility was optimised by exclusion of images with heavy calcification and image blurring (23).

### **Assessment of Coronary Arteries with High Calcium Score**

The “Achilles heel” of cardiac CT is calcification, which hampers diagnostic accuracy by causing blooming artefact (Fig 4). As a result, the specificity of CCTA in calcified vessels is significantly

reduced. Recent studies have shown that a higher coronary artery calcium score (CACS  $\geq 400$  or  $\geq 600$ ) resulted in reduction in specificity by 35 to 48% (24, 25). Therefore, current guidelines do not recommend CCTA for patients with very high CACS. These patients should instead undergo a functional assessment or ICA based on their pre-test probability of CAD. Subtraction algorithms have been developed to be applied on CT images acquired using dual energy CT scanners which may remove calcium and improve the evaluation of coronary artery segments with heavy calcification (26, 27). Clinical studies examining the utility of this technique to assess CAD are currently underway.

### **Assessment of Coronary Artery Bypass Grafts**

CCTA is also used to assess coronary bypass grafts with the accuracy being higher in grafts than in native vessels. This superior diagnostic accuracy may be due to larger vessel diameter of the grafts, lower propensity to develop calcified plaque and due to lower motion artefacts in the grafts (Fig 5) (28-30). In addition, grafts that cannot be detected or accessed by ICA can be visualised with CCTA. 32 detector CCTA was used in a study to evaluate 52 patients with a mean follow up period of 9.6 $\pm$ 7.2 years following CABG surgery (31). The diagnostic accuracy of CCTA for the detection or exclusion of significant stenosis in arterial and venous grafts on per segment analysis was 100%. The sensitivity and specificity were lower in the distal runoffs and in the native vessels. In a meta-analysis by Hamon et al. (32), the diagnostic accuracy of assessing grafts by 16 and 64 slice CCTA was exceptionally high (sensitivity, 97.6%; specificity, 96.7%; and NPV, 98.9%).

### **Assessment of In-stent Restenosis**

The evaluation of stents by CCTA is more challenging than that of native coronary arteries (33). This is predominantly attributable to beam hardening and partial volume artefact from stent struts. It has been demonstrated that a difference in CT density in Hounsfield units (HU) of  $\leq 19\%$  between a reference vessel (aorta) and inside the lumen of a stent, along with a mean CT density of  $\geq 300$

inside a stent correlated with a patent stent with high sensitivity and specificity (34). According to a meta-analysis, the diagnostic accuracy of 64 slice CCTA for stents was 90%, with sensitivity of 89.7%, specificity of 92.2%, positive predictive value (PPV) of 72.5%, and NPV of 97.4%. When non-assessable segments were included, the sensitivity and specificity significantly decreased to 79% and 81% respectively (35). The diagnostic accuracy is also influenced by the diameter of the stent. Overall, diagnostic accuracy is significantly higher in stents with diameter  $\geq 3$ mm (Fig 6) (35-38). When CCTA was used to evaluate in-stent restenosis using IVUS as reference standard, it was demonstrated that the sensitivity, specificity, PPV, NPV, and accuracy were 67%, 78%, 57%, 85%, and 75%, respectively, for stents  $< 3.0$ mm in diameter; whereas for stents  $\geq 3.0$ mm in diameter, the sensitivity, specificity, PPV, NPV, and accuracy were 89%, 100%, 100%, 97%, and 98%, respectively (39). Moreover, the diagnostic performance of CCTA has been found to be superior in stents with thinner struts ( $< 100\mu\text{m}$ ) compared to stents with thicker struts (40, 41). Due to these limitations, use of CCTA for evaluation of in-stent restenosis is not considered for routine clinical use, except for the assessment of unprotected left main stent (42). High definition cardiac tomography (HDCT) equipped with superior spatial resolution of 0.23mm compared to 0.625mm offered by standard CCTA, may improve the accuracy of CCTA in assessing stents. HDCT improved coronary stent visualisation with an increase in luminal stent diameter from 42.3% to 54.1% and area visualisation from 25.8 to 54% when compared to standard CCTA in an ex vivo phantom model (43). In a comparison study of HDCT vs. standard definition CCTA, 25 stents were assessed in 14 patients who were examined by both the scanners on the same day. Partial volume effects were significantly reduced by HDCT resulting in an increase in percentage of stents with no or only minor artefacts, from 44% to 96% (44).

### **Assessment of Plaque progression**

While invasive imaging modalities such as IVUS and OCT have been used to evaluate the efficacy of various anti-atherosclerotic therapies on plaque progression, a non-invasive test would be more

assessable and safe. CCTA has been touted as the non-invasive imaging modality to study the surrogate end points for cardiovascular outcomes, such as plaque progression. Several studies have explored this potential. Zeb et al. (45) studied the effect of statin on plaque progression in 100 patients using CCTA with a mean follow up of  $406 \pm 92$  days. Total plaque progression was significantly reduced among subjects on statin compared to those who were not ( $-33.3\text{mm}^3 \pm 90.5$  vs.  $31.0\text{mm}^3 \pm 84.5$ ,  $p = 0.0006$ ). Statin use was associated with reduced progression of non-calcified plaque (NCP) volume ( $-47.7\text{mm}^3 \pm 71.9$  vs.  $13.8\text{mm}^3 \pm 76.6$ ,  $p < 0.001$ ) and low attenuation plaque (LAP) volume ( $-12.2\text{mm}^3 \pm 19.2$  vs.  $5.9\text{mm}^3 \pm 23.1$ ,  $p < 0.0001$ ) as quantified on CT. Similar reduction in total plaque volumes and LAP volumes were demonstrated in two other studies in patients on statin therapy. These changes were more pronounced in non-calcified and in mixed plaque (46, 47). Although these studies highlight the potential use of CCTA to monitor plaque progression/regression, studies comparing CCTA to IVUS in the longitudinal assessment of plaque progression are scarce.

### **Assessment of the Hemodynamic Significance of Coronary Atherosclerosis**

Although CCTA accurately assesses coronary plaque and stenosis, it is limited in evaluating the hemodynamic significance of coronary stenosis. As functional significance of coronary stenosis determines prognosis and the need for revascularisation, it is of relevance in the management of patients with stable CAD (55-57). Recently, three novel techniques have been demonstrated to accurately detect vessel-specific ischemia using the gold standard invasive fractional flow reserve (FFR) as a reference (48-50). They are 1) Non-invasive FFR (CT FFR) 2) Transluminal attenuation gradient (TAG) and 3) CT perfusion imaging (CTP). These techniques may broaden the use of CCTA to assess coronary ischemia in addition to anatomy (51-53).

### **CT FFR**

Non-invasive FFR or CT FFR is derived by applying computational fluid dynamics. Using a supercomputer, three dimensional models throughout the cardiac cycle representing the pressure and flow along all points of the arteries are generated during rest and simulated maximal hyperaemic conditions. Blood viscosity is assumed to be constant and CT features that affect coronary flow are taken into consideration. Currently, the technique requires 5 hours of processing time and a non-invasive FFR is derived based on approximated pressure measurements (54, 55). In a multicentre, prospective cohort of 159 vessels in 103 patients, Koo et al. demonstrated that CT FFR, using a threshold of  $\leq 0.8$ , detected FFR-significant ( $\leq 0.8$ ) stenoses with a sensitivity of 84% and specificity of 82% (56). Overall, there was a good correlation between CT FFR and FFR ( $r = 0.72$ ,  $p < 0.001$ ) and the area under the ROC curve (AUC) was 0.90, which was significantly higher than CCTA alone (0.70,  $p < 0.0001$ ). A similar improvement in ROC curve was reported when the study was repeated in a larger multicentre prospective cohort of 285 patients. (57). In a recent prospective multicentre study (the NXT trial), diagnostic accuracy, sensitivity and specificity for CT FFR were 81%, 86% and 79% respectively. Again, there was an improvement in ROC curve (CCTA AUC = 0.8 vs. FFR CT AUC = 0.90,  $p = 0.0008$ ) (58).

## **TAG**

TAG is defined as the linear regression coefficient between intraluminal attenuation (HU) and axial distance. TAG evaluates the slope of decline in intraluminal contrast attenuation from the ostium to the distal coronary vessel (Fig. 7). Choi et al. demonstrated that in a cohort of 127 patients (370 vessels) with multivessel disease, TAG performed on resting CCTA was significantly lower in occluded vessels compared to those with lesions of 0 – 49% stenosis on quantitative coronary angiography (QCA) ( $-13.46 \pm 9.59\text{HU} / 10\text{mm}$  vs.  $-2.37 \pm 4.67\text{HU} / 10\text{mm}$ ,  $p < 0.001$ ) (59). The addition of TAG to the interpretation of CCTA improved diagnostic accuracy for anatomical stenosis severity ( $p = 0.001$ ), especially in vessels with calcified lesions and provided a net reclassification improvement of 0.095 (59). As the 320 detector row scanner allows isophasic,

single beat imaging of the entire coronary tree, it was postulated that it would be the ideal platform for TAG assessment. The accuracy and incremental value of TAG on a 320-detector row scanner has been evaluated by Wong et al. in a cohort of 53 stable CAD patients. TAG assessed in FFR-significant vessels was significantly lower than that found in FFR non-significant vessels ( $-21$  vs.  $-11$  HU / 10mm,  $p < 0.001$ ) (50). Using a retrospectively determined TAG320 cut-off of  $-15.1$  HU / 10mm, TAG320 was reported to predict  $FFR \leq 0.8$  with 77% sensitivity and 74% specificity. Importantly, the AUC for the combined use of TAG320 and CCTA was 0.88.

### **CT Stress Myocardial Perfusion Imaging**

Myocardial perfusion imaging on CCTA is the acquisition of images during the first pass of iodinated contrast from the arteries into the myocardium where hypo perfusion is represented by hypo-attenuated areas (Fig 8). CTP has been evaluated in numerous single centre studies to date. The sensitivity ranges from 71 to 100% and specificity from 72 to 98% depending on the scanner type and the studied population when compared with single-photon emission computed tomography - myocardial perfusion imaging (SPECT-MPI), invasive FFR and magnetic resonance imaging (MRI) perfusion imaging. In a study by George et al., CTP had a sensitivity of 81% and a specificity of 85% when compared with SPECT-MPI (60). More recently, in the Core320 study, which is a multicentre study with a cohort of 381 patients, the combined protocol of CCTA and CTP was compared to SPECT-MPI. The sensitivity and specificity for the combined protocol was 80% and 74% respectively (61). Four studies thus far have compared CTP with FFR, all demonstrating that the use of CTP provided incremental diagnostic accuracy when added to CCTA alone, by increasing the specificity and positive predictive value for FFR-significant stenoses (48, 49, 62, 63). Ko et al. (62) demonstrated using a 320-detector CT, in a prospective cohort of 40 patients including 120 vessels with suspected CAD, that CCTA detected FFR-significant stenoses ( $\leq 0.8$ ) with 95% sensitivity and 78% specificity (62). The additional use of CTP increased the per-vessel specificity to 95% while sensitivity was maintained at 87%. The combined use of CCTA and

CTP was associated with an increase in the ROC AUC from 0.93 vs. 0.85 using CCTA alone ( $p = 0.0003$ ). In a study by Bettencourt et al., improved diagnostic accuracy was noted for FFR  $<0.8$ , from 78% using 64 detector CCTA alone, to 85% with combined protocol, which was non inferior to the accuracy of MR perfusion imaging of 88%.

### **Prediction of Clinical Outcomes Using Cardiac CT**

A number of studies have demonstrated that the presence and burden of calcified plaque as represented by the CACS is associated with an increased risk of future adverse cardiovascular events (64-66). A direct relationship was observed between plaque burden and the rate of plaque progression to cardiovascular outcomes in a study that used IVUS to assess coronary atherosclerotic burden (67). Similarly, plaque burden assessed by CCTA predicts prognosis. In addition, the location of the lesions, number of vessels with lesions and, the presence of normal, non-obstructive and obstructive vessels determine prognosis..

CCTA meets three fundamental criteria as a good prognostic test: (1) it identifies patients at very low risk for events (2) it provides definition of clear gradations of risk based on test results and (3) it enables the concentration of resources in management of patients with abnormal tests (68).

**Presence of Obstructive Disease predicts prognosis:** In a single-centre consecutive cohort of 1,127 symptomatic patients, Min et al. demonstrated that all-cause mortality was predicted by a number of angiographic features as assessed on CCTA. This included the presence of moderate ( $\geq 50\%$ ) or severe ( $\geq 70\%$ ) coronary stenosis in any coronary artery ( $p = 0.007$  and  $p < 0.001$ , respectively) (Fig. 9), the presence of a severe stenosis in any proximal segment of a major epicardial vessel ( $p = 0.001$ ) and the presence of obstructive left main or left anterior descending artery stenosis ( $p = 0.001$ ). It was also demonstrated that CCTA-derived Duke prognostic CAD index, clinical coronary artery plaque score including a segment stenosis score and segment involvement score, were significant predictors of all-cause mortality ( $p < 0.001$ ) (69).

In a pooled analysis of 18 CCTA prognostic studies involving 9,592 symptomatic patients with predominantly suspected CAD (70), Hulten et al. (Fig 10) analysed the annual event rates for major cardiac events and death. The event rates in obstructive coronary disease defined as the presence of any lesion with  $\geq 50$  % stenosis was 8.8 and 3.2 % which was significantly higher ( $p < 0.005$ ) than patients with non-obstructive disease (1.4 and 0.74 %) and normal coronary arteries on CCTA (0.17 and 0.15 %), respectively.

In the CONFIRM Registry, a large international multicentre registry which included 24, 775 patients at a mean follow up of 2.3 years, it was demonstrated that the presence of obstructive disease on CCTA not only risk stratified patients into clinically important risk tertiles (71), but was also a significant predictor of all-cause mortality and provided significant incremental value to LVEF and clinical variables with a net reclassification index of 17.8 % ( $p < 0.001$ ) (72). Furthermore, using data from the same registry, Hadamitzky described the novel use of an optimised score which accounted for the number of proximal segments with a stenosis  $> 50$  % or with mixed or calcified plaque (73). The use of this CCTA-based scoring system was demonstrated to significantly improve overall risk prediction beyond the National Cholesterol Education Program Expert Panel on Detection, Evaluation and Treatment of High Blood Cholesterol in Adults (ATP III) score (73).

**Presence of Non-obstructive Disease predicts prognosis:** Lin et al. (74) demonstrated that the presence of non-obstructive coronary artery stenosis ( $< 50\%$ ) on CCTA was associated with higher mortality (hazard ratio (HR) 1.98,  $p = 0.03$ ) when compared with normal findings. The highest risk was among those who had non-obstructive CAD in three epicardial vessels (HR 4.75,  $p = 0.0002$ ) and  $\geq 5$  coronary segments (HR 5.12,  $p = 0.0002$ ) in a cohort of 2,583 symptomatic patients with mean follow up of 3.1 years. Importantly the higher mortality for non-obstructive disease was

observed even in patients with low 10-year Framingham risk (3.4%,  $p < 0.0001$ ), as well as those with no traditional, medically treatable cardiovascular risk factors including diabetes mellitus, hypertension and dyslipidemia (5.7%,  $p < 0.0001$ ).

**Presence of normal findings predicts prognosis:** Lastly, normal findings on CCTA were found to be associated with very low event rates (69-72). This is comparable to the background event rate among healthy low-risk individuals (<1%) (75) and is similar to that reported in patients with normal stress testing evaluated on echocardiography or nuclear myocardial perfusion imaging (76).

**CT Plaque Quantification predicts prognosis:** Verheylen et al. demonstrated that the use of a semi-automated plaque quantification algorithm may provide additional prognostic value in prediction of future ACS beyond conventional CT assessment of stenosis alone and Framingham risk scores (77). At a mean  $26 \pm 10$  months, patients with ACS were found to have higher total plaque volume (94 vs. 29 mm<sup>3</sup>,  $p < 0.001$ ), non-calcified plaque volume (28 vs. 4 mm<sup>3</sup>,  $p < 0.001$ ) and plaque burden (57% vs. 36%,  $p < 0.01$ ).

## **CCTA - Acute Coronary Syndrome**

### **Predicting Acute Coronary Syndrome**

There is growing evidence to suggest that the susceptibility of an individual to develop an acute coronary event is determined by plaque morphology rather than the extent of luminal stenosis. In the COURAGE study (78) where patients who received optimal medical management, the consistent predictor of death, myocardial infarction and non-ST segment elevation ACS was the anatomic burden and not the ischemic burden. The occurrence of major adverse clinical outcomes may be because of the disruption rather than by the ischemia-producing nature of obstructive plaques. In this context, the prognostic significance of CCTA assumes importance as it has the

advantage of being a non invasive test that can be used to assess individual plaque characteristics apart from the assessment of luminal stenosis.

### **CT Plaque Characteristics Predict Future ACS**

Two-thirds of ACS is caused by atherosclerotic plaque rupture. A number of CT-based coronary plaque characteristics of a “vulnerable plaque” associated with culprit lesions for future ACS have been identified in retrospective observational studies (Fig. 11).

#### *CCTA features of LAP, positive remodelling and spotty calcification predict ACS*

Motoyama et al. compared CCTA features of 38 patients with ACS to 33 patients with stable angina (79). Plaques in ACS group had higher frequency of non-calcified plaque NCP <30HU (79% vs. 9%,  $p < 0.0001$ ), spotty calcification (63% vs. 21%,  $p = 0.0005$ ) and positive remodelling (87% vs. 12%,  $p < 0.0001$ ). Presence of all 3 features showed a high positive predictive value, and their absence demonstrated a high negative predictive value for future ACS. Furthermore, mean plaque volumes were higher in ACS group  $192.8 \pm 114.9 \text{mm}^3$  vs.  $103.8 \pm 51.8 \text{mm}^3$  ( $p=0.001$ ) (80). It has been shown in pathological studies, that the size of necrotic core in TCFA ranges from 1.6 to 1.7mm<sup>2</sup> with a length of 8mm (range, 2–17mm), and in ruptured plaques ranges from 2.2 to 3.8mm<sup>2</sup> with a length of 9mm (range, 2.5–22mm) (81, 82). Imazeki and colleagues demonstrated that remodelling detected on CCTA correlated with IVUS and Remodelling Index (RI) was significantly larger in patients with ACS ( $1.19 \pm 0.18$ ) than in those with stable angina ( $0.89 \pm 0.10$ ,  $p < 0.0001$ ) (83, 84). Pathological studies have established a relationship between positive vessel remodelling and plaque vulnerability, showing an increase in inflammatory marker concentrations, larger lipid cores, paucity of smooth muscle cells, and medial thinning in positively remodelled vessels (84). In a large prospective study with a cohort of 1,059 patients, Motoyama et al. demonstrated that the CT angiographic features of LAP and positive remodelling were associated with subsequent development of acute coronary events (85). ACS developed in 10 (22%) of 45

patients who had these two CT features against 4 (0.5%) in 820 patients who did not have LAP or positive remodelling. None of the 167 patients with normal CCTA sustained acute events ( $p < 0.001$ ). Both features were independent predictors of acute coronary events (hazard ratio = 23, 95% confidence interval 7–75,  $p < 0.001$ ). Importantly, the plaques associated with early ACS when compared with late ACS had larger LAP volume.

*CCTA features of Napkin ring sign, plaque ulceration and intraplaque dye penetration predict ACS*

Vulnerable or rupture prone atherosclerotic plaques have histologically been described as thin-cap fibroatheroma (TCFA), distinguished by a large necrotic core with an overlying thin intact fibrous cap, macrophage infiltration and often increased number of intraplaque vasa vasorum (81). Pathological studies have demonstrated the thickness of the fibrous cap thickness is the most important plaque characteristic to identify plaque vulnerability, followed by the magnitude of macrophage inflammation and the size of necrotic core (86). Kashiwagi and colleagues proposed that the presence of *a ring-like attenuation* in a CT angiographic cross section may be a surrogate marker of TCFA after comparing optical coherence tomography (OCT) and CCTA findings (87). In a total of 100 patients with ACS, coronary lesions were divided into TCFA and non-TCFA group based on OCT findings. CCTA-verified positive remodelling was observed more frequently in the TCFA (75%) than in the non-TCFA group (30 %,  $p < 0.001$ ). The TCFA group also demonstrated LAP more frequently; CT attenuation value in the TCFA group ( $35 \pm 32$  HU) was significantly lower than the non-TCFA group ( $62 \pm 34$  HU,  $p < 0.001$ ). Notably a ring-like attenuation in the TCFA group was found to be 11-fold more frequent than in the non-TCFA group (44% vs. 4%,  $p < 0.001$ ). The sensitivity, specificity, positive predictive value, and negative predictive value of ring-like enhancement for detecting TCFA are 44%, 96%, 79%, and 85%, respectively (41). In another study by Tanaka and colleagues, 67 patients with de novo angina were divided into a plaque rupture group ( $n=27$ ) and a non-rupture group ( $n=40$ ) based on the IVUS. The 64-slice CCTA revealed that the prevalence of an ulcer-like enhancement space (37% vs. 5%,  $p < 0.01$ ), a ring-like sign (41% vs.

18%,  $p=0.04$ ), in the plaque rupture group was higher than those in the non-rupture group (88). It is postulated that the ring like enhancement represents highly active vasa vasorum neovascularisation. Vasa vasorum density is seen as surrogate marker of plaque vulnerability as it strongly correlated with macrophage infiltration in atherosclerotic plaque (89). In addition, it has also been postulated that the ring-like enhancement may be due to large central lipid core surrounded by fibrous plaque tissue or intra mural thrombus (90).

Lastly, CT feature of plaque disruption including plaque ulceration and intraplaque dye penetration in patients with unstable angina, have been described to be modestly sensitive (53–81%) and highly specific (82–95%) for plaque erosion and / or intraplaque haemorrhage as demonstrated on invasive angiography. Madder, R.D et al. demonstrated that in 294 plaques with  $>25\%$  stenosis on CCTA, 37% had features of disruption, including 27% with intraplaque dye penetration and 18% with ulceration. In addition, when compared with non-disrupted lesions, they were more voluminous ( $313\pm 356 \text{ mm}^3$  versus  $18\pm 93 \text{ mm}^3$   $p<0.0001$ ) and were more often complex by ICA (57.8% versus 8.1%,  $p<0.0001$ ) (91).

### **Use of CCTA in the assessment of acute chest pain in Emergency Departments**

Acute chest pain is one of the leading symptoms in emergency departments all over the world. Exclusion of ACS is difficult when patients with typical chest pain have normal initial ECG and biomarkers (92). The standard evaluation of these patients includes hospital admission to undergo serial ECG's, troponin assessment with or without additional stress testing and only a minority of such patients are eventually diagnosed with cardiac ischemia (93). Despite this expensive and comprehensive approach, 2 to 5 % of ACS is still missed (94). The high sensitivity and negative predictive value of CCTA for the detection of coronary stenosis allows safe rule-out of CAD, especially in population with low to intermediate risk.

## **Use of CCTA in ED**

CCTA has been studied in comparison with invasive coronary angiography for detection of ACS in several observational cohort studies. The Rule Out Myocardial Infarction / Ischemia Using Computer Assisted Tomography (ROMICAT) study, found that CCTA had excellent sensitivity and negative predictive value to rule out ACS in 368 subjects with inconclusive clinical evaluation of chest pain in ED (95). Hollander et al (96) demonstrated that 84% of 568 patients with potential ACS and low Thrombolysis In Myocardial Infarction (TIMI) risk score, were discharged after CCTA. Compared to standard evaluation, when CCTA was included in triaging patients who presented with chest pain to ED, there was a reduction in the length of stay in hospital and increased discharge rates from ED without hospitalisation (97, 98). These studies demonstrate that CCTA is an efficient and safe tool to assess patients with chest pain, particularly those with low to intermediate likelihood of CAD. In a meta-analysis of 64-detector CCTA, which included 1559 patients presenting with chest pain, CCTA had a 99.3% negative predictive value in excluding major adverse cardiac events (MACE) for 30 days after initial symptom presentation in 85.2% of the study population (99). The ROMICAT and CT-STAT studies showed that the absence of significant coronary atherosclerosis is associated with the absence or a minimum number of MACE at 6 months of follow-up (95, 100). Nasis et al followed up 506 patients without plaque, patients with nonobstructive plaque and at most mild to moderate stenosis (<40% luminal narrowing). These patients were discharged from ED without further investigation and some of them, after a single troponin measurement. At median 47.4 month follow-up there were no major adverse events (0% for all; 95% CI: 0%, 0.7%) (101).

## **Better risk stratification**

Among low to intermediate risk patients who presented with chest pain to the ED, CCTA was found to be a better predictor of CAD and cardiovascular outcomes than the use of TIMI score, global registry of acute coronary events (GRACE) score and risk assessment by traditional risk factors. In

a study involving 250 patients evaluated by CCTA, correlation with CAD was poor for the TIMI ( $r = 0.12$ ) and GRACE ( $r = 0.09-0.23$ ) scores. Only older age and male sex were significant independent predictors of CAD while CCTA identified severe CAD in all subjects with adverse outcomes (102). In another study involving 93 patients, CCTA accurately identified ten patients (8.13%) with obstructive CAD requiring myocardial revascularization; all had a low TIMI score (0-2) and eight had a low GRACE score (103). Similarly, Linde et al evaluated the clinical impact of CCTA on 600 patients who were randomised to a CCTA-guided strategy (299 patients) or standard care (301 patients). Referral rate for ICA was 17% with CCTA vs. 12% with standard care ( $p=0.1$ ). ICA confirmed significant coronary artery stenoses in 12% vs. 4% ( $p=0.001$ ), and 10% vs. 4% were subsequently revascularised ( $p=0.005$ ). The positive predictive value for the detection of significant stenoses was 71% with CCTA vs. 36% with standard care ( $p=0.001$ ) (104).

### **Costs and resource utilization**

Poon et al demonstrated that the routine use of CCTA in ED evaluation of chest pain may reduce healthcare resource utilization. The overall admission rate was lower with CCTA (14% vs. 40%;  $p < 0.001$ ). Standard evaluation was associated with a 5.5-fold greater risk for admission (odds ratio [OR]: 5.53;  $p < 0.001$ ), 1.6 times longer expected ED length of stay (OR: 1.55;  $p < 0.001$ ), 5 times greater likelihood of returning to ED with chest pain within 30 days (OR: 5.06;  $p = 0.022$ ) and a 7-fold greater likelihood of invasive coronary angiography without revascularization (OR: 7.17;  $p < 0.001$ ). There were no differences in the rates of death and acute myocardial infarction within 30 days of the index visit between the two groups (105). CCTA was found to be cost-effective compared to myocardial perfusion imaging (106). In a comprehensive cost-effectiveness model by Ladapo et al. (107), the increased overall cost of CCTA due to detection of CAD was partially offset by reduction of event rates by 3% and by lower costs of care for myocardial infarction and stroke.

## **CONCLUSION**

Coronary CT angiography provides robust non-invasive, qualitative and quantitative assessment of coronary atherosclerosis with high reproducibility and accuracy. The constant advances in scanner technology; image acquisition and reconstruction techniques have expanded the use of CCTA. In addition to the anatomical information, it is now possible to assess the hemodynamic significance of atherosclerotic plaque and to predict clinical outcomes based on plaque burden and plaque morphology.

## **Disclosures**

We have no disclosures to make.

## **References**

1. Go AS, Mozaffarian D, Roger VL, et al. Executive summary: heart disease and stroke statistics--2013 update: a report from the American Heart Association. *Circulation* 2013;127:143-52.
2. Mallika V, Goswami B, Rajappa M. Atherosclerosis pathophysiology and the role of novel risk factors: a clinicobiochemical perspective. *Angiology* 2007;58:513-22.
3. Narula J, Finn AV, Demaria AN. Picking plaques that pop. *J Am Coll Cardiol* 2005;45:1970-3.
4. Muller JE, Abela GS, Nesto RW, et al. Triggers, acute risk factors and vulnerable plaques: the lexicon of a new frontier. *J Am Coll Cardiol* 1994;23:809-13.
5. Ehara S, Kobayashi Y, Yoshiyama M, et al. Spotty calcification typifies the culprit plaque in patients with acute myocardial infarction: an intravascular ultrasound study. *Circulation* 2004;110:3424-9.
6. Schoenhagen P, Ziada KM, Kapadia SR, et al. Extent and direction of arterial remodeling in stable versus unstable coronary syndromes : an intravascular ultrasound study. *Circulation* 2000;101:598-603.

7. Raff GL, Gallagher MJ, O'Neill WW, et al. Diagnostic accuracy of noninvasive coronary angiography using 64-slice spiral computed tomography. *J Am Coll Cardiol* 2005;46:552-7.
8. Pundziute G, Schuijf JD, Jukema JW, et al. Evaluation of plaque characteristics in acute coronary syndromes: non-invasive assessment with multi-slice computed tomography and invasive evaluation with intravascular ultrasound radiofrequency data analysis. *Eur Heart J* 2008;29:2373-81.
9. Miller JM, Rochitte CE, Dewey M, et al. Diagnostic performance of coronary angiography by 64-row CT. *N Engl J Med* 2008;359:2324-36.
10. Meijboom WB, Meijis MF, Schuijf JD, et al. Diagnostic accuracy of 64-slice computed tomography coronary angiography: a prospective, multicenter, multivendor study. *J Am Coll Cardiol* 2008;52:2135-44.
11. Budoff MJ, Dowe D, Jollis JG, et al. Diagnostic performance of 64-multidetector row coronary computed tomographic angiography for evaluation of coronary artery stenosis in individuals without known coronary artery disease: results from the prospective multicenter ACCURACY (Assessment by Coronary Computed Tomographic Angiography of Individuals Undergoing Invasive Coronary Angiography) trial. *J Am Coll Cardiol* 2008;52:1724-32.
12. Schuetz GM, Zacharopoulou NM, Schlattmann P, et al. Meta-analysis: noninvasive coronary angiography using computed tomography versus magnetic resonance imaging. *Ann Intern Med* 2010;152:167-77.
13. Rinehart S, Vazquez G, Qian Z, et al. Quantitative measurements of coronary arterial stenosis, plaque geometry, and composition are highly reproducible with a standardized coronary arterial computed tomographic approach in high-quality CT datasets. *J Cardiovasc Comput Tomogr* 2011;5:35-43.
14. Lehman SJ, Schlett CL, Bamberg F, et al. Assessment of coronary plaque progression in coronary computed tomography angiography using a semiquantitative score. *JACC Cardiovasc Imaging* 2009;2:1262-70.
15. Fihn SD, Gardin JM, Abrams J, et al. 2012 ACCF/AHA/ACP/AATS/PCNA/SCAI/STS Guideline for the diagnosis and management of patients with stable ischemic heart disease: a report of the American College of Cardiology Foundation/American Heart Association Task Force on Practice Guidelines, and the American College of Physicians, American Association for Thoracic Surgery, Preventive Cardiovascular Nurses

- Association, Society for Cardiovascular Angiography and Interventions, and Society of Thoracic Surgeons. *J Am Coll Cardiol* 2012;60:e44-e164.
16. Task Force M, Montalescot G, Sechtem U, et al. 2013 ESC guidelines on the management of stable coronary artery disease: the Task Force on the management of stable coronary artery disease of the European Society of Cardiology. *Eur Heart J* 2013;34:2949-3003.
17. Taylor AJ, Cerqueira M, Hodgson JM, et al. ACCF/SCCT/ACR/AHA/ASE/ASNC/NASCI/SCAI/SCMR 2010 Appropriate Use Criteria for Cardiac Computed Tomography. A Report of the American College of Cardiology Foundation Appropriate Use Criteria Task Force, the Society of Cardiovascular Computed Tomography, the American College of Radiology, the American Heart Association, the American Society of Echocardiography, the American Society of Nuclear Cardiology, the North American Society for Cardiovascular Imaging, the Society for Cardiovascular Angiography and Interventions, and the Society for Cardiovascular Magnetic Resonance. *J Cardiovasc Comput Tomogr* 2010;4:407 e1-33.
18. Voros S, Rinehart S, Qian Z, et al. Coronary atherosclerosis imaging by coronary CT angiography: current status, correlation with intravascular interrogation and meta-analysis. *JACC Cardiovasc Imaging* 2011;4:537-48.
19. Papadopoulou SL, Neefjes LA, Schaap M, et al. Detection and quantification of coronary atherosclerotic plaque by 64-slice multidetector CT: a systematic head-to-head comparison with intravascular ultrasound. *Atherosclerosis* 2011;219:163-70.
20. Voros S, Rinehart S, Qian Z, et al. Prospective validation of standardized, 3-dimensional, quantitative coronary computed tomographic plaque measurements using radiofrequency backscatter intravascular ultrasound as reference standard in intermediate coronary arterial lesions: results from the ATLANTA (assessment of tissue characteristics, lesion morphology, and hemodynamics by angiography with fractional flow reserve, intravascular ultrasound and virtual histology, and noninvasive computed tomography in atherosclerotic plaques) I study. *JACC Cardiovasc Interv* 2011;4:198-208.
21. Nakazato R, Shalev A, Doh JH, et al. Aggregate plaque volume by coronary computed tomography angiography is superior and incremental to luminal narrowing for diagnosis of ischemic lesions of intermediate stenosis severity. *J Am Coll Cardiol* 2013;62:460-7.

22. Cheng VY, Nakazato R, Dey D, et al. Reproducibility of coronary artery plaque volume and composition quantification by 64-detector row coronary computed tomographic angiography: an intraobserver, interobserver, and interscan variability study. *J Cardiovasc Comput Tomogr* 2009;3:312-20.
23. Otsuka M, Bruining N, Van Pelt NC, et al. Quantification of coronary plaque by 64-slice computed tomography: a comparison with quantitative intracoronary ultrasound. *Invest Radiol* 2008;43:314-21.
24. Arbab-Zadeh A, Miller JM, Rochitte CE, et al. Diagnostic accuracy of computed tomography coronary angiography according to pre-test probability of coronary artery disease and severity of coronary arterial calcification. The CORE-64 (Coronary Artery Evaluation Using 64-Row Multidetector Computed Tomography Angiography) International Multicenter Study. *J Am Coll Cardiol* 2012;59:379-87.
25. Abdulla J, Pedersen KS, Budoff M, et al. Influence of coronary calcification on the diagnostic accuracy of 64-slice computed tomography coronary angiography: a systematic review and meta-analysis. *Int J Cardiovasc Imaging* 2012;28:943-53.
26. Yoshioka K, Tanaka R, Muranaka K. Subtraction coronary CT angiography for calcified lesions. *Cardiol Clin* 2012;30:93-102.
27. Yamada M, Jinzaki M, Imai Y, et al. Evaluation of severely calcified coronary artery using fast-switching dual-kVp 64-slice computed tomography. *Circ J* 2011;75:472-3.
28. Chiurlia E, Menozzi M, Ratti C, et al. Follow-up of coronary artery bypass graft patency by multislice computed tomography. *Am J Cardiol* 2005;95:1094-7.
29. Jabara R, Chronos N, Klein L, et al. Comparison of multidetector 64-slice computed tomographic angiography to coronary angiography to assess the patency of coronary artery bypass grafts. *Am J Cardiol* 2007;99:1529-34.
30. Pache G, Saueressig U, Frydrychowicz A, et al. Initial experience with 64-slice cardiac CT: non-invasive visualization of coronary artery bypass grafts. *Eur Heart J* 2006;27:976-80.
31. Weustink AC, Nieman K, Pugliese F, et al. Diagnostic accuracy of computed tomography angiography in patients after bypass grafting: comparison with invasive coronary angiography. *JACC Cardiovasc Imaging* 2009;2:816-24.

32. Hamon M, Lepage O, Malagutti P, et al. Diagnostic performance of 16- and 64-section spiral CT for coronary artery bypass graft assessment: meta-analysis. *Radiology* 2008;247:679-86.
33. Mark DB, Berman DS, Budoff MJ, et al. ACCF/ACR/AHA/NASCI/SAIP/SCAI/SCCT 2010 expert consensus document on coronary computed tomographic angiography: a report of the American College of Cardiology Foundation Task Force on Expert Consensus Documents. *Catheter Cardiovasc Interv* 2010;76:E1-42.
34. Abdelkarim MJ, Ahmadi N, Gopal A, et al. Noninvasive quantitative evaluation of coronary artery stent patency using 64-row multidetector computed tomography. *J Cardiovasc Comput Tomogr* 2010;4:29-37.
35. Andreini D, Pontone G, Mushtaq S, et al. Multidetector computed tomography coronary angiography for the assessment of coronary in-stent restenosis. *Am J Cardiol* 2010;105:645-55.
36. Rixe J, Achenbach S, Ropers D, et al. Assessment of coronary artery stent restenosis by 64-slice multi-detector computed tomography. *Eur Heart J* 2006;27:2567-72.
37. Carbone I, Francone M, Algeri E, et al. Non-invasive evaluation of coronary artery stent patency with retrospectively ECG-gated 64-slice CT angiography. *Eur Radiol* 2008;18:234-43.
38. de Graaf FR, Schuijf JD, van Velzen JE, et al. Diagnostic accuracy of 320-row multidetector computed tomography coronary angiography to noninvasively assess in-stent restenosis. *Invest Radiol* 2010;45:331-40.
39. Andreini D, Pontone G, Bartorelli AL, et al. Comparison of feasibility and diagnostic accuracy of 64-slice multidetector computed tomographic coronary angiography versus invasive coronary angiography versus intravascular ultrasound for evaluation of in-stent restenosis. *Am J Cardiol* 2009;103:1349-58.
40. Andreini D, Pontone G, Mushtaq S, et al. Coronary in-stent restenosis: assessment with CT coronary angiography. *Radiology* 2012;265:410-7.
41. Sun Z, Almutairi AM. Diagnostic accuracy of 64 multislice CT angiography in the assessment of coronary in-stent restenosis: a meta-analysis. *Eur J Radiol* 2010;73:266-73.
42. Task Force on Myocardial Revascularization of the European Society of C, the European Association for Cardio-Thoracic S, European Association for Percutaneous Cardiovascular I, et al. Guidelines on myocardial revascularization. *Eur Heart J* 2010;31:2501-55.

43. Min JK, Swaminathan RV, Vass M, et al. High-definition multidetector computed tomography for evaluation of coronary artery stents: comparison to standard-definition 64-detector row computed tomography. *J Cardiovasc Comput Tomogr* 2009;3:246-51.
44. Fuchs TA, Stehli J, Fiechter M, et al. First in vivo head-to-head comparison of high-definition versus standard-definition stent imaging with 64-slice computed tomography. *Int J Cardiovasc Imaging* 2013;29:1409-16.
45. Zeb I, Li D, Nasir K, et al. Effect of statin treatment on coronary plaque progression - a serial coronary CT angiography study. *Atherosclerosis* 2013;231:198-204.
46. Inoue K, Motoyama S, Sarai M, et al. Serial coronary CT angiography-verified changes in plaque characteristics as an end point: evaluation of effect of statin intervention. *JACC Cardiovasc Imaging* 2010;3:691-8.
47. Hamirani YS, Kadakia J, Pagali SR, et al. Assessment of progression of coronary atherosclerosis using multidetector computed tomography angiography (MDCT). *Int J Cardiol* 2011;149:270-4.
48. Ko BS, Cameron JD, Meredith IT, et al. Computed tomography stress myocardial perfusion imaging in patients considered for revascularization: a comparison with fractional flow reserve. *Eur Heart J* 2012;33:67-77.
49. Bettencourt N, Chiribiri A, Schuster A, et al. Direct comparison of cardiac magnetic resonance and multidetector computed tomography stress-rest perfusion imaging for detection of coronary artery disease. *J Am Coll Cardiol* 2013;61:1099-107.
50. Wong DT, Ko BS, Cameron JD, et al. Transluminal attenuation gradient in coronary computed tomography angiography is a novel noninvasive approach to the identification of functionally significant coronary artery stenosis: a comparison with fractional flow reserve. *J Am Coll Cardiol* 2013;61:1271-9.
51. Tonino PA, De Bruyne B, Pijls NH, et al. Fractional flow reserve versus angiography for guiding percutaneous coronary intervention. *N Engl J Med* 2009;360:213-24.
52. De Bruyne B, Pijls NH, Kalesan B, et al. Fractional flow reserve-guided PCI versus medical therapy in stable coronary disease. *N Engl J Med* 2012;367:991-1001.

53. Hachamovitch R, Berman DS, Kiat H, et al. Incremental prognostic value of adenosine stress myocardial perfusion single-photon emission computed tomography and impact on subsequent management in patients with or suspected of having myocardial ischemia. *Am J Cardiol* 1997;80:426-33.
54. Taylor CA, Fonte TA, Min JK. Computational fluid dynamics applied to cardiac computed tomography for noninvasive quantification of fractional flow reserve: scientific basis. *J Am Coll Cardiol* 2013;61:2233-41.
55. Min JK, Berman DS, Budoff MJ, et al. Rationale and design of the DeFACTO (Determination of Fractional Flow Reserve by Anatomic Computed Tomographic Angiography) study. *J Cardiovasc Comput Tomogr* 2011;5:301-9.
56. Koo BK, Erglis A, Doh JH, et al. Diagnosis of ischemia-causing coronary stenoses by noninvasive fractional flow reserve computed from coronary computed tomographic angiograms. Results from the prospective multicenter DISCOVER-FLOW (Diagnosis of Ischemia-Causing Stenoses Obtained Via Noninvasive Fractional Flow Reserve) study. *J Am Coll Cardiol* 2011;58:1989-97.
57. Min JK, Leipsic J, Pencina MJ, et al. Diagnostic accuracy of fractional flow reserve from anatomic CT angiography. *JAMA* 2012;308:1237-45.
58. Norgaard BL, Leipsic J, Gaur S, et al. Diagnostic performance of noninvasive fractional flow reserve derived from coronary computed tomography angiography in suspected coronary artery disease: the NXT trial (Analysis of Coronary Blood Flow Using CT Angiography: Next Steps). *J Am Coll Cardiol* 2014;63:1145-55.
59. Choi JH, Min JK, Labounty TM, et al. Intracoronary transluminal attenuation gradient in coronary CT angiography for determining coronary artery stenosis. *JACC Cardiovasc Imaging* 2011;4:1149-57.
60. George RT, Arbab-Zadeh A, Miller JM, et al. Adenosine stress 64- and 256-row detector computed tomography angiography and perfusion imaging: a pilot study evaluating the transmural extent of perfusion abnormalities to predict atherosclerosis causing myocardial ischemia. *Circ Cardiovasc Imaging* 2009;2:174-82.
61. Rochitte CE, George RT, Chen MY, et al. Computed tomography angiography and perfusion to assess coronary artery stenosis causing perfusion defects by single photon emission computed tomography: the CORE320 study. *Eur Heart J* 2014;35:1120-30.

62. Ko BS, Cameron JD, Leung M, et al. Combined CT coronary angiography and stress myocardial perfusion imaging for hemodynamically significant stenoses in patients with suspected coronary artery disease: a comparison with fractional flow reserve. *JACC Cardiovasc Imaging* 2012;5:1097-111.
63. Bamberg F, Becker A, Schwarz F, et al. Detection of hemodynamically significant coronary artery stenosis: incremental diagnostic value of dynamic CT-based myocardial perfusion imaging. *Radiology* 2011;260:689-98.
64. Detrano R, Guerci AD, Carr JJ, et al. Coronary calcium as a predictor of coronary events in four racial or ethnic groups. *N Engl J Med* 2008;358:1336-45.
65. Greenland P, LaBree L, Azen SP, et al. Coronary artery calcium score combined with Framingham score for risk prediction in asymptomatic individuals. *JAMA* 2004;291:210-5.
66. Polonsky TS, McClelland RL, Jorgensen NW, et al. Coronary artery calcium score and risk classification for coronary heart disease prediction. *JAMA* 2010;303:1610-6.
67. Nicholls SJ, Hsu A, Wolski K, et al. Intravascular ultrasound-derived measures of coronary atherosclerotic plaque burden and clinical outcome. *J Am Coll Cardiol* 2010;55:2399-407.
68. Hachamovitch R, Di Carli MF. Methods and limitations of assessing new noninvasive tests: Part II: Outcomes-based validation and reliability assessment of noninvasive testing. *Circulation* 2008;117:2793-801.
69. Min JK, Shaw LJ, Devereux RB, et al. Prognostic value of multidetector coronary computed tomographic angiography for prediction of all-cause mortality. *J Am Coll Cardiol* 2007;50:1161-70.
70. Hulten EA, Carbonaro S, Petrillo SP, et al. Prognostic value of cardiac computed tomography angiography: a systematic review and meta-analysis. *J Am Coll Cardiol* 2011;57:1237-47.
71. Min JK, Dunning A, Lin FY, et al. Age- and sex-related differences in all-cause mortality risk based on coronary computed tomography angiography findings results from the International Multicenter CONFIRM (Coronary CT Angiography Evaluation for Clinical Outcomes: An International Multicenter Registry) of 23,854 patients without known coronary artery disease. *J Am Coll Cardiol* 2011;58:849-60.

72. Chow BJ, Small G, Yam Y, et al. Incremental prognostic value of cardiac computed tomography in coronary artery disease using CONFIRM: COroNary computed tomography angiography evaluation for clinical outcomes: an InteRnational Multicenter registry. *Circ Cardiovasc Imaging* 2011;4:463-72.
73. Hadamitzky M, Achenbach S, Al-Mallah M, et al. Optimized prognostic score for coronary computed tomographic angiography: results from the CONFIRM registry (COroNary CT Angiography Evaluation For Clinical Outcomes: An InteRnational Multicenter Registry). *J Am Coll Cardiol* 2013;62:468-76.
74. Lin FY, Shaw LJ, Dunning AM, et al. Mortality risk in symptomatic patients with nonobstructive coronary artery disease: a prospective 2-center study of 2,583 patients undergoing 64-detector row coronary computed tomographic angiography. *J Am Coll Cardiol* 2011;58:510-9.
75. Wilson PW, D'Agostino RB, Levy D, et al. Prediction of coronary heart disease using risk factor categories. *Circulation* 1998;97:1837-47.
76. Metz LD, Beattie M, Hom R, et al. The prognostic value of normal exercise myocardial perfusion imaging and exercise echocardiography: a meta-analysis. *J Am Coll Cardiol* 2007;49:227-37.
77. Versteyleen MO, Kietselaer BL, Dagnelie PC, et al. Additive value of semiautomated quantification of coronary artery disease using cardiac computed tomographic angiography to predict future acute coronary syndrome. *J Am Coll Cardiol* 2013;61:2296-305.
78. Mancini GB, Hartigan PM, Shaw LJ, et al. Predicting outcome in the COURAGE trial (Clinical Outcomes Utilizing Revascularization and Aggressive Drug Evaluation): coronary anatomy versus ischemia. *JACC Cardiovasc Interv* 2014;7:195-201.
79. Motoyama S, Kondo T, Sarai M, et al. Multislice computed tomographic characteristics of coronary lesions in acute coronary syndromes. *J Am Coll Cardiol* 2007;50:319-26.
80. Pfleiderer T, Marwan M, Schepis T, et al. Characterization of culprit lesions in acute coronary syndromes using coronary dual-source CT angiography. *Atherosclerosis* 2010;211:437-44.
81. Virmani R, Burke AP, Farb A, et al. Pathology of the vulnerable plaque. *J Am Coll Cardiol* 2006;47:C13-8.
82. Cheruvu PK, Finn AV, Gardner C, et al. Frequency and distribution of thin-cap fibroatheroma and ruptured plaques in human coronary arteries: a pathologic study. *J Am Coll Cardiol* 2007;50:940-9.

83. Imazeki T, Sato Y, Inoue F, et al. Evaluation of coronary artery remodeling in patients with acute coronary syndrome and stable angina by multislice computed tomography. *Circ J* 2004;68:1045-50.
84. Wu YW, Kao HL, Huang CL, et al. The effects of 3-month atorvastatin therapy on arterial inflammation, calcification, abdominal adipose tissue and circulating biomarkers. *Eur J Nucl Med Mol Imaging* 2012;39:399-407.
85. Motoyama S, Sarai M, Harigaya H, et al. Computed tomographic angiography characteristics of atherosclerotic plaques subsequently resulting in acute coronary syndrome. *J Am Coll Cardiol* 2009;54:49-57.
86. Narula J, Nakano M, Virmani R, et al. Histopathologic characteristics of atherosclerotic coronary disease and implications of the findings for the invasive and noninvasive detection of vulnerable plaques. *J Am Coll Cardiol* 2013;61:1041-51.
87. Kashiwagi M, Tanaka A, Kitabata H, et al. Feasibility of noninvasive assessment of thin-cap fibroatheroma by multidetector computed tomography. *JACC Cardiovasc Imaging* 2009;2:1412-9.
88. Tanaka A, Shimada K, Yoshida K, et al. Non-invasive assessment of plaque rupture by 64-slice multidetector computed tomography--comparison with intravascular ultrasound. *Circ J* 2008;72:1276-81.
89. Fleiner M, Kummer M, Mirlacher M, et al. Arterial neovascularization and inflammation in vulnerable patients: early and late signs of symptomatic atherosclerosis. *Circulation* 2004;110:2843-50.
90. Zerhouni EA, Barth KH, Siegelman SS. Demonstration of venous thrombosis by computed tomography. *AJR Am J Roentgenol* 1980;134:753-8.
91. Madder RD, Chinnaiyan KM, Marandici AM, et al. Features of disrupted plaques by coronary computed tomographic angiography: correlates with invasively proven complex lesions. *Circ Cardiovasc Imaging* 2011;4:105-13.
92. Swap CJ, Nagurney JT. Value and limitations of chest pain history in the evaluation of patients with suspected acute coronary syndromes. *JAMA* 2005;294:2623-9.
93. Amsterdam EA, Kirk JD, Bluemke DA, et al. Testing of low-risk patients presenting to the emergency department with chest pain: a scientific statement from the American Heart Association. *Circulation* 2010;122:1756-76.

94. Pope JH, Aufderheide TP, Ruthazer R, et al. Missed diagnoses of acute cardiac ischemia in the emergency department. *N Engl J Med* 2000;342:1163-70.
95. Hoffmann U, Bamberg F, Chae CU, et al. Coronary computed tomography angiography for early triage of patients with acute chest pain: the ROMICAT (Rule Out Myocardial Infarction using Computer Assisted Tomography) trial. *J Am Coll Cardiol* 2009;53:1642-50.
96. Hollander JE, Chang AM, Shofer FS, et al. Coronary computed tomographic angiography for rapid discharge of low-risk patients with potential acute coronary syndromes. *Ann Emerg Med* 2009;53:295-304.
97. Hoffmann U, Truong QA, Schoenfeld DA, et al. Coronary CT angiography versus standard evaluation in acute chest pain. *N Engl J Med* 2012;367:299-308.
98. Litt HI, Gatsonis C, Snyder B, et al. CT angiography for safe discharge of patients with possible acute coronary syndromes. *N Engl J Med* 2012;366:1393-403.
99. Takakuwa KM, Keith SW, Estepa AT, et al. A meta-analysis of 64-section coronary CT angiography findings for predicting 30-day major adverse cardiac events in patients presenting with symptoms suggestive of acute coronary syndrome. *Acad Radiol* 2011;18:1522-8.
100. Goldstein JA, Chinnaiyan KM, Abidov A, et al. The CT-STAT (Coronary Computed Tomographic Angiography for Systematic Triage of Acute Chest Pain Patients to Treatment) trial. *J Am Coll Cardiol* 2011;58:1414-22.
101. Nasis A, Meredith IT, Sud PS, et al. Long-term Outcome after CT Angiography in Patients with Possible Acute Coronary Syndrome. *Radiology* 2014:132680.
102. Halpern EJ, Deutsch JP, Hannaway MM, et al. Cardiac risk factors and risk scores vs cardiac computed tomography angiography: a prospective cohort study for triage of ED patients with acute chest pain. *Am J Emerg Med* 2013;31:1479-85.
103. Hascoet S, Bongard V, Chabbert V, et al. Early triage of emergency department patients with acute coronary syndrome: contribution of 64-slice computed tomography angiography. *Arch Cardiovasc Dis* 2012;105:338-46.

104. Linde JJ, Kofoed KF, Sorgaard M, et al. Cardiac computed tomography guided treatment strategy in patients with recent acute-onset chest pain: results from the randomised, controlled trial: CARDiac cT in the treatment of acute Chest pain (CATCH). *Int J Cardiol* 2013;168:5257-62.
105. Poon M, Cortegiano M, Abramowicz AJ, et al. Associations between routine coronary computed tomographic angiography and reduced unnecessary hospital admissions, length of stay, recidivism rates, and invasive coronary angiography in the emergency department triage of chest pain. *J Am Coll Cardiol* 2013;62:543-52.
106. Min JK, Shaw LJ, Berman DS, et al. Costs and clinical outcomes in individuals without known coronary artery disease undergoing coronary computed tomographic angiography from an analysis of Medicare category III transaction codes. *Am J Cardiol* 2008;102:672-8.
107. Ladapo JA, Jaffer FA, Hoffmann U, et al. Clinical outcomes and cost-effectiveness of coronary computed tomography angiography in the evaluation of patients with chest pain. *J Am Coll Cardiol* 2009;54:2409-22.

## FIGURES

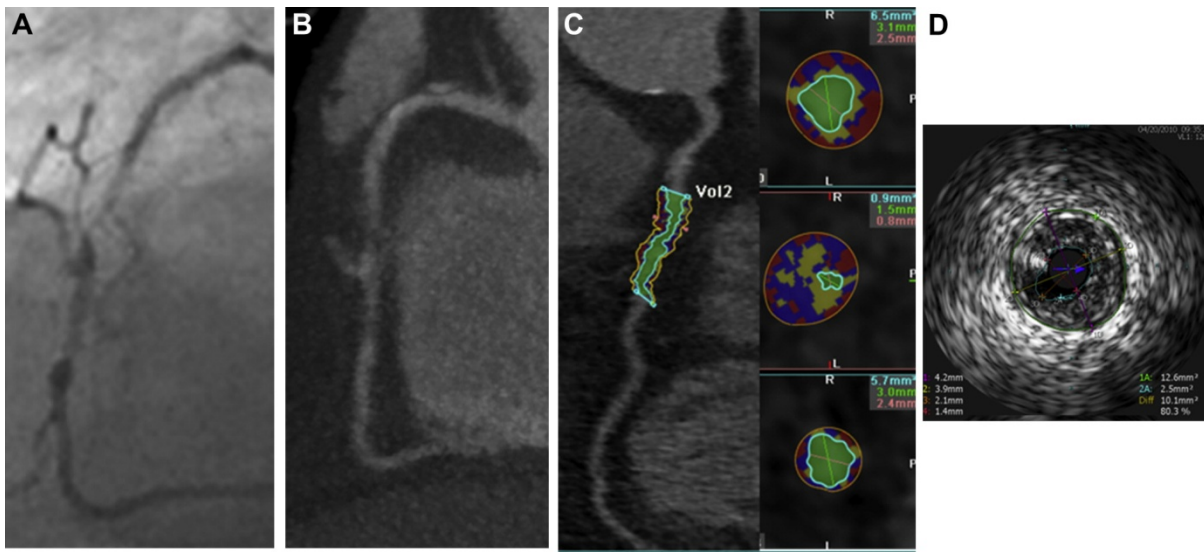


**Figure 1.** A: Invasive coronary angiography, B: CCTA , C: automated assessment of plaque on CCTA, D: IVUS assessment of plaque. There is a severe complex lesion in mid RCA. Adapted from Collin Fischer et al, Coronary CT angiography versus intravascular ultrasound for estimation of coronary stenosis and atherosclerotic plaque burden: a meta-analysis. Journal of cardiovascular computed tomography ,2013.

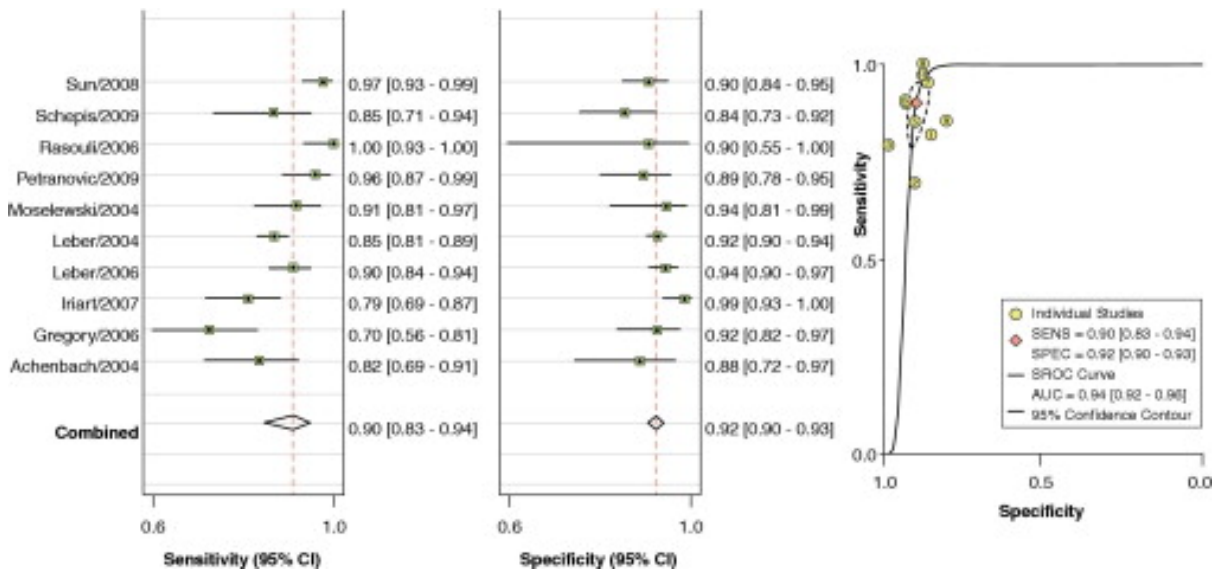


**Figure 2. Pooled Sensitivity and Specificity for Coronary CTA Versus IVUS**

Pooled sensitivity and specificity for coronary CTA vs. IVUS (Adapted from Voros S, Rinehart S, Qian Z et al. Coronary atherosclerosis imaging by coronary CT angiography: current status, correlation with intravascular interrogation and meta-analysis. JACC Cardiovasc Imaging 2011;4:537–48. With permission from Elsevier)

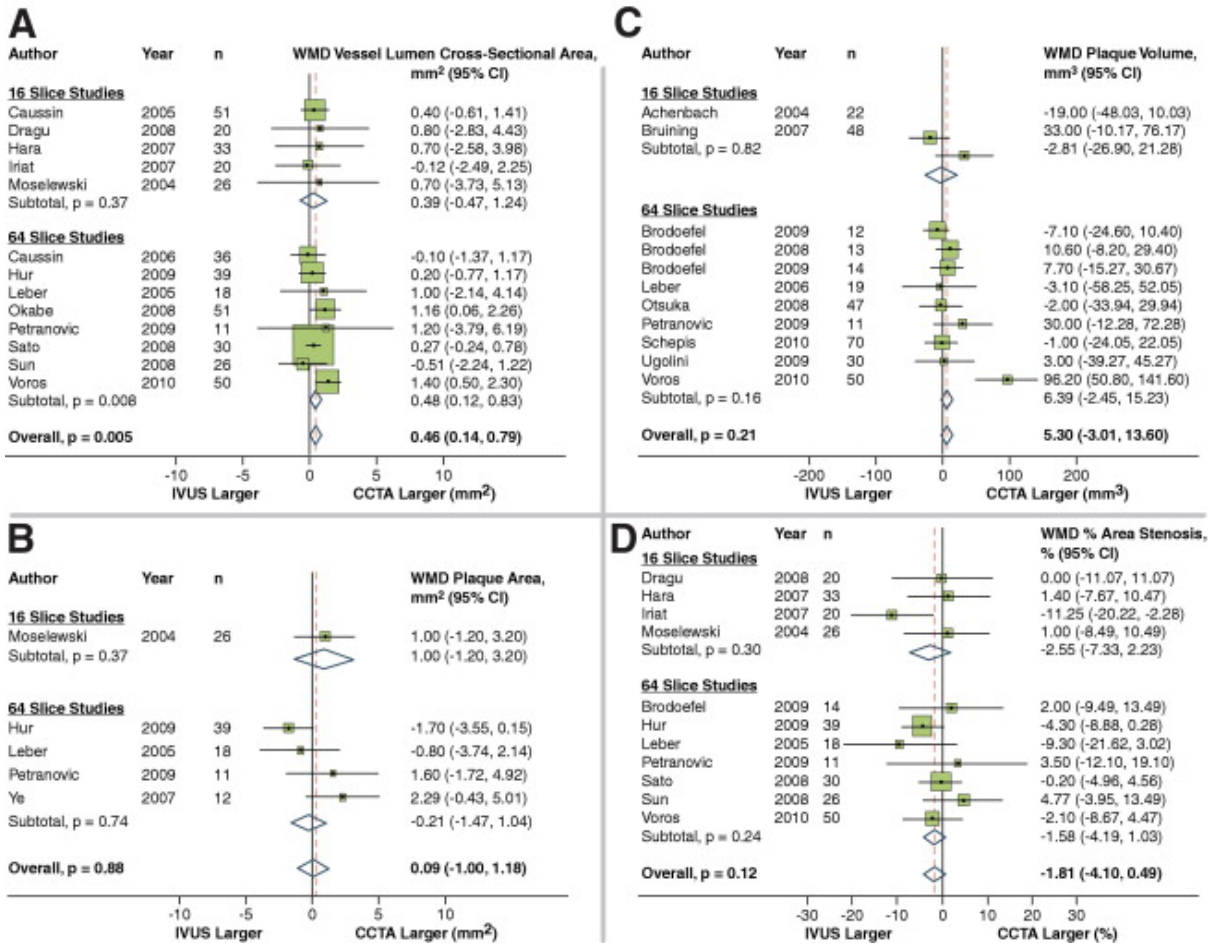


**Figure 3.** Coronary CTA vs. IVUS to compare vessel lumen area (a), plaque area (b), plaque volume (c) and percent area stenosis (d) (Adapted from Voros S, Rinehart S, Qian Z et al. Coronary atherosclerosis imaging by coronary CT angiography: current status, correlation with intravascular interrogation and meta-analysis. JACC Cardiovasc Imaging 2011;4:537–48. With permission from Elsevier)

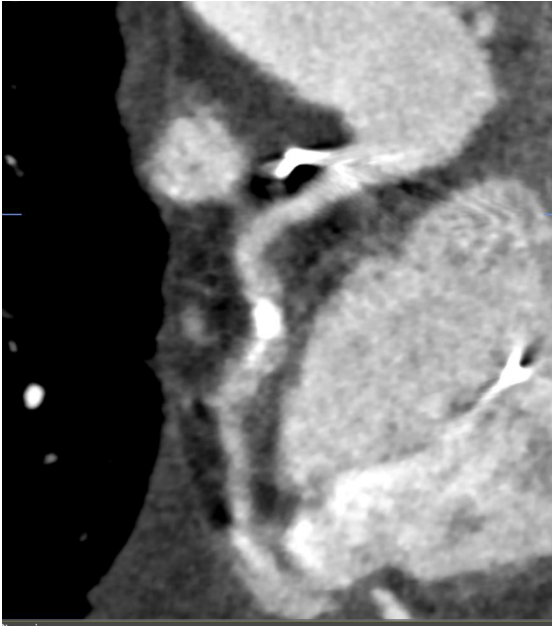


**Figure 4.** A heavily calcified mid right coronary artery. Due to blooming artefact from calcium, accurate assessment of luminal stenosis is not possible. In addition, this is a poor quality image with motion artefacts which may prohibit accurate image interpretation.

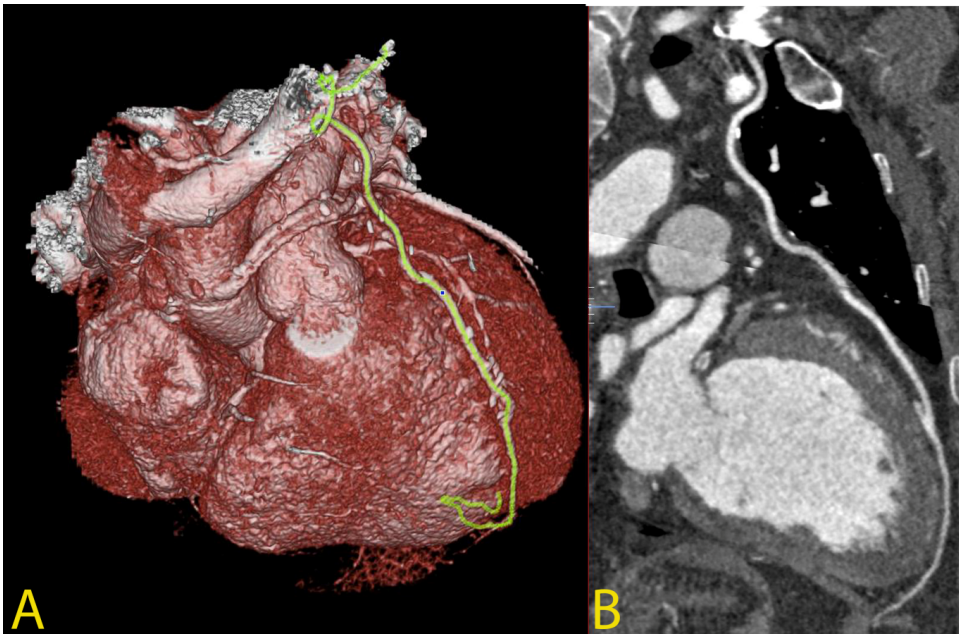


**Figure 5.** (A) 3D rendered image showing left internal thoracic artery (LIMA) graft insertion into mid left anterior descending artery (B) A well opacified LIMA with no obvious stenosis. The insertion of graft into LAD is visible with good distal run off.

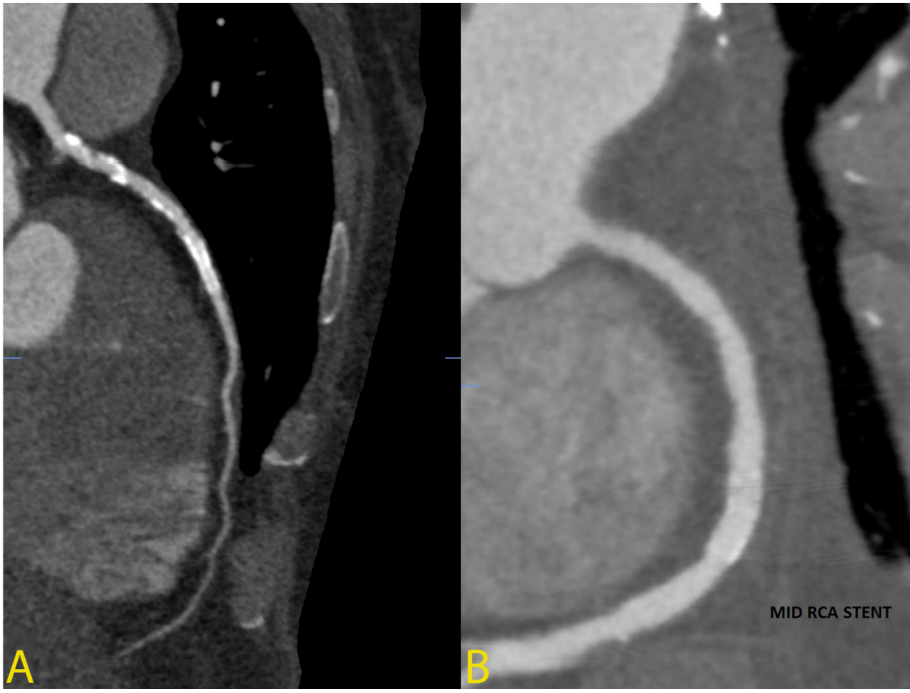


**Figure 6.** (A) < 3mm Stent in mid LAD. Partial volume artefact duet to stent makes assessment difficult. (B) > 3mm stent in mid RCA. The lumen is well visualised and there is no significant instent restenosis.

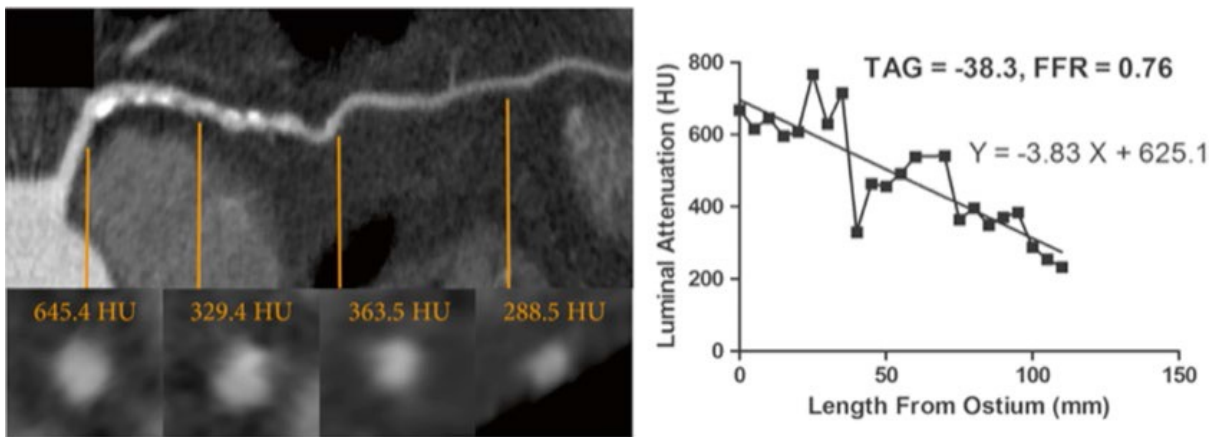


**Figure 7.** Transluminal attenuation gradient. Left anterior descending artery with significant obstructive plaque burden imaged by CCTA. Axial and representative cross-sectional views with corresponding luminal attenuation (HU) of CCTA. *Black square dots* represent 5 mm intervals at which intraluminal attenuation (HU) was measured. TAG was  $-38.3$ , and the FFR was  $0.76$  (Adapted from Wong DT, Ko BS, Cameron JD et al. Transluminal Attenuation Gradient in Coronary Computed Tomography Angiography Is a Novel Non-invasive Approach to the Identification of Functionally Significant Coronary Artery Stenosis: A Comparison With Fractional Flow Reserve. Journal of the American College of Cardiology 2013 Mar 26;61(12):1271–9. With permission from Elsevier)

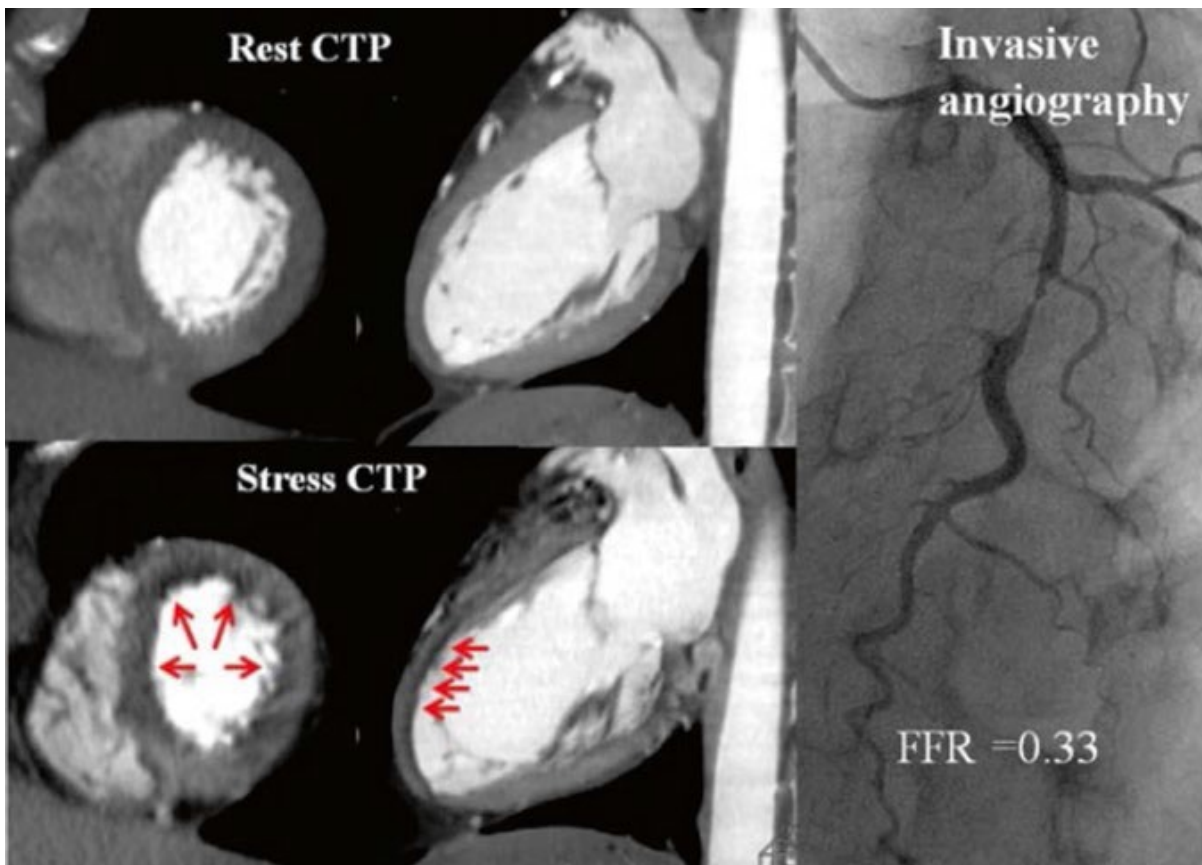
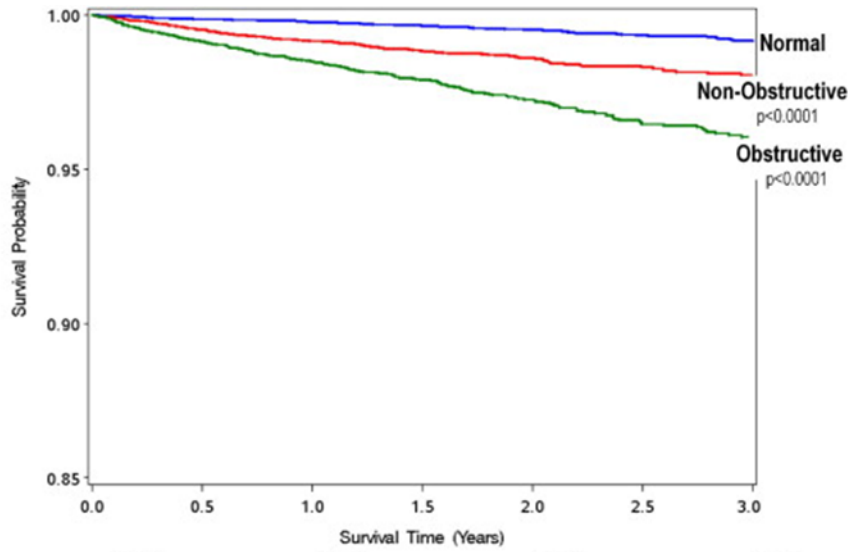


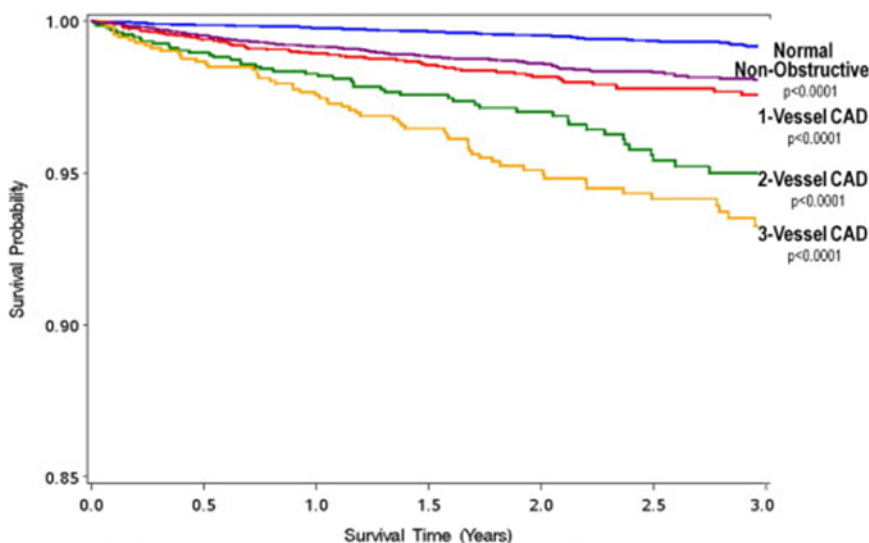
**Figure 8.** CT perfusion imaging and invasive angiography. Stress perfusion defects are demonstrated on CT in the mid and distal anterior wall corresponding to a severe stenosis in the mid LAD associated with an FFR of 0.33 (Adapted from Ko BS, Cameron JD, Meredith IT et al. Computed tomography stress myocardial perfusion imaging in patients considered for revascularization: a comparison with fractional flow reserve. *Eur Heart J* 2012;33:67–77. With permission from Oxford University Press)

a



At Risk	Year 0	Year 1	Year 2	Year 3
Normal	10146	9357	5800	2907
Non-Obstructive (1-49%)	8114	7437	4081	1930
Obstructive (≥50%)	5594	5135	3153	1430

b



At Risk	Year 0	Year 1	Year 2	Year 3
Normal	10146	9357	5800	2907
Non-Obstructive	8114	7437	4081	1930
1-Vessel	3118	2873	1747	782
2-Vessel	1346	1228	742	324
3-Vessel/Left Main	1130	1034	664	324

**Figure 9.** Cumulative survival in patients with severe plaque. (a) 3-year Kaplan Meier Survival by the maximal per-patient presence of none, nonobstructive and obstructive CAD. (b) 3-year Kaplan Meier Survival by the presence, extent and severity of CAD by CCTA (Adapted from Min JK et al. J Am Coll Cardiol 2011;58:849–60. With permission from Elsevier)

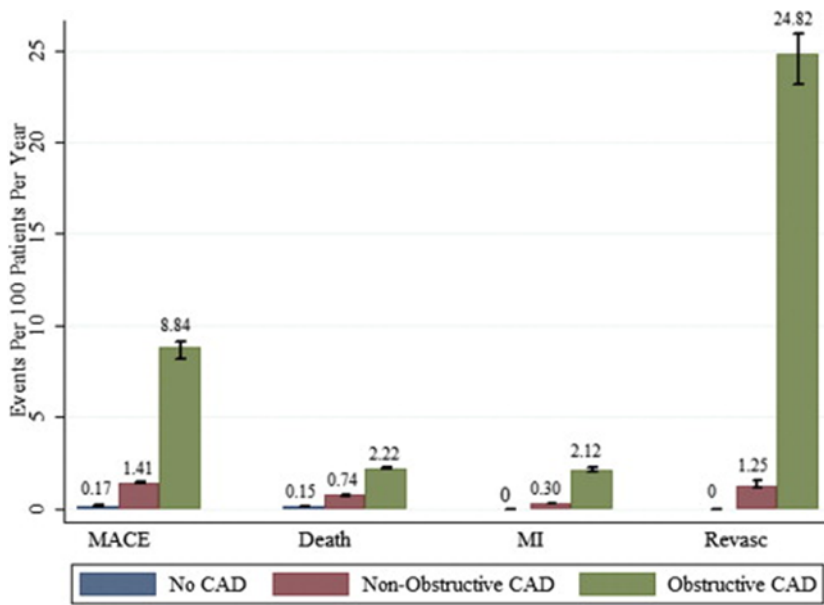


**Figure 10.** Annual event rates stratified by CTA result (Adapted from Hulten EA, Carbonaro S, Petrillo SP, Mitchell JD, Villines TC. Prognostic value of cardiac computed tomography angiography: a systematic review and meta-analysis. *J Am Coll Cardiol* 2011;57:1237–47. With permission from Elsevier)

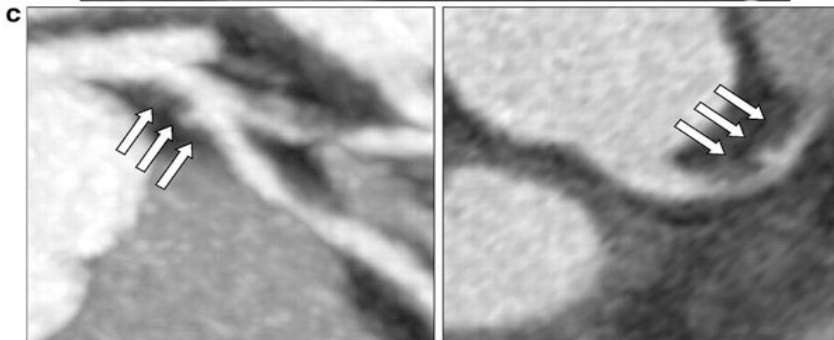
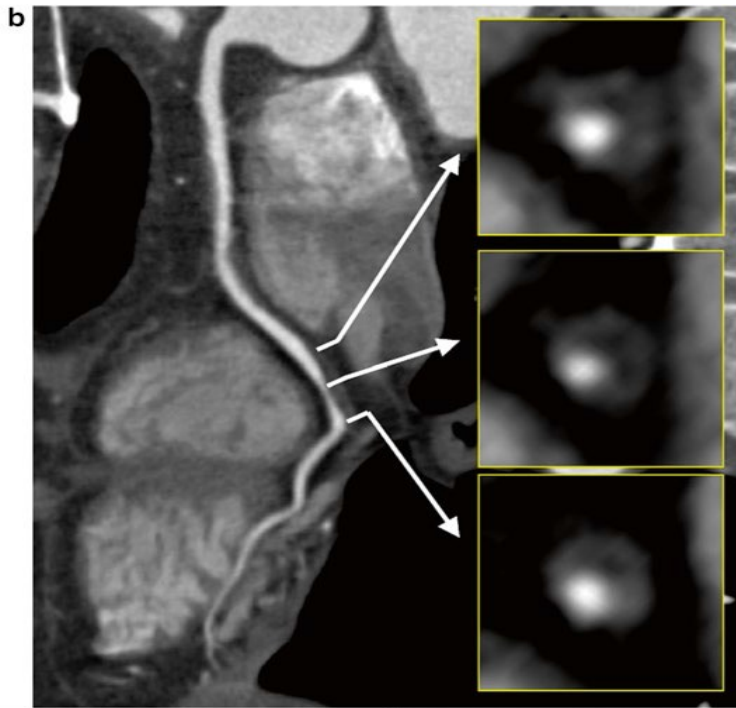
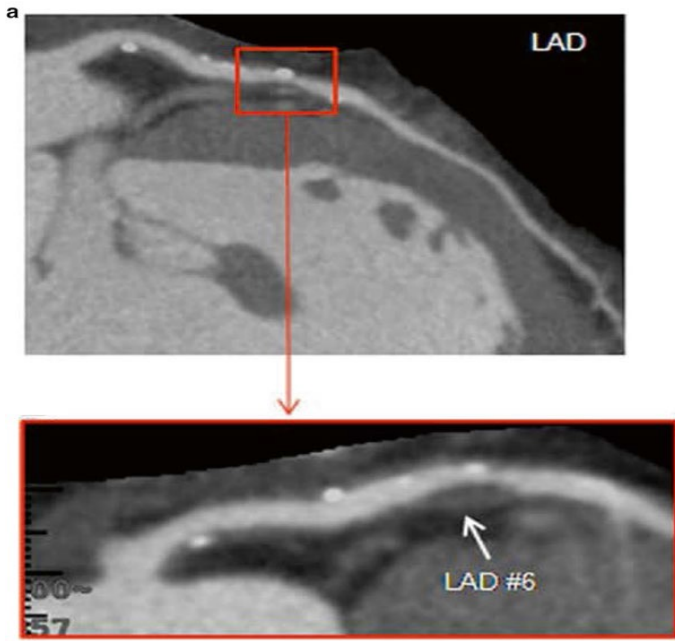


**Figure 11.** Vulnerable plaque characteristics. Features of vulnerable plaque including the presence of low attenuation plaque, positive remodelling, spotty calcification **(a)**, ring-like sign **(b)** and plaque ulceration with intraplaque contrast penetration **(c)**. **(a)** Adapted from Motoyama S, Sarai M, Harigaya H et al. Computed tomographic angiography characteristics of atherosclerotic plaques subsequently resulting in acute coronary syndrome. *J Am Coll Cardiol* 2009;54: 49–57. With permission from Elsevier. **(b)** Adapted from Kashiwagi M, Tanaka A, Kitabata H et al. Feasibility of noninvasive assessment of thin-cap fibroatheroma by multidetector computed tomography. *JACC Cardiovasc Imaging* 2009;2:1412–9. With permission from Elsevier. **(c)** Adapted from Madder RD, Chinnaiyan KM, Marandici AM, Goldstein JA. Features of disrupted plaques by coronary computed tomographic angiography: correlates with invasively proven complex lesions. *Circ Cardiovasc Imaging* 2011;4:105–13. With permission from Wolters Kluwer Health

# **Chapter 3: Quantitative and Qualitative Coronary Plaque Assessment using Computed Tomography Coronary Angiography: A comparison with Intravascular Ultrasound**

*Ravi Kiran Munnur MBBS<sup>1\*</sup>, Jordan Andrews<sup>2,3</sup>, Yu Kataoka MBBS, PhD<sup>4</sup>, Nitesh Nerlekar<sup>1</sup>, Peter J Psaltis MBBS (Hons), PhD<sup>1,3</sup>, Stephen J Nicholls MBBS, PhD<sup>2,3</sup>, Yuvaraj Malaiapan MBBS, MD<sup>1</sup>, James D Cameron MBBS, MD<sup>1</sup>, Ian T Meredith MBBS (Hons), PhD<sup>1</sup>, Sujith Seneviratne MBBS (Hons)<sup>1</sup>, Dennis TL Wong MBBS (Hons), MD, PhD<sup>1,2</sup>*

**Submitted: International Journal of Cardiology**

<sup>1</sup> Monash Cardiovascular Research Centre, Department of Medicine (Monash Medical Centre) Monash University and Monash Heart, Monash Health, 246 Clayton Road, Clayton, 3168 VIC, Australia

<sup>2</sup> South Australian Medical Research Institute (SAHMRI), Adelaide, Australia

<sup>3</sup> Discipline of Medicine, University of Adelaide, Adelaide, Australia

<sup>4</sup> Department of Cardiovascular Medicine, National Cerebral & Cardiovascular Centre, Suita, Japan

\* Corresponding author

Ravi Kiran Munnur

Monash Heart, Monash Cardiovascular Research Centre

Monash Health, [REDACTED]  
[REDACTED]

## **ABSTRACT**

### **Objective**

To compare coronary angiography (CTCA) with intravascular ultrasound (IVUS) in quantitative and qualitative plaque assessment.

### **Methods**

Patients who underwent IVUS and CTCA within 3 months for suspected coronary artery disease were retrospectively studied. Plaque volumes on CTCA were quantified manually and with automated-software and were compared to IVUS. High-risk plaque features were compared between CTCA and IVUS.

### **Results**

There were 769 segments in 32 vessels (27 patients) included. Manual plaque quantification on CTCA was comparable to IVUS per slice (mean difference of  $0.06 \pm 0.07 \text{ mm}^3$ ,  $p=0.44$ ; Bland-Altman 95% limits of agreement  $-2.19$  to  $2.08 \text{ mm}^3$ , bias of  $-0.06 \text{ mm}^3$ ) and per vessel ( $3.1 \text{ mm}^3 \pm 2.85 \text{ mm}^3$ ,  $p=0.92$ ). In contrast, there was significant difference between automated-software and IVUS per slice ( $2.3 \pm 0.09 \text{ mm}^3$ ,  $p<0.001$ ; 95% LoA  $-6.78$  to  $2.25 \text{ mm}^3$ , bias of  $-2.2 \text{ mm}^3$ ) and per vessel ( $33.04 \pm 10.3 \text{ mm}^3$ ,  $p < 0.01$ ).

The sensitivity, specificity, positive and negative predictive value of CTCA to detect plaques that had features of echo-attenuation (EA) on IVUS was 93.3%, 99.6%, 93.3% and 99.6% respectively. The association of  $\geq 2$  high-risk plaque features on CTCA with EA plaque features on IVUS was excellent (86.7%, 99.6%, 92.9% and 99.2%). In comparison, the association of high-risk plaque features on CTCA and plaques with echo-lucency on IVUS was only modest.

## **Conclusion**

Plaque volume quantification by manual CTCA method is accurate when compared to IVUS. The presence of at least two high-risk plaque features on CTCA is associated with plaque features of echo attenuation on IVUS.

## **Keywords**

Computed Tomography coronary angiography, Intravascular Ultrasound, Echo-attenuated plaques, Plaque quantification, Low-attenuation plaque

## **Key Points**

- Manual plaque volume quantification on CTCA is highly comparable to IVUS
- Accurate quantitative and qualitative analysis of plaques on CTCA is feasible with appropriate window setting
- Plaques with features of echo attenuation on IVUS are detectable on CTCA
- CTCA was poor in detecting plaques with features of echo lucency on IVUS

## **Abbreviations**

CTCA: Computed tomography coronary angiography

IVUS: Intravascular Ultrasound

ICA: Invasive coronary angiography

HU: Hounsfield units

PR: Positive remodelling

LAP: Low attenuation plaque

SC: Spotty Calcification

EEM: External elastic membrane

EA: Echo-attenuated

EL: Echo-lucent

## **Introduction**

Computed tomography coronary angiography (CTCA) is an established non-invasive test to assess coronary stenosis with excellent negative predictive value and correlates favourably with invasive coronary angiography (ICA) (1). CTCA is also an emerging tool for detection, quantification and characterisation of high-risk plaque (2, 3). Intravascular ultrasound (IVUS) is the gold standard for plaque volume quantification and in serial IVUS evaluation studies it has been observed that clinical events are linked to atheroma burden and to the rate of plaque progression (4, 5). However, IVUS is limited by the high cost and invasive nature of the test. It is therefore desirable to have a non-invasive tool for serial plaque volume assessment, which can serve as a surrogate for future clinical trials of atherosclerosis evaluation. Although some studies have described satisfactory correlation of CTCA vs. IVUS-derived plaque quantification, wide limits of agreement on Bland-Altman analysis suggests only modest agreement (6). Moreover, majority of these studies were performed on older generation CT scanners with variable scanning protocols and parameters. In the current era of 320-detector row CT with improved scanning techniques and iterative reconstruction, the accuracy of plaque quantification requires further validation. Additional refinements in techniques as well as algorithms are necessary as plaque quantification on CTCA is affected by several factors such as mean luminal Hounsfield units (HU), window settings, image quality and calcium blooming (7).

Manual, semi-automated and automated methods have been described to quantify plaque on CTCA (8-11). Even though manual quantification has been the most accurate, it is time consuming and technically difficult, requiring specific expertise and therefore prone to inter-observer variability (12, 13). Meanwhile, automated plaque assessment using dedicated software (14, 15) is

appealing as it is quick and reproducible but is less accurate (16). The diagnostic accuracy of these techniques needs further rigorous comparison against each other using IVUS as the reference gold standard.

The detection of high-risk plaque before it ruptures would be a watershed moment in the management of atherosclerotic coronary artery disease. Recently, plaques with IVUS features of echo-lucency (EL) and echo-attenuation (EA) have been shown to be associated with the presence of fibroatheroma with a necrotic core on autopsy studies and may represent a high-risk plaque (17). High-risk plaque features on CTCA such as positive remodelling (PR), low attenuation plaque (LAP), spotty calcification (SC) and napkin ring sign (NR) have also been described and are associated with adverse outcomes (18-21). Very few studies however have assessed the association of these high-risk plaque features on CTCA with IVUS features of echo-lucency and echo-attenuation(8, 22).

The primary objective of this study is to compare the accuracy of plaque quantification by automated and manual methods on CTCA using IVUS as the reference standard.

Secondary objectives were to assess the association between plaques with features of EA and EL on IVUS with high-risk plaque features on CTCA.

## **Methods**

This was a retrospectively performed study of patients who underwent clinically indicated CTCA for suspected coronary artery disease and also had subsequent invasive coronary angiography with concomitant IVUS imaging. Specific inclusion on the basis of CTCA was the presence of atherosclerotic plaque in the proximal or mid segments of any major epicardial coronary vessel. Patients had to have angiography and IVUS performed within a three-month period of initial CTCA. Patients were excluded if they had impaired left ventricular function, moderate or greater valvular heart disease, severely calcified vessels that precluded CTCA interpretation, poor

quality CTCA and/or IVUS images and if CTCA or IVUS segments were unable to be matched due to a lack of fiducial points. The institutional ethics committee approved this study.

### CT coronary angiography

CT coronary angiography was performed using 320-detector row CT scanner (Aquilion Vision; Toshiba Medical Systems, Nasu, Japan). Pre-scanning heart rate of 65 beats per minute was achieved using beta-blockers, and nitroglycerine was administered to optimise vasodilatation in accordance with previous institutional protocol and major society guidelines (23). A bolus of 70 ml of 100% iohexol 56.6-g/75 ml (Omnipaque 350; GE Healthcare, Princeton, NJ) was injected into an antecubital vein at a flow rate of 6 ml/sec, followed by 30 ml of saline. Scan parameters for CTCA were: detector collimation: 320 x 0.5 mm; tube current: 300 to 500 mA; tube voltage: 100 to 120 kV; gantry rotation time: 270 ms; and temporal resolution: 135 ms. Prospective electrocardiogram gating was used, covering 70% to 99% of the R-R interval. For images acquired at heart rate of 65 beats per minute or slower, scanning was completed with a single R-R interval utilizing an 180° segment. In patients with heart rate greater than 65 beats per minute, data segments from two consecutive beats were used for multisegment reconstruction with an improved temporal resolution of 87 msec.

### Invasive Coronary Angiography

All the patients in the study underwent clinically indicated coronary angiography. Invasive coronary angiography was performed as per the standard catheterisation in accordance with the American College of Cardiology guidelines for coronary angiography (24).

### IVUS acquisition

IVUS was done for clinical indications and in a standard fashion using commercially available catheters (40MHz, Atlantis SR Pro, Boston Scientific, Boston, Massachusetts and Volcano Eagle Eye IVUS-catheter 20 MHz, electronic transducer or Volcano Inc., Rancho

Cordova, California). After intracoronary administration of 100-200 µg of nitroglycerine, IVUS images were acquired using automated mechanical pullback devices at a continuous pull back speed of 0.5 mm/s (25). The images were stored on a CD-ROM for offline analysis in a core lab (South Australian Health and Medical Research institute, Adelaide, Australia).

#### Analysis of CT coronary angiograms

Data was transferred to an external workstation (Vitrea 6, version 6.0; Vital Images, Minnetonka, Minnesota) for further analysis. Quantitative plaque burden analysis was done using attenuation-based-automated SurePlaque (Vitrea 6, version 3.0; Vital Images and Toshiba Medical Systems) software for vessel and plaque analysis. The coronary vessels were assessed on a 0.5mm slice-by-slice basis from ostium proximally and distally to the point of IVUS pull back. These slices were matched to IVUS images based on fiduciary points. Plaque area was defined as the area between the vessel wall and the lumen. Manual quantification of plaque was performed after delineation of the lumen and the vessel wall using the window settings of 230W and 83 L [if the luminal Hounsfield unit (HU) was <500]; and 300W and 150 L [if the luminal HU was >500] (26). Additional window and level settings of 740W and 220L were used if necessary to assess the outer vessel wall (7, 10) (**Figure 1**). These window and level settings were adopted as they best suited our vendor, contrast and acquisition protocols. In the presence of calcium, settings were modified according to luminal HU ( $W = \text{Luminal HU} \times 2.07$ ;  $L = \text{luminal HU} \times 0.72$ )(27). Two experienced cardiologists (KM, DW) who were blinded to the results of coronary angiography and IVUS measurements performed the analysis independently.

The segments on CTCA were matched to the IVUS segments based on fiduciary points such as branch points or calcified plaques. The reference diameter and area were determined as an average of the vessel dimension immediately proximal and distal to the lesion where there was minimal or no plaque. In ostial lesions, only distal reference was used. Remodelling was calculated as the ratio of the

diameter of the vessel at the lesion site to the reference segment, and positive remodelling was defined as ratio > 1.1(20)

Total atheroma volume was calculated as the summation of plaque area in each measured image.

In a second step, plaque characterization was defined based on HU (< 56 HU for LAP, 56 – 150 HU for fibrous plaque and > 150 HU for calcified plaque) (28). The presence of high-risk plaque features on CTCA such as positive remodelling, low attenuation plaque, spotty calcification and napkin ring sign (NR) were evaluated. NR sign on CTCA is the presence of a ring like attenuation and has been suggested to be a marker for thin cap fibro atheroma (29) (SM **Figure 2**). In addition, the location of the high-risk plaque was noted based on the American College of Cardiology (ACC) 17 segment model of coronary arteries

#### IVUS plaque volume measurements

All the images were analysed in a core laboratory (South Australian Medical Research Institute) that was blinded to the CT results and patient demographics. The cross-sectional images that were analysed were 0.5 mm in thickness. Lumen and vessel wall (external elastic membrane) were manually traced. The measurements were performed according to the American College of Cardiology recommendations(25). The leading edges of the lumen and external elastic membrane (EEM) were traced by manual planimetry. Plaque area was defined as the area occupied between these leading edges. Total atheroma volume was calculated as the summation of plaque area in each measured image.

Echo-attenuated plaque (EA) was identified by plaque that was either hypo-echoic or isoechoic to the reference adventitia with no bright calcium and by the absence of ultrasound signal behind the plaque. Echo-lucent (EL) plaque contained an intraplaque zone of low or absent echogenicity which is lower than that of reference adventitia and is surrounded by tissue of greater echodensity (30). The location of EA and EL plaque was noted based on the American College of Cardiology (ACC) 17 segment model of

coronary arteries. The association of EL and EA on IVUS to the presence of high-risk plaque features on CTCA was assessed on per segment / plaque based analysis. **(Figure 3)**

## **Statistical Analysis**

Continuous variables were expressed as mean  $\pm$  standard deviation. Pearson's correlation, paired t-test and Bland Altman analysis with 95% limits of agreement were used to assess agreement between CTCA to IVUS measurement and for intra and inter observer variability for CTCA measurements. A 2-sided p-value  $< 0.05$  was considered statistically significant. Sensitivity, specificity, positive and negative predicate values were calculated with confidence intervals adjusted for clustered data at a per patient level. Statistical analysis was performed using statistical software (SPSS, 20 Chicago, IL, USA and Stata MP/14, StataCorp).

## **Results**

There were 769 segments analysed from 32 vessels in 27 patients. The patient characteristics are shown in Table 1. The distribution of stenosis was: left main (n = 9), left anterior descending artery (n = 16), left circumflex artery (n = 4) and right coronary artery (n = 3). The average time interval between CTCA and IVUS examinations was  $< 90$  days.

### Automated CTCA luminal cross section area, vessel cross section area and plaque volume compared to IVUS

When automated software was used for plaque quantification on CTCA, there was a significant plaque volume difference compared to IVUS, on per slice analysis ( $5.51 \pm 0.08$  vs.  $3.26 \pm 0.05$  mm<sup>3</sup>, mean difference  $2.3 \pm 0.09$ , p  $< 0.0001$ ) and per vessel ( $126.04 \pm 17.55$  vs.  $93 \pm 11.58$  mm<sup>3</sup>,

mean difference of  $33.04 \pm 10.3$ ,  $p < 0.01$ ). The difference was less for calcified vessels ( $0.4 \pm 0.12 \text{ mm}^3$ ) ( $p = 0.001$ ) compared to non-calcified vessels ( $1.78 \pm 0.4 \text{ mm}^3$ ) ( $p < 0.001$ ).

On per slice analysis, there was no significant difference between luminal cross-section area on CTCA and IVUS lumen ( $8.422 \pm 0.1171$  vs.  $8.346 \pm 0.1228 \text{ mm}^2$ , mean difference  $0.07338 \pm 0.1697$ , CI:  $-0.2595$  to  $0.4062$ ,  $p = 0.6655$ )

There was significant difference between vessel cross sectional area on CTCA and IVUS ( $19.51 \pm 0.223 \text{ mm}^2$ ,  $n = 765$  vs.  $14.88 \pm 0.1843$ ,  $n = 769$ , mean difference of  $4.635 \pm 0.2892$ , CI:  $4.067$  to  $5.202$ ,  $p = < 0.0001$ ) (Table 2)

Bland Altman analysis demonstrated satisfactory bias and 95% limits of agreement between IVUS and CTCA for lumen volume ( $-5.3$  to  $5.17 \text{ mm}^3$ , bias of  $-0.06$ ), vessel volume ( $-14.84$  to  $5.6 \text{ mm}^3$ , bias of  $-4.61 \text{ mm}^3$ ) and plaque volume ( $-6.78$  to  $2.25 \text{ mm}^3$ , bias of  $-2.26$ ) (SM Figure 4).

#### Manual CTCA luminal cross section area, vessel cross section area and plaque volume compared to IVUS

When plaque volumes were quantified manually on CTCA, there was no significant difference when compared to IVUS, on per slice analysis ( $3.31 \pm 0.05 \text{ mm}^3$  vs.  $3.26 \pm 0.05 \text{ mm}^3$ , mean difference of  $0.06 \pm 0.07$ ,  $p = 0.44$ ) and per vessel ( $96.1 \pm 11.56$  vs.  $93 \pm 11.58 \text{ mm}^3$ , mean difference of  $-3.1 \text{ mm}^3 \pm -2.85 \text{ mm}^3$ ,  $p = 0.92$ ). The difference was lower in non-calcified vessels ( $0.19 \pm 0.09 \text{ mm}^3$ ,  $p = 0.25$ ) compared to calcified vessels ( $0.25 \pm 0.6 \text{ mm}^3$ ,  $p < 0.001$ ).

On per slice analysis, there was no significant difference between CTCA and IVUS for luminal cross sectional area and ( $8.54 \pm 0.12$  and  $8.39 \pm 0.12 \text{ mm}^2$ , mean difference of  $0.19 \pm 0.17$ , CI:  $-0.15$

to 0.53,  $p=0.26$ ) and for vessel cross sectional area ( $15.1 \pm 0.17$  and  $14.88 \pm 0.18 \text{ mm}^2$ , mean difference of  $0.22 \pm 0.25$ , CI:  $-0.27$  to  $0.72$ ,  $p=0.37$ ) (**Table 2**).

Bland Altman 95% limits of agreement and bias between IVUS and CTCA were excellent for lumen volume ( $-3.85$  to  $3.56 \text{ mm}^3$ , bias of  $-0.14$ ), vessel volume ( $-5.23$  to  $4.8 \text{ mm}^3$ , bias of  $-0.19 \text{ mm}^3$ ) and plaque volume ( $-2.19$  to  $2.08 \text{ mm}^3$ , bias of  $-0.06$ ) (SM Figure 5).

#### Inter-observer and Intra-observer variability for manual and automated CTCA plaque volume quantification

Manual plaque volume measurement was highly reproducible with intra-observer intra-class correlation coefficient of 0.99 (95% CI: 0.90 - 0.99) and inter-observer intra-class correlation coefficient of 0.85 (95% CI: 0.40 - 0.96).

Automated plaque volume quantification had excellent reproducibility with intra-observer intraclass correlation coefficient of 1 (95% CI: 1 - 1) and inter-observer intraclass correlation coefficient of 1 (95% CI: 1 - 1) (SM **Table 3**).

#### High-risk plaque features on CTCA and IVUS

The sensitivity, specificity, PPV and NPV of CTCA to detect an echolucent plaque compared to IVUS were 52.4%, 98.4%, 73.3% and 96.1% respectively with AUC of 0.75. The association of EL on IVUS with the presence of  $\geq 2$  HRP features on CTCA was modest with sensitivity, specificity, PPV and NPV of 47.6%, 98.4%, 71.4% and 95.7% with AUC of 0.73.

Notably, the sensitivity, specificity, PPV and NPV of CTCA to identify EA when compared to IVUS was 93.3%, 99.6%, 93.3% and 99.6% with AUC of 0.93. The association of EA on IVUS with the presence of  $\geq 2$  HRP features on CTCA was excellent with sensitivity, specificity, PPV and NPV of 86.7%, 99.6%, 92.9% and 99.2% and AUC of 0.93 (SM Table 4).

## **Discussion**

Our results confirm that 1) manual plaque volume quantification on CTCA is comparable to IVUS with good agreement 2) manual CTCA plaque volume quantification is superior to automated software with IVUS as the reference standard 3) Automated software is accurate in luminal assessment and has agreement with IVUS 4) The high risk CTCA plaque features of positive remodelling and low attenuation plaque are significantly correlated with echo-attenuated plaque detected on IVUS. 5) There is modest correlation between echo-lucent plaque on IVUS and high-risk CTCA plaque features.

### Automated CTCA plaque volume compared to IVUS

Plaque quantification using automated software in our study was inferior to manual plaque quantification. However, the results were better compared to previous studies that assessed plaque quantification using automated software with IVUS as reference (14, 16). Automated software used for plaque quantification relies on threshold levels that allow rapid assessment of volume of plaque. Software differentiates between tissues based on the difference in HU and appears to perform best for luminal assessment. Delineation of the outer wall was less accurate and inconsistencies were also observed at branch points and in the presence of calcified or low attenuation plaque. In previous studies and in our experience, automated plaque quantification potentially can over estimate and underestimate plaque volume (16). The challenge and further research would therefore be in refining algorithms that would allow automated software to better detect vessel wall edge.

### Manual CTCA plaque volume compared to IVUS

Manual quantification of plaque volume on CTCA was comparable to IVUS in our study. Using specific window settings that allowed proper visualization of outer wall, vessel cross sectional area was more accurate and this lead to improvement in plaque volume quantification. The window settings (W 230, L 83 & W 300, L 150) adopted for this study significantly brighten the

lumen and the plaque in relation to the surrounding tissue making it easy for delineation. The additional settings aid in accurately delineating the outer wall in the presence of non-calcified plaque or calcified plaque. In previous studies comparing CTCA to IVUS, although the mean plaque volumes were similar, the limits of agreement were generally wide suggesting only modest agreement (6, 8-11, 14, 15, 31, 32). Moreover, significant inter-observer variability has been reported (8, 9, 33). The improved accuracy and agreement, and excellent inter-observer and intra-observer variability in our study with manual plaque quantification may have been contributed by the pre-specified window settings

### High-risk plaque features

In a large post mortem study of human coronary samples; it was observed that echo-attenuated plaque on IVUS was the most reliable signature for identifying a high-risk plaque and corresponded to a fibroatheroma with a necrotic core (frequently > 40% of the plaque volume). Cardiovascular deaths were more frequent compared to non-cardiovascular deaths in patients with echo-attenuation compared to those with echo-lucency, which had significantly smaller necrotic core. In our study, all echo-attenuated plaques on IVUS were identifiable on CTCA with the presence of at least two high-risk CTCA plaque features. In contrast, echo-lucent plaques on IVUS did not correspond with high-risk features on CTCA and may be less identifiable on CTCA due to blooming effect from the lumen and adjacent plaque with higher HU. Of note, we defined low attenuation plaque as < 56 HU based on a recent study involving 320 row detector CTCA with contemporary radiation doses where the cut-off for the discrimination between lipid pool and fibrous plaque was 56 HU (28). The cut off HU of 56 for LAP with our CT acquisition protocols is also validated by the excellent agreement in our study between echo-attenuated plaques on IVUS with low attenuation plaques on CTCA. Previous studies that defined low attenuation plaque as HU < 30 were performed on older generation scanners with higher radiation doses (34).

## Future directions

For plaque quantification purposes, it is imperative that institutions adopt or derive customised optimal window and level setting for the assessment of outer wall and lumen, as image acquisition techniques, contrast protocols and vendors vary. Accurate quantification of plaque on CTCA is essential for it to become the non-invasive tool to measure plaque progression or regression, which would greatly assist in testing the efficacy of novel anti-atherosclerotic drugs. Improvement in automated methods would be ideal if plaque quantification is to be applied as routine practice to predict outcomes and for risk stratification. Identification of patients at increased risk of future events based on non-invasive quantitative and qualitative plaque assessment may aid in the development of personalized preventative therapies.

## **Limitations**

This is a small, retrospective single centre study and larger prospective studies are needed to confirm our findings. There are several technical limitations in any comparative studies between CTCA and IVUS for plaque volume quantification. Manual plaque quantification is time consuming and is operator dependent. Spatial and temporal resolution constraints of CTCA and partial volume effects of calcium and lumen contrast enhancement may have affected plaque quantification. In addition, severely calcified plaques are difficult to analyse on CTCA and on IVUS due to problems of blooming artefact and acoustic shadowing respectively, and these were excluded from our cohort. Despite diligent effort using fiduciary points for co-registration between CTCA and IVUS, some discrepancies may have also affected the results. Lastly the different IVUS catheters used in the study could have been a source of bias-error.

## Conclusion

Plaque volume quantification by manual CTCA method is accurate when compared to IVUS. The presence of at least two high-risk plaque features on CTCA highly corresponds to echo attenuated plaques on IVUS.

## Acknowledgements

RKM is a recipient of Cardiac Society of Australia and New Zealand (CSANZ) scholarship and Australian Post Graduate (APA) scholarship.

DW is supported by National Health & Medical Research Institute (NHMRC) Australia Early Career Fellowship

PP is supported by National Heart Foundation Australia Career Development Fellowship

NN is supported by the National Heart Foundation Australia and National Health & Medical Research Institute (NHMRC) Australia Postgraduate Scholarship

*Disclosure:* The authors declare no conflict of interest.

## Références

1. Miller JM, Rochitte CE, Dewey M, Arbab-Zadeh A, Niinuma H, Gottlieb I, et al. Diagnostic performance of coronary angiography by 64-row CT. *The New England journal of medicine*. 2008;359(22):2324-36.
2. Cordeiro MA, Lima JA. Atherosclerotic plaque characterization by multidetector row computed tomography angiography. *Journal of the American College of Cardiology*. 2006;47(8 Suppl):C40-7.
3. Hoffmann U, Moselewski F, Nieman K, Jang IK, Ferencik M, Rahman AM, et al. Noninvasive assessment of plaque morphology and composition in culprit and stable lesions in acute coronary syndrome and stable lesions in stable angina by multidetector computed tomography. *Journal of the American College of Cardiology*. 2006;47(8):1655-62.
4. Ringqvist I, Fisher LD, Mock M, Davis KB, Wedel H, Chaitman BR, et al. Prognostic value of angiographic indices of coronary artery disease from the Coronary Artery Surgery Study (CASS). *The Journal of clinical investigation*. 1983;71(6):1854-66.
5. Nicholls SJ, Hsu A, Wolski K, Hu B, Bayturan O, Lavoie A, et al. Intravascular ultrasound-derived measures of coronary atherosclerotic plaque burden and clinical outcome. *J Am Coll Cardiol*. 2010;55(21):2399-407.
6. Voros S, Rinehart S, Qian Z, Joshi P, Vazquez G, Fischer C, et al. Coronary atherosclerosis imaging by coronary CT angiography: current status, correlation with intravascular interrogation and meta-analysis. *JACC Cardiovascular imaging*. 2011;4(5):537-48.

7. Heo R, Park HB, Lee BK, Shin S, Arsanjani R, Min JK, et al. Optimal boundary detection method and window settings for coronary atherosclerotic plaque volume analysis in coronary computed tomography angiography: comparison with intravascular ultrasound. *European radiology*. 2016;26(9):3190-8.
8. Leber AW, Becker A, Knez A, von Ziegler F, Sirol M, Nikolaou K, et al. Accuracy of 64-slice computed tomography to classify and quantify plaque volumes in the proximal coronary system: a comparative study using intravascular ultrasound. *Journal of the American College of Cardiology*. 2006;47(3):672-7.
9. Petranovic M, Soni A, Bezzera H, Loureiro R, Sarwar A, Raffel C, et al. Assessment of nonstenotic coronary lesions by 64-slice multidetector computed tomography in comparison to intravascular ultrasound: evaluation of nonculprit coronary lesions. *Journal of cardiovascular computed tomography*. 2009;3(1):24-31.
10. Papadopoulou SL, Neefjes LA, Schaap M, Li HL, Capuano E, van der Giessen AG, et al. Detection and quantification of coronary atherosclerotic plaque by 64-slice multidetector CT: a systematic head-to-head comparison with intravascular ultrasound. *Atherosclerosis*. 2011;219(1):163-70.
11. Nakazato R, Shalev A, Doh JH, Koo BK, Dey D, Berman DS, et al. Quantification and characterisation of coronary artery plaque volume and adverse plaque features by coronary computed tomographic angiography: a direct comparison to intravascular ultrasound. *Eur Radiol*. 2013;23(8):2109-17.
12. Burgstahler C, Reimann A, Beck T, Kuettner A, Baumann D, Heuschmid M, et al. Influence of a lipid-lowering therapy on calcified and noncalcified coronary plaques monitored by multislice detector computed tomography: results of the New Age II Pilot Study. *Investigative radiology*. 2007;42(3):189-95.
13. Schmid M, Achenbach S, Ropers D, Komatsu S, Ropers U, Daniel WG, et al. Assessment of changes in non-calcified atherosclerotic plaque volume in the left main and left anterior descending coronary arteries over time by 64-slice computed tomography. *The American journal of cardiology*. 2008;101(5):579-84.
14. Dey D, Schepis T, Marwan M, Slomka PJ, Berman DS, Achenbach S. Automated three-dimensional quantification of noncalcified coronary plaque from coronary CT angiography: comparison with intravascular US. *Radiology*. 2010;257(2):516-22.
15. Otsuka M, Bruining N, Van Pelt NC, Mollet NR, Ligthart JM, Vourvouri E, et al. Quantification of coronary plaque by 64-slice computed tomography: a comparison with quantitative intracoronary ultrasound. *Investigative radiology*. 2008;43(5):314-21.
16. Park HB, Lee BK, Shin S, Heo R, Arsanjani R, Kitslaar PH, et al. Clinical Feasibility of 3D Automated Coronary Atherosclerotic Plaque Quantification Algorithm on Coronary Computed Tomography Angiography: Comparison with Intravascular Ultrasound. *European radiology*. 2015;25(10):3073-83.
17. Pu J, Mintz GS, Biro S, Lee JB, Sum ST, Madden SP, et al. Insights into echo-attenuated plaques, echolucent plaques, and plaques with spotty calcification: novel findings from comparisons among intravascular ultrasound, near-infrared spectroscopy, and pathological histology in 2,294 human coronary artery segments. *J Am Coll Cardiol*. 2014;63(21):2220-33.
18. Motoyama S, Sarai M, Harigaya H, Anno H, Inoue K, Hara T, et al. Computed tomographic angiography characteristics of atherosclerotic plaques subsequently resulting in acute coronary syndrome. *J Am Coll Cardiol*. 2009;54(1):49-57.
19. Park HB, Heo R, o Hartaigh B, Cho I, Gransar H, Nakazato R, et al. Atherosclerotic plaque characteristics by CT angiography identify coronary lesions that cause ischemia: a direct comparison to fractional flow reserve. *JACC Cardiovascular imaging*. 2015;8(1):1-10.

20. Motoyama S, Ito H, Sarai M, Kondo T, Kawai H, Nagahara Y, et al. Plaque Characterization by Coronary Computed Tomography Angiography and the Likelihood of Acute Coronary Events in Mid-Term Follow-Up. *Journal of the American College of Cardiology*. 2015;66(4):337-46.
21. Nerlekar N, Ha FJ, Cheshire C, Rashid H, Cameron JD, Wong DT, et al. Computed Tomographic Coronary Angiography-Derived Plaque Characteristics Predict Major Adverse Cardiovascular Events: A Systematic Review and Meta-Analysis. *Circ Cardiovasc Imaging*. 2018;11(1):e006973.
22. Nakazato R, Shalev A, Doh JH, Koo BK, Gransar H, Gomez MJ, et al. Aggregate plaque volume by coronary computed tomography angiography is superior and incremental to luminal narrowing for diagnosis of ischemic lesions of intermediate stenosis severity. *Journal of the American College of Cardiology*. 2013;62(5):460-7.
23. Abbara S, Arbab-Zadeh A, Callister TQ, Desai MY, Mamuya W, Thomson L, et al. SCCT guidelines for performance of coronary computed tomographic angiography: a report of the Society of Cardiovascular Computed Tomography Guidelines Committee. *J Cardiovasc Comput Tomogr*. 2009;3(3):190-204.
24. Scanlon PJ, Faxon DP, Audet AM, Carabello B, Dehmer GJ, Eagle KA, et al. ACC/AHA guidelines for coronary angiography. A report of the American College of Cardiology/American Heart Association Task Force on practice guidelines (Committee on Coronary Angiography). Developed in collaboration with the Society for Cardiac Angiography and Interventions. *Journal of the American College of Cardiology*. 1999;33(6):1756-824.
25. Mintz GS, Nissen SE, Anderson WD, Bailey SR, Erbel R, Fitzgerald PJ, et al. American College of Cardiology Clinical Expert Consensus Document on Standards for Acquisition, Measurement and Reporting of Intravascular Ultrasound Studies (IVUS). A report of the American College of Cardiology Task Force on Clinical Expert Consensus Documents. *Journal of the American College of Cardiology*. 2001;37(5):1478-92.
26. Utsunomiya M, Hara H, Moroi M, Sugi K, Nakamura M. Relationship between tissue characterization with 40 MHz intravascular ultrasound imaging and 64-slice computed tomography. *J Cardiol*. 2011;57(3):297-302.
27. Saba L, Mallarin G. Window settings for the study of calcified carotid plaques with multidetector CT angiography. *AJNR Am J Neuroradiol*. 2009;30(7):1445-50.
28. Takahashi S, Kawasaki M, Miyata S, Suzuki K, Yamaura M, Ido T, et al. Feasibility of tissue characterization of coronary plaques using 320-detector row computed tomography: comparison with integrated backscatter intravascular ultrasound. *Heart and vessels*. 2016;31(1):29-37.
29. Kashiwagi M, Tanaka A, Kitabata H, Tsujioka H, Kataiwa H, Komukai K, et al. Feasibility of noninvasive assessment of thin-cap fibroatheroma by multidetector computed tomography. *JACC Cardiovascular imaging*. 2009;2(12):1412-9.
30. Pu J, Mintz GS, Brilakis ES, Banerjee S, Abdel-Karim AR, Maini B, et al. In vivo characterization of coronary plaques: novel findings from comparing greyscale and virtual histology intravascular ultrasound and near-infrared spectroscopy. *European heart journal*. 2012;33(3):372-83.
31. Pohle K, Achenbach S, Macneill B, Ropers D, Ferencik M, Moselewski F, et al. Characterization of non-calcified coronary atherosclerotic plaque by multi-detector row CT: comparison to IVUS. *Atherosclerosis*. 2007;190(1):174-80.
32. Stolzmann P, Schlett CL, Maurovich-Horvat P, Maehara A, Ma S, Scheffel H, et al. Variability and accuracy of coronary CT angiography including use of iterative reconstruction algorithms for plaque burden assessment as compared with intravascular ultrasound-an ex vivo study. *European radiology*. 2012;22(10):2067-75.

33. Pflederer T, Schmid M, Ropers D, Ropers U, Komatsu S, Daniel WG, et al. Interobserver variability of 64-slice computed tomography for the quantification of non-calcified coronary atherosclerotic plaque. *Rofo*. 2007;179(9):953-7.
34. Motoyama S, Kondo T, Anno H, Sugiura A, Ito Y, Mori K, et al. Atherosclerotic plaque characterization by 0.5-mm-slice multislice computed tomographic imaging. *Circulation journal : official journal of the Japanese Circulation Society*. 2007;71(3):363-6.

**Table 1. Baseline Patient Characteristics (n= 27)**

Age, years	64.29 ± 8.4
Male	16 (59 %)
<b>Risk factors</b>	
Hypertension	59 % (16)
Diabetes mellitus	15 % (4)
Dyslipidaemia	74 % (20)
Current smoker	26 % (7)
Obesity	19 % (5)
Ex Smokers	26 % (7)
Family history of IHD	56 % (15)
<b>Distribution of Vessels (32)</b>	
Left main artery	28% (9)
Left anterior descending artery	50% (16)
Left circumflex artery	12.5 % (4)
Right coronary artery	9 % (3)

**Table 2: Comparison between manual and automated using IVUS as reference**

Parameter	Manual		Automated	
	Mean difference +/- SEM between CTCA and IVUS	P value	Mean difference +/- SEM between CTCA and IVUS	P value
LCSA	0.19 ± 0.17mm <sup>2</sup>	0.26	0.07 ± 0.16mm <sup>3</sup>	0.66
VCSA	0.22 ± 0.25 mm <sup>2</sup>	0.37	4.6 ± 0.28mm <sup>3</sup>	<0.001
Plaque volume (Per slice)	0.06±0.07mm <sup>3</sup>	0.44	2.3 ± 0.09mm <sup>3</sup>	<0.001
Calcified	0.25 ± 0.6mm <sup>3</sup>	<0.001	0.4 ± 0.12mm <sup>3</sup>	0.001
Non Calcified	0.19 ± 0.09mm <sup>3</sup>	0.25	1.78 ± 0.4mm <sup>3</sup>	<0.001
Plaque volume (per vessel)	3.1 ± 2.8mm <sup>3</sup>	0.92	33.04 ± 9 mm <sup>3</sup>	<0.01

*LCSA: luminal cross sectional area, VCSA: vessel cross sectional area*

Table 3. Intra and Inter observer variability for manual plaque volume quantification on CTCA

Manual Plaque quantification	Intra observer	Inter observer
Intra class correlation Coefficient	0.99 (95% CI: 0.9 - 0.99).	0.85(0.4 – 0.96)
Bland Altman		
Mean difference	0.114±1.96%	0.54±3.66%
P value	p =0.86	p=0.65
Limits of agreement	3.84 - 3.62	7.72 - 6.64

Table 4. Association between high-risk plaque features (HRP) on CTCA and plaques with features of echolucency (EL) and echo attenuation (EA) on IVUS

	EL on IVUS Vs. HRP features on CTCA	EA on IVUS Vs. HRP feature on CTCA	EL on IVUS Vs. $\geq 2$ HRP feature on CTCA	EA on IVUS Vs. $\geq 2$ HRP feature on CTCA
Sensitivity	52.4	93.3	47.6	86.7
Specificity	98.4	99.6	98.4	99.6
Positive Predictive Value	73.3	93.3	71.4	92.9
Negative Predictive Value	96.1	99.6	95.7	99.2
AUC	0.75	0.93	0.73	0.93

**Figure 1:** (A) Cross section of a vessels with a non-calcified plaque on unadjusted window settings (B) The lumen and the outer wall are better delineated on window settings of width 230 and level of 83. (C) The outer vessel wall (yellow line) and the lumen (blue line) are drawn (D) Various components of plaque are represented in colour (red – low attenuation plaque, blue – fibrous plaque and green – lumen).

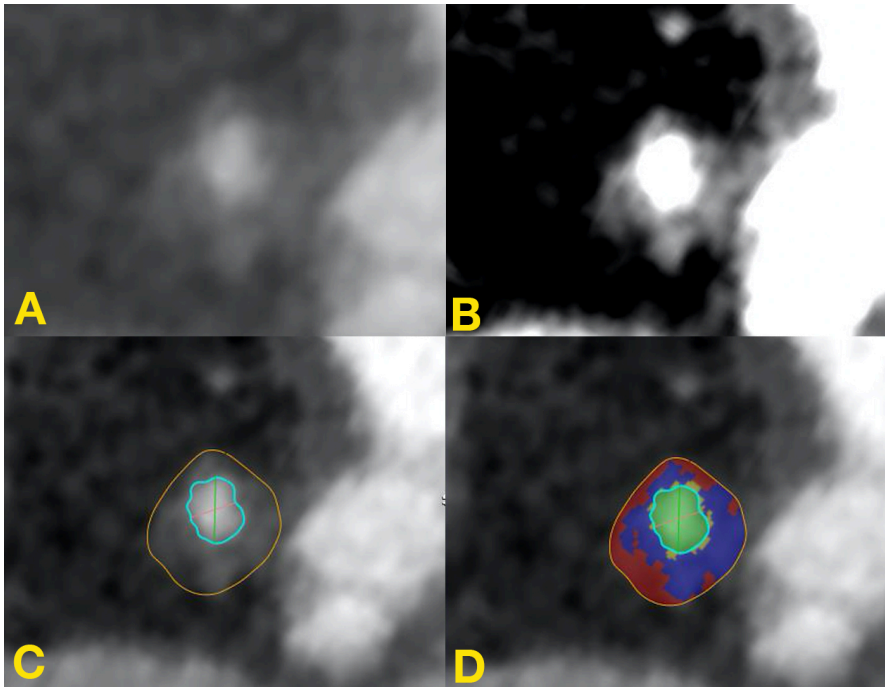


**Figure 2:** High-risk plaque A) Yellow arrow indicating plaque at the distal segment of left main artery extending into proximal left anterior descending artery. The plaque displays high-risk features such as positive remodelling and low attenuation plaque B) Cross section of the high-risk plaque C) Cross section of the high-risk plaque with various plaque components depicted in colour. Napkin ring sign: Low attenuation plaque (lipid pool) is shown in red surrounded by fibrous plaque (blue). Lumen is represented by green colour.

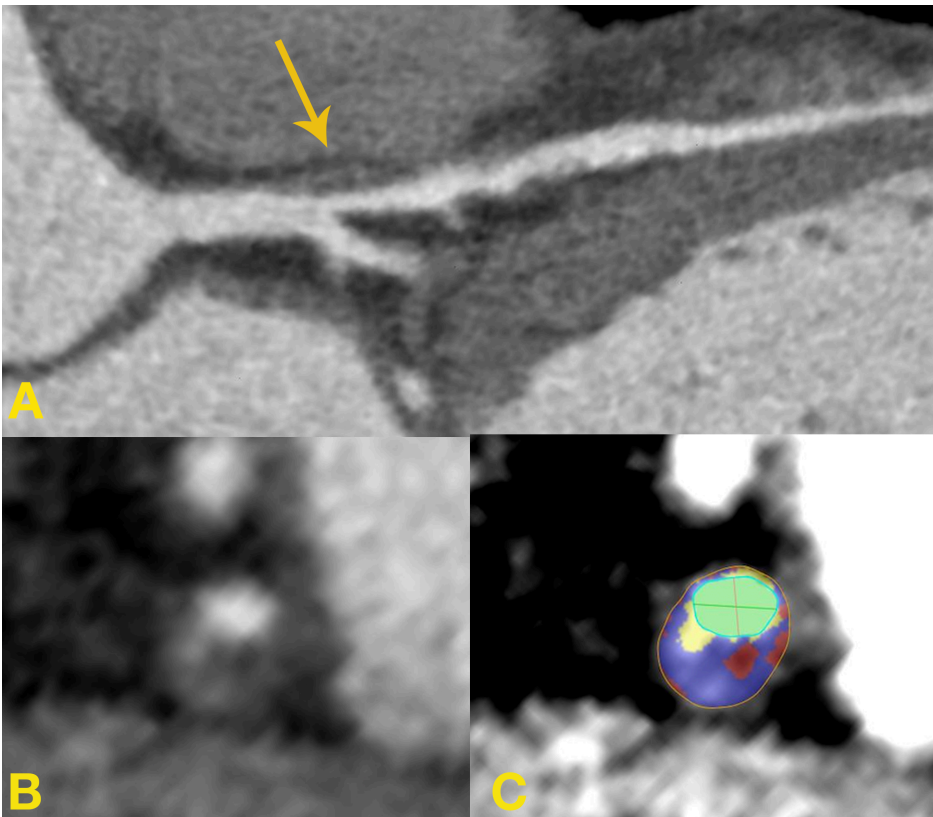


**Figure 3:** A) Multiplanar reconstruction image of left main and left circumflex artery (LCx). There is a non-calcified plaque at the distal left main extending into the proximal segment of LCx. B) Cross section of the distal left main on CTCA with plaque components shown. Low attenuation plaque is represented in red colour, fibrous plaque in blue, calcified plaque in yellow and the lumen in green. C) IVUS image of the same plaque in the distal left main artery showing echo attenuation due to the deep lipid pool close to the outer wall.

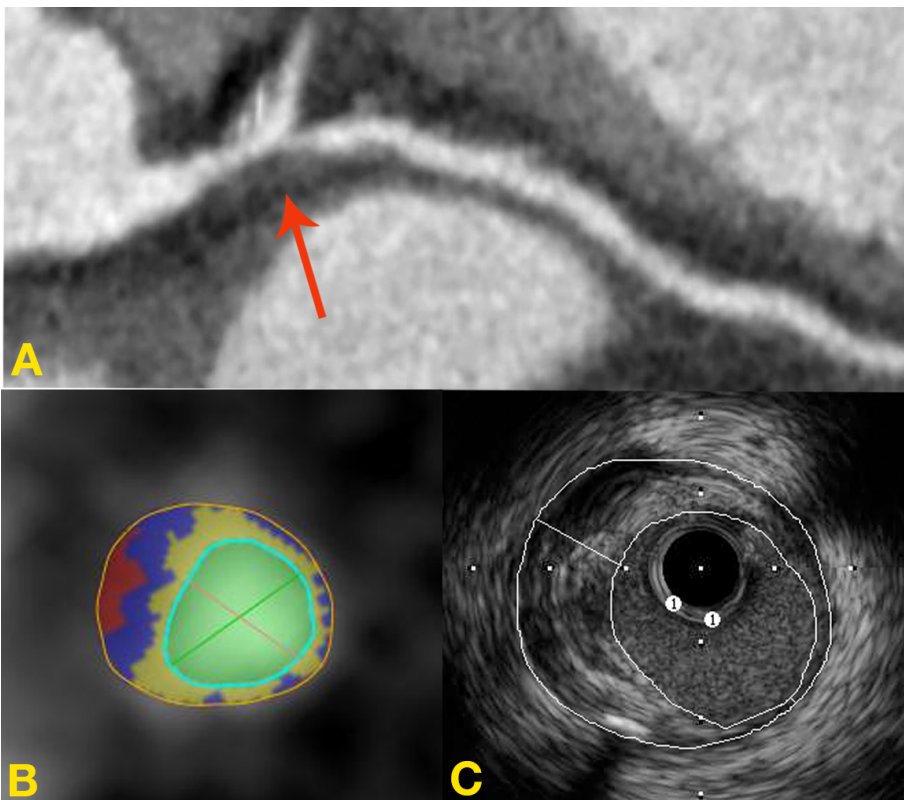
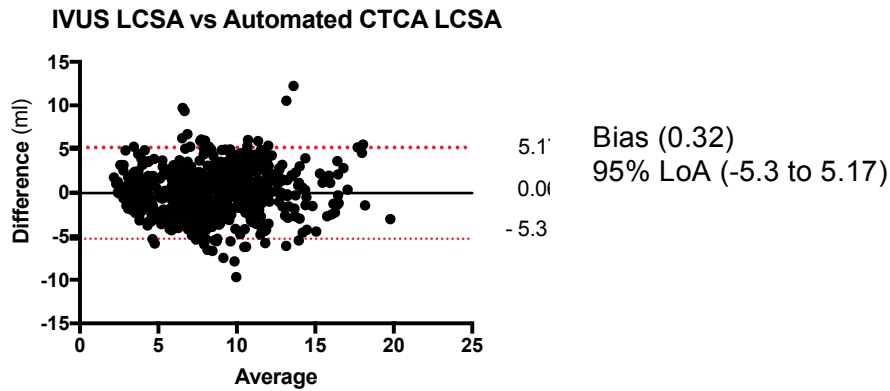
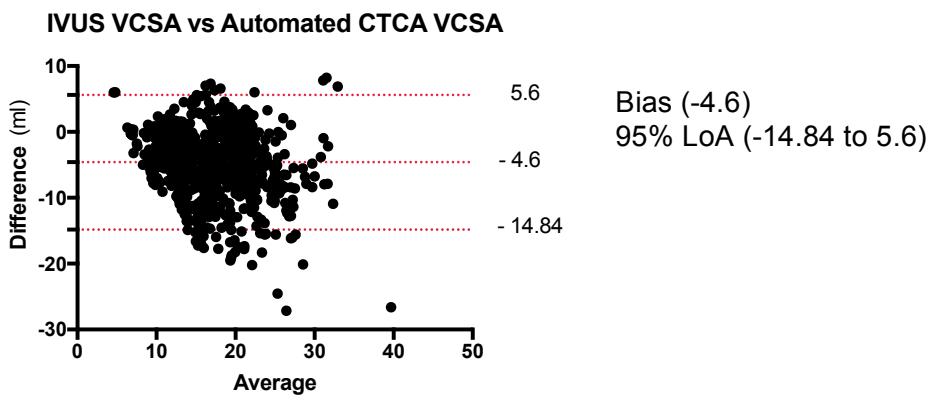


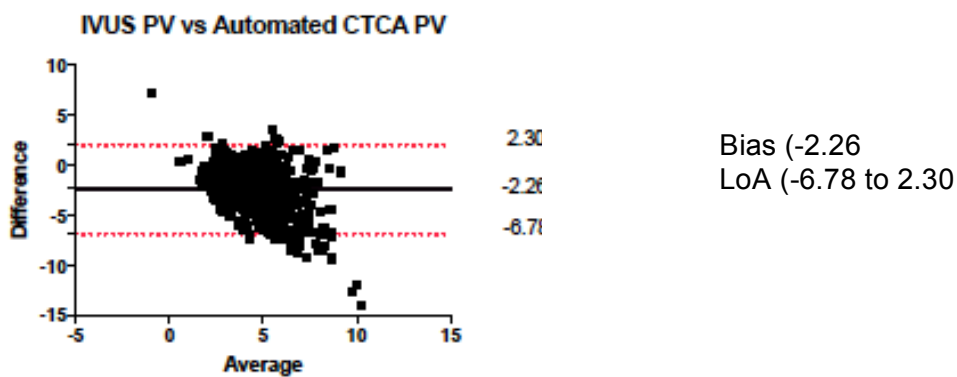
**Figure 4:** Bland-Altman plots A) lumen B) Vessel Volume and C) plaque volume between intravascular ultrasound and Computed tomography coronary angiography using automated software.



A

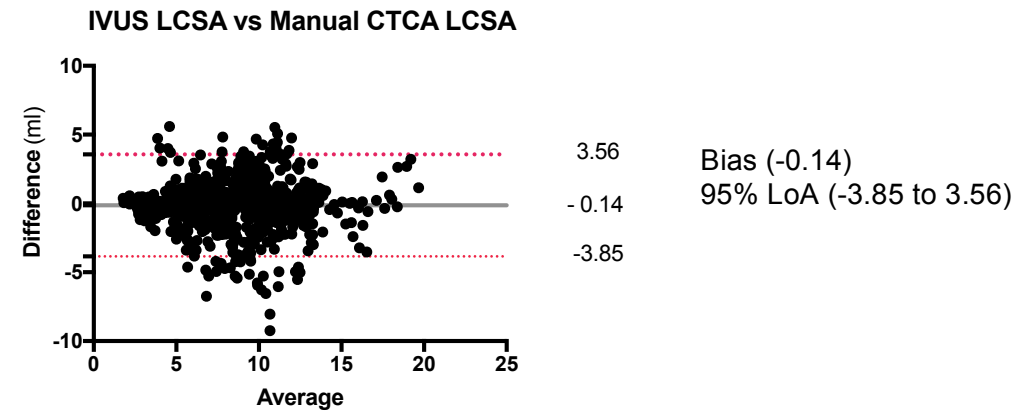


B

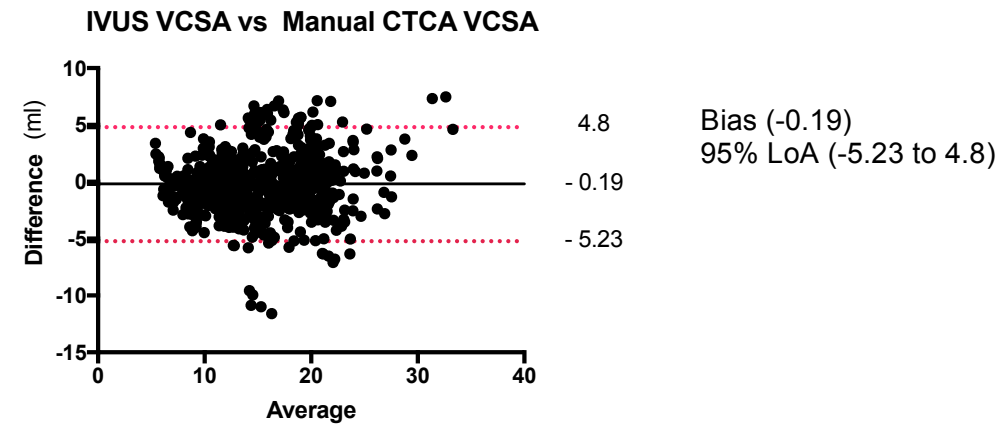


C

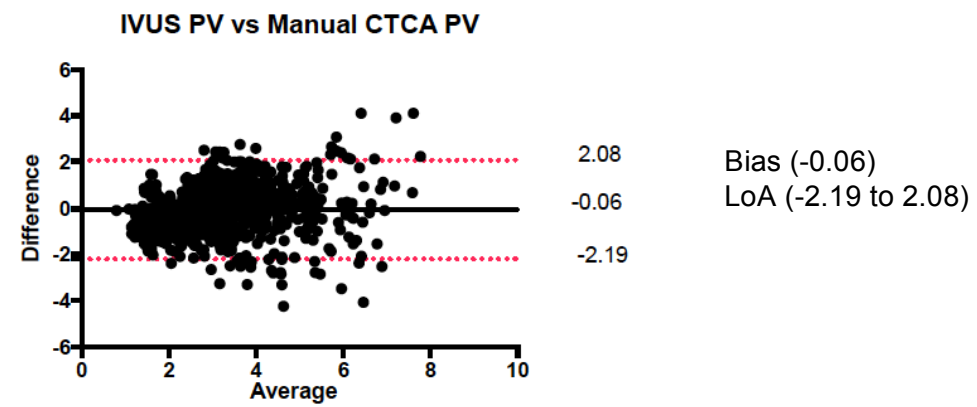
**Figure 5:** Bland-Altman plots for limits of agreement for A) lumen B) Vessel volume and C) plaque volume between intravascular ultrasound and computed tomography coronary angiography using manual methods for plaque quantification.



A

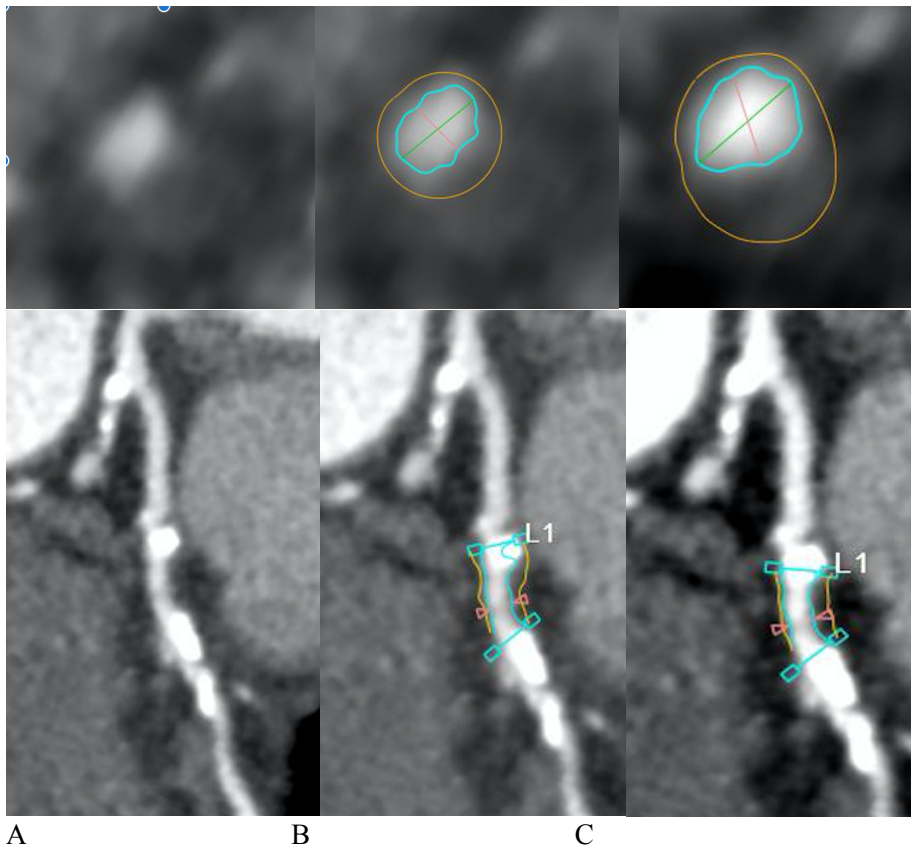


B



C

**Figure 6:** Plaque quantification on CTCA. A) Unadjusted cross sectional image showing non-calcified plaque with positive remodelling and the corresponding multiplanar reconstruction (MPR) image below B) Automated plaque assessment where the outer wall passes through the plaque with underestimation of plaque volume shown in MPR image C) Manual plaque quantification with adjusted vessel wall and corresponding MPR image accounting for the entire plaque.



## **Chapter 4: Longitudinal assessment of coronary Plaque using Computed Tomography Coronary Angiography (CTCA) and Intravascular Ultrasound (IVUS)**

*Ravi Kiran Munnur MBBS<sup>1</sup>, Jordan Andrews<sup>2,3</sup>, Yu Kataoka MBBS, PhD<sup>2</sup>, Peter J*

*Psaltis MBBS (Hons), PhD<sup>1,3</sup>, Stephen J Nicholls MBBS, PhD<sup>2,3</sup>, Yuvaraj Malaiapan MBBS, MD<sup>1</sup>, Sujith*

*Seneviratne MBBS (Hons), James D Cameron MBBS, MD<sup>1</sup>, Dennis TL Wong MBBS (Hons), MD, PhD<sup>1,2\*</sup>*

1 Monash Cardiovascular Research Centre, Department of Medicine (Monash Medical Centre) Monash University and Monash Heart, Monash Health, 246 Clayton Road, Clayton, 3168 VIC, Australia

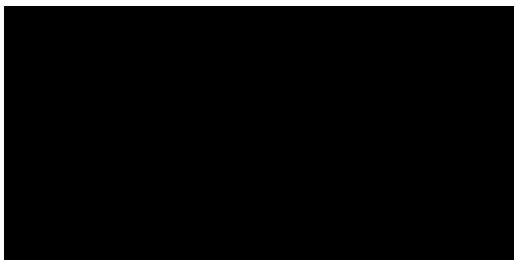
2 South Australian Medical Research Institute (SAHMRI), Adelaide, Australia

3 Discipline of Medicine, University of Adelaide, Adelaide, Australia

### **Unpublished / to be submitted**

\* Associate Professor Dennis Wong

Monash Cardiovascular Research Centre, Monash University and MonashHeart, Monash Health, Clayton, Victoria, Australia



## **Abstract**

**Objective:** To determine the accuracy of quantitative Computed Tomography Coronary Angiography (CTCA) coronary plaque progression / regression against Intravascular Ultrasound (IVUS).

### **Background:**

Intravascular ultrasound (IVUS) is the current gold standard test to evaluate the efficacy of medical therapies on coronary atheroma progression. Although studies have shown that measurement of coronary plaque on computed tomography coronary angiography (CTCA) correlates with IVUS, serial quantitative CTCA plaque measurements have never been compared to IVUS.

### **Methods:**

Ten patients (7 men, ages  $61 \pm 5.4$  years) in a prospective study underwent serial invasive coronary angiography, IVUS and CTCA with a median interval of 334.5 (IQR: 288 – 438) days. Plaque geometry and composition was quantified after spatial co-registration using fiducial points on segmental and slice-by-slice (0.5mm) basis on IVUS and CTCA. Baseline and follow up total atheroma volume, percent atheroma volume (PAV) and normalised total atheroma volume (nTAV) were assessed. PAV and nTAV change were calculated and compared between CTCA and IVUS.

### **Results:**

Analysis was performed on 300 slices and each patient had a median of 31.5 slices. There was no significant difference in total atheroma volume measurement between CTCA and IVUS at baseline ( $202.1 \pm 122.1$  vs  $195.4 \pm 111.7$ ,  $p=0.49$ ;  $r=0.97$ ) and at follow up ( $195 \pm 134.3$  vs.  $182.33 \pm 127.3$ ,  $p=0.21$ ;  $r=0.96$ ). Between CTCA and IVUS, PAV change ( $-2.61 \pm 3.44$  vs.  $0 \pm 4.88$ ,  $p=0.53$ ,  $r=0.65$ ) was moderately correlated with no significant difference and nTAV change ( $-17.98 \pm 28.8$ ,  $p=0.26$ ,  $r=0.84$ ) was strongly correlated with no significant difference.

**Conclusion:**

This is the first validation that serial CTCA quantitative measurements of coronary plaque change correlate with IVUS. There was good agreement between CTCA and IVUS in plaque measurement at baseline and follow up. CTCA was comparable to IVUS in the measurement of plaque volume change over time.

**Key words**

Computed Tomography Coronary Angiography, Intravascular Ultrasound, Plaque quantification, plaque progression, Coronary Artery Disease

**Abbreviations**

CTCA: Computed Tomography Coronary Angiography

IVUS: Intravascular Ultrasound

PAV: Percent atheroma Volume

TAV: Total atheroma Volume

CAD: Coronary artery disease

ICA: Invasive coronary angiography

ACS: Acute coronary syndrome

nTAV: Normalised Total atheroma volume

PAV: Percent atheroma volume

EEM: External elastic membrane

IQR: Interquartile range

QCT: Quantitative computed tomography

## **Introduction**

Atherosclerotic coronary artery disease (CAD) is the leading cause of morbidity and mortality in the developed world (1). Sub clinical disease develops slowly and progresses over many decades before abruptly causing clinical manifestations (2). There is a large body of evidence that has established the direct relationship between burden of coronary atherosclerosis, its progression and adverse cardiovascular events (3-6). Intravascular ultrasound (IVUS) is the current gold standard for precise quantitative assessment of plaque volume and has been used in clinical trials to evaluate the efficacy of medical therapies on coronary atheroma progression (7-10). IVUS is however limited by invasive nature of the test and high cost.

Computed tomography coronary angiography (CTCA) is an established non-invasive test to assess coronary stenosis with excellent negative predictive value and correlates favourably with invasive coronary angiography (ICA) (11). Quantitative measurements of coronary plaque using CTCA have been shown in previous studies to correlate with IVUS (12-16). Although CTCA has been touted as a promising non-invasive tool to assess coronary atheroma progression in response to antiatherosclerotic therapies, serial quantitative CTCA plaque measurements have never been compared to IVUS. The objective of this study is to determine the accuracy of quantitative CTCA coronary plaque progression / regression against IVUS.

## **Methods**

From August 2014 to March 2016, patients who underwent clinically indicated CTCA or invasive coronary angiography (ICA) were prospectively recruited. ACS patients with non-culprit artery stenosis on invasive coronary angiography and patients referred for CTCA with suspected coronary artery disease were approached to participate in this study. In ACS patients undergoing invasive ICA, IVUS assessment of the non-culprit vessel with mild to moderate stenosis was performed. In patients with stable coronary artery disease, any epicardial coronary artery with mild to moderate stenosis was also assessed by IVUS. At baseline and at follow up after 9-15months,

CTCA and IVUS were performed within two weeks interval. Institutional ethic committee approved the study and informed consent was obtained from participants. All patients included in this study had coronary artery disease in major epicardial vessels in the proximal or mid segments with at least 30% stenosis. Excluded were patients with allergy to contrast material, renal insufficiency, acute ST-segment elevation myocardial infarction, impaired left ventricular function, valvular heart disease, severely calcified vessels precluding CTCA interpretation, poor quality CTCA and IVUS images, and CTCA/IVUS segments that could not be matched due to lack of fiducial points.

#### CT coronary angiography

Patients underwent cardiac CT assessment using a 320-row detector CT scanner (Aquilion One Vision; Toshiba Medical Systems Corp., Tokyo, Japan). All patients received sublingual nitroglycerine, and additional beta-blockers were administered to achieve a pre-scan heart rate of <60 beats/min in accordance with Society of Cardiovascular Computed Tomography guidelines (17).

A bolus of 55 mL of 100% iohexol 56.6 g/75 mL (Omnipaque 350; GE Healthcare, Princeton, NJ) was injected into an antecubital vein at a low rate of 5 mL/sec, followed by 20 mL of a 30:70 mixture of contrast material and saline, followed by 30 mL of saline. Scanning parameters were as follows: detector collimation: 320 x 0.5 mm; tube current: 300–500 mA (depending on body mass index), tube voltage: 120 kV; gantry rotation time: 350 msec; and temporal resolution: 175 msec. Prospective electrocardiographic gating was used; covering phases 70%– 80% of the R-R interval. For images acquired at heart rates of 65 beats per minute or slower, scanning was completed with a single R-R interval utilizing a 180° segment. In patients with a heart rate greater than 65 beats per minute, data segments from two consecutive beats were used for multi-segment reconstruction with an improved temporal resolution of 87 msec.

#### Invasive Coronary Angiography

All the patients in the study underwent clinically indicated coronary angiography. Invasive coronary angiography was performed as per the standard catheterisation in accordance with the American College of Cardiology guidelines for coronary angiography (18).

#### IVUS acquisition

IVUS was done in a standard fashion using commercially available catheters (40MHz, Atlantis SR Pro, Boston Scientific, Boston, Massachusetts or Volcano Eagle Eye IVUS-catheter, 20 MHz, electronic transducer or Volcano Inc., Rancho Cordova, California). After intracoronary administration of 100-200 µg of nitroglycerine, IVUS images were acquired using automated mechanical pullback devices at a continuous pull back speed of 0.5 mm/s (19). The images were stored on a CD-ROM for offline analysis in a core lab (South Australian Health and Medical Research institute).

#### Analysis of CT coronary angiograms

Data was transferred to an external workstation (Vitrea 6, version 6.0; Vital Images, Minnetonka, Minnesota) for further analysis. Plaque quantification was performed using a dedicated attenuation based software tool (Sure Plaque, Vitrea 6, version 3.0; Vital Images and Toshiba Medical Systems). Manual quantification of plaque was performed after delineation of the lumen and the outer vessel wall using the window settings of 230W and 83 L if the luminal Hounsfield unit (HU) was <500; and if the luminal HU was >500, settings of 300W and 150 L were used (20). Additional window and level settings of 740W and 220L was used if necessary to assess outer vessel wall (21) (**Figure 1**). In the presence of calcium, outer wall was assessed with modified setting according to luminal HU ( $W = \text{Luminal HU} \times 2.07$ ;  $L = \text{luminal HU} \times 0.72$ )(22). Two experienced cardiologists (KM, DW) who were blinded to the results of coronary angiography and IVUS measurements performed the analysis independently. Vessels with stenosis in proximal or mid segment were included in the study after agreement between the cardiologists.

Normalised total atheroma volume (TAV) was calculated as follows

$$TAV_{\text{normalized}} = (\Sigma (\text{outerwall}_{\text{area}} - \text{lumen}_{\text{area}}) / \text{no. of images analysed}) \times \text{median no. of images in cohort.}$$

Firstly, plaque volume was calculated by subtracting lumen area from outer wall followed by summation. The summated plaque areas (TAV) were multiplied by the number of images in the cohort divided by the number of images analysed for the patient. Normalisation of TAV was done to compensate for the differences in the segment length between subjects.

*Percent atheroma volume (PAV) was calculated as follows:*

$$PAV = (\Sigma (\text{Outer wall}_{\text{area}} - \text{lumen}_{\text{area}}) / \Sigma \text{outerwall}_{\text{area}}) \times 100,$$

PAV was calculated by first summing the plaque area. This value was then divided by summation of outer-wall area multiplied by 100.

#### IVUS plaque volume measurements

All the images were analysed in a core laboratory (South Australian Medical Research Institute) that was blinded to the CTCA results. The cross sectional images that were analysed were 0.5 mm in thickness. Lumen and vessel (external elastic membrane) were manually traced. The measurements were performed according to the American College of Cardiology recommendations (19). The leading edges of the lumen and external elastic membrane (EEM) were traced by manual planimetry. Plaque area was defined as the area occupied between these leading edges. Total atheroma volume was calculated as the summation of plaque area in each measured image.

PAV and TAV were calculated. The IVUS images and CTCA images were analysed on a 0.5mm segments commencing from a major landmark such as a branch. The analysed sections on both the

imaging modalities were matched based on branch points and calcified plaques. A maximal discrepancy of 1.5 mm of segment length was considered acceptable between the two imaging modalities (13)

The inter and intra observer variability of CTCA plaque volume measurements were assessed for 20% of the CTCA segments.

## Results

Of the 15 patients enrolled, five patients were excluded. In 3 of these patients, the IVUS image quality was not sufficient for analysis due to unsteady pullbacks, 1 patient had myocardial infarction prior to follow up and 1 patient withdrew from the study. Of the ten patients included in the study, 2 had ACS whilst 8 patients had stable coronary artery disease. The mean age was  $61 \pm 5.4$  years and 7 patients were male. The median duration between CTCA and IVUS was 29 (IQR: 25.5-31.5) days at baseline and 6.5 (IQR: 6-11) days at follow up. The median duration between baseline and follow up investigations was 334.5 (IQR: 288 – 438) days. The baseline characteristic of the patients is shown in **Table 1**. There were ten vessels comprising seven anterior descending arteries, three left circumflex arteries and one ramus intermediate artery. There was a total of 300 slices analysed and median number of slices per patient was 31.5.

There was excellent correlation and no significant difference in total atheroma volume measurement between IVUS and CTCA at baseline ( $195.4 \pm 111.7$  vs.  $202.1 \pm 122.1$ ,  $p=0.49$ ;  $r=0.97$ ). There was also excellent correlation and no significant difference between means of follow up plaque volume between IVUS and CTCA ( $182.33 \pm 127.3$  vs.  $195.2 \pm 134.3$ ,  $p=0.21$ ;  $r=0.96$ ) (**SM Table 3**).

There was no significant difference in baseline %PAV between IVUS and CTCA ( $41.6 \pm 8.4$  vs.  $38.7 \pm 7.1$ ,  $p=0.11$ ,  $r=0.7$ ) and the agreement was good for follow up %PAV ( $39.01 \pm 9.4$  vs.

38.76±10.5, p=0.9, r=0.96). There was no significant difference between IVUS and CTCA for PAV change with moderate correlation (-2.61±3.44 vs. 0±4.88, p=0.53, r=0.65) (**SM Table 4**) (**Fig 2**). Nine out of 10 vessels had PAV regression as assessed on IVUS compared to 6 out of 10 vessels as assessed on CTCA. The classification of progression or regression of PAV was concordant in 7 vessels between IVUS and CTCA (**Table 2**). The PAV change between CTCA and IVUS was comparable with low bias (-2.28) with narrow limits of agreement (-9.67 to 5.11) (**Fig 3**).

There was excellent agreement between IVUS and CTCA for baseline nTAV (211.9±58.9 vs. 209.9±49.9, p=0.84, r=0.84) and for follow up nTAV (193.96±67.35 vs. 197.62±53.3, p=0.7, r=0.9). There was no significant difference between IVUS and CTCA for nTAV change (-17.98±28.8, p=0.26, r=0.84) (**SM 5**) (**Fig 2 & 3**). Eight vessels had nTAV regression as assessed on IVUS and CTCA. The classification of progression or regression of nTAV was concordant in all 10 vessels between IVUS and CTCA. The nTAV change between CTCA and IVUS was comparable with low bias (-2.28) with narrow limits of agreement (-17.64 to 10.39) (**Fig 3**).

Plaque quantification was highly reproducible with an intraobserver mean difference of 0.114±1.96%, p =0.86, limits of agreement: 3.84 - 3.62 and a correlation coefficient of 0.99 (95% CI: 0.9 - 0.99). There was good interobserver variability with mean difference of 0.54±3.66%, p=0.65, limits of agreement 7.72 - 6.64 and a correlation coefficient of 0.85(0.4 – 0.96) (**Table 3**)

## **Discussion**

This study has demonstrated that serial assessment of plaque progression / regression on CTCA was feasible and comparable to the gold standard IVUS. Our finding also lends support to the numerous studies that have shown good correlation between CTCA and plaque measurements. We found

excellent correlation and no significant difference in plaque volume measurement between IVUS and CTCA at baseline ( $p=0.49$ ,  $r=0.97$ ) at follow up ( $p=0.21$ ,  $r=0.96$ ).

Although past studies have shown good correlation between CTCA and IVUS for plaque measurements with small mean differences for various geometrical parameters, the limits of agreement have generally been wide (23). This implies that quantitative CTCA assessment might be suitable for population studies with suitable sample size but has limited accuracy on a per-patient basis. In our study, in addition to good correlation between CTCA and IVUS for PAV and nTAV change, we found low bias and narrow limits of agreement for PAV and nTAV change. The classification of progression or regression of nTAV and PAV was concordant in all 10 vessels and 7 vessels respectively between CTCA and IVUS. Our results suggest that it is feasible to study plaque progression using CTCA in an individual patient. Our findings lend support to a recent study that found good correlation between segmental plaque volume changes on IVUS with total plaque volume change on CTCA (24). Whilst the authors noted no correlation between IVUS and CTCA for plaque volume measurements, there was correlation ( $r=0.62$ ) for plaque volume change on per patient analysis. The correlation improved significantly ( $r=0.82$ ) when changes in normalised coronary plaque volume were considered. We have also observed that when normalised for mean length of all the vessels included in the study, nTAV change had a better correlation ( $r=0.84$ ) compared to PAV change ( $r=0.65$ ). In addition, we found excellent agreement and correlation between CTCA and IVUS for baseline plaque volume, follow up plaque volume, baseline normalised TAV and follow up normalised TAV. As the plaque change over time can be small, considering total coronary segment length would be of importance for the determination of TPV in serial IVUS or CTCA studies (25). The luminal volume and vessel volume on CTCA can be influenced by timing or dose of nitroglycerin and the measurements can be influenced by image quality and contrast load. Hence, normalised TPV taking into account the mean length of assessed

coronary segment of all the subjects in the study may be a more reliable measure of plaque volume change in serial CTCA studies.

There have been a few retrospective studies that assessed plaque progression using CTCA (26-29). Notably, in a prospective randomised double blind trial, lipid therapy was tested in human immunodeficiency virus (HIV) patients and CTCA measured total plaque volume change of +12% was observed in placebo group vs -4.7% in atorvastatin group (30). These studies are encouraging and demonstrate the feasibility of CTCA for plaque progression studies. In this context, demonstration of the accuracy of CTCA to track plaque volume changes over time that is comparable IVUS as shown in our study assumes importance.

Despite the advancements in the treatment of coronary artery disease, patients with coronary disease continue to be at risk of cardiovascular events. In the Prove-It Trial, 22.4% of patients experienced a coronary event during 2 years of intensive statin therapy (31). It is possible that these treatments fail to target some of the inflammatory pathways implicated in the disease and novel therapies are required to prevent plaque growth and to promote plaque stabilisation. Measurement of subclinical disease with a non-invasive test such as CTCA will greatly assist in designing clinical trials that determine the efficacy of various therapies and in monitoring of preventive treatments to reduce the risk of clinical cardiovascular disease.

#### Differences between CTCA and IVUS

There are several differences between IVUS and CT that can potentially lead to inter-method variability. Firstly, the resolution of IVUS is superior to CTCA. Secondly, the plaque measure on IVUS is between the intima and the external elastic lamina, whereas, on CT, the outer-wall could include adventitia, as the EEM is not visualised on CT. Thirdly, there is blooming artefact on CT

due to the contrast in the lumen with the potential to overestimate the luminal area. Calcium also causes blooming artefact on CTCA and acoustic shadowing from calcium makes it challenging for analysis even on IVUS. Due to these inter method variability, differences in plaque volume measurement between the modalities is inevitable. We have shown in this study that with appropriate window settings and manual adjustment, accuracy and reproducibility of plaque measurement on CTCA correlates well with IVUS. Specifically, appropriate window settings are required to improve the accuracy of delineating the vessel wall, which is usually the biggest limitation when it comes to plaque quantification due to the low HU difference between vessel wall and the adjacent tissues.

These window settings have been derived based on the acquisition protocols at our institution and based on a relatively higher HU contrast intensity in the lumen. Hence, it is imperative that to improve accuracy, institutions adopt the window settings based on vendor, contrast and acquisition protocols.

#### Manual vs. Automated plaque quantification

Manual plaque quantification using appropriate window setting is the most accurate method but is time consuming and is expert dependant. Accurate fully automated software that is reproducible would be ideally suited for plaque progression studies and it has been shown in a few studies to be comparable to IVUS for plaque quantification (12). Automated software differentiates between tissues based on HU and appears to perform best for luminal assessment. Delineation of outer wall was less accurate and inconsistencies were observed, especially at branch points and in the presence of non-calcified plaque requiring additional contouring adjustments. In our experience, automated QCT can potentially overestimate as well as underestimate plaque volume. In a study by Park et al, automated plaque assessment was compared to manual plaque quantification by expert and non-

expert readers quantitative computed tomography (QCT). Although there was no significant difference in the mean plaque volume between the groups, it was significantly underestimated by automated QCT ( $152.20 \pm 87.20$  vs.  $129.92 \pm 75.26$ ,  $p < 0.001$ ). As several serial imaging studies have shown that plaque volume change over time is small, improvement in the accuracy of automated plaque quantification is desirable (6). The challenge and further research is needed in refining algorithms that would allow automated software to better detect the outer wall.

### **Serial CTCA imaging**

For serial CTCA plaque quantification, high quality CTCA images are essential as the plaque volume changes over time are small. Moreover, CTCA has poor tissue penetration and the outer wall demarcation is optimised at low noise, which usually requires higher radiation doses. However, serial CTCA also exposes patients to additional radiation. Over the years, there has been substantial reduction in radiation doses for CTCA acquisition. In a multicentre analysis, a median dose of 12.5 mSv was reported in 2009 and in contrast, the latest third generation CT scanners report comparable image quality at sub millisievert dosage (32, 33). Technical improvements such as multi energy CT, improved detector systems and faster acquisition speeds may help plaque quantification at low radiation doses(34). In addition, of aid would be improvements in image reconstruction algorithms aimed at improving resolution and reducing noise and artefacts(35).

### **Future directions**

We have shown in this study that with appropriate window settings and manual adjustment, accuracy and reproducibility of plaque measurement on CTCA correlates well with IVUS. We acknowledge that ours was a small study but a step in the right direction.

Larger studies are needed to compare CTCA and IVUS in serial plaque assessment using rigorous methodology. Careful planning and standardization of CTCA protocols is also needed to ensure that baseline and follow up scan parameters are similar. Lastly, appropriate window settings according

to the vendor, contrast and acquisition protocols are essential.

### **Limitations**

Ours was a single centre; single vendor study with limited number of patients and requires confirmation in larger studies. Although the segments on IVUS and CTCA were matched diligently based on fiduciary points, some discrepancies may have influenced the results.

### **Conclusions**

Manual plaque assessment on CTCA had good correlation and agreement with IVUS in the longitudinal assessment of coronary plaque. CTCA was comparable to IVUS in tracking plaque changes over time.

### **Acknowledgements**

RKM is a recipient of Cardiac Society of Australia and New Zealand (CSANZ) scholarship and Australian Post Graduate (APA) scholarship.

DW is supported by National Health & Medical Research Institute (NHMRC) Australia Early Career Fellowship

*Disclosure:* The authors declare no conflict of interest.

### **References:**

1. Murray CJ, Lopez AD. Mortality by cause for eight regions of the world: Global Burden of Disease Study. *Lancet*. 1997;349(9061):1269-76.
2. Libby P, Theroux P. Pathophysiology of coronary artery disease. *Circulation*. 2005;111(25):3481-8.
3. Cliff WJ, Heathcote CR, Moss NS, Reichenbach DD. The coronary arteries in cases of cardiac and noncardiac sudden death. *The American journal of pathology*. 1988;132(2):319-29.

4. Ringqvist I, Fisher LD, Mock M, Davis KB, Wedel H, Chaitman BR, et al. Prognostic value of angiographic indices of coronary artery disease from the Coronary Artery Surgery Study (CASS). *The Journal of clinical investigation*. 1983;71(6):1854-66.
5. Ellis S, Alderman EL, Cain K, Wright A, Bourassa M, Fisher L. Morphology of left anterior descending coronary territory lesions as a predictor of anterior myocardial infarction: a CASS Registry Study. *Journal of the American College of Cardiology*. 1989;13(7):1481-91.
6. Nicholls SJ, Hsu A, Wolski K, Hu B, Bayturan O, Lavoie A, et al. Intravascular ultrasound-derived measures of coronary atherosclerotic plaque burden and clinical outcome. *Journal of the American College of Cardiology*. 2010;55(21):2399-407.
7. Nissen SE, Tuzcu EM, Schoenhagen P, Brown BG, Ganz P, Vogel RA, et al. Effect of intensive compared with moderate lipid-lowering therapy on progression of coronary atherosclerosis: a randomized controlled trial. *JAMA : the journal of the American Medical Association*. 2004;291(9):1071-80.
8. Nicholls SJ, Puri R, Anderson T, Ballantyne CM, Cho L, Kastelein JJ, et al. Effect of Evolocumab on Progression of Coronary Disease in Statin-Treated Patients: The GLAGOV Randomized Clinical Trial. *JAMA : the journal of the American Medical Association*. 2016;316(22):2373-84.
9. Kini AS, Baber U, Kovacic JC, Limaye A, Ali ZA, Sweeny J, et al. Changes in plaque lipid content after short-term intensive versus standard statin therapy: the YELLOW trial (reduction in yellow plaque by aggressive lipid-lowering therapy). *Journal of the American College of Cardiology*. 2013;62(1):21-9.
10. Hirohata A, Yamamoto K, Miyoshi T, Hatanaka K, Hirohata S, Yamawaki H, et al. Impact of olmesartan on progression of coronary atherosclerosis a serial volumetric intravascular ultrasound analysis from the OLIVUS (impact of OLmesarten on progression of coronary atherosclerosis: evaluation by intravascular ultrasound) trial. *Journal of the American College of Cardiology*. 2010;55(10):976-82.
11. Miller JM, Rochitte CE, Dewey M, Arbab-Zadeh A, Niinuma H, Gottlieb I, et al. Diagnostic performance of coronary angiography by 64-row CT. *N Engl J Med*. 2008;359(22):2324-36.
12. Dey D, Schepis T, Marwan M, Slomka PJ, Berman DS, Achenbach S. Automated three-dimensional quantification of noncalcified coronary plaque from coronary CT angiography: comparison with intravascular US. *Radiology*. 2010;257(2):516-22.
13. Leber AW, Becker A, Knez A, von Ziegler F, Sirol M, Nikolaou K, et al. Accuracy of 64-slice computed tomography to classify and quantify plaque volumes in the proximal coronary system: a comparative study using intravascular ultrasound. *Journal of the American College of Cardiology*. 2006;47(3):672-7.
14. Park HB, Lee BK, Shin S, Heo R, Arsanjani R, Kitslaar PH, et al. Clinical Feasibility of 3D Automated Coronary Atherosclerotic Plaque Quantification Algorithm on Coronary Computed Tomography Angiography: Comparison with Intravascular Ultrasound. *European radiology*. 2015;25(10):3073-83.
15. Nakazato R, Shalev A, Doh JH, Koo BK, Dey D, Berman DS, et al. Quantification and characterisation of coronary artery plaque volume and adverse plaque features by coronary computed tomographic angiography: a direct comparison to intravascular ultrasound. *European radiology*. 2013;23(8):2109-17.
16. Otsuka M, Bruining N, Van Pelt NC, Mollet NR, Ligthart JM, Vourvouri E, et al. Quantification of coronary plaque by 64-slice computed tomography: a comparison with quantitative intracoronary ultrasound. *Investigative radiology*. 2008;43(5):314-21.
17. Raff GL, Chinnaiyan KM, Cury RC, Garcia MT, Hecht HS, Hollander JE, et al. SCCT guidelines on the use of coronary computed tomographic angiography for patients presenting with acute chest pain to the emergency department: a report of the Society of Cardiovascular Computed Tomography Guidelines Committee. *Journal of cardiovascular computed tomography*. 2014;8(4):254-71.

18. Scanlon PJ, Faxon DP, Audet AM, Carabello B, Dehmer GJ, Eagle KA, et al. ACC/AHA guidelines for coronary angiography. A report of the American College of Cardiology/American Heart Association Task Force on practice guidelines (Committee on Coronary Angiography). Developed in collaboration with the Society for Cardiac Angiography and Interventions. *Journal of the American College of Cardiology*. 1999;33(6):1756-824.
19. Mintz GS, Nissen SE, Anderson WD, Bailey SR, Erbel R, Fitzgerald PJ, et al. American College of Cardiology Clinical Expert Consensus Document on Standards for Acquisition, Measurement and Reporting of Intravascular Ultrasound Studies (IVUS). A report of the American College of Cardiology Task Force on Clinical Expert Consensus Documents. *Journal of the American College of Cardiology*. 2001;37(5):1478-92.
20. Utsunomiya M, Hara H, Moroi M, Sugi K, Nakamura M. Relationship between tissue characterization with 40 MHz intravascular ultrasound imaging and 64-slice computed tomography. *J Cardiol*. 2011;57(3):297-302.
21. Papadopoulou SL, Neefjes LA, Schaap M, Li HL, Capuano E, van der Giessen AG, et al. Detection and quantification of coronary atherosclerotic plaque by 64-slice multidetector CT: a systematic head-to-head comparison with intravascular ultrasound. *Atherosclerosis*. 2011;219(1):163-70.
22. Saba L, Mallarin G. Window settings for the study of calcified carotid plaques with multidetector CT angiography. *AJNR Am J Neuroradiol*. 2009;30(7):1445-50.
23. Voros S, Rinehart S, Qian Z, Vazquez G, Anderson H, Murrieta L, et al. Prospective validation of standardized, 3-dimensional, quantitative coronary computed tomographic plaque measurements using radiofrequency backscatter intravascular ultrasound as reference standard in intermediate coronary arterial lesions: results from the ATLANTA (assessment of tissue characteristics, lesion morphology, and hemodynamics by angiography with fractional flow reserve, intravascular ultrasound and virtual histology, and noninvasive computed tomography in atherosclerotic plaques) I study. *JACC Cardiovascular interventions*. 2011;4(2):198-208.
24. Nakanishi R, Alani A, Matsumoto S, Li D, Fahmy M, Abraham J, et al. Changes in Coronary Plaque Volume: Comparison of Serial Measurements on Intravascular Ultrasound and Coronary Computed Tomographic Angiography. *Tex Heart Inst J*. 2018;45(2):84-91.
25. Mintz GS, Garcia-Garcia HM, Nicholls SJ, Weissman NJ, Bruining N, Crowe T, et al. Clinical expert consensus document on standards for acquisition, measurement and reporting of intravascular ultrasound regression/progression studies. *EuroIntervention*. 2011;6(9):1123-30, 9.
26. Zeb I, Li D, Nasir K, Malpeso J, Batool A, Flores F, et al. Effect of statin treatment on coronary plaque progression - a serial coronary CT angiography study. *Atherosclerosis*. 2013;231(2):198-204.
27. Papadopoulou SL, Neefjes LA, Garcia-Garcia HM, Flu WJ, Rossi A, Dharampal AS, et al. Natural history of coronary atherosclerosis by multislice computed tomography. *JACC Cardiovascular imaging*. 2012;5(3 Suppl):S28-37.
28. Lehman SJ, Schlett CL, Bamberg F, Lee H, Donnelly P, Shturman L, et al. Assessment of coronary plaque progression in coronary computed tomography angiography using a semiquantitative score. *JACC Cardiovascular imaging*. 2009;2(11):1262-70.
29. Inoue K, Motoyama S, Sarai M, Sato T, Harigaya H, Hara T, et al. Serial coronary CT angiography-verified changes in plaque characteristics as an end point: evaluation of effect of statin intervention. *JACC Cardiovascular imaging*. 2010;3(7):691-8.
30. Lo J, Lu MT, Ihenachor EJ, Wei J, Looby SE, Fitch KV, et al. Effects of statin therapy on coronary artery plaque volume and high-risk plaque morphology in HIV-infected patients with subclinical atherosclerosis: a randomised, double-blind, placebo-controlled trial. *Lancet HIV*. 2015;2(2):e52-63.

31. Ridker PM, Morrow DA, Rose LM, Rifai N, Cannon CP, Braunwald E. Relative efficacy of atorvastatin 80 mg and pravastatin 40 mg in achieving the dual goals of low-density lipoprotein cholesterol <70 mg/dl and C-reactive protein <2 mg/l: an analysis of the PROVE-IT TIMI-22 trial. *Journal of the American College of Cardiology*. 2005;45(10):1644-8.
32. Hausleiter J, Meyer T, Hermann F, Hadamitzky M, Krebs M, Gerber TC, et al. Estimated radiation dose associated with cardiac CT angiography. *JAMA : the journal of the American Medical Association*. 2009;301(5):500-7.
33. Chen MY, Shanbhag SM, Arai AE. Submillisievert median radiation dose for coronary angiography with a second-generation 320-detector row CT scanner in 107 consecutive patients. *Radiology*. 2013;267(1):76-85.
34. Donnino R, Jacobs JE, Doshi JV, Hecht EM, Kim DC, Babb JS, et al. Dual-source versus single-source cardiac CT angiography: comparison of diagnostic image quality. *AJR American journal of roentgenology*. 2009;192(4):1051-6.
35. Wang R, Schoepf UJ, Wu R, Nance JW, Jr., Lv B, Yang H, et al. Diagnostic accuracy of coronary CT angiography: comparison of filtered back projection and iterative reconstruction with different strengths. *Journal of computer assisted tomography*. 2014;38(2):179-84.

**Table 1. Patient characteristics (n=10)**

Hypertension	7
Hyperlipidaemia	6
Ex smoker	2
Current smoker	1
Diabetes Mellitus	1
Family history of ischaemic heart disease	3
Obesity	1
Acute coronary syndrome at initial presentation	2

**Table 2. Baseline and follow up TAV, PAV, nTAV, %PAV change and %nTAV change: Comparison between CTCA and IVUS**

	CTCA	IVUS	P Value	Correlation	P Value	Mean difference (95%CI)
<b>Baseline</b>						
TAV (mm <sup>3</sup> )	195.4±111.7	202±122	0.49	0.97	<0.001	6.7 (-27.9, 14.5)
PAV (%)PAPA	41.6±8.4	38.8±7.1	0.11	0.79	0.007	2.9 (-0.8, 6.6)
Baseline nTAV (mm <sup>3</sup> )	211.9±58.9	209.9±49.9	0.84	0.84	0.002	2.1 (-20.5, 24.7)
<b>Follow up</b>						
TAV (mm <sup>3</sup> )	182.3±127.3	195.2±134.3	0.21	0.97	<0.001	12.9 (-34.6, 8.8)
PAV (%)PAV	39.0±9.4	38.8±10.5	0.9	0.8	0.005	0.25 (-4.3, 4.8)
NTAV (mm <sup>3</sup> )	194.0±67.4	197.6±53.3	0.7	0.9	<0.001	3.7 (-25.1, 17.8)
<b>Change</b>						
PAV (%)	-2.6±3.4	0±4.9	0.05	0.65	0.04	2.6 (-5.3, 0)
nTAV (mm <sup>3</sup> )	-18.0±28.8	-12.3±22.2	0.26	0.85	0.002	5.7 (-16.6, 5.1)

**Table 3. Inter and Intra observer variability for plaque volume quantification on CTCA**

Plaque quantification	Intra observer	Inter observer
Intra class correlation Coefficient	0.99 (95% CI: 0.9 - 0.99).	0.85(0.4 – 0.96)
<b>Bland Altman</b>		
Mean difference	0.114±1.96%	0.54±3.66%
P value	p =0.86	p=0.65
Limits of agreement	3.84 - 3.62	7.72 - 6.64

**Table 4. Baseline and follow up plaque volumes of IVUS and CTCA**

Patient No.	Baseline IVUS TAV	Follow-up IVUS TAV	Change in IVUS TAV	Baseline CT TAV	Follow up CT TAV	Change in CT TAV
1	465.19	502.85	-37.66	467.3	498.4	-31.1
2	239.2	215.5	23.7	236.8	226.6	10.2
3	71.96	64.3	7.66	72.9	60.4	12.5
4	199.4	103.7	95.7	187.5	131.9	55.6
5	138.4	132.24	6.16	116.1	114.2	1.9
6	74.82	67.73	7.09	58	56	2
7	246.87	248.79	-1.92	330.3	336	-5.7
8	157.79	143	14.79	174.2	171.5	2.7
9	178.3	166.23	12.07	181.9	166.8	15.1
10	182	179	3	195.9	190.4	5.5

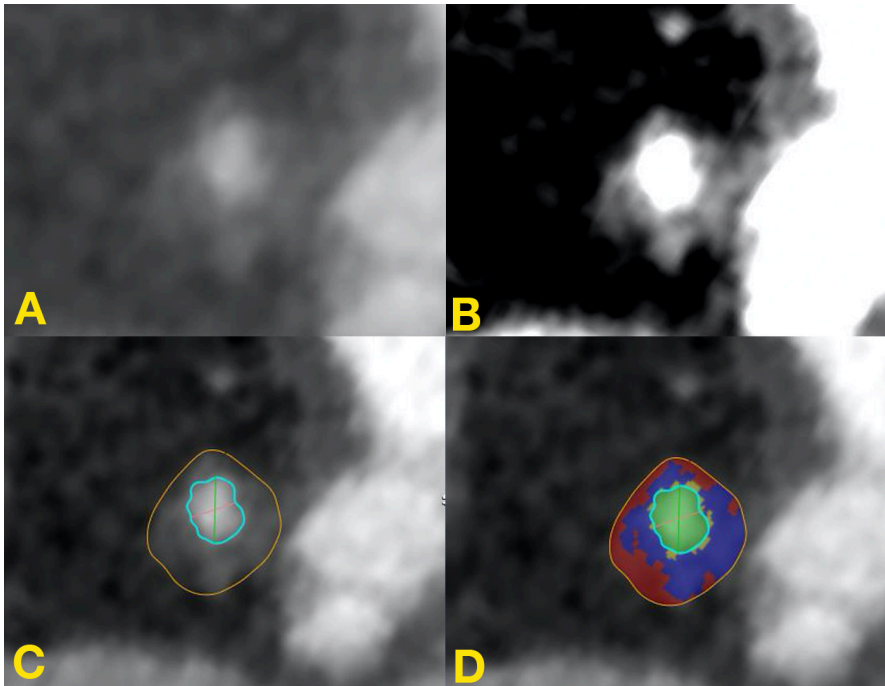
**Table 5. Baseline and follow up PAV on IVUS and CTCA**

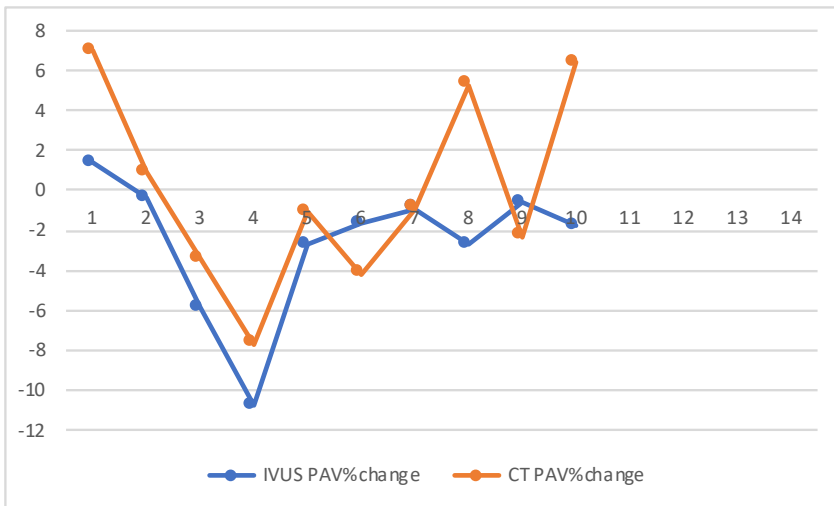
Pt. no.	Baseline IVUS PAV	Follow up IVUS PAV	Change in IVUS PAV	Baseline CT PAV	Follow up CT PAV	Change in CT PAV
1	47.3	502.85	1.34	45.3	498.4	7
2	30.8	215.5	-0.4	27.5	226.6	0.9
3	37.5	64.3	-5.9	36.6	60.4	-3.4
4	38.3	103.7	-10.8	32.3	131.9	-7.7
5	41.7	132.24	-2.7	34.9	114.2	-1.1
6	53.7	67.73	-1.7	41.7	56	-4.2
7	37.5	248.79	-0.9	44.8	336	-0.9
8	55.9	143	-2.7	51.3	171.5	5.3
9	32	166.23	-0.6	33.7	166.8	-2.3
10	41.6	179	-1.8	39.5	190.4	6.4

**Table 6. Baseline and follow up nTAV on IVUS and CTCA**

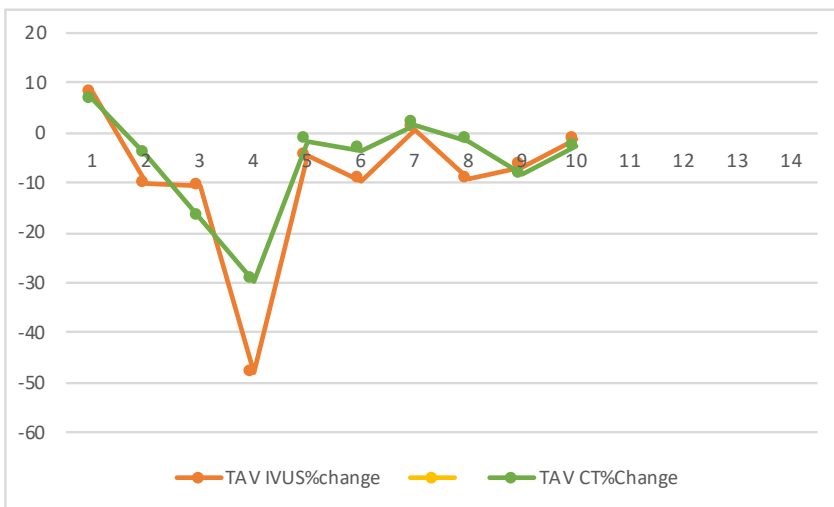
Pt. no.	Baseline IVUS nTAV	Follow up IVUS nTAV	Change in PAV on nTAV	Baseline CT nTAV	Follow up CT nTAV	Change in CT nTAV
1	271.4	293.3	21.9	272.6	290.7	18.1
2	123.5	110.8	-12.7	122.3	117	-5.3
3	283.3	253.1	-30.2	287	237.8	-49.2
4	184.7	96	-88.7	173.7	122.2	-51.5
5	272.5	260	-12.5	228.6	224.8	-3.8
6	261.87	237	-24.87	203	196	-7
7	162	163.3	1.3	216.8	220.5	3.7
8	171.4	155.3	-16.1	189.2	186.3	-2.9
9	233.9	218.2	-15.7	238.7	218.9	-19.8
10	154.9	152.6	-2.3	166.8	162	-4.8

**Figure 1:** (A) Cross section of a vessels with a non-calcified plaque on unadjusted window settings (B) The lumen and the outer wall are better delineated on window settings of width 230 and level of 83. (C) The outer vessel wall (yellow line) and the lumen (blue line) are drawn using window setting of W740 L 220 (D) Various components of plaque are represented in colour (red – low attenuation plaque, blue – fibrous plaque and green – lumen).



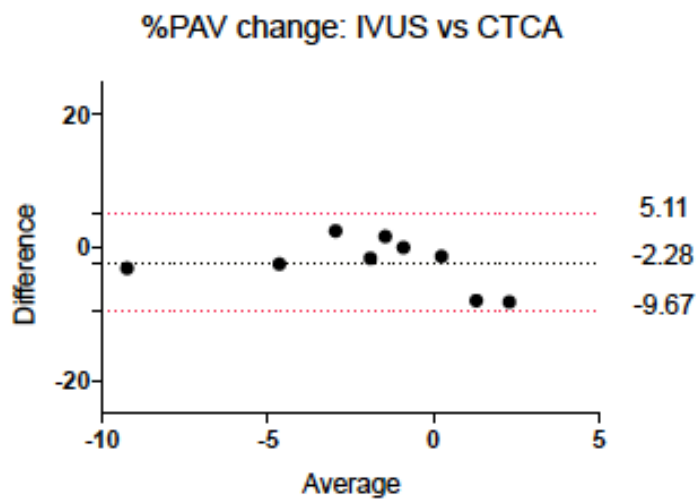


A



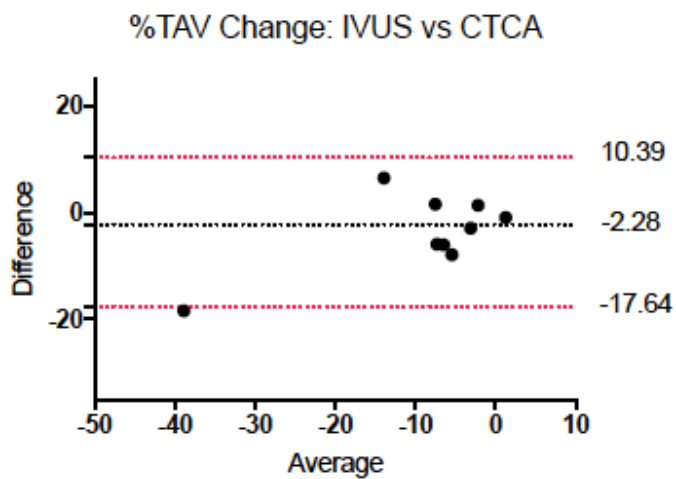
B

Fig 2. Line graph showing (A) Moderate correlation for % PAV change between CTCA and IVUS ( $r = 0.65$ ,  $p = 0.53$ ) and (B) excellent correlation for % TAV change between CTCA and IVUS ( $r = 0.84$ ,  $p = 0.26$ )



Bias -2.28  
LoA -9.67 to 5.11

**A**



Bias of - 2.28  
LoA: -17.64 to 10.39

**B**

Fig 3. Bland Altman plot for (A)% PAV change between CTCA and IVUS. There was small difference in mean values with narrow limits of agreement and (B) % TAV change between CTCA and IVUS. There was small mean difference with relatively narrow limits of agreement.

## **Chapter 5: Quantitative plaque characterisation and association with acute coronary syndrome on medium to long term follow up: Insights from computed tomography coronary angiography**

*Ravi Kiran Munnur MBBS<sup>1</sup>, Nitesh Nerlekar MBBS<sup>1</sup>, Andrew Talman MBBS<sup>1</sup>, Rahul Muthalaly MBBS<sup>1</sup>, Yee Way Baey MBBS<sup>1\*</sup>, Jason Nogie MBBS<sup>1</sup>, Jordan Laggoune, Andrew Lin MBBS<sup>1</sup>, James Cameron MBBS PhD<sup>1</sup>, Brian Ko MBBS MBBS PhD<sup>1</sup>, Sujith Seneviratne MBBS (Hons)<sup>1</sup>, Dennis TL Wong MBBS, MD, PhD<sup>1</sup>*

<sup>1</sup> Monash Cardiovascular Research Centre, Department of Medicine (Monash Medical Centre) Monash University and Monash Heart, Monash Health, 246 Clayton Road, Clayton, 3168 VIC, Australia

**Unpublished: To be submitted**

*\* Corresponding author*

*Ravi Kiran Munnur*

*Monash Medical Centre, Monash Cardiovascular Research Centre, VIC, Australia*

## **ABSTRACT**

### **Objectives**

To study the association between computed tomography coronary angiography (CTCA) derived high-risk plaques (HRP) and subsequent acute coronary syndrome on a medium to long term follow up. To assess the utility of quantitative analysis to further discriminate HRP that are likely to cause ACS.

### **Background**

Although several studies have identified the association of HRP on CTCA and future ACS, there is paucity of studies that examined predictors for ACS amongst HRPs.

Culprit precursor lesions have been found to cause only mild stenosis in several studies and the relevance of stenosis severity to ACS occurrence is not completely understood.

### **Methods**

Retrospective study of patients who underwent CTCAA for suspected coronary artery disease (CAD). Plaque composition, and the presence of HRP and its constituents: positive remodelling (PR), low attenuation plaque (LAP < 56HU) and spotty calcification (SC) were recorded. Cross sectional quantitative analysis of HRP was performed at the site of minimum luminal area (MLA), which included plaque burden, plaque volume (PV), LAP volume, minimum luminal diameter (MLD). Other assessed parameters included lesion length, obstructive stenosis (OS) defined as  $\geq 50\%$  stenosis, plaque, composition (calcified, non calcified and mixed plaque), segmental involvement score (SIS) and segmental stenosis score (SSS) scores. Primary end point was fatal or non-fatal ACS on follow up.

### **Results**

Included were 1254 patients (mean age and 50.9% male) with a median follow up period of 7.24 years (IQR 5.53 yrs. to 7.7years). ACS occurred in 45 patients (3.6%): 34 (13.9%) of 243 HRP (+) patients and 11 (1%) of 1011 HRP (-)(HR 14.5: 95% CI 7.3 -28.6;  $p < 0.001$ ). The occurrence of ACS was significantly higher in HRP (+) patients compared to HRP (-) patients and patients with no plaques (20.5% vs. 1.6% vs. 0.4%, log-rank test  $p < 0.001$ ). Only the presence of HRP was an independent predictor of ACS (HR 14.99, 7.47-30.06,  $p < 0.001$ ) and none of the cardiovascular risk factors were significant. Among patients with ACS, the time to event was shorter in patients with HRP features (HR 3.34 (1.16-9.63),  $p=0.03$ ; Kaplan Meier log-rank 0.02) and 100% of HRP(-) patients were event free at the end of one year and had lower event rates up to five years of follow up.

ACS occurred in 24 (11.4%) of 209 OS (+) patients compared to 21 (2%) of 1045 OS (-) patients (HR 6.3: 3.5-11.4;  $p < 0.001$ ). ACS was more frequent in HRP (+)/ (OS (+) patients with 22 (20.7%) of 106 developing ACS. In comparison, 12 (8.6%) of 136 HRP (+)/OS (-) patients, 2 (1.8%) of 111 HRP (-)/ OS (+) patients and 9 (1.0%) of 900 HRP (-)/OS (-) patients developed ACS

Obstructive stenosis, cross sectional PV and the presence of very low attenuated plaque ( $< 30$ HU) identified those HRP lesions that were more likely to cause future ACS. ACS occurred early (mean duration of 2.6 yrs) and more frequently in HRP lesions with obstructive stenosis [22 (17%) of 128 lesions] compared to ACS occurring later (mean duration of 3.75 yrs) and less frequently [13(7.1%) of 182 HRP lesions] in HRP lesions with non-obstructive stenosis. Cross-sectional LAP volume in HRP lesions with obstructive stenosis added incremental prognostic value in predicting ACS ( $p=0.008$ ). SIS and SSS scores were not predictive of ACS.

## **Conclusions**

CTCA derived HRP is an independent predictor of future ACS beyond traditional cardiovascular risk factors. The absence of HRP features was associated with event free survival at one year and reduced annual risk compared to those with HRP features up to five years of follow up. The risk of future ACS appears directly related to the degree of stenosis caused by the high-risk plaque components with plaque volume and LAP volume being the important determinants. ACS occurred early and more frequently in HRP lesions with obstructive stenosis and cross-sectional LAP volume provided further incremental prognostic value in predicting ACS. Irrespective of the presence of obstructive stenosis, absence of HRP was associated with low rates of ACS.

**Key Words:** Coronary artery disease, High-risk plaque, acute coronary syndrome, Computed tomography coronary angiography

### **Abbreviations**

ACS: Acute coronary syndrome

CAD: Coronary artery disease

CTCAA: Computed Tomography Coronary Angiography

IVUS: Intravascular Ultrasound

TCFA: Thin cap fibroatheroma

MLA: Minimum luminal area

PR: Positive remodelling

LAP: Low attenuation plaque

SC: Spotty Calcification

NR: Napkin ring

SIS: Segmental involvement score

SSS: Segment stenosis score

HRP: High risk plaque

MLD: Minimum luminal diameter

FFR: Fractional flow reserve

PB: Plaque burden

PV: Plaque volume

OS: Obstructive stenosis

## **Introduction**

Acute coronary syndrome is a major public health issue (1). It can be the initial manifestation in many patients with coronary artery disease causing significant mortality and morbidity. Majority of acute coronary syndromes are due to plaque rupture and pathological studies have identified plaque characteristics of thin cap fibroatheroma (TCFA), lipid rich necrotic pool and inflammation as key determinants (2). Despite our improved understanding of the disease process and management, appropriate risk stratification is lacking. Identification of at risk-patients and development of preventative strategies is a major public health issue. Although, in vivo identification of these rupture prone plaque is possible with intra coronary imaging techniques and a wealth of data is available in patients for secondary prevention, their utility in primary prevention population is limited (3,4). Computed tomography coronary angiography (CTCA) is a non-invasive test that in addition to the diagnosis of luminal stenosis, provides information on degree of atherosclerotic plaque burden and plaque composition (5-7). CTCA derived high-risk plaque (HRP) features of positive remodelling (PR), low attenuation plaque (LAP), spotty calcification (SC) and napkin ring sign (NR) correlate well with adverse plaque characteristics on intracoronary imaging. Despite the association between HRP and ACS being shown in short to medium term follow up studies, only a minority of patients develop ACS (8,9). Apart from the presence of HRP, the underlying atherosclerotic plaque burden assessed by Agatston score, segmental involvement score (SIS), segmental stenosis score (SSS) have also been shown to offer prognostic information (10,11).

Additionally in PROSPECT trial which studied non culprit lesion lesions in ACS patients, IVUS derived predictors of future ACS were thin-cap fibroatheroma, plaque burden and minimal luminal area and majority of culprit lesion precursors had only mild stenosis (12). These observations highlight the relevance of plaque burden, plaque composition and stenosis severity to future ACS. Given that CTCAA is now a front line investigation in the assessment of chest pain, it is uniquely positioned to study the natural progression of coronary atherosclerosis leading to ACS in primary prevention population.

Further differentiation of the HRP lesions that are rupture prone on CTCA is needed for optimisation of risk stratification in stable patients. There have been very few studies have assessed the incremental benefit of quantitative plaque analysis in patients with HRP (13,14). Specifically, lesion based analyses of HRP on CTCA that includes assessment of plaque burden, plaque volume, LAP volume, MLD and MLA may aid further in prognostication. We sought to study the association between ACS and CTCA derived HRP, plaque burden and stenosis severity on a medium to long term follow up. By employing quantitative plaque analysis and various CT scores, we aimed to differentiate the HRP lesions that are at a higher risk of causing ACS.

## **Methods**

Of the 1735 eligible patients with follow up data that underwent CTCA at our institution from January 2008 to March 2013, patients with prior CABG (103), previous ACS or PCI (84), 29 patients with poor CT images, 128 patients with early revascularisation, 157 deaths from non-cardiac causes were excluded. The remaining 1254 patients were followed up until 30<sup>th</sup> November 2017 for development of ACS (**Figure 1**). A structured questionnaire was completed for every patient prior to CTCA and it captured patient information such as age, height, weight, symptoms and cardiac risk factors. Follow up information on patient outcomes was obtained by assessment of hospital medical records, detailed structured questionnaires sent by mail/email, or, if the

questionnaire was not returned, by telephone contact. Records from the registry of birth and deaths were also obtained. All reported events were verified by hospital records and adjudicated by two cardiologists in consensus. It was ensured that subsequent ACS events and corresponding culprit lesion geographically matched the precise location of HRP that was analysed on CTCA. The institutional Human Research and Ethics Committee approved the study.

The primary end-point of this study was MACE defined by a composite of cardiac death and acute coronary syndrome (myocardial infarction and unstable angina). Cardiac death was defined as any death caused by acute myocardial infarction. Acute coronary syndrome was defined as per the basis of the third universal definition of myocardial infarction (15) and the Canadian Cardiovascular Society grading of angina pectoris (16) that included presentation with typical sounding chest pain associated with troponin elevation with or without ECG changes. In the event of no troponin rise, chest pain that was Canadian Cardiovascular Society class 3 or 4 was considered significant. Determination of the culprit vessel was done by a combination of electrocardiographic and invasive coronary angiographic findings.

### **CT coronary angiography**

Patients underwent cardiac CT assessment using a 320-row detector CT scanner (Aquilion One Vision; Toshiba Medical Systems Corp., Tokyo, Japan). All patients received sublingual nitroglycerine, and additional beta-blockers were administered to achieve a pre-scan heart rate of <60 beats/min in accordance with Society of Cardiovascular Computed Tomography guidelines (17). The studies were performed according to established guidelines(18) and departmental protocols (19,20) at the time of the scan.

### **CTCA Analysis**

Data was transferred to an external workstation (Vitrea 6, version 6.0; Vital Images, Minnetonka, Minnesota) for further analysis. Two level III experienced readers (DW and RKM) who were blinded to the patient's clinical information evaluated all the scans. In case of disagreement, a joint reading was performed and a consensus decision was reached. All the CTCA images were analysed on axial, coronal, sagittal, cross-sectional and curved multiplanar reconstructed images. Studies were interpreted according to current guidelines (21) using a 16-segment model. Plaque was defined as tissue structures  $>1 \text{ mm}^2$  within the coronary artery lumen or adjacent to the lumen that could be discriminated from the surrounding pericardial tissue, epicardial fat, or vessel lumen itself. Each coronary segment  $>2\text{mm}$  in diameter was analysed for the presence of plaque and the diameter stenosis of each lesion was visually graded and categorised as follows: no stenosis (0%), minimal ( $<25\%$ ), mild (25 – 49%), moderate (50 -69%), severe (70 -99%), occluded (100%) (22). Obstructive disease was defined as  $>50\%$  stenosis. Plaque composition was classified as non-calcified, calcified, or mixed.

The measure of total coronary atherosclerotic plaque burden was performed using the segmental involvement score (SIS) and segmental stenosis score (SSS). SIS was calculated as the total number of coronary segments with plaque, irrespective of the degree of luminal stenosis within each segment (range 0 to 16). SSS was calculated by grading each coronary segment as having no to severe plaque (scores from 0 to 3) based on stenosis severity followed by summation of the scores of all 16 individual segments to yield a total score (range 0 to 48) (23).

#### *High-risk plaque characteristics*

Binary evaluation of HRP characteristics included low attenuation plaque (LAP), spotty calcification and positive remodelling was done. Low attenuation plaque is defined as plaques with  $<30$  Hounsfield unit (HU) (24). Spotty calcification was defined when calcification was  $< 3 \text{ mm}$  in size. Positive

remodelling was defined as remodelling index  $\geq 1.1$ (8). The napkin ring sign on CTCA is another previously described HRP feature but was not included in this analysis due to its infrequent presence.

### *Quantitative plaque analysis*

Quantitative plaque analysis was performed on all plaques with HRP features using attenuation-based-automated SurePlaque (Vitrea 6, version 3.0; Vital Images and Toshiba Medical Systems) software (25) with appropriate manual correction. Cross sectional quantitative analysis was performed solely at the site of MLA in HRP lesions and assessed parameters included, plaque volume (PV), plaque burden (PB), minimal luminal area (MLA), minimal luminal diameter (MLD) and plaque composition using predefined HU thresholds: low attenuation plaque ( $< 56$  HU), fibrofatty (56 to 130 HU), fibrous (131 to 350 HU), and calcified plaque ( $\geq 350$  HU) (26). The cut off  $< 30$  HU has been found to be specific for lipid rich plaque with higher positive predictive value but lacked sensitivity. The cut-off of  $< 56$  HU was more sensitive with higher negative predictive value and was more suitable for quantification purposes. It has previously been shown to be more suited for current CT scanners and scanning protocols studies to identify LAP. (27,28)

The LAP volumes were classified according to tertiles of low, mid and high LAP volume. Each of these groups was further divided into OS (-) or OS (+) groups. There were six group comprising: OS (-)/Low LAP, OS (+)/Low LAP, OS (-)/mid LAP, OS (+)/mid LAP, OS (-)/high LAP and OS (+)/high LAP.

### **Statistical Analysis**

Categorical data are presented as raw numbers and percentages and compared with chi-square test. Continuous data is displayed as mean  $\pm$  standard deviation if data was normally distributed, or medians [interquartile range] for non-normal data and compared with t-tests or Mann-Whitney tests as appropriate. Kaplan-Meier plots were constructed and the log-rank test used to assess the differences in equality of curves. Univariable Cox proportional hazard regression models were

performed to assess clinically relevant variables on the outcome of interest. Variables of clinical relevance or with a  $p < 0.20$  on univariate assessment were considered for the multivariable model. Final multivariable covariates included gender, hyperlipidaemia, smoking, presence of vulnerable plaques and obesity. Conditional proportional hazards assumptions were visually inspected by plotting Schoenfeld residuals. The incremental prognostic value of including assessment of low attenuation plaque values and obstructive stenosis  $> 50\%$  was compared by Harrell's c-statistic. A 2-sided p-value of  $< 0.05$  was considered statistically significant. Statistical analysis was performed using Stata MP/14 (StataCorp, College Station, Texas).

## Results

### *Study population and clinical characteristics*

Included in the study were 1254 patients (Mean age  $60.9 \pm 13.7$ , 50.9% were male) with a median follow up period of 7.24 years (IQR 5.53 yrs. to 7.7 years). Of these, 583 patients had hypertension (46%), 581 hyperlipidaemia (46%), 138 had diabetes mellitus (10.9%), 128 (10.2%) patients were active smokers and 152 patients (12.1%) were obese. On comparison of the traditional risk factors, only smoking was associated with ACS (**Table 1**).

### *Coronary computed tomography angiography results*

Of 1254 patients, 209 patients (16.6%) had a  $\geq 50\%$  stenotic lesion in at least 1 coronary artery, only 17 (0.6%) patients had severe stenosis ( $\geq 70\%$ ) and 475 (37.8%) patients had no coronary atherosclerosis. There were 243 (19.3%) patients who had HRP with at least one high-risk feature and 106 (8.4%) patients had HRP with obstructive stenosis. On comparison of the traditional risk factors, only diabetes mellitus and smoking were associated with the presence of HRP (**Table 2**). There were 195 HRP (+) patients with  $\geq 2$  features (plaques with  $\geq 2$  of PR, LAP and SC), 48 HRP

(+) patients with 1 feature (either PR, LAP or SC), 539 HRP (-) patients had plaques with no HRP features and 475 patients had no plaques.

#### *Patient level analysis*

Of the 1254 patients, 45 (3.6%) patients had ACS during the follow up. Three patients had ACS related death, 34 (2.7%) patients had myocardial infarction and 8 (0.6%) patients had unstable angina. Culprit lesion precursors were identified by both invasive coronary angiography (ICA) and CTCA in 42 (93%) patients and were not known in three patients who died of acute myocardial infarction. The culprit lesion was found in 21 left anterior descending arteries, 3 left circumflex arteries and 19 right coronary arteries.

#### *Plaque composition and stenosis severity: Association with ACS*

Of the 45 patients who had ACS, 34 patients had HRP while 11 patients had no HRP. During follow up, 32 (16.4%) of 195 patients with HRP (+) patients with  $\geq 2$  features developed ACS. In comparison, 2 (4.1%) of 48 HRP (+) patients with one HRP feature, 9 (1.6%) of the 539 HRP (-) patients and 2 (0.4%) of the 475 patients without any plaque developed ACS. **(Figure 1 and 2)**

Compared to 9 HRP (+) patients who had ACS, none of the HRP (-) patients developed ACS within the first year of follow up. From year one to year five of the follow up duration, HRP (+) patients had more events compared to HRP (-) patients (1-2yrs: 6 vs. 3 patients; 2-3yrs: 5 vs. 0 patients; 3-4yrs: 2 vs. 1 patients; 4-5yrs: 4 vs. 3 patients; >5yrs: 8 vs. 4 patients).

Overall, ACS occurred in 24 (11.4%) of 209 OS (+) patients compared to 21 (2%) of 1045 OS (-) patients. When the relationship between HRP and OS was assessed, ACS was more frequent in HRP (+)/ (OS (+) patient with 22 (20.7%) of 106 developing ACS. In comparison, 12 (8.6%) of

136 HRP (+)/OS (-) patients, 2 (1.8%) of 111 HRP (-)/ OS (+) patients and 9 (1.0%) of 900 HRP (-)/OS (-) patients developed ACS (**Figure 3 and 4**).

#### *Predictive value of plaque characteristics*

The presence of HRP was associated with ACS (HR 14.5: 95% CI 7.3 -28.6;  $p < 0.001$ ) as were its constituents PR (HR 14.5: 7.3-28.7;  $p < 0.001$ ), SC (HR 5.4: 3-9.9;  $p < 0.001$ ) and LAP 30 (HR 16.7: 9.1-30.5;  $p < 0.001$ ). The presence of  $\geq 2$  HRP features (HR 14.4: 7.46-26.44;  $p < 0.001$ ), obstructive stenosis  $\geq 50\%$  (HR 6.3: 3.5-11.4;  $p < 0.001$ ) and plaques with any HRP features and obstructive stenosis (10.3: 5 – 21.2;  $p < 0.001$ ) were associated with ACS (**Table 3**).

On multivariate Cox regression analysis of variables comprising sex, hyperlipidaemia, smoking, diabetes mellitus, obesity and presence of at least one HRP feature, only the presence of HRP was an independent predictor of ACS (HR 14.99, 7.47-30.06,  $p < 0.001$ ). The occurrence of ACS was significantly higher in HRP (+) patients compared to HRP (-) patients and patients with no plaques (20.5% vs. 1.6% vs. 0.4%, log-rank test  $p < 0.001$ ). Significantly higher rate of ACS was observed in HRP(+)/OS(+) patients compared to (HRP+)/OS(-) and HRP(-)/OS(+) patients (20.7% vs. 8.6% vs. 1.8%, log-rank test  $p < 0.001$ ).

#### *Survival Analysis*

On survival analysis of patients with events limited to five years of follow up, the time interval between the CTCA and event was shorter in HRP (+) patients (HR 3.34 (1.16-9.63),  $p = 0.03$ ; Kaplan Meier log-rank 0.02). The comparison of proportion of patients surviving, between HRP(+) patients to HRP(-) annually was 73% and 100%; 56% and 82%; 41% and 82%; 35% and 82%; 24% and 64% respectively for up to 5 years follow up (**Table 6, Figure 5**).

#### *Lesion level analysis: Assessment of ACS predictors among plaques with HRP features*

Among 234 HRP (+) patients with at least one HRP feature, there were 310 HRP lesions. 11 patients had 3 HRP lesions, 44 patients had 2 HRP lesions and 188 patients had 1 HRP lesion. PR was a feature in all HRP lesions while LAP was present in 161 lesions. Obstructive stenosis was present in 128 lesions (41.2%). The mean SIS score was  $3.6 \pm 0.9$  and the mean SSS score was  $6.1 \pm 4.32$ .

During follow up, ACS developed in 34 HRPs (10.9%). LAP was the most common determinant of ACS in a HRP with 28 (17.3%) of 161 HRPs with LAP developing ACS. In comparison 7 (4.6%) of 149 HRPs without LAP developed ACS. The development of ACS was more frequent in HRP(+)/OS(+) lesions with ACS occurring in 22 (17%) of 128 lesions compared to the ACS occurring in 13(7.1%) of 182 HRP (+)/OS(-) lesions . In addition, patients with HRP(+)/OS(+) lesions presented earlier with ACS (mean duration of 2.6 yrs.) compared to those with HRP(+)/OS(-) lesions (mean duration of 3.75 yrs.).

On quantitative plaque analysis of HRPs, only the presence of LAP (HR 3.77: 1.64-8.67;  $p=0.002$ ) and PV (HR 1.08: 1.02-1.14;  $p=0.007$ ) were associated with ACS (**Table 4**). The lesions that lead to ACS had larger mean LAP volume ( $2.9 \pm 1.9\text{mm}^3$  vs.  $2.1 \pm 2.1\text{mm}^3$ ,  $p = 0.04$ ) and PV ( $13.9 \pm 5.9\text{mm}^3$  vs.  $11.2 \pm 4.9\text{mm}^3$ ,  $p = 0.005$ ) compared to the lesions that did not lead to ACS. Lesions with  $\geq 50\%$  stenosis (HR 2.46: 1.23-4.91;  $p=0.01$ ) but not MLA ( $p=0.61$ ) or MLD ( $p=0.73$ ) was associated with ACS. Plaque composition such as calcified, mixed or non-calcified plaque was not associated with ACS ( $p=0.56$ ,  $0.27$  and  $0.97$  respectively). Plaque length ( $p=0.78$ ), plaque burden ( $p=0.58$ ) and in addition, the measures of total atherosclerotic plaque burden such as SIS ( $p=0.11$ ) and SSS ( $p=0.09$ ) were also not associated with ACS.

In the 11 HRP (-) patients who developed ACS during follow up, all culprit lesions were identified. On assessment of CTCA, only 2 patients had stenosis  $\geq 50\%$ , 4 lesions had  $<25\%$  stenosis, 3 culprit

lesions had 25-49% stenosis and 2 culprit lesions had no plaque. The mean SIS and SSS in these patients were 2.9 and 5.1.

#### *Obstructive disease and LAP volume*

On comparison of the HRP at lesion level using OS (-)/low LAP as reference, lesions with OS (+)/mid LAP (HR 4.08: 1.06 – 15.79; p=0.04) and OS (+)/high LAP (HR 5.68: 1.59- 20.2; p=0.007) were associated with ACS (**Table 5**).

#### *Predictive value of HRP and obstructive stenosis of ACS*

The predictive value of each quantitative plaque characteristics of ACS during follow up was evaluated by ROC analysis. The AUC for OS (+) was 0.64 and LAP volume was 0.65. The predictive value increased to AUC of 0.71 when obstructive stenosis and LAP 56 volume were combined. On comparison of AUC, this was statistically significant when compared to obstructive stenosis alone (p=0.008).

### **Discussion**

We investigated the predictors of ACS in low risk population undergoing CTCA on a medium to long term follow up and the salient findings of our study are 1) CTCA derived HRP is an independent predictor of future ACS beyond traditional cardiovascular risk factors 2) The absence of HRP features was associated with event free survival at one year and reduced annual risk compared to those with HRP features up to five years of follow up 3) Obstructive stenosis, cross sectional PV and the presence of very low attenuated plaque (<30HU) identified those HRP lesions that were more likely to cause future ACS 4) ACS occurred early and more frequently in HRP lesions with obstructive stenosis and cross-sectional LAP volume added further incremental prognostic value in predicting ACS. 5) Irrespective of the presence of obstructive stenosis, absence of HRP was associated with low rates of ACS.

CTCA is an established non-invasive imaging modality for the assessment of coronary artery disease and is now a front line test in the investigation of chest pain (29). We observed increased rates of ACS in patients with HRP (+) patients compared to HRP (-) patient or those with no plaques, which is in agreement with several previous studies that have established an association between the presence of HRP and future ACS on a short to medium term follow up (8,9,24). We demonstrated that this association exists even at a significantly longer duration of follow up. HRP (+) patients presented early with events and had more events per year for up to five years of follow up compared to HRP (-) patients. Our study differs from previous studies as we excluded patients with prior ACS. Our cohort also had low prevalence of patients with severe stenosis ( $\geq 70\%$ ) with overall low atherosclerotic plaque burden reflected in the low SIS and SSS scores. Furthermore, 82% of ACS events in our study were due to myocardial infarction as compared to  $< 5\%$  in previous studies (12,13). The patients in this study may therefore potentially represent the “real world” population with stable chest pain.

We observed that HRP (+) patients with  $\geq 2$  had more events compared to HRP (+) patient with only one HRP feature. Low attenuation plaque was an important determinant with ACS occurring more frequently in HRP (+) plaques with LAP compared to HRP (+) plaque without LAP (17.3% vs. 4.6%). Majority of ACS are caused by plaque rupture and is related to the size of necrotic core (30). The CTCA derived LAP volumes in HRPs were found to be larger in those that resulted in ACS compared to stable HRPs and strikingly, even larger in those presenting with ACS in the first year. In such cases, LAP occupied 21% of plaque area similar to pathological descriptions of ruptured plaques (2,24). In our study, HRPs with obstructive lesions had more frequent events and presented early. Despite the presence of expansive remodelling, presence of obstructive stenosis

signifies a large LAP volume in these plaques. We observed that cross sectional LAP56 volume just at the site of MLA, added further incremental predictive value in predicting ACS obstructive HRP lesions and may act as a surrogate for entire LAP quantification. In the ICONIC (Incident coronary syndrome identified by computed tomography) nested case control study, fibrofatty plaque and necrotic core were observed to be a consistent predictor of ACS, albeit with a relatively low sensitivity of 69%(26). This may be due to the low prevalence of LAP (24.03%) in culprit lesion precursors and LAP presence may have been underestimated as the study consisted of subjects from different countries with a wide array of CTCA scanner and acquisition protocols. Plaque density is affected by lumen contrast density and tube voltage and more contemporary CT studies have used <56HU for LAP definition (27). This could be explained by the fact that the definition of LAP as < 30HU was validated against IVUS on old generation CT scanners with tube voltage of 135KV (31). Considerable overlap exists between LAP and fibrous plaque and a recent histopathological validation study observed that LAP30 had high specificity and positive predictive value but had low sensitivity. In comparison higher cut off values were sensitive with higher negative predictive value but had low specificity (28). Hence, in modern CT acquisition protocols with low KV as demonstrated in our study, the presence of very low attenuation plaque measuring < 30 HU signifies true presence of necrotic core, whereas LAP 56 with higher negative predictive value was more suitable for quantification of the entire LAP volume with fibro fatty components.

In several previous studies, majority of culprit precursor lesions were non-obstructive. However, angiographic studies have demonstrated that culprit lesions were more likely to be > 50% stenosis when evaluated close to an event and < 50% stenosis when assessed many months prior (32-34). Pathological studies of ruptured plaques demonstrated layering from multiple healed plaque ruptures suggesting that silent plaque ruptures and healing may contribute to rapid plaque growth in HRP prior to an event (35). In this study, 53% of culprit precursor lesions had obstructive stenosis and overall ACS occurred in 11.4 % in OS (+) patients vs. 1.6% in OS (-) patients. However, it was

not the stenosis severity but the presence of concomitant HRP that determined future events as only 1.8% of HRP (-)/OS(+) patients developed ACS. Events rarely occurred from non-fibroatheromas regardless of stenosis severity even in PROSPECT study. From these observations we can conclude that underlying plaque composition determines whether stenosis severity becomes a prognostic indicator, greater the stenosis in a lesion with high-risk plaque features, greater the future risk of ACS. This is supported by our findings that HRP(+)/OS(+) patients had more frequent ACS and presented early compared to HRP(+)/OS(-). Additionally, on quantitative analysis of HRP lesions we found that only OS(+)/mid or high LAP were predictive whereas OS(+)/low LAP did not.

The interplay between plaque burden, plaque progression and plaque composition and their role in future events is complex and our understanding of the pathophysiology is still evolving. In the ICONIC study, when stenosis severity was accounted for, it was observed that culprit precursor lesions compared to control lesions had greater overall PV as well as fibrofatty and necrotic core components. We made similar observation that PV and presence of very low attenuated plaque measuring  $< 30\text{HU}$  in a cross section at site of MLA in a HRP further differentiated the ones that were more likely to result in ACS. These observations are also in keeping with findings made in ACS patients that whilst the dimensions of fibrous cap thickness differentiated between ruptured and unruptured plaques, ruptured culprit plaque had greater necrotic plaque burden and lesser luminal area compared to the ruptured non-culprit lesions(36). It has therefore been suggested that there is a potential gap in the predictive ability of CT scores such as Agatston score, SIS score and SSS scores that determine plaque burden, as they do not account for plaque composition (37,38). This is confirmed in a quantitative CTCA study, which demonstrated that LAP volume provided incremental prognostic information beyond calcium score (13). It has been shown in intra coronary imaging studies that multiple plaques exist at different stages of evolution in the same coronary tree and atherosclerosis is a dynamic process (39,40). Although stenosis severity and plaque burden are relevant, it may be assumed that plaque progression and conversion to HRP may be the final

pathway before plaque ruptures, with the burden of adverse plaque composition being an important determinant. This is well illustrated in patients who underwent serial CTCA's, where it was observed that several HRP (-) plaques that become HRP (+) plaques and subsequently developed ACS and HRP(-) plaques that had plaque progression had worse outcomes compared to HRP(+) plaques at baseline that did not progress and remained free of events (8). Hence, any prognostication should consider PV as well as plaque composition. Lastly, adverse haemodynamic parameters measured on CTCA including  $\Delta$  FFR CT, wall shear stress and plaque stress in non-culprit lesions were also found to predict ACS. Interestingly, plaques exhibiting these parameters were more likely to have greater diameter stenosis, LAP and spotty calcification (14,41).

Consistent with previous studies, we observed that compared to HRP(+) patients, HRP(-) patients had low events and those with no plaques had even lower event rate. We also observed that the absence of HRP features confers 100% event free survival rate up to one year. Compared to HRP (+) patients, patients with HRP (-) continued to have survival advantage up to five years of follow up.

None of the traditional risk factors apart from the presence of HRP features were predictive of ACS. The presence HRP identifies a cohort of patients from primary prevention group to have a higher risk of ACS and their prognostic importance is now recognised and is reflected in the recommendation on CTCA reporting (22). Despite the known increased risk, the event rate even among patients with HRP is overall low and current guidelines do not recommend treatment or management of CTCA identified HRPs (42). Our findings suggest that a prediction model similar to PROSPECT study could potentially be applied to HRP(+) patients on CTCA. In HRP (+) patients, along with obstructive stenosis, cross sectional examination at the site of MLA for PV and the presence of very low attenuation plaque measuring  $< 30$  appears to identify those patients in this high-risk group who are at an even higher risk of ACS.

Based on the results of our study, perhaps a higher proportion of plaques with obstructive stenosis with large PV and LAP volumes are more likely to progress and rupture. Quantitative plaque analysis on CTCA is time consuming and expert dependent and for it to be used as a tool for risk stratification, incremental benefit over and above the existing scores should be proven. It appears that we get the relevant information if quantification is performed just at the site of MLA, which can be readily performed in a short duration at the time of reporting CTCA as against quantification of entire plaque.

Atherosclerosis is a result of complex interplay between genetic, environmental and various cardiovascular risk factors and whilst the local plaque features may grab our attention, they may help identify at-risk patient and addressing entire atherosclerotic process and prevention of plaque progression through aggressive risk factor modification is important. Even in patients with HRP features, the slow progression of disease and the long time interval between CTCA and coronary events makes designing any trial that involves intervention difficult. Given the dynamic nature of these plaques, selecting at risk patients with HRP with moderate stenosis and significant LAP volume for future trials aimed at intense medical or other preventative therapies with assessment of progress through serial imaging may be the way forward.

### **Limitations**

Ours was single centre retrospective study. Treatment information following CTCA and compliance to medications was not known. Patients included in the study had CTCA from 2008 to 2012 on old generation scanners and do not represent the current generation of CT scanners. Patients included were investigated for chest pain and there may have also been some referral bias. Several aspects may have influenced our results: Firstly, patients with incomplete datasets were excluded from the study, which may have lead to information bias. Secondly, patients with significant baseline plaque burden who underwent early revascularisation were excluded from the

study. Thirdly, we did not assess those patients who needed late revascularisation due to progression of disease without ACS. Lastly, assessment of luminal stenosis may have been over estimated in calcified lesions and under estimated in non-calcified lesions.

## **Conclusion**

Absence of CTCA derived HRP features confers event free survival for one year and low events rates up to five years when compared to the presence of HRP features. CTCA derived HRP is an independent predictor of future ACS beyond traditional cardiovascular risk factors. All the HRP features of PR, LAP, SC were associated with increased risk. The risk of future ACS appears directly related to the degree of stenosis caused by the high-risk plaque component with plaque volume and LAP volume being the important determinants. In this very high-risk group of patients with obstructive HRP lesions, LAP volume had incremental predictive value to predict ACS. Stenosis severity in the absence of HRP was a not a predictor of ACS.

## **Disclosures**

DW has received speaking fees from Bayer, AstraZeneca, Novartis, Merck Sharp & Dome and Boehringer Ingelheim.

## **Acknowledgements**

RKM is a recipient of Cardiac Society of Australia and New Zealand (CSANZ) scholarship and Australian Post Graduate (APA) scholarship.

AL is supported by a Postgraduate Scholarship from the National Health and Medical Research Council. NN is supported by a Postgraduate Scholarship from the National Health and Medical Research Council and National Heart Foundation.

DW is supported by National Health & Medical Research Institute (NHMRC) Australia Early Career Fellowship

## References

1. Go AS, Mozaffarian D, Roger VL et al. Heart disease and stroke statistics--2014 update: a report from the American Heart Association. *Circulation* 2014;129:e28-e292.
2. Virmani R, Burke AP, Farb A, Kolodgie FD. Pathology of the vulnerable plaque. *Journal of the American College of Cardiology* 2006;47:C13-8.
3. Yamagishi M, Terashima M, Awano K et al. Morphology of vulnerable coronary plaque: insights from follow-up of patients examined by intravascular ultrasound before an acute coronary syndrome. *Journal of the American College of Cardiology* 2000;35:106-11.
4. Schoenhagen P, Ziada KM, Kapadia SR, Crowe TD, Nissen SE, Tuzcu EM. Extent and direction of arterial remodeling in stable versus unstable coronary syndromes : an intravascular ultrasound study. *Circulation* 2000;101:598-603.
5. Miller JM, Rochitte CE, Dewey M et al. Diagnostic performance of coronary angiography by 64-row CT. *N Engl J Med* 2008;359:2324-36.
6. Cordeiro MA, Lima JA. Atherosclerotic plaque characterization by multidetector row computed tomography angiography. *Journal of the American College of Cardiology* 2006;47:C40-7.
7. Hoffmann U, Moselewski F, Nieman K et al. Noninvasive assessment of plaque morphology and composition in culprit and stable lesions in acute coronary syndrome and stable lesions in stable angina by multidetector computed tomography. *Journal of the American College of Cardiology* 2006;47:1655-62.
8. Motoyama S, Ito H, Sarai M et al. Plaque Characterization by Coronary Computed Tomography Angiography and the Likelihood of Acute Coronary Events in Mid-Term Follow-Up. *J Am Coll Cardiol* 2015;66:337-46.
9. Puchner SB, Liu T, Mayrhofer T et al. High-risk plaque detected on coronary CT angiography predicts acute coronary syndromes independent of significant stenosis in acute chest pain: results from the ROMICAT-II trial. *Journal of the American College of Cardiology* 2014;64:684-92.
10. Pletcher MJ, Tice JA, Pignone M, Browner WS. Using the coronary artery calcium score to predict coronary heart disease events: a systematic review and meta-analysis. *Arch Intern Med* 2004;164:1285-92.
11. Min JK, Shaw LJ, Devereux RB et al. Prognostic value of multidetector coronary computed tomographic angiography for prediction of all-cause mortality. *J Am Coll Cardiol* 2007;50:1161-70.
12. Stone GW, Maehara A, Lansky AJ et al. A prospective natural-history study of coronary atherosclerosis. *The New England journal of medicine* 2011;364:226-35.
13. Nadjiri J, Hausleiter J, Jahnichen C et al. Incremental prognostic value of quantitative plaque assessment in coronary CT angiography during 5 years of follow up. *Journal of cardiovascular computed tomography* 2016;10:97-104.
14. Lee JM, Choi G, Koo BK et al. Identification of High-Risk Plaques Destined to Cause Acute Coronary Syndrome Using Coronary Computed Tomographic Angiography and Computational Fluid Dynamics. *JACC Cardiovascular imaging* 2018.
15. Thygesen K, Alpert JS, Jaffe AS et al. Third universal definition of myocardial infarction. *Journal of the American College of Cardiology* 2012;60:1581-98.

16. Campeau L. The Canadian Cardiovascular Society grading of angina pectoris revisited 30 years later. *The Canadian journal of cardiology* 2002;18:371-9.
17. Raff GL, Chinnaiyan KM, Cury RC et al. SCCT guidelines on the use of coronary computed tomographic angiography for patients presenting with acute chest pain to the emergency department: a report of the Society of Cardiovascular Computed Tomography Guidelines Committee. *Journal of cardiovascular computed tomography* 2014;8:254-71.
18. Abbara S, Arbab-Zadeh A, Callister TQ et al. SCCT guidelines for performance of coronary computed tomographic angiography: A report of the Society of Cardiovascular Computed Tomography Guidelines Committee. *Journal of Cardiovascular Computed Tomography* 2009;3:190-204.
19. Wong DTL, Soh SY, Ko BSH et al. Superior CT coronary angiography image quality at lower radiation exposure with second generation 320-detector row CT in patients with elevated heart rate: a comparison with first generation 320-detector row CT. *Cardiovascular Diagnosis and Therapy* 2014;4:299-306.
20. Nerlekar N, Ko BS, Nasis A et al. Impact of heart rate on diagnostic accuracy of second generation 320-detector computed tomography coronary angiography. *Cardiovascular Diagnosis and Therapy* 2017;7:296-304.
21. Raff GL, Chair A, Abidov S et al. SCCT guidelines for the interpretation and reporting of coronary computed tomographic angiography. *Journal of Cardiovascular Computed Tomography* 2009;3:122-136.
22. Cury RC, Abbara S, Achenbach S et al. Coronary Artery Disease - Reporting and Data System (CAD-RADS): An Expert Consensus Document of SCCT, ACR and NASCI: Endorsed by the ACC. *JACC Cardiovascular imaging* 2016;9:1099-1113.
23. Min JK, Shaw LJ, Devereux RB et al. Prognostic Value of Multidetector Coronary Computed Tomographic Angiography for Prediction of All-Cause Mortality. *Journal of the American College of Cardiology* 2007;50:1161-1170.
24. Motoyama S, Sarai M, Harigaya H et al. Computed tomographic angiography characteristics of atherosclerotic plaques subsequently resulting in acute coronary syndrome. *Journal of the American College of Cardiology* 2009;54:49-57.
25. Psaltis PJ, Talman AH, Munnur K et al. Relationship between epicardial fat and quantitative coronary artery plaque progression: insights from computer tomography coronary angiography. *Int J Cardiovasc Imaging* 2016;32:317-28.
26. Chang HJ, Lin FY, Lee SE et al. Coronary Atherosclerotic Precursors of Acute Coronary Syndromes. *Journal of the American College of Cardiology* 2018;71:2511-2522.
27. Takahashi S, Kawasaki M, Miyata S et al. Feasibility of tissue characterization of coronary plaques using 320-detector row computed tomography: comparison with integrated backscatter intravascular ultrasound. *Heart and vessels* 2016;31:29-37.
28. Han D, Torii S, Yahagi K et al. Quantitative measurement of lipid rich plaque by coronary computed tomography angiography: A correlation of histology in sudden cardiac death. *Atherosclerosis* 2018.
29. Moss AJ, Williams MC, Newby DE, Nicol ED. The Updated NICE Guidelines: Cardiac CT as the First-Line Test for Coronary Artery Disease. *Curr Cardiovasc Imaging Rep* 2017;10:15.
30. Tian J, Dauerman H, Toma C et al. Prevalence and characteristics of TCFA and degree of coronary artery stenosis: an OCT, IVUS, and angiographic study. *Journal of the American College of Cardiology* 2014;64:672-80.

31. Motoyama S, Kondo T, Anno H et al. Atherosclerotic plaque characterization by 0.5-mm-slice multislice computed tomographic imaging. *Circulation journal : official journal of the Japanese Circulation Society* 2007;71:363-6.
32. Zaman T, Agarwal S, Anabtawi AG et al. Angiographic lesion severity and subsequent myocardial infarction. *The American journal of cardiology* 2012;110:167-72.
33. Ellis S, Alderman EL, Cain K, Wright A, Bourassa M, Fisher L. Morphology of left anterior descending coronary territory lesions as a predictor of anterior myocardial infarction: a CASS Registry Study. *J Am Coll Cardiol* 1989;13:1481-91.
34. Alderman EL, Corley SD, Fisher LD et al. Five-year angiographic follow-up of factors associated with progression of coronary artery disease in the Coronary Artery Surgery Study (CASS). CASS Participating Investigators and Staff. *Journal of the American College of Cardiology* 1993;22:1141-54.
35. Burke AP, Kolodgie FD, Farb A et al. Healed plaque ruptures and sudden coronary death: evidence that subclinical rupture has a role in plaque progression. *Circulation* 2001;103:934-40.
36. Tian J, Ren X, Vergallo R et al. Distinct morphological features of ruptured culprit plaque for acute coronary events compared to those with silent rupture and thin-cap fibroatheroma: a combined optical coherence tomography and intravascular ultrasound study. *Journal of the American College of Cardiology* 2014;63:2209-16.
37. Naghavi M, Libby P, Falk E et al. From vulnerable plaque to vulnerable patient: a call for new definitions and risk assessment strategies: Part II. *Circulation* 2003;108:1772-8.
38. Lee MS, Chun EJ, Kim KJ, Kim JA, Yoo JY, Choi SI. Asymptomatic subjects with zero coronary calcium score: coronary CT angiographic features of plaques in event-prone patients. *Int J Cardiovasc Imaging* 2013;29 Suppl 1:29-36.
39. Kubo T, Maehara A, Mintz GS et al. The dynamic nature of coronary artery lesion morphology assessed by serial virtual histology intravascular ultrasound tissue characterization. *Journal of the American College of Cardiology* 2010;55:1590-7.
40. Narula J, Kovacic JC. Putting TCFA in clinical perspective. *Journal of the American College of Cardiology* 2014;64:681-3.
41. Brown AJ, Teng Z, Calvert PA et al. Plaque Structural Stress Estimations Improve Prediction of Future Major Adverse Cardiovascular Events After Intracoronary Imaging. *Circulation Cardiovascular imaging* 2016;9.
42. Mark DB, Berman DS, Budoff MJ et al. ACCF/ACR/AHA/NASCI/SAIP/SCAI/SCCT 2010 expert consensus document on coronary computed tomographic angiography: a report of the American College of Cardiology Foundation Task Force on Expert Consensus Documents. *Catheterization and cardiovascular interventions : official journal of the Society for Cardiac Angiography & Interventions* 2010;76:E1-42.

**Table 1. Patient characteristics**

	Overall (1254)	ACS (45)	No ACS (1192)	P value
Age	60.9±13.7	59.9 ± 11.7	61 ± 13.8	0.86
Male gender	638 (50.9%)	29 (64%)	610 (51%)	0.41
Hypertension	583 (46%)	23 (51%)	560(45%)	0.76
Hypercholesterolemia	581 (46%)	18(40%)	563 (45%)	0.05
Diabetes mellitus	1398(11.2%)	8 (18%)	131 (11%)	0.39
Smoker	128 (10.3%)	9 (20%)	119 (10%)	0.03
Ex smoker	223 (18%)	8 (18%)	215 (18%)	0.84
Family history of IHD	536 (43.3%)	19 (42%)	517 (43%)	0.42
Obesity (BMI >30)	152 (12.2%)	7 (16%)	145 (13%)	0.16

<b>Table 2. Patient characteristics – Variables associated with HRP</b>			
	HRP (243)	No HRP (991)	P value
Age	63.5±12.9	60.5±13.8	0.7
Male gender	160 (66%)	482 (49%)	0.42
Hypertension	113 (47%)	461 (47%)	0.99
Hypercholesterolemia	123 (51%)	446 (45%)	0.12
Diabetes mellitus	38 (16%)	100 (10%)	0.015
Smoker	35 (14%)	94 (9%)	0.03
Ex smoker	48 (20%)	174 (18%)	0.43
Family history of IHD	99 (41%)	437 (44%)	0.34
Obesity (BMI >30)	26 (11%)	126 (13%)	0.39

<b>Table 3. ACS development per patient and stenosis characteristics</b>		
Parameter	Hazard Ration	P value
HRP presence	14.5 (7.3-28.6)	< 0.001
HRP – PR	14.5 (7.3-28.7)	<0.001
HRP – SC	5.4 (3.0-9.9)	< 0.001
HRP – LAP	16.7 (9.1-30.5)	< 0.001
HRP ≥ 2 features	14.04 (7.46-26.44)	< 0.001
Stenosis ≥ 50	6.3 (3.5-11.4)	< 0.001
HRP + Stenosis ≥ 50	10.3 (5-21.2)	< 0.001
Remodelling index	0.98 (0.96-0.99)	< 0.004

**Table 4. Quantitative plaque analysis of HRP segments and association with ACS**

Parameter	ACS	No ACS	HR	P value
Stenosis $\geq$ 50	22	83	2.4 (1.19-4.83)	0.01
SC	17	127	0.76 (0.38-1.50)	0.42
Presence of LAP	31	132	3.77 (1.64-7.72)	0.005
$\geq$ 2 HRP features	32	167	2.66 (0.81-8.67)	0.11
MLA	6.54	6.5	1.02 (0.94-1.12)	0.43
MLD	2.27	2.23	1.08(0.7-1.65)	0.55
SIS	1.61	1.9	0.71 (0.47-1.08)	0.08
SSS	2.17	2.6	0.8 (0.62-1.04)	0.37
Calcified plaque	2	5	1.53 (0.37-6.38)	0.38
Non-Calcified plaque	8	35	0.98 (0.44-2.18)	0.72
Mixed plaque	20	123	0.68(0.34-1.35)	0.34
Total plaque length	14.9	14.8	1.0 (0.96-1.06)	0.64
Total plaque burden	56.7	56.7	1.00 (0.97-1.04)	0.84
Total plaque volume	170	169.5	1.00 (0.99-1.00)	0.32
LL plaque burden	64.8	64.9	1.01 (0.98-1.03)	0.57
LL Plaque volume	11.9	11.9	1.08 (1.02-1.15)	0.007

<b>Table 5. ACS predictors – Per plaque at lesion level analysis determined by stenosis and LAP volume</b>			
Parameter	n	Hazard ratio	P value
Non-obstructive + Lap low LAP	53	Reference	
Obstructive + Lap low LAP	29	1.72 (0.35-8.54)	0.51
Non-obstructive + mid LAP	46	0.65 (0.11-3.91),	0.64
Obstructive + mid LAP	32	4.08 (1.06-15.79)	0.04
Non-obstructive + high LAP	46	2.26 (0.58-8.81)	0.24
Obstructive + high LAP	37	5.68 (1.59 -20.2)	0.007

**Table 6. Survival analysis in only patients with events limited to 5 year follow-up**

HRP: HR 3.34 (1.16-9.63), p=0.03; Kaplan Meier log-rank 0.02

Comparing proportion surviving at annual time point

<b>Year</b>	<b>HRP absent</b>	<b>HRP present</b>
<b>0</b>	100%	100%
<b>1</b>	100%	73%
<b>2</b>	82%	56%
<b>3</b>	82%	41%
<b>4</b>	82%	35%
<b>5</b>	64%	24%

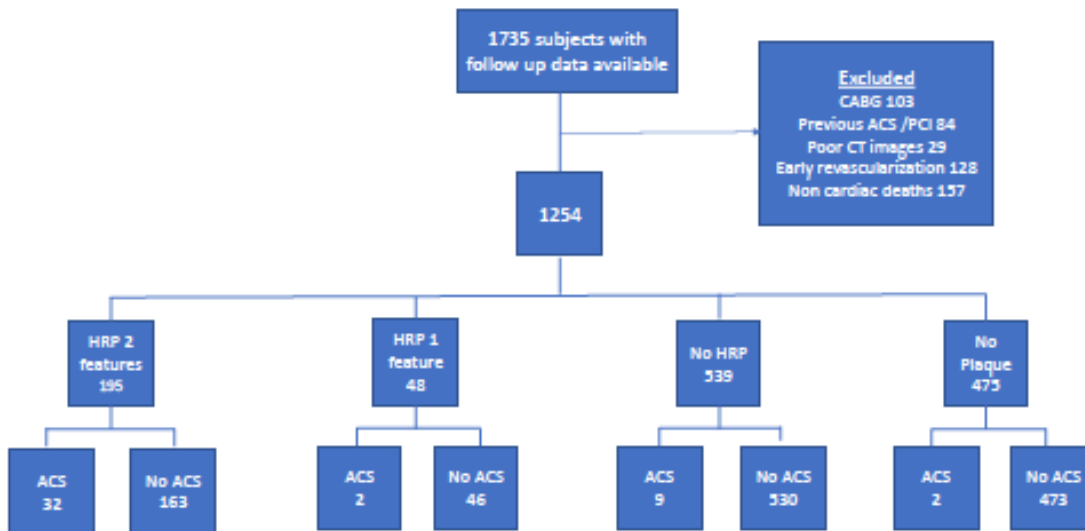
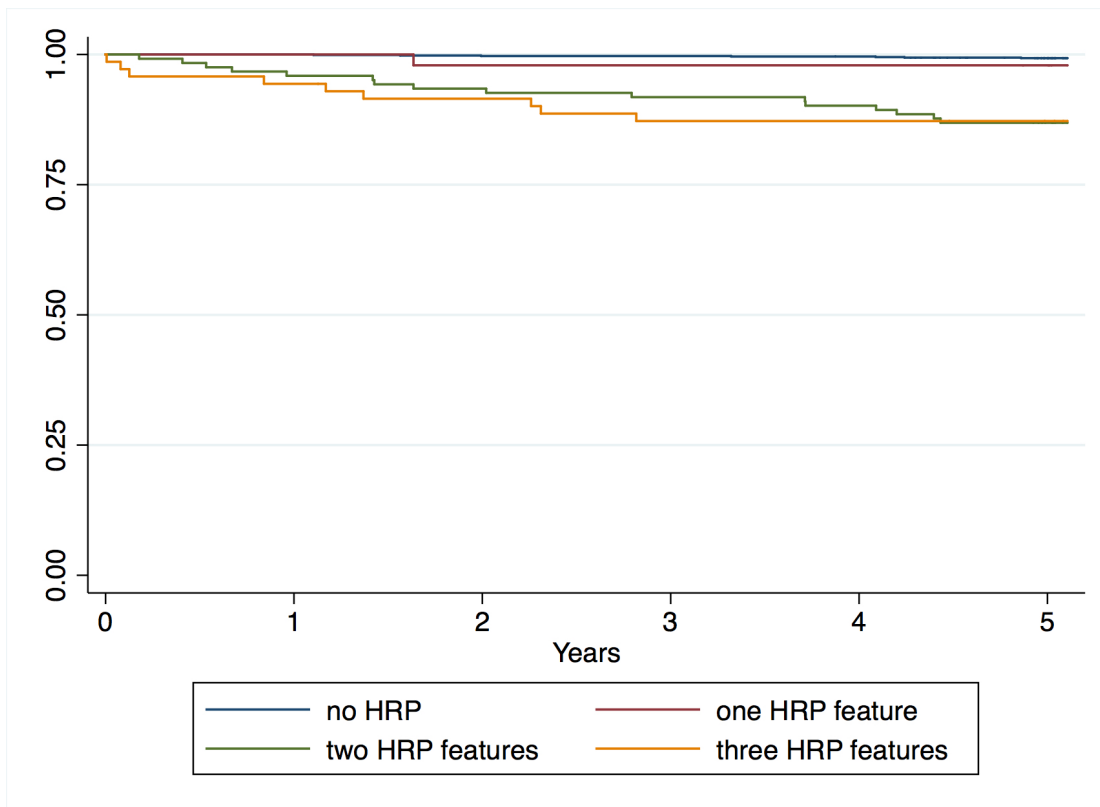


Figure1: Acute Coronary Events in Patients based on plaque characteristics

During follow up ACS occurred in 32 (16.4%) of 195 HRP(+) patients with  $\geq 2$  features compared to 2 (4.1%) of 48 HRP(+) patients with one feature, 9 patients (1.6%) of the 539 HRP(-) patients and 2 (0.4%) of the 475 patients without any plaque.

CABG = Coronary artery bypass grafting, ACS = acute coronary syndrome



**Figure 2; Kaplan Myer curve of patients with 3HRP with 3 features vs. HRP with 2 features vs. HRP with 1 feature vs. No HRP features**

Of the 45 patients who had ACS, 34 patients had HRP while 11 patients had no HRP. During follow up, 32 (16.4%) of 195 patients with HRP (+) patients with  $\geq 2$  features developed ACS. In comparison, 2 (4.1%) of 48 HRP (+) patients with one HRP feature, 9 (1.6%) of the 539 HRP (-) patients and 2 (0.4%) of the 475 patients without any plaque developed ACS.

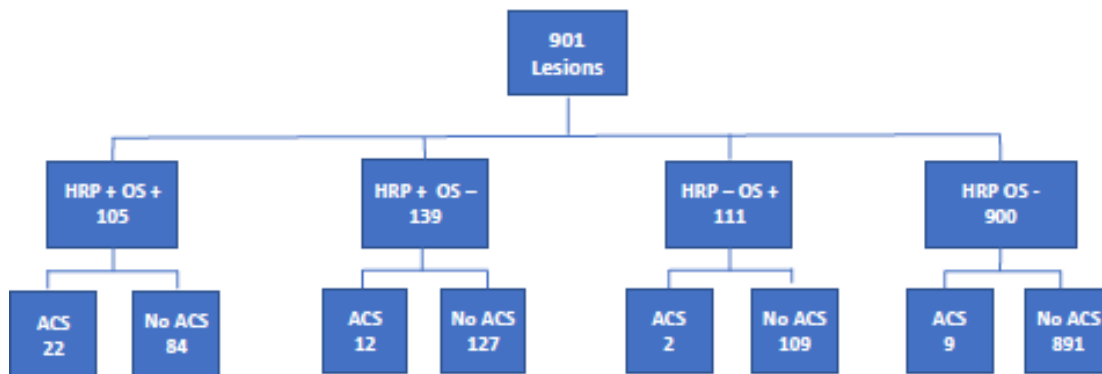


**Figure 3. Acute coronary syndrome based on stenosis severity**

Overall, ACS occurred in 24 (11.4%) of 209 OS(+) patients compared to 21 (2%) of 1045 OS(-) patients. When the relationship between HRP and OS was assessed, ACS was more frequent in HRP(+)/(OS(+)) patient with 22 (20.7%) of 106 developing ACS. In comparison, 12 (8.6%) of 139 HRP(+)/OS(-) patients, 2 (1.8%) of 111 HRP(-)/OS(+) patients and 9 (1.0%) of 900 HRP(-)/OS(-) patients developed ACS.

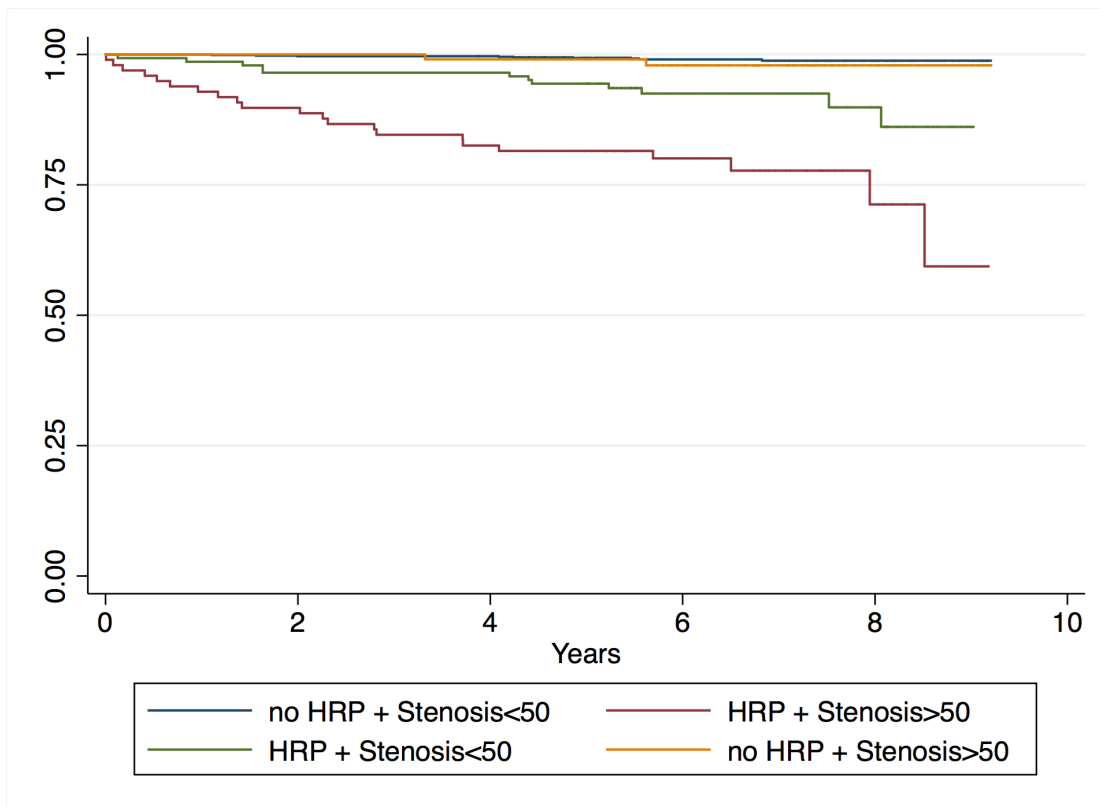
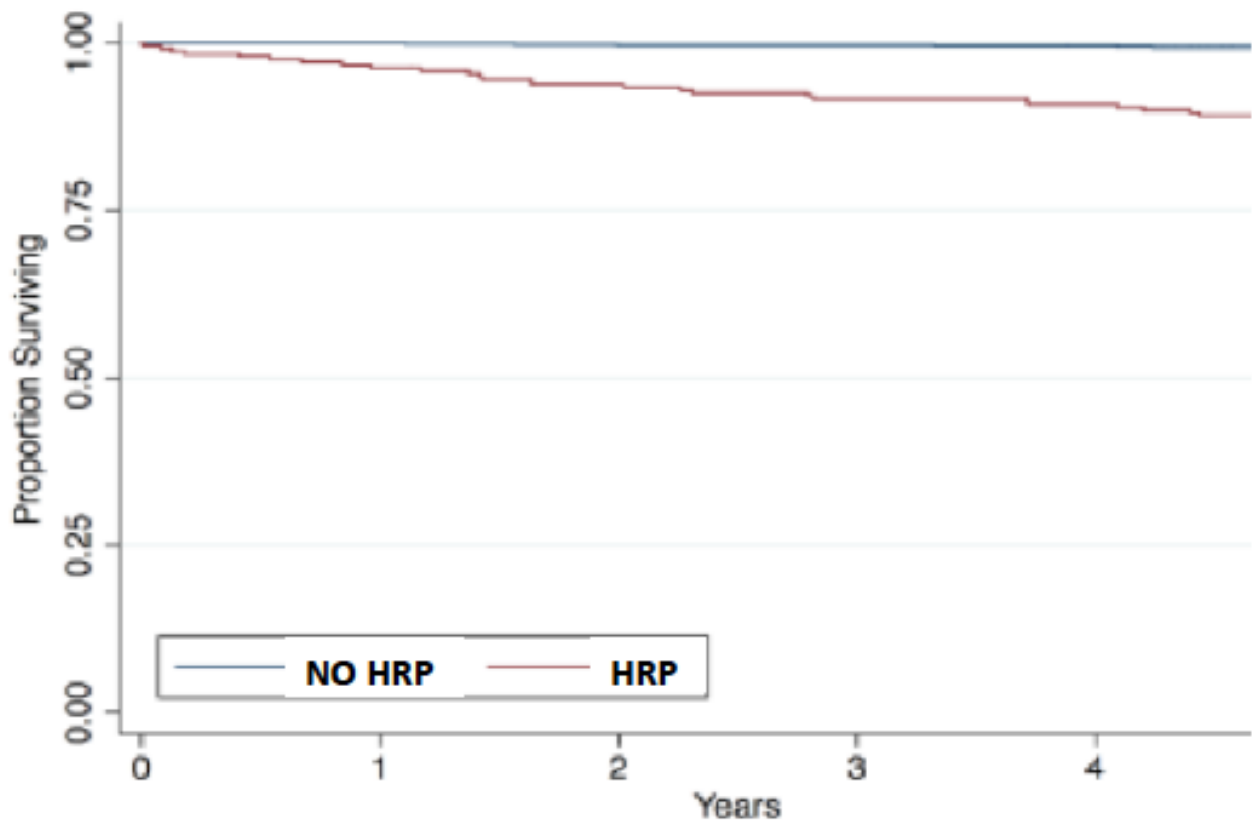


Figure 4: Kaplan Meier curve of patient with HRP(+)/OS(+) vs. HRP(+)/OS(-) vs. HRP(-)/OS(+) vs. HRP(-)/OS(-).

ACS was more frequent in HRP (+)/ (OS (+) patient with 22 (20.7%) of 106 developing ACS. In comparison, 12 (8.6%) of 136 HRP (+)/OS (-) patients, 2 (1.8%) of 111 HRP (-)/ OS (+) patients and 9 (1.0%) of 900 HRP (-)/OS (-) patients developed ACS



**Figure 5: Kaplan Myer curve of patients with HRP vs. patients with no HRP**

On survival analysis of patients with events limited to five years of follow up, the time interval between the CCTA and event was shorter in HRP(+) patients (HR 3.34 (1.16-9.63), p=0.03; Kaplan Meier log-rank 0.02). The comparison of proportion of patients surviving, between HRP(+) patients to HRP(-) annually was 73% and 100%; 56% and 82%; 41% and 82%; 35% and 82%; 24% and 64% respectively for up to 5 years follow up

## **Chapter 6: Diagnostic Accuracy of ASLA Score (A Novel CT Angiographic Index) and Aggregate Plaque Volume in the Assessment of Functional Significance of Coronary Stenosis**

*Ravi Kiran Munnur\* MBBS<sup>1</sup>, James D Cameron MBBS, MD<sup>1</sup>, Liam M McCormick MBBS, MD<sup>1</sup>, Peter J Psaltis MBBS (Hons), PhD<sup>2,3</sup>, Nitesh Nerlekar MBBS<sup>1</sup>, Brian SH Ko MBBS (Hons), PhD<sup>1</sup>, Ian T Meredith MBBS (Hons), PhD<sup>1</sup>, Sujith Seneviratne MBBS (Hons)<sup>1</sup>, Dennis TL Wong MBBS (Hons), MD, PhD<sup>1,2</sup>*

<sup>1</sup> *Monash Cardiovascular Research Centre, Department of Medicine (Monash Medical Centre) Monash University and Monash Heart, Monash Health, 246 Clayton Road, Clayton, 3168 VIC, Australia*

<sup>2</sup> *South Australian Medical Research Institute (SAHMRI), Adelaide, Australia*

<sup>3</sup> *Discipline of Medicine, University of Adelaide, Adelaide, Australia*

**Accepted and Published Int J Cardiol. 2018 Jun 8. pii: S0167-5273(18)30781-2**

*Corresponding author*

*Ravi Kiran Munnur*

*Monash Medical Centre, Monash Cardiovascular Research Centre, VIC, Australia*

## ABSTRACT

**BACKGROUND:** Visual assessment of diameter-stenosis on Computed tomography coronary angiography (CTCA) lacks specificity to determine functional significance of coronary artery stenosis. Percent-aggregate plaque volume (%APV) and ASLA score, which incorporates Area of Stenosis, Lesion length, and area of myocardium subtended estimated by APPROACH score (Alberta Provincial Project for Outcome Assessment in Coronary Heart Disease) have been described to predict lesion specific ischaemia in focal lesions with intermediate stenosis.

**METHODS AND RESULTS:** Included were 81 patients (mean age  $64.7 \pm 9$  years, 62% male; 94 vessels) who underwent 320- detector-row CTCA, invasive coronary angiography and fractional-flow-reserve (FFR). We examined vessels with wide range of diameter stenosis (mid to severe) and with multiple lesions. Invasive FFR of  $\leq 0.8$  was considered functionally significant.

The first 54 patients (62 vessels) formed the derivation cohort. ASLA score was the best predictor of  $\text{FFR} \leq 0.8$  (AUC 0.83,  $p < 0.001$ ) compared to %APV (0.72),  $\text{CT} > 50\%$  (0.76), APPROACH score (0.79), area-stenosis (0.73), diameter-stenosis (0.74), minimum-luminal-diameter (0.74), minimal-luminal-area (0.72), and lesion-length (0.67). ASLA score and not %APV, provided incremental predictive value when added to  $\text{CT} > 50$  [(NRI 0.71,  $p = 0.005$ ) vs. (NRI 0.01,  $p = 0.96$ )]. In the validation cohort of 27 patients (32 vessels), the ASLA score (AUC 0.85) was again a better predictor of  $\text{FFR} \leq 0.8$  compared to %APV (0.71),  $\text{CT} > 50\%$  (0.66) and other CT indices. The AUC of ASLA score was superior to  $\text{CTCA} > 50\%$  ( $p = 0.001$ ).

**CONCLUSION:** ASLA score is a novel predictor of functional significance of coronary stenosis and adds incremental predictive value to  $\text{CT} > 50$  but %APV did not.

**Key Words:** Coronary artery disease, Fractional Flow Reserve, ASLA score Computed Tomography Coronary Angiography, percent Aggregate Plaque Volume

## ABBREVIATIONS

CTCA: Computed Tomography Coronary Angiography

ICA: Invasive coronary angiography

CAD: Coronary artery disease

APV: Aggregate Plaque Volume

ASLA: Area stenosis, lesion length, area of myocardium subtended by APPROACH score

IVUS: Intravascular Ultrasound

FFR: Fractional flow reserve

APPROACH: Alberta Provincial Project for Outcome Assessment in Coronary Heart Disease

ASLA: Area stenosis Lesion length Approach Score

SM: Supplementary material

## **Introduction**

Computed Tomography Coronary Angiography (CTCA) is an established non-invasive test to detect coronary stenosis in individuals with low to intermediate risk of coronary artery disease (CAD) (1, 2). However, CTCA is limited by low specificity to predict lesion specific ischaemia and visual or quantitative assessments of coronary stenosis do not correlate well to fractional flow reserve (FFR)(3). In addition, even the presence of obstructive disease on CTCA had poor predictive value of ischaemia on myocardial perfusion tests (4-6). Studies have shown that besides diameter stenosis, predictors of fractional flow reserve (FFR)  $\leq 0.8$  are area stenosis, lesion length and ischaemic burden (7-9). In addition, for intermediate stenosis, lesions in proximal LAD with larger myocardial supply and ischaemic burden had more significant FFR values compared to distal LAD, left circumflex artery and right coronary artery(10). Based on these observations, the ASLA (Area Stenosis Lesion length and APPROACH score) score has been described. It was demonstrated to predict significant FFR and provide incremental predictive value over individual indexes alone(11). It incorporates lesion length, area of stenosis and the area of myocardium subtended by coronary stenosis estimated by APPROACH score (Alberta Provincial Project for Outcome Assessment in Coronary Heart Disease).

In addition to the identification of luminal stenosis, plaque quantification can also be derived from CTCA (12). Nakazato et al demonstrated that percent aggregate plaque volume (% APV) was the best

predictor of FFR significant lesions amongst various CTCA indexes and it was shown to provide incremental diagnostic value when added to individual CTCA indexes (13). To date, diagnostic accuracy of the ASLA score and percent APV have been evaluated only in vessels with focal lesions with intermediate diameter stenosis severity. In this study, we assessed and compared the diagnostic accuracy of ASLA score and percent APV in vessels with wide range of stenosis severity and in vessels with multiple stenoses.

## **Methods**

We included consecutive patients with suspected coronary artery disease who underwent clinically indicated 320 detector–row CTCA and ICA with FFR within a three month period between December 2013 and January 2015. FFR assessment was performed in at least one lesion of mild (>30%) severity as visually assessed on CTCA. Our institutional Human Research Ethics Committee approved the study. Excluded were patients with > 3 months duration between CTCA an FFR, poor quality images, prior coronary artery bypass grafting, left ventricular dysfunction, acute coronary syndrome and vessels with more than one severe lesion, severe calcification, diffuse disease, severe stenosis in the distal segment, intra coronary stents and small vessel diameter (<2mm).

### CT coronary angiography

Patients underwent cardiac CT assessment using a 320-row detector CT scanner (Aquilion One Vision; Toshiba Medical Systems Corp., Tokyo, Japan). All patients received sublingual nitroglycerine, and additional beta-blockers were administered to achieve a pre-scan heart rate of <60 beats/min in accordance with Society of Cardiovascular Computed Tomography guidelines (14).

A bolus of 55 mL of 100% iohexol 56.6 g/75 mL (Omnipaque 350; GE Healthcare, Princeton, NJ) was injected into an antecubital vein at a low rate of 5 mL/sec, followed by 20 mL of a 30:70 mixture of contrast material and saline, followed by 30 mL of saline. Scanning parameters were as

follows: detector collimation: 320 3 0.5 mm; tube current:300–500 mA (depending on body mass index), tube voltage: 120 kV; gantry rotation time: 350 msec; and temporal resolution: 175 msec. Prospective electrocardiographic gating was used, covering phases 70%– 80% of the R-R interval. Scanning was completed with a single R-R interval utilizing a 180° segment if heart rate was < 65 beats per minute or slower and data segments from two consecutive beats were used for multi-segment reconstruction with an improved temporal resolution of 87 msec in patients with a heart rate greater than 65 beats per minute,

#### Analysis of CT coronary angiograms

Data was transferred to an external workstation (Vitrea 6, version 6.0; Vital Images, Minnetonka, Minnesota) for further analysis. Two experienced cardiologists (KM & DW) who were blinded to the results of coronary angiography and FFR measurements performed the analysis independently. Plaque quantification was performed using a dedicated software tool (Sure Plaque, Vitrea 6, version 3.0; Vital Images and Toshiba Medical Systems). Further manual adjustments were performed for the lumen and the outer vessel wall using dedicated window settings [230W and 83 L if the luminal Hounsfield unit (HU) was <500; and 300W and 150 L if the luminal HU was >500] (15). If necessary, additional window setting of 740W / 220L and 1400W / 400L were used in the presence of non-calcified and calcified plaque respectively, to assess outer vessel wall (16) (Figure 1) (SM Fig 4).

Vessels were categorised based on visual diameter stenosis of >50% (CT>50) and quantitative computed tomography (QCT) stenosis > 70%. APPROACH score was used to evaluate the proportion of the myocardium perfused by each artery as previously described (17, 18) (SM Table 3). The modified score considers the location of the lesion (proximal, middle, or distal) and the dominance and size of the secondary branches and provides an estimate of the percentage of supplied myocardium beyond the considered coronary lesion. For the assessment of ASLA score, each lesion was assigned individual score based on lesion length, area stenosis and APPROACH

score as previously described (11). ASLA score was derived after addition of individual scores for a possible total of 18 points (Table 1). In vessels with multiple stenoses, the most significant lesion was analysed for minimal luminal area (MLA), minimal luminal diameter (MLD), lesion length and ASLA score (SM Fig 3).

For the assessment of percent APV, ostium to the distal edge of the lesion in vessels with single lesion and from the ostium to the distal edge of the distal lesion in vessels with multiple lesions was considered. As a first step, plaque area defined as the area between the outer contour of the vessel (vessel area) and the lumen at each slice (0.5mm) was determined. Secondly, aggregate plaque volume was obtained by summation of all plaque areas. Thirdly, total vessel volume was derived from the summation of all vessel areas. Percent aggregate plaque volume was calculated as aggregate plaque volume divided by total vessel volume and reported as percentage (13).

#### Invasive coronary angiography and FFR measurement

Invasive coronary angiography was performed as per standard catheterisation procedure in accordance with the American College of Cardiology guidelines for coronary angiography (19). FFR was measured using pressure sensor tipped guide wire (Pressure wire Certus; St Jude Medical, St Paul, Minn) as previously described. Intracoronary glyceryl trinitrate (100 µg) was injected to minimise vasospasm. Intravenous adenosine was administered at 140 µg/kg/min through an intravenous line in the antecubital fossa. At steady state hyperaemia, FFR was assessed by using the Radi Analyser Xpress (St Jude Medical) and was calculated by dividing the pressure obtained distal to the stenosis to the mean aortic pressure measured through the guide catheter. An FFR of 0.8 or less was considered to indicate lesion-specific ischaemia (20).

#### Statistical analysis

Continuous variables are expressed as mean  $\pm$  standard deviations or with 95% confidence interval. Categorical variables are expressed as percentages. Continuous and categorical variables were compared using *t* test, Mann-Whitney or chi-square as appropriate. Correlations between coronary CTA parameters and FFR were assessed by calculating Pearson's correlation coefficient. Inter-observer variability was assessed by using the intra-class coefficient and Bland Altman test. For Univariate binary logistic regression analysis, standardised odds ratio coefficients were added to enable direct comparison of predictors. Any cut off value of 0.25 on univariate analysis are usually included in the multivariate analysis and we chose covariates with  $P < 0.2$  on univariate analysis to be included in the multivariate analysis by using the "enter" approach. For the multivariate logistic regression analysis, odds ratios were reported.

To examine discrimination, area under the receiver operating characteristic curves (AUC) were calculated and compared for the different CTCA parameters using De Long method (21). We determined the net reclassification improvement of ASLA score and percent APV over  $CT > 50$  to predict  $FFR \leq 0.8$ . To determine intra-observer and inter-observer variability for calculation of percent APV and ASLA score, eighteen random subjects were selected (eight patients with  $FFR \leq 0.8$ ). A *p* value of  $< 0.05$  was considered statistically significant. Statistical analysis was performed with SPSS 18 (SPSS, Chicago, III).

## **Results**

### Patient characteristics

There were 145 patients who underwent CT and FFR assessment in our institution during the study period. All the patients in the study had CTCA initially for assessment of chest pain and the treating physician decided on the need for further investigations. Patients were excluded from the study for the following reasons: presence of minimal stenosis  $< 30\%$  ( $n=16$ ), poor image quality ( $n=7$ ), vessel diameter  $< 2\text{mm}$  ( $n=14$ ), excessive calcification ( $n=17$ ) and multiple severe tandem lesions ( $n=10$ ).

The remaining 81 patients (mean age  $64.7 \pm 9$  years, 62% male) with 94 vessels were included for analysis. The time interval between CTCA and FFR was less than three months. Of the 94 vessels (56 - LAD, 16 - LCx and 22 - RCA) included in the study, 42 vessels were FFR significant, 41 vessels had single lesion and 63 vessels had multiple lesions. There were 29 vessels with non-calcified plaque and remaining vessels had calcified or partially calcified plaque. Participants in the study did not undergo revascularisation between CTCA acquisition and FFR measurement and there were no events during this period. Patient characteristics are shown in table 2.

The first 62 vessels were analysed for the assessment of diagnostic accuracy of ASLA score, %APV and various CT indices and formed the derivation cohort. The subsequent 32 vessels formed the validation cohort where the results were tested again.

### **DERIVATION COHORT (54 patients and 62 vessels)**

#### Relationship between CTCA parameters and significant FFR.

There were 39 vessels (61%) with CT>50 stenosis. On per vessel analysis, the sensitivity, specificity, negative predictive value (NPV) and positive predictive value (PPV) of CT>50 for predicting significant FFR were 95%, 59%, 90% and 68% respectively. There were 22 vessels (35%) with CT>70 stenosis and on per vessel analysis, the sensitivity, specificity, NPV and PPV of CT > 70 were 57%, 84%, 68% and 77% respectively. On univariate analysis, there was significant association between FFR  $\leq 0.8$  and CT>50 (AUC: 0.76; 95% CI: 0.64, 0.89,  $p=0.004$ ), CT >70 (AUC: 0.71; 95% CI: 0.57, 0.84,  $p=0.001$ ), diameter stenosis (AUC: 0.74; 95% CI: 0.61, 0.87;  $p < 0.004$ ), MLD (AUC: 0.74; 95% CI: 0.61, 0.87;  $p < 0.004$ ), MLA (AUC: 0.72, 95% CI: 0.59, 0.85;  $p = 0.005$ ), CTCA QCT (0.68; 95% CI: 0.55, 0.82,  $p < 0.004$ ) and APPROACH score (0.79; 95% CI: 0.68, 0.9;  $p < 0.001$ ). There was no significant association between lesion length and FFR  $\leq 0.8$  (AUC: 0.67; 95% CI: 0.54, 0.81;  $p < 0.077$ ) (SM Table 4 and Fig 5).

#### Relationship between ASLA score and significant FFR

The mean ASLA score in vessels with  $\text{FFR} \leq 0.8$  was  $13.6 \pm 4.06$  compared to  $7.6 \pm 4.4$  versus for vessels with  $\text{FFR} > 0.8$  ( $p < 0.001$ ). On a per vessel analysis, the AUC of ASLA score for predicting  $\text{FFR} \leq 0.8$  was 0.83 (95% CI: 0.73-0.93;  $p < 0.001$ ) and was superior compared to area stenosis, lesion length and APPROACH score. The measurement of ASLA score was highly reproducible with excellent intra-observer and inter-observer intra-class correlation coefficient of 0.99 (95% CI: 0.99 – 0.99) and 0.99 (95% CI: 0.99 – 0.99) respectively (SM Table 5). The ASLA score  $\leq 4$  (100 % sensitivity and NPV) and ASLA score  $\geq 15$  (94% specificity and 86% PPV) were able to identify FFR insignificant and FFR significant lesions respectively (Figure 2). On an average it took 4.7 minutes (range: 3 to 8 minutes) to calculate ASLA score.

#### Relationship between percent APV and significant FFR

The mean percent APV in vessels with  $\text{FFR} \leq 0.8$  was  $54.9 \pm 9 \text{ mm}^3$  compared to  $48.8 \pm 12.6 \text{ mm}^3$  for vessels with  $\text{FFR} > 0.8$  ( $p < 0.03$ ). On a per vessel analysis, the AUC for percent APV to identify lesion specific ischaemia was 0.72 (95% CI: 0.59-0.85;  $p < 0.039$ ). The percent APV measurements was reproducible with intra-observer and inter observer intra-class correlation coefficient of 0.99 (95% CI: 0.90 - 0.99) and 0.85 (95% CI: 0.40 - 0.96) respectively (SM Table 6). On an average, it took 42 minutes to calculate percent APV.

We performed 2 multivariate models. Model 1 included ASLA score,  $\text{CT} > 50$ , lesion length, area stenosis and APPROACH score. Model 2 included percent APV as a co-variate in addition to the parameters in Model 1. Only ASLA score was predictive for lesion specific ischemia in both the models whilst the other parameters were not significant.

#### Incremental predictive value of ASLA score to predict significant FFR

When added to CT>50%, only ASLA score provided incremental predictive value [Net reclassification index 0.71,  $p < 0.005$ ] and percent APV did not (NRI 0.01,  $p = 0.96$ ). On direct comparison of AUC, ASLA score (0.83) had a trend of being superior to APV (0.72) for predicting significant FFR but did not reach statistical significance ( $p = 0.07$ ).

### **VALIDATION COHORT (27 patients, 32 vessels)**

The results from the validation cohort confirmed that ASLA (AUC of 0.85,  $p = 0.007$ ) was the best predictor of significant FFR compared to % APV (0.71), CT> 50 (0.66), MLD (0.80), MLA (0.81), area stenosis (0.81), diameter stenosis (0.79), lesion length (0.81), Approach score (0.73). CT>50 [OR 8.3 (CI: 0.88 – 0.78)  $p = 0.07$ ,  $n = 10$ ] and CT>70 [OR 2.5 (CI: 0.55-11.33),  $p = 0.24$ ,  $n = 10$ ] were not significant in predicting functionally significant lesions. On comparison of AUC of ASLA score to CT>50, ASLA score was found to be superior ( $p = 0.001$ ).

ASLA score  $< 5$  (100% sensitivity and 100% NPV) and ASLA score of  $> 14$  (94 % specificity and 94% PPV) were able to identify FFR insignificant and FFR significant vessels respectively. ASLA score of 10 had sensitivity of 86% and specificity of 71% in the identification of lesion specific ischaemia.

### **Discussion**

To our knowledge, this study is the first to compare the diagnostic accuracy of ASLA score and aggregate plaque volume using 320-detector row CT with invasive functional standard FFR as reference. ASLA score was the best parameter at predicting functional significance of stenosis. ASLA score but not aggregate plaque volume, added incremental predictive value when added to CT >50 for predicting significant FFR.

#### ASLA score is a predictor of functionally significant lesions

Following a CTCA, although visually determined diameter stenosis greatly determines the need for further investigations, it lacks specificity in identifying functionally significant lesions (22). In our

study, only ASLA score provided incremental predictive value when added to CT > 50 suggesting that there may be a role for ASLA score to further streamline patient management. Our findings indicate that lesions on CTCA with ASLA score  $\leq 4$  could potentially be managed conservatively while those with ASLA score of  $\geq 15$  referred for cardiac catheterisation. Patients with scores between 5 and 14 require further assessment by a functional test or FFR (SM Fig 6). The addition of ASLA score is attractive as on average it takes < 5 minutes to calculate at point of care, is reproducible and improves the diagnostic ability of CTCA without the need for additional imaging, reconstruction or cost.

Coronary flow is complex and is determined by various factors. Poiseuille equation illustrates that the pressure gradient across a coronary lesion is directly proportional to the coronary blood flow, blood viscosity and lesion length, and is inversely proportional to the 4<sup>th</sup> power of the radius. ASLA score takes into account most of these components and its performance in our study is consistent with previous observations and broadens the use of ASLA score beyond its application in focal lesions of intermediate stenosis. In vessels with multiple lesions, the ASLA score was superior to percent APV and other CT parameters in predicting significant FFR, when the score was applied to the most severe lesion. There are several other CT parameters that have been studied to assess their suitability to identify haemodynamically significant lesions. Non-invasive CT-FFR (23) appears to be the best tool available but is limited by high cost and long processing time involving the use of an offsite super computer. Computational CT-FFR using novel algorithms with prototype software appears promising. In two small studies, CT-FFR was found to be the best predictor of lesion specific ischaemia (AUC of 0.91 and AUC of 0.85) compared to various other CT parameters (24, 25). As the technology further improves and until CT-FFR is more readily available, ASLA may serve as a complementary technique to CTCA visual diameter stenosis assessment.

Although lesion length and percent APV were shown to be associated with lesion specific ischaemia (7, 11, 13), Park et al demonstrated the association of these parameters to significant FFR only in lesions

with stenosis > 50% (26). Whereas in our study, whilst significant association between lesion length and FFR  $\leq 0.8$  was observed only in the validation cohort, we found no association between percent APV and FFR significant lesions, and percent APV did not add incremental value to CT>50. We differ from previous studies as we assessed vessels with varying degree of stenosis and number of lesions, which may have contributed to the difference in the significance of lesion length and percent APV. Several IVUS studies have found inconsistent relationship between plaque burden and FFR. The location of the lesion (proximal vs. distal) and the vessel involved (LAD vs. non-LAD) appear to influence the results, which may be due to the difference in the myocardium subtended. In addition, it has been observed in post mortem studies that positive or negative remodelling affects lumen differently regardless of the plaque size (27, 28). Hence, it is possible for the effect of percent APV to vary depending on the location of the lesion and extent of remodelling.

### **Limitations**

Our study was retrospective and limited to a single centre involving a selected small number of patients and the results need confirmation in larger multicentre studies. The ASLA score is also of clinical utility at extremes of scores and is applicable in selected patients. Calcification limits application of ASLA score due to blooming artefacts. In addition, there is a possibility of missing mild calcification due to high luminal HU leading to an error in the assessment of stenosis severity (29). The performance of ASLA score was not tested in vessels with severe stenosis in distal segments, in bypass graft lesions and in patients with impaired left ventricular function.

Furthermore, we have not assessed the clinical impact of plaque composition in our study.

Fractional flow reserve was clinically indicated at physician's discretion, which may have lead to a selection bias. In vessels with more than one lesion, the most severe lesion was considered for analysis and the other less severe lesions in the same vessel could also have influenced FFR results.

In our study, we assessed only the images with Likert score of  $\geq 3$  and we acknowledge that it may

have impacted our results. Lastly, this is a single vendor study and only one platform was used for imaging analysis. Therefore, result may not be universally applicable.

## **Conclusion**

ASLA score is a novel predictor of functional significance of coronary stenosis. ASLA score adds incremental predictive value to CT>50 but percent APV did not. If the performance of ASLA score is confirmed in larger studies, it has the potential to be used in routine clinical practice to improve the diagnostic accuracy of CTCA.

## **Acknowledgements**

RKM is a recipient of Cardiac Society of Australia and New Zealand (CSANZ) scholarship and Australian Post Graduate (APA) scholarship.

DW is supported by National Health & Medical Research Institute (NHMRC) Australia Early Career Fellowship

PP is supported by National Heart Foundation Australia Career Development Fellowship

NN is supported by the National Heart Foundation Australia and National Health & Medical Research Institute (NHMRC) Australia Postgraduate Scholarship

Dr. Liam McCormick is supported by Robertson Family Fellowship.

*Disclosure:* The authors declare no conflict of interest.

## **References**

1. Miller JM, Rochitte CE, Dewey M, Arbab-Zadeh A, Niinuma H, Gottlieb I, et al. Diagnostic performance of coronary angiography by 64-row CT. The New England journal of medicine. 2008;359(22):2324-36.
2. Taylor AJ, Cerqueira M, Hodgson JM, Mark D, Min J, O'Gara P, et al. ACCF/SCCT/ACR/AHA/ASE/ASNC/NASCI/SCAI/SCMR 2010 Appropriate Use Criteria for Cardiac Computed Tomography. A Report of the American College of Cardiology Foundation Appropriate Use Criteria Task Force, the Society of Cardiovascular Computed Tomography, the American College of Radiology, the American Heart Association, the American Society of Echocardiography, the American Society of Nuclear Cardiology, the North American Society for Cardiovascular Imaging, the Society for Cardiovascular Angiography and Interventions, and the Society for Cardiovascular Magnetic Resonance. Circulation. 2010;122(21):e525-55.

3. Meijboom WB, Meijs MF, Schuijf JD, Cramer MJ, Mollet NR, van Mieghem CA, et al. Diagnostic accuracy of 64-slice computed tomography coronary angiography: a prospective, multicenter, multivendor study. *Journal of the American College of Cardiology*. 2008;52(25):2135-44.
4. Min JK, Hachamovitch R, Rozanski A, Shaw LJ, Berman DS, Gibbons R. Clinical benefits of noninvasive testing: coronary computed tomography angiography as a test case. *JACC Cardiovascular imaging*. 2010;3(3):305-15.
5. Dorbala S, Hachamovitch R, Di Carli MF. Myocardial perfusion imaging and multidetector computed tomographic coronary angiography: appropriate for all patients with suspected coronary artery disease? *Journal of the American College of Cardiology*. 2006;48(12):2515-7.
6. Schuijf JD, Wijns W, Jukema JW, Atsma DE, de Roos A, Lamb HJ, et al. Relationship between noninvasive coronary angiography with multi-slice computed tomography and myocardial perfusion imaging. *Journal of the American College of Cardiology*. 2006;48(12):2508-14.
7. Kristensen TS, Engstrom T, Kelbaek H, von der Recke P, Nielsen MB, Kofoed KF. Correlation between coronary computed tomographic angiography and fractional flow reserve. *International journal of cardiology*. 2010;144(2):200-5.
8. Rossi A, Papadopoulou SL, Pugliese F, Russo B, Dharampal AS, Dedic A, et al. Quantitative computed tomographic coronary angiography: does it predict functionally significant coronary stenoses? *Circulation Cardiovascular imaging*. 2014;7(1):43-51.
9. Jogiya R, Kozerke S, Morton G, De Silva K, Redwood S, Perera D, et al. Validation of dynamic 3-dimensional whole heart magnetic resonance myocardial perfusion imaging against fractional flow reserve for the detection of significant coronary artery disease. *Journal of the American College of Cardiology*. 2012;60(8):756-65.
10. Leone AM, De Caterina AR, Basile E, Gardi A, Laezza D, Mazzari MA, et al. Influence of the amount of myocardium subtended by a stenosis on fractional flow reserve. *Circulation Cardiovascular interventions*. 2013;6(1):29-36.
11. Ko BS, Wong DT, Cameron JD, Leong DP, Soh S, Nerlekar N, et al. The ASLA Score: A CT Angiographic Index to Predict Functionally Significant Coronary Stenoses in Lesions with Intermediate Severity-Diagnostic Accuracy. *Radiology*. 2015;276(1):91-101.
12. Voros S, Rinehart S, Qian Z, Joshi P, Vazquez G, Fischer C, et al. Coronary atherosclerosis imaging by coronary CT angiography: current status, correlation with intravascular interrogation and meta-analysis. *JACC Cardiovasc Imaging*. 2011;4(5):537-48.
13. Nakazato R, Shalev A, Doh JH, Koo BK, Gransar H, Gomez MJ, et al. Aggregate Plaque Volume by Coronary Computed Tomography Angiography Is Superior and Incremental to Luminal Narrowing for Diagnosis of Ischemic Lesions of Intermediate Stenosis Severity. *J Am Coll Cardiol*. 2013;62(5):460-7.
14. Raff GL, Chinnaiyan KM, Cury RC, Garcia MT, Hecht HS, Hollander JE, et al. SCCT guidelines on the use of coronary computed tomographic angiography for patients presenting with acute chest pain to the emergency department: a report of the Society of Cardiovascular Computed Tomography Guidelines Committee. *Journal of cardiovascular computed tomography*. 2014;8(4):254-71.
15. Utsunomiya M, Hara H, Moroi M, Sugi K, Nakamura M. Relationship between tissue characterization with 40 MHz intravascular ultrasound imaging and 64-slice computed tomography. *J Cardiol*. 2011;57(3):297-302.
16. Papadopoulou SL, Neefjes LA, Schaap M, Li HL, Capuano E, van der Giessen AG, et al. Detection and quantification of coronary atherosclerotic plaque by 64-slice multidetector CT: a systematic head-to-head comparison with intravascular ultrasound. *Atherosclerosis*. 2011;219(1):163-70.

17. Ortiz-Perez JT, Meyers SN, Lee DC, Kansal P, Klocke FJ, Holly TA, et al. Angiographic estimates of myocardium at risk during acute myocardial infarction: validation study using cardiac magnetic resonance imaging. *European heart journal*. 2007;28(14):1750-8.
18. Moral S, Rodriguez-Palomares J, Descalzo M, Marti G, Pineda V, Otaegui I, et al. Quantification of Myocardial Area at Risk: Validation of Coronary Angiographic Scores With Cardiovascular Magnetic Resonance Methods. *Rev Esp Cardiol*. 2012;65(11):1010-7.
19. Scanlon PJ, Faxon DP, Audet AM, Carabello B, Dehmer GJ, Eagle KA, et al. ACC/AHA guidelines for coronary angiography. A report of the American College of Cardiology/American Heart Association Task Force on practice guidelines (Committee on Coronary Angiography). Developed in collaboration with the Society for Cardiac Angiography and Interventions. *Journal of the American College of Cardiology*. 1999;33(6):1756-824.
20. Tonino PA, De Bruyne B, Pijls NH, Siebert U, Ikeno F, van't Veer M, et al. Fractional flow reserve versus angiography for guiding percutaneous coronary intervention. *The New England journal of medicine*. 2009;360(3):213-24.
21. DeLong ER, DeLong DM, Clarke-Pearson DL. Comparing the areas under two or more correlated receiver operating characteristic curves: a nonparametric approach. *Biometrics*. 1988;44(3):837-45.
22. Shaw LJ, Hausleiter J, Achenbach S, Al-Mallah M, Berman DS, Budoff MJ, et al. Coronary computed tomographic angiography as a gatekeeper to invasive diagnostic and surgical procedures: results from the multicenter CONFIRM (Coronary CT Angiography Evaluation for Clinical Outcomes: an International Multicenter) registry. *Journal of the American College of Cardiology*. 2012;60(20):2103-14.
23. Koo BK, Erglis A, Doh JH, Daniels DV, Jegere S, Kim HS, et al. Diagnosis of ischemia-causing coronary stenoses by noninvasive fractional flow reserve computed from coronary computed tomographic angiograms. Results from the prospective multicenter DISCOVER-FLOW (Diagnosis of Ischemia-Causing Stenoses Obtained Via Noninvasive Fractional Flow Reserve) study. *Journal of the American College of Cardiology*. 2011;58(19):1989-97.
24. Wang R, Renker M, Schoepf UJ, Wichmann JL, Fuller SR, Rier JD, et al. Diagnostic value of quantitative stenosis predictors with coronary CT angiography compared to invasive fractional flow reserve. *European journal of radiology*. 2015;84(8):1509-15.
25. Tesche C, De Cecco CN, Caruso D, Baumann S, Renker M, Mangold S, et al. Coronary CT angiography derived morphological and functional quantitative plaque markers correlated with invasive fractional flow reserve for detecting hemodynamically significant stenosis. *Journal of cardiovascular computed tomography*. 2016;10(3):199-206.
26. Park HB, Heo R, O'Hartaigh B, Cho I, Gransar H, Nakazato R, et al. Atherosclerotic plaque characteristics by CT angiography identify coronary lesions that cause ischemia: a direct comparison to fractional flow reserve. *JACC Cardiovascular imaging*. 2015;8(1):1-10.
27. Pasterkamp G, Schoneveld AH, van Wolferen W, Hillen B, Clarijs RJ, Haudenschild CC, et al. The impact of atherosclerotic arterial remodeling on percentage of luminal stenosis varies widely within the arterial system. A postmortem study. *Arteriosclerosis, thrombosis, and vascular biology*. 1997;17(11):3057-63.
28. Cho YK, Nam CW, Han JK, Koo BK, Doh JH, Ben-Dor I, et al. Usefulness of combined intravascular ultrasound parameters to predict functional significance of coronary artery stenosis and determinants of mismatch. *EuroIntervention*. 2015;11(2):163-70.
29. La Grutta L, Galia M, Gentile G, Lo Re G, Grassedonio E, Coppolino F, et al. Comparison of iodinated contrast media for the assessment of atherosclerotic plaque attenuation values by CT coronary angiography: observations in an ex vivo model. *Br J Radiol*. 2013;86(1021):20120238.

**Table 1: ASLA Score**

Variable and Value	Score assigned
Area of Stenosis	
> 63	7
47- 63	2
31- 46	1
<31	0
Lesion Length	
>28	6
10.8 - 28	1
< 10.8	0
APPROACH Score	
>44	5
25.1- 44	2
18 - 25	1
< 18	0
TOTAL	MAX = 18

**Table 2. Baseline Patient Characteristics**

	<b>Derivation Cohort (n=54)</b>	<b>Validation Cohort (n=27)</b>
Age, years	64.7 ± 9	63.2± 7
Male	62 %	66% (18)
<b>Risk factors</b>		
Hypertension	64% (32)	88% (24)
Diabetes mellitus	18% (9)	33% (9)
Dyslipidaemia	58% (29)	66% (18)
Current smoker	18% (9)	14% (4)
Obesity	4% (2)	11% (3)
Prior AMI / Prior PCI	6% (3)	7% (2)
Family history of IHD	46% (23)	40% (11)
<b>Distribution of Vessels</b>		
Left anterior descending artery	59% (56)	65% (21)
Left circumflex artery	17% (16)	21% (7)
Right coronary artery	25% (24)	12% (4)
<b>Lesion Characteristics</b>		
Obstructive lesions (> 50% stenosis)	43% (41)	75% (24)
Vessels with non-calcified plaques	30% (29)	18% (6)
Vessels with mixed / calcified plaques	70% (13)	81% (26)

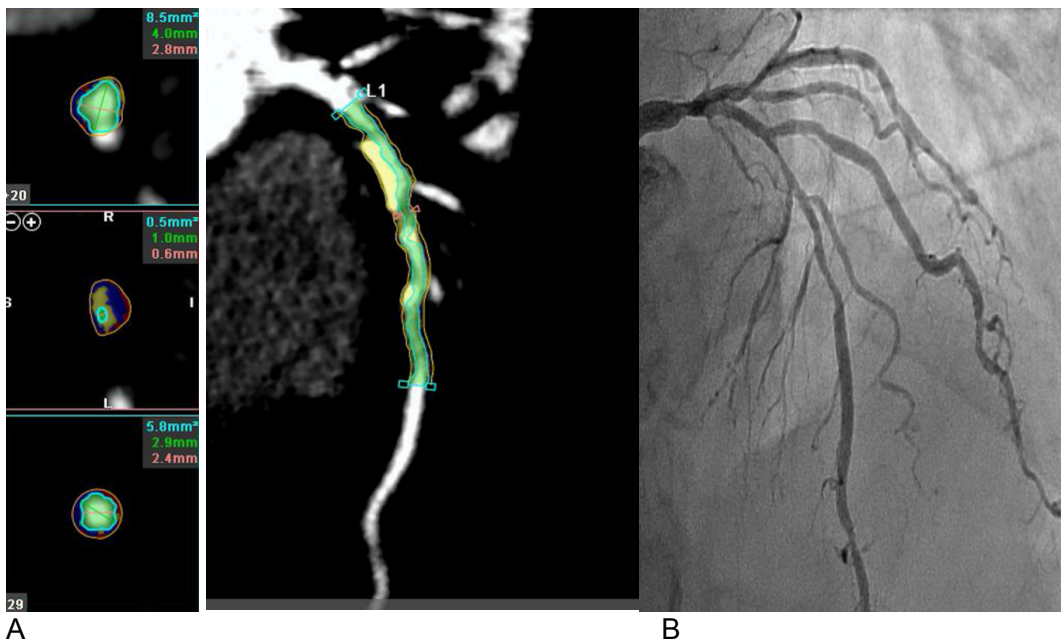


**Figure 1:** A- CTCA image with an analysed left anterior descending artery (LAD) segment with severe stenosis. Lumen is depicted in green, non-calcified plaque in blue with low attenuation plaque in red and calcium in yellow. The % APV was 45.2%. ASLA score was 18 [6 for lesion length (59.5mm) + 7 for area stenosis (91%) + 5 (44.5) for APPROACH score]. B- Corresponding LAD image on invasive angiogram with significant FFR (0.53)

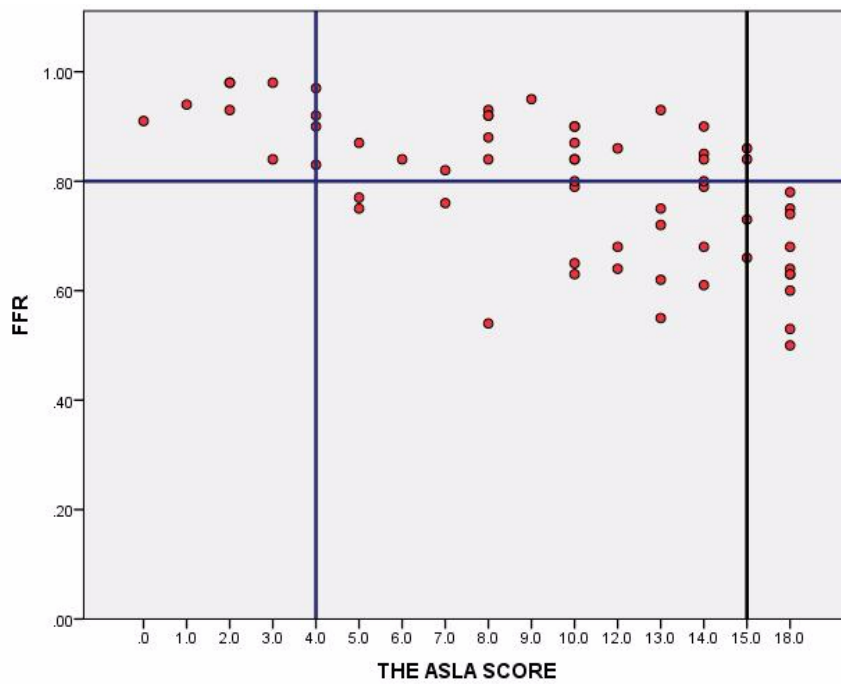


**Figure 2:** Scatter Plot showing distribution of FFR values and ASLA scores. ASLA score of  $4 \leq$  had 100% sensitivity and negative predictive value of 100% in excluding lesion specific ischaemia. ASLA score  $\geq 15$  had 94% specificity and positive predictive value of 86% in predicting FFR significant lesions.

Culprit lesion location	Infarct related artery Side branches →  ↓		Diagonal artery for LAD occlusion only Or Posterolateral artery for all others		
			Small or absent	Medium	Large
LAD (RD or LD)		Distal	13.75	14.8	15.9
		Mid	27.5	29.7	31.8
		Proximal	41.25	44.5	47.75
Proximal LCx (RD)	OM	Small or absent	9.25	12.5	15.75
		Medium	15.25	18.5	21.75
		Large	21.25	24.5	27.75
Proximal LCx (LD)	PDA	Small or absent	23.5	28	32.5
		Medium	29.5	34	38.5
		Large	35.5	40	44.5
Mid LCx (LD) or RCA (RD)	PDA	Small or absent	9.25	12.5	15.75
		Medium	15.25	18.5	21.75
		Large	21.25	24.5	27.75
Mid LCx (RD)			3.25	6.5	9.75

**Table 3: APPROACH Score.** APPROACH score is calculated based on the culprit lesion location (represented in the table in the first column) and the size of the side branches (represented by the second column and the top right row). For instance, APPROACH score for a lesion in proximal LAD with a large diagonal artery would be 47.75. On the other hand, APPROACH score for a lesion in RCA with a small PDA and a small PLV would be 9.25.

**Table 4. Computed tomography coronary angiography parameters of studied lesions as a function of fractional flow reserve**

Parameter	FFR > 0.8 (34)	FFR ≤ 0.8 (34)	P Value
Percent APV (%)	48.8 ± 12.6	54.9 ± 9	0.03
Length (mm)	22.8 ± 14.8	29.7 ± 14.4	0.07
Area Stenosis (mm <sup>2</sup> )	60.6 ± 23.8	79.3 ± 17.5	0.001
Diameter Stenosis (mm)	51.2 ± 22.6	68.5 ± 17.2	0.001
MLD (mm)	1.7 ± 0.87	1.09 ± 0.67	0.002
MLA (mm <sup>2</sup> )	5.04 ± 3.37	2.6 ± 2.44	0.002
ASLA Score	7.6 ± 4.4	13.6 ± 4.06	<0.001
APPROACH score	25.3 ± 11.9	37.2 ± 9.6	<0.001

**Table 5. ASLA score: Interobserver Variability**

Assessment of ASLA score parameters and Interobserver Variability (Lesion characteristics quantified according to CT and Interobserver Variability)		
Characteristic	Mean ± Standard Deviation	Interobserver interclass Correlation Coefficient
Area of Stenosis (%)	47.8 ± 24	0.977 (0.91,0.99)
Lesion Length (mm)	19.5 ±11.4	0.954 (0.824,0.988)
APPROACH Score	26.5 ±11.9	1.0 (1.0,1.0)
ASLA Score	8.85 ± 4.84	0.97 (0.88, 0.99)

**Table 6: Intraobserver and interobserver variability of percent APV**

Percent aggregate plaque volume	Intraobserver	Interobserver
Intraclass coefficient (35)		
Bland Altman	0.991 (0.903 - 0.999)	0.851 (0.401 – 0.963)
Mean difference	0.114 ± 1.96%	-0.544 ± 3.663%
p value	0.86	0.65
Limits of agreement	-3.84 – 3.62	-7.72 – 6.64

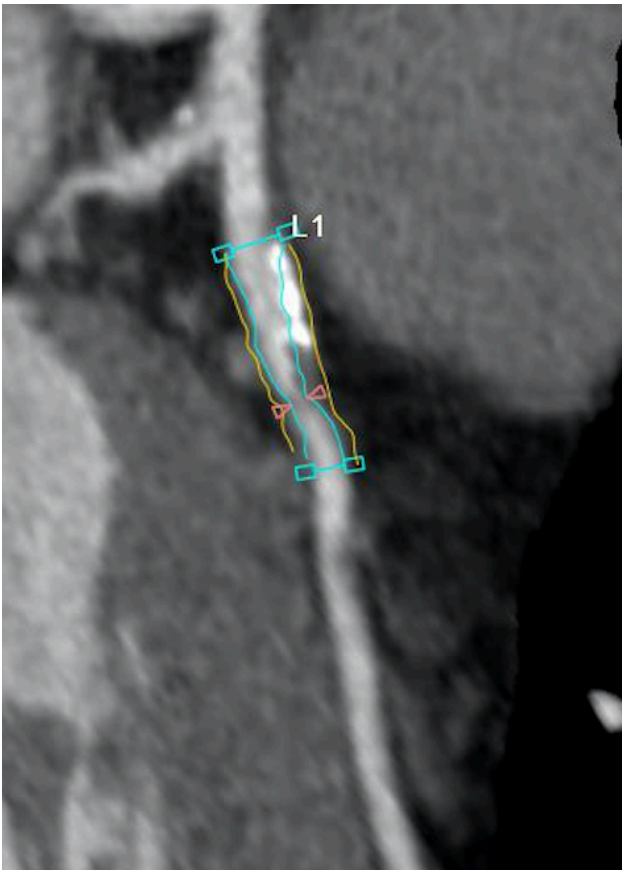


**Figure 3:** CTCA image of LAD with severe proximal segment stenosis and further moderate mid segment stenosis. ASLA score was calculated for the proximal lesion. The ASLA score was 18 (7 for area stenosis, 6 for lesion length and 5 for Approach score). Invasive FFR was 0.73. Percent APV was calculated from the ostium to the distal edge of the distal lesion.

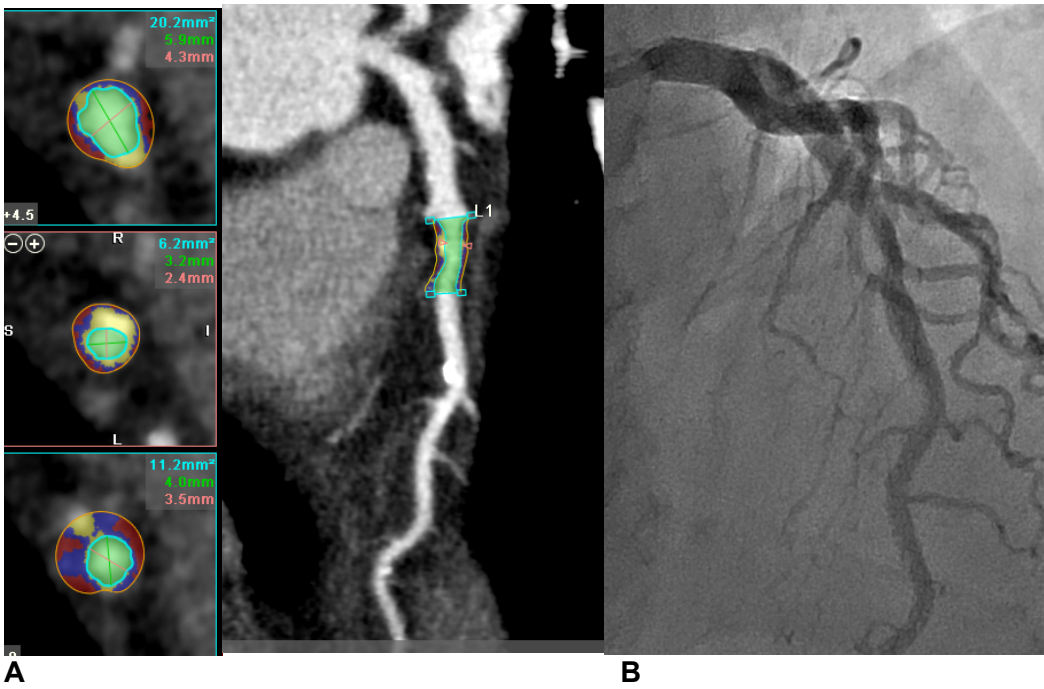


**Figure 4:** A- CTCA image with an analysed mid segment of left anterior descending artery (LAD) with moderate stenosis. The % APV was 52.9%. ASLA score was 5 [1 for lesion length (19.3mm) + 2 for area stenosis (58%) + 2 for APPROACH score (29.75)].

B- Corresponding LAD image on invasive angiogram with an FFR of 0.86 which was not significant

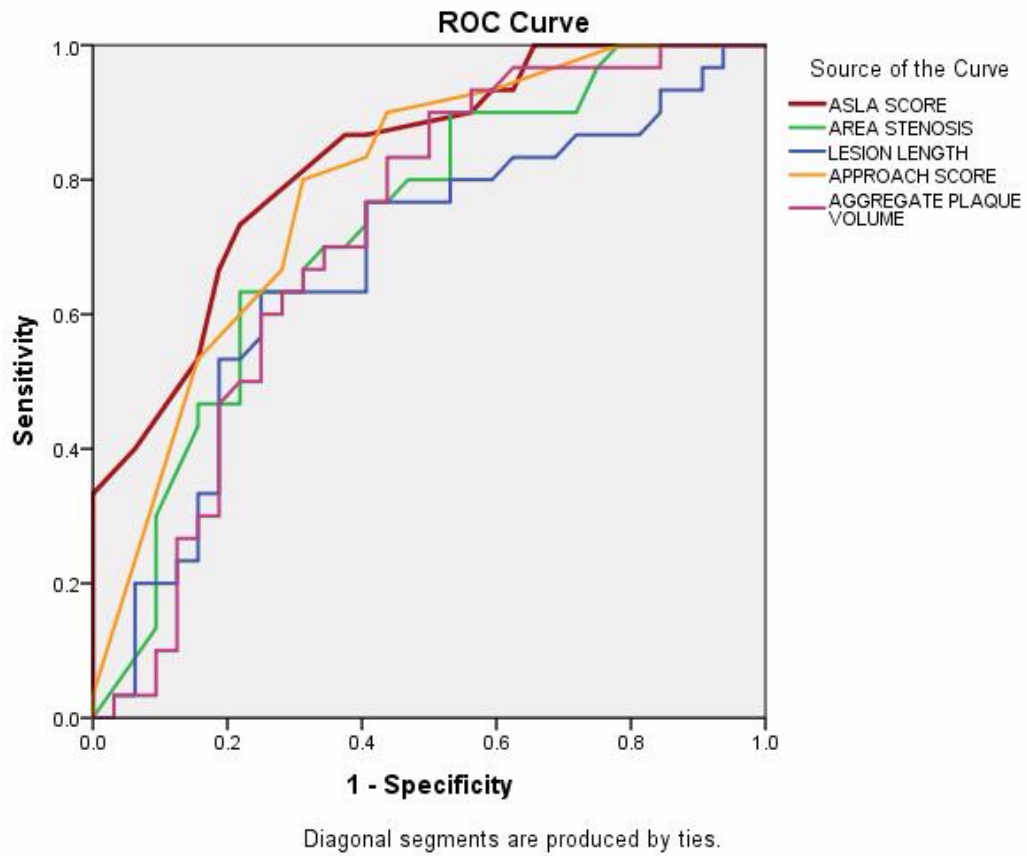
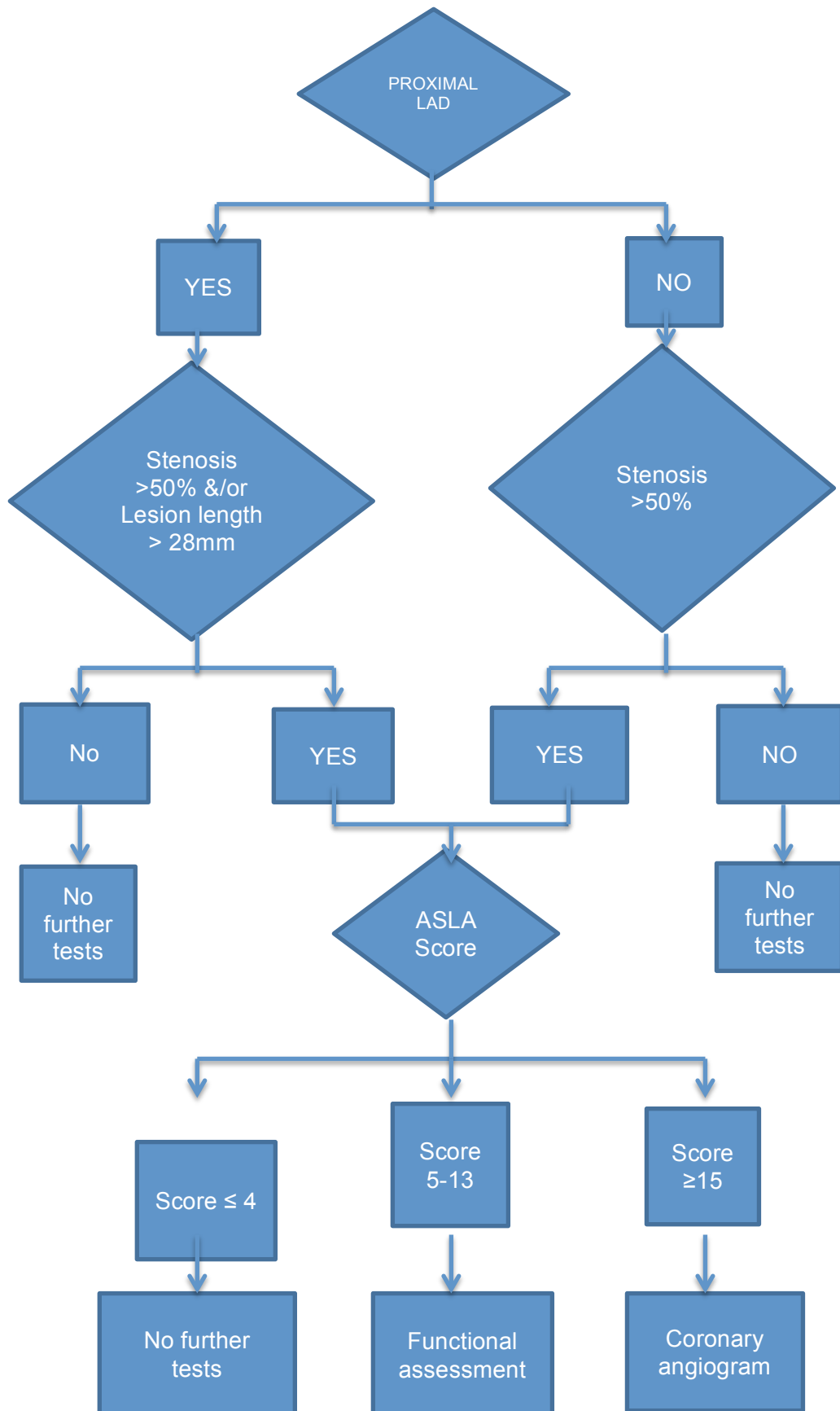


**Figure 5.** Receiver operating characteristic curves of ASLA score, APPROACH score, area of stenosis, lesion length and percent aggregate plaque volume (from derivation cohort). The AUC for ASLA score, area stenosis, lesion length, APPROACH score and percent APV were 0.83, 0.77, 0.67, 0.79 and 0.72 respectively.

Figure 6: Flow chart for ASLA score application



## **Chapter 7: Novel Non-Invasive CT-Derived Fractional Flow Reserve Based on Structural and Fluid Analysis (CT-FFR) for Detection of Functionally Significant Stenosis: a Comparison with Invasive Fractional Flow Reserve.**

*Brian S Ko<sup>a</sup>, MBBS (Hons), PhD; James D Cameron<sup>a</sup>, MBBS, BE, MD; Ravi K Munnur<sup>a</sup>, MBBS; Dennis TL Wong<sup>a</sup>, MBBS (Hons), PhD; Yasuko Fujisawa<sup>b</sup>, BSci; Takuya Sakaguchi<sup>b</sup>, MSci; Kenji Hirohata<sup>c</sup>, PhD; Jacqui Hislop-Jambrich<sup>d</sup>, PhD; Shinichiro Fujimoto<sup>e</sup>, MD, PhD; Kazuhisa Takamura<sup>e</sup>, MD, PhD; Marcus Crossett<sup>a,f</sup>, BSc; Michael Leung<sup>a</sup>, MBBS (Hons), PhD; Ahilan Kuganesan<sup>a,f</sup>, BSc; Yuvaraj Malaiapan<sup>a</sup>, MBBS; Arthur Nasis<sup>a</sup>, MBBS (Hons), PhD; John Troupis<sup>a,f</sup>, MBBS; Ian T Meredith<sup>a</sup>, MBBS (Hons), PhD; Sujith K Seneviratne<sup>a</sup>, MBBS.*

<sup>a</sup> Monash Cardiovascular Research Centre, MonashHEART, Department of Medicine Monash Medical Centre (MMC), Monash Health and Monash University, Melbourne, Australia

<sup>b</sup> Toshiba Medical Systems Corporation, Otawara, Japan.

<sup>c</sup> Toshiba Corporation, Kawasaki, Japan

<sup>d</sup> Toshiba Medical, Melbourne, Australia

<sup>e</sup> Department of Cardiovascular Medicine, Juntendo University Graduate School of Medicine, Tokyo, Japan

<sup>f</sup> Department of Diagnostic Imaging, MMC, Monash Health, Melbourne, Australia

**Accepted and Published: JACC Cardiovasc Imaging. 2017 Apr;10(4):498-499**

### **Corresponding Author**

Dr Brian S Ko

Monash Heart, [REDACTED]

[REDACTED]

[REDACTED]

## **Keywords**

Imaging, Coronary Disease, Ischemia, Computed Tomography, Fractional Flow Reserve, Quantitative Coronary Angiography.

## **Abbreviations**

CT = computed tomography

CTCA = Computed tomography coronary angiography

CT-FFR = Non-invasive fractional flow reserve

ICA = Invasive coronary angiography

FFR = Fractional flow reserve

CFD = Computational fluid dynamics

ROC = Receiver-operating characteristics curve

AUC = Area under the curve

NRI = Net reclassification index

IDI = Integrated discrimination improvement index

## **Conflicts of interest**

Dr Brian Ko has been an invited speaker at symposiums sponsored by St Jude, Pfizer, Bristol-Myers Squibb and Lilly. Ms Yasuko Fujisawa, Mr Takuya Sakaguchi and Dr Jacqui Hislop-Jambrich are employees of Toshiba Medical Systems Corporation. Dr Kenji Hirohata is an employee of Toshiba Corporation. Professor Ian Meredith has received honoraria for serving on strategic advisory boards of Boston Scientific and Medtronic. Dr Sujith Seneviratne has been an invited speaker at a Toshiba sponsored meeting.

**Objectives:** To describe the feasibility and accuracy of a novel CT technique (CT-FFR) to derive fractional flow reserve based on alternative boundary conditions.

**Background:** Techniques used to compute fractional flow reserve (FFR) based on images acquired from coronary CT angiography (CTCA) have been described. Boundary conditions are typically determined by allometric scaling laws and assumptions regarding microvascular resistance. Alternatively boundary conditions can be derived from the structural deformation of coronary lumen and aorta though its accuracy remains unknown.

**Methods:** Forty-two patients (78 vessels) in a single institution prospectively underwent 320-detector-CTCA and FFR. Deformation of coronary cross-sectional lumen and aorta, computed from CTCA images acquired over diastole, was used to determine the boundary conditions based on Hierarchical-Bayes modelling. CT-FFR was derived using a reduced-order model performed on a standard desktop computer and dedicated software. First 12 patients (20 vessels) formed the derivation-cohort to determine optimal CT-FFR threshold to detect functional stenosis defined as  $FFR \leq 0.8$ , which was validated in the subsequent 30 patients (58 vessels).

**Results:** Derivation-cohort results demonstrated optimal threshold for CT-FFR was 0.8, with 67% sensitivity, 91% specificity. In the validation-cohort, CT-FFR was successfully computed in 56/58 vessels (97%). Compared with CTCA, CT-FFR  $\leq 0.8$  demonstrated a higher specificity (87% vs 74%) and positive predictive value (74% vs 60%), with comparable sensitivity (78% vs 79%), negative predictive value (89% vs 88%) and accuracy (AUC 0.88 vs 0.77,  $P=0.22$ ). Based on Bland-Altman analysis, mean intra-observer and inter-observer variability for CT-FFR was  $-0.02 \pm 0.05$  (95% limit of agreement  $-0.12$  to  $0.08$ ) and  $0.03 \pm 0.06$  ( $0.07$ - $0.19$ ). Mean per-patient time for CT-FFR analysis was  $27.07 \pm 7.54$  minutes.

**Conclusions:** CT-FFR based on alternative boundary conditions and reduced-order fluid model is feasible, highly reproducible and may be accurate in detecting  $FFR \leq 0.8$ . It requires a short processing time and can be completed at point-of-care. Further validation is required in large prospective multicentre settings.

**Clinical Perspective:****Competency in medical knowledge**

Non-invasive CT fractional flow reserve (CT-FFR) using boundary conditions determined by assessing coronary luminal and aortic deformation during diastole and a reduced-order fluid model is feasible, highly reproducible and may be accurate in detecting  $FFR \leq 0.8$ . It requires a short processing time and can be completed at point-of-care.

**Translational Outlook**

The diagnostic performance of CT-FFR requires further evaluation and validation using on large prospective multicentre observational studies.

## Introduction

Ischemia assessment remains the cornerstone management of stable coronary artery disease (CAD), as its presence and burden determine outcomes and benefit from revascularization (1). Traditional stress tests and imaging modalities provide assessment of overall ischemic burden, yet remain limited in ischemia localisation and guiding revascularization on per vessel basis. Invasive fractional flow reserve (FFR) is the established standard to assess the functional significance of coronary stenosis. It represents the ratio of distal coronary and aortic pressure and leads to improved clinical outcomes when used to guide revascularization compared to invasive angiography (1,2).

HeartFlow FFR<sub>CT</sub> is a technique used to non-invasively derive invasive FFR by applying the principles of computational fluid dynamics (CFD) and image based modelling on typically acquired CT coronary angiography (CTCA) images which permit computation of coronary flow and pressures along the length of the entire coronary tree. Compared with invasive FFR, the diagnostic accuracy range between 73-81%, with sensitivity of 86-93%, and specificity of 54-79% (3,4), and its potential cost effectiveness when compared with invasive angiography has been described (5,6).

In CFD-based techniques, pressure and flow along the coronary tree are derived using 3 broad steps (7), 1) generation of an anatomical model using CT data, 2) application of mathematical principles to derive coronary boundary conditions 3) the use of a numerical solution which accounts for fluid dynamics to simulate flow and pressure.

In FFR<sub>CT</sub>, the boundary conditions are determined by allometric scaling laws and assumptions regarding coronary microvascular resistance (7) and the numerical solution used to simulate fluid dynamics permits three dimensional pressure and flow evaluation in each pixel of the coronary tree.

In this paper, we describe a novel technique (CT-FFR) in which boundary conditions are derived by accounting for the structural deformation changes in the coronary lumen and adjacent aorta across

the entire diastolic phase of the cardiac cycle (8,9). The numerical solution used to simulate fluid dynamics in CT-FFR is a reduced order (one dimensional) fluid model which permits evaluation of pressure and flow at each luminal cross-section of the coronary tree. (10).

Phantom feasibility studies using a pump connected to flexible tubes with varying degrees of stenosis have demonstrated excellent correlation between CT-FFR and invasive FFR measurements (8,9). However the feasibility and diagnostic performance of CT-FFR in human populations, and its incremental value when compared with CTCA remain unknown. Our primary aim is to determine the feasibility and diagnostic accuracy of CT-FFR to detect functionally significant stenosis. Our secondary aim is to evaluate the incremental value of CT-FFR upon CTCA. Fractional flow reserve was used as the reference standard.

## **Methods**

Symptomatic patients with no known CAD who were at intermediate or high risk (11) and were scheduled for clinically mandated elective invasive coronary angiography (ICA) at Monash Medical Centre were screened. Exclusion criteria included age <40 years, atrial fibrillation, renal insufficiency (eGFR <60mL/min/1.73m<sup>2</sup>), bronchospastic lung disease requiring long term steroid therapy, morbid obesity (BMI≥40) and contraindications to iodinated contrast. Screened patients were included in the study upon providing consent to undergo a research indicated CTCA and invasive FFR in a least one major epicardial vessel with > 2mm diameter during invasive coronary angiography. Among the 42 patients who were recruited in the study, the first twelve patients formed the derivation cohort and the subsequent thirty patients formed the validation cohort. The study was approved by the institutional human research ethics committee and all participants gave written informed consent.

### Computed tomography imaging protocol

Patients underwent cardiac CT assessment using a 320-row detector CT scanner (Aquilion ONE ViSION™, Toshiba Medical Systems Corporation, Japan). The CT protocol consisted of calcium score followed by CT coronary angiography. All patients received sublingual nitroglycerine and additional beta-blockers were administered to achieve a pre-scan heart rate of <60 beats per minute (bpm) in accordance to societal guidelines (12). Scanning was triggered in the arterial phase using automated contrast bolus tracking with a region of interest placed in the descending aorta, and automatically triggered at 300 Hounsfield units. Scan parameters for CTCA were: Detector collimation 320x0.5mm; tube current 300-500mA; tube voltage 100-120kV; gantry rotation time 270ms; and temporal resolution 135ms. Prospective electrocardiogram (ECG) gating was used covering 70-99% of the R-R interval. Effective radiation dose was calculated by multiplying the dose-length product (DLP) by a constant ( $k=0.014\text{mSv/mGy/cm}$ ) (13).

#### CTCA analysis

Stenosis severity on CTCA were interpreted on a dedicated workstation (Vitrea Fx 6, Vital Images, MN, USA) by two experienced CT angiographers (SF, KT) at the Juntendo CTCA core laboratory, blinded to the results of ICA and FFR in accordance to the 18 coronary segment model (14) with disagreement resolved by consensus. A vessel was considered significant if there was  $\geq 1$  segment which was non-evaluable or with a >50% luminal stenosis.

#### CT-FFR analysis

The CT-FFR analysis was performed by two experienced post processing technicians (YF, TS) at the Toshiba Medical Systems Corporation core laboratory blinded to the results of the invasive FFR using a standard desktop computer (Intel Xeon E5-2620, 6 core x 2 processor) and dedicated software (Toshiba Medical Systems, Japan) (Figure 1). Three-dimensional models of the coronary tree were constructed from the CT slice data using the FC03 reconstruction kernel (SurePlaque, Toshiba, Japan). Vessel centerline and luminal contours were automatically processed. Manual adjustments were performed as required.

Four CT images were reconstructed from the available phases (at 70, 80, 90, and 99% of R-R interval). Each mm of the coronary tree from the vessel inlet to outlet (up to 1.8mm in diameter) was registered and permitted calculation of structural data including the cross sectional luminal deformation, volume variation in the vessels and aortic root. Blood was modelled as a non-Newtonian fluid using the Herschel-Bulkley fluid constitutive model.

A number of physical principles and relationships were used to derive the boundary conditions 1) the volume variation in the aorta is related to inlet coronary flow rate during diastole (70-100%), 2) the boundary pressures of the coronary outlets during diastole relate to the cross sectional luminal deformation, vessel stiffness, cross sectional luminal shape and the pressure at when flow rate is 0, 3) the extent of pressure loss between the aorta and coronary artery outlets relates to the flow rate of the coronary outlets, 4) microvascular resistance is minimized during diastole and constant such that pressure is proportional to flow (15).

Hierarchical Bayes modelling was used to integrate the CT data and structural and fluid analysis conditions. This model takes into account the probability distribution based on observed structural measurements and prior data, the latter is generated using simulation-based parameter surveys and Markov-Chain Monte Carlo simulation.

Based on the finite element mesh model reconstructed from the CT data, structural and fluid analysis was performed using the finite-difference method based on the continuity, momentum and constitutive equations. A reduced order fluid model was used with a fluid resistance database which provided one-dimensional pressure and flow simulations across the coronary tree. The clinical site provided the Toshiba core laboratory with the distance measured from the vessel ostium to pressure sensor of FFR wire for each interrogated vessel in order to directly match the FFR result with CT-FFR estimate. CT-FFR values were calculated from the derived pressures along the length of the vessel to a minimum diameter width of 1.8mm.

### Invasive angiography and FFR

Invasive coronary angiography was performed as per standard practice either via the femoral or radial approach. FFR was performed during ICA in at least 1 vessel with diameter  $\geq 2$ mm and 10% to 90% visual stenosis, and was chosen at the discretion of the operator blinded to the CT findings. The pressure wire (Pressure wire Certus 7, St Jude Medical, USA) was calibrated and electronically equalised with the aortic pressure before being placed in the distal third of the coronary artery being interrogated. Intracoronary glyceryl trinitrate (100mcg) was injected to minimise vasospasm. Intravenous adenosine was administered (140mcg/kg/min) through an intravenous line in the antecubital fossa. At steady-state hyperaemia, FFR was recorded and calculated by dividing the mean coronary pressure measured with the pressure sensor placed distal to the stenosis by the mean aortic pressure measured through the guide catheter. The pressure sensor was then pulled back into the tip of the guiding catheter, and only runs with  $\leq 0.03$  drift were accepted for analysis. A FFR value  $\leq 0.8$  was chosen to define functionally significant stenosis (1).

### Quantitative coronary angiography

Quantitative coronary angiography was performed using a 18-segment coronary model (14). This was performed using a semi-automated edge detection system (Xcelera Cath R3.2, Philips, Netherlands) by two experienced cardiologists (YM, ML) at the Monash Heart core laboratory who were blinded to FFR and CT findings with disagreement resolved by consensus. Each coronary segment was visually assessed for degree of luminal stenosis and a vessel was considered significant if there was  $\geq 1$  segment which was non-evaluable or with a  $>50\%$  luminal stenosis.

### Statistical analysis

Continuous variables are presented as mean  $\pm$  standard deviation if normally distributed. Categorical variables are displayed as frequencies (percentage). Sensitivity, specificity, positive (PPV) and negative predictive value (NPV) were calculated to predict the ability of each modality to identify functionally significant stenoses on per vessel basis. The association between the studied

CT technique and FFR was assessed using a generalised estimating approach. Patient identity was included as a cluster variable to account for likely within-individual correlations, given that repeated measures were made from each individual. FFR as a dichotomous variable was assumed to have a binomial probability distribution. Interobserver and intraobserver reproducibility was performed on 16 randomly selected vessels. Receiver-operating characteristic curve (ROC) analysis was undertaken to evaluate the discriminatory ability of CTCA and CT-FFR for  $FFR \leq 0.8$ . The optimal CT-FFR threshold in the derivation cohort that provided at least 65% sensitivity and maximised the sum of sensitivity and specificity was chosen as threshold for the validation cohort. Areas under the ROC curves (AUC) were compared using the approach of DeLong et al. (16) with Bonferroni's adjustment for pair-wise comparisons. The incremental value of CT-FFR to CTCA in discriminating significant FFR was assessed by 2 methods. The integrated discrimination improvement (IDI) index and category-free net reclassification index (17) were used to determine whether CT-FFR improve vessel classification as hemodynamically significant, compared with CTCA alone (18). An IDI index that is significantly greater than zero is taken to demonstrate the incremental value of the studied technique when added to coronary CTCA. The NRI can be calculated by consideration of the sum of two separate components: vessels with  $FFR \leq 0.8$  and vessels with  $FFR > 0.8$ . For vessels with  $FFR \leq 0.8$ , we assign 1 for upward reclassification, -1 for downward and 0 for vessels which do not change their risk category by applying CT-FFR when compared with CTA alone. For vessels with  $FFR > 0.8$ , the opposite is performed. The sum of the individual scores is divided against the number of vessels in each group. Intra-observer and inter-observer variability in assessment of CT-FFR were determined using Bland-Altman analysis. Statistical analysis was performed with SPSS version 20 (SPSS, Chicago, Illinois) and STATA version 13.1 (STATA Corp, College Station, Texas). A P value  $< 0.05$  was considered statistically significant.

## Results

In the derivation cohort, twelve patients including twenty vessels were retrospectively studied. A CT-FFR threshold  $\leq 0.8$  provided optimal sum of sensitivity and specificity. The ROC AUC using this threshold was 0.87 (95% confidence interval 0.68-1.0), with a sensitivity of 66.7% and specificity of 90.9%.

In the validation cohort, thirty-four consecutive patients with suspected coronary artery disease underwent 320 detector CTCA and invasive coronary angiography with FFR measurement in Monash Medical Centre (n=34) between July 2014 and January 2016 (Table 1). Four patients were excluded due to inaccurate FFR assessment (n=1), inability to perform CT assessment due to deviation from image acquisition protocol (n=1), intramyocardial bridging (n=1) and poor image quality (n=1). Finally 58 vessels were analysed from 30 patients.

Mean age was 60 years and 70% were male. Of the 58 coronary arteries, 24 were left anterior descending (LAD), 2 diagonal branches, 20 left circumflex arteries (LCx) or marginal branches, 2 ramus branches, and 10 right coronary arteries (RCA). Baseline patient and vessel characteristics are listed in tables 1 & 2. CT scan parameters are listed in Table 3. The number (percentage) of vessels with  $FFR \leq 0.80$  was 19 (33%).

#### Relationship of CT-FFR with FFR

CT-FFR was successfully computed in 56/58 vessels (97%). The CT data in one patient (including 2 vessels) was corrupted and precluded analysis. CT-FFR was significantly lower in vessels with hemodynamically significant stenoses compared to vessels without hemodynamically significant stenosis, 0.63 vs 0.87 ( $P < 0.0001$ ). Figure 2 illustrates the correlation between CT-FFR and invasive FFR. CT-FFR demonstrated a statistically significant yet modest correlation with invasive FFR (Pearson's  $R = 0.57$ ,  $P < 0.0001$ ). On Bland Altman analysis, there was good agreement between FFR and CT-FFR with a difference of  $0.065 \pm 0.137$  (95% CI -0.20 to 0.33) (Figure 3).

### Diagnostic performance of CTCA, and CT-FFR

The diagnostic performance of CTCA and CT-FFR for diagnosis of hemodynamically significant stenosis is summarised in Table 4 and Figure 4. Two case examples of correlation are provided in Figures 5 and 6. The ROC curve analysis for CTCA alone showed an AUC of 0.77 (P=0.001). Sensitivity, specificity, PPV and NPV were 78.9%, 74.3%, 60% and 87.9% respectively. Four hemodynamically significant stenoses (3 LAD, 1 LCx, FFR range 0.68-0.78) were identified as <50% stenosis on CTCA.

Using a CT-FFR threshold of  $\leq 0.80$ , the ROC curve analysis for CT-FFR demonstrated an AUC of 0.88 (P<0.001), which was comparable with CTCA (P= 0.22). This resulted in 14 true positives, 33 true negatives, 5 false positives (1 in LAD, 2 in LCx, 2 in RCA) and 4 false negatives (2 in LAD, 1 in LCx, 1 in RCA). Sensitivity, specificity, PPV and NPV of CT-FFR were 78%, 87%, 74% and 89%. The net reclassification index for CT-FFR when compared with CTCA was 1.29 (SE 0.29, P <0.0001). The integrated discrimination improvement for CT-FFR was 0.21 with standard error of 0.06, (P=0.0002).

### Time taken and reproducibility of CT-FFR analysis

The mean per patient time required for CT-FFR analysis was  $27.07 \pm 7.54$  mins. There was a mean intraobserver variability of  $-0.02 \pm 0.05$ , and the 95% limit of agreement was  $-0.12$  to  $0.08$ . The mean interobserver variability was  $0.03 \pm 0.06$  ( $-0.07$ - $0.19$ )

## **Discussion**

In this prospective study, we demonstrate the feasibility and high diagnostic accuracy of a novel CT-based technique CT-FFR to assess the functional significance of coronary stenosis as determined by invasive fractional flow reserve. When compared with CTCA alone, our results demonstrate CT-FFR provides superior specificity and positive predictive value, while the sensitivity, negative predictive and accuracy are comparable. CT-FFR also provided incremental benefit when compared with CTCA alone. The lack of difference in overall accuracy as represented by the ROC AUC may be attributed to an underpowered sample size.

CT-based techniques to derive non-invasive FFR all require three broad steps, 1) generation of an anatomical model based on CT data, 2) application of mathematical principles to derive boundary inlet and outlet conditions which represent cardiac output, aortic pressures, outlet coronary flow and pressure and microvascular resistance and 3) to perform a fluid simulation using identified boundary conditions to derive flow and pressures along the entire coronary tree. The differences in methodology between CT-FFR and HeartFlow FFR<sub>CT</sub> are highlighted in Table 5. They differ primarily in the mathematical principles in which boundary conditions are derived and the fluid model in which coronary flow and pressure are simulated. In FFR<sub>CT</sub>, form and function relationships of arteries and the myocardium were used to derive boundary conditions. Typically the technique only requires one CT acquisition phase (for example at 75% of R-R interval) during diastole. In CT-FFR, boundary outlet and inlet pressure conditions are derived from determining the change in the cross sectional area of coronary vessels and aorta across the entire diastole. This information is obtained using 4 phases of CT acquisition typically at 70%, 80%, 90% and 99% of the R-R interval.

The ideal CTCA based CFD technique is one which permits accurate and timely functional assessment of coronary stenosis. The numerical solution to simulate fluid dynamics for FFR<sub>CT</sub> is one which is based on a 3-dimensional fluid model, which permits pressure and flow estimation for

each point or pixel along the coronary tree. This rigorous process is aimed to provide added information and accuracy though requires a prolonged processing time and the use of a supercomputer at HeartFlow in California USA. For this reason, the technique currently requires a turnover time of 24 hours which includes the need for offsite image transfer and an image processing time of 1-4 hours depending on disease burden and CT image quality (4). In CT-FFR, fluid simulation is based on a reduced-order (one dimensional) model (9,19), which permits assessment of pressure and flow at each luminal cross section of the coronary tree. The theoretical concern is that this may reduce diagnostic performance when compared with the 3 dimensional model. This report demonstrates the promise of CT-FFR which was found to have a high diagnostic accuracy despite the use of the reduced order fluid model comparable with that reported for other resting CTCA based CFD techniques (19,20). The advantage offered by this model is the much reduced processing time required and the ability to derive this information without the use of a supercomputer. Our results demonstrate the feasibility to process CT-FFR in less than 30 minutes, using standard desktop computers which permits point of care CT-FFR calculation. Notably our results demonstrate excellent reproducibility, with little inter-observer and intra-observer variability on repeated measures.

The study has a number of inherent limitations. It is a single centre study with a small sample of subjects and vessels. Accordingly it is not powered to detect AUC differences when compared with CTCA alone, as such numerical comparisons with previous CFD-based CT studies should be interpreted cautiously. Larger multicentre, well powered prospective studies are required to further establish the diagnostic performance of CT-FFR. For the same reason, sub-analyses into intermediate, major sub-branch or calcified lesions will be vastly underpowered and only hypothesis generating. The population studied were patients awaiting elective invasive coronary angiography, hence the potential for selection bias. Patients with previous revascularisation or myocardial infarction were excluded from the study, for that reason, the accuracy of CT-FFR in

these populations remain unknown. All scans were performed using 320-detector CT, and the feasibility of this technique when applied to narrow detector CT is not known. Finally the influence of heart rate, motion and calcification which may affect image quality and impact diagnostic performance has not been evaluated in this study.

### **Conclusion**

Non-invasive fractional flow reserve based on structural and fluid analysis using a reduced order flow model is a highly reproducible technique. This pilot data suggests that it may provide accurate detection of functionally significant coronary stenosis and can be processed over < 30 mins. Larger multicentre prospective studies are required to further establish its diagnostic performance and incremental value upon CTCA.

## Reference

1. Tonino PA, De Bruyne B, Pijls NH et al. Fractional flow reserve versus angiography for guiding percutaneous coronary intervention. *N Engl J Med* 2009;360:213-24.
2. De Bruyne B, Fearon WF, Pijls NH et al. Fractional flow reserve-guided PCI for stable coronary artery disease. *N Engl J Med* 2014;371:1208-17.
3. Min JK, Leipsic J, Pencina MJ et al. Diagnostic Accuracy of Fractional Flow Reserve From Anatomic CT Angiography. *JAMA* 2012;1-9.
4. Norgaard BL, Leipsic J, Gaur S et al. Diagnostic performance of non-invasive fractional flow reserve derived from coronary CT angiography in suspected coronary artery disease: The NXT trial. *J Am Coll Cardiol* 2014;63:1145-55.
5. Douglas PS, Pontone G, Hlatky MA et al. Clinical outcomes of fractional flow reserve by computed tomographic angiography-guided diagnostic strategies vs. usual care in patients with suspected coronary artery disease: the prospective longitudinal trial of FFRct: outcome and resource impacts study. *Eur Heart J* 2015.
6. Hlatky MA, De Bruyne B, Pontone G et al. Quality-of-Life and Economic Outcomes of Assessing Fractional Flow Reserve With Computed Tomography Angiography: PLATFORM. *J Am Coll Cardiol* 2015;66:2315-23.
7. Taylor CA, Fonte TA, Min JK. Computational fluid dynamics applied to cardiac computed tomography for noninvasive quantification of fractional flow reserve: scientific basis. *Journal of the American College of Cardiology* 2013;61:2233-41.
8. Hirohata K, Kano A, Goryu A et al. A novel CT-FFR method for the coronary artery based on 4D-CT image analysis and structural fluid analysis. *SPIE Medical Imaging* 2015;9412-94:26.
9. Kato M, Hirohata K, Kano A et al. Fast CT-FFR analysis method for the coronary artery based on 4D-CT image analysis and structural and fluid analysis. *Proceedings of the ASME International Mechanical Engineering Congress and Exposition* 2015.
10. Coenen A, Lubbers MM, Kurata A et al. Fractional flow reserve computed from noninvasive CT angiography data: diagnostic performance of an on-site clinician-operated computational fluid dynamics algorithm. *Radiology* 2015;274:674-83.
11. Gibbons RJ, Chatterjee K, Daley J et al. ACC/AHA/ACP-ASIM guidelines for the management of patients with chronic stable angina: executive summary and recommendations. A Report of the American College of Cardiology/American Heart Association Task Force on Practice Guidelines (Committee on Management of Patients with Chronic Stable Angina). *Circulation* 1999;99:2829-48.
12. Raff GL, Chinnaiyan KM, Cury RC et al. SCCT guidelines on the use of coronary computed tomographic angiography for patients presenting with acute chest pain to the emergency department: a report of the Society of Cardiovascular Computed Tomography Guidelines Committee. *Journal of cardiovascular computed tomography* 2014;8:254-71.
13. Hausleiter J, Meyer T, Hermann F et al. Estimated radiation dose associated with cardiac CT angiography. *JAMA* 2009;301:500-7.
14. Raff GL, Abidov A, Achenbach S et al. SCCT guidelines for the interpretation and reporting of coronary computed tomographic angiography. *Journal of cardiovascular computed tomography* 2009;3:122-36.
15. Sen S, Escaned J, Malik IS et al. Development and validation of a new adenosine-independent index of stenosis severity from coronary wave-intensity analysis: results of the ADVISE (ADenosine Vasodilator Independent Stenosis Evaluation) study. *J Am Coll Cardiol* 2012;59:1392-402.
16. DeLong ML, Duncan BD, Parker JH. Parametric Extension of the Classical Exposure-Schedule Theory for Angle-Multiplexed Photorefractive Recording over Wide Angles. *Appl Opt* 1998;37:3015-30.
17. Langheinrich AC, Kampschulte M, Buch T, Bohle RM. Vasa vasorum and atherosclerosis - Quid novi? *Thrombosis and haemostasis* 2007;97:873-9.
18. Pencina MJ, D'Agostino RB, Sr., D'Agostino RB, Jr., Vasan RS. Evaluating the added predictive ability of a new marker: from area under the ROC curve to reclassification and beyond. *Statistics in medicine* 2008;27:157-72; discussion 207-12.

19. Coenen A, Lubbers MM, Kurata A et al. Coronary CT angiography derived fractional flow reserve: Methodology and evaluation of a point of care algorithm. *J Cardiovasc Comput Tomogr* 2015.
20. Koo BK, Erglis A, Doh JH et al. Diagnosis of ischemia-causing coronary stenoses by noninvasive fractional flow reserve computed from coronary computed tomographic angiograms. Results from the prospective multicenter DISCOVER-FLOW (Diagnosis of Ischemia-Causing Stenoses Obtained Via Noninvasive Fractional Flow Reserve) study. *Journal of the American College of Cardiology* 2011;58:1989-97.

## **Acknowledgements**

Dr Brian Ko and Dr Dennis Wong are funded by the National Heart Foundation of Australia and Robertson Family Scholarship. Dr Dennis Wong is also funded by the National Health and Medical Research Council of Australia. We acknowledge Mr Shigeo Kaminaga for advice on study design, Mr Norikazu Yamada for his contribution to assessment of the reproducibility of CT-FFR, Ms Nozomi Masubuchi for her work as a member of the core laboratory staff, Dr Mitsuaki Kato and Mr Akira Kano for work related to CT-FFR algorithm optimisation, Dr Rich Mather for technical support and Ms Chloe Steveson for support in scan protocol.

## Figures

### Figure 1 – CT-FFR Methodology

An anatomical luminal model is reconstructed from CTCA (Steps 1 and 2), the boundary conditions are determined by assessment of luminal deformation of coronary arteries and aorta during diastole and Hierarchical Bayes modelling (Steps 3 and 4). Fluid simulation is based on a reduced order model using standard desktop computer. Pressure, flow and CT-FFR are determined along coronary tree (Steps 5 and 6).

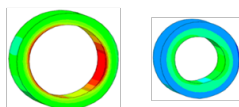
**Step 1:** CT acquisition



**Step 2:** Image reconstruction, centreline and contour adjustments



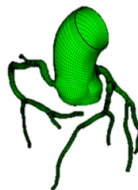
**Step 3:** Four diastolic phases (btw 70-99%) chosen to assess luminal deformation of coronaries and aorta



**Step 4:** Application of mathematical principles and Hierarchical Bayes modelling to derive boundary conditions and vessel stiffness



**Step 5:** Fluid simulation using a finite-element mesh and reduced order fluid model on standard desktop computer



**Step 6:** Pressure & flow determined along coronary tree and CT-FFR is determined

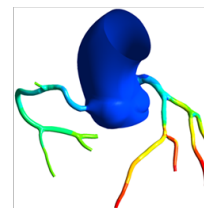


### Figure 2 – Correlation of CT-FFR & invasive FFR

FFR = fractional flow reserve, CT-FFR = Non-invasive fractional flow reserve derived from CT coronary angiography.

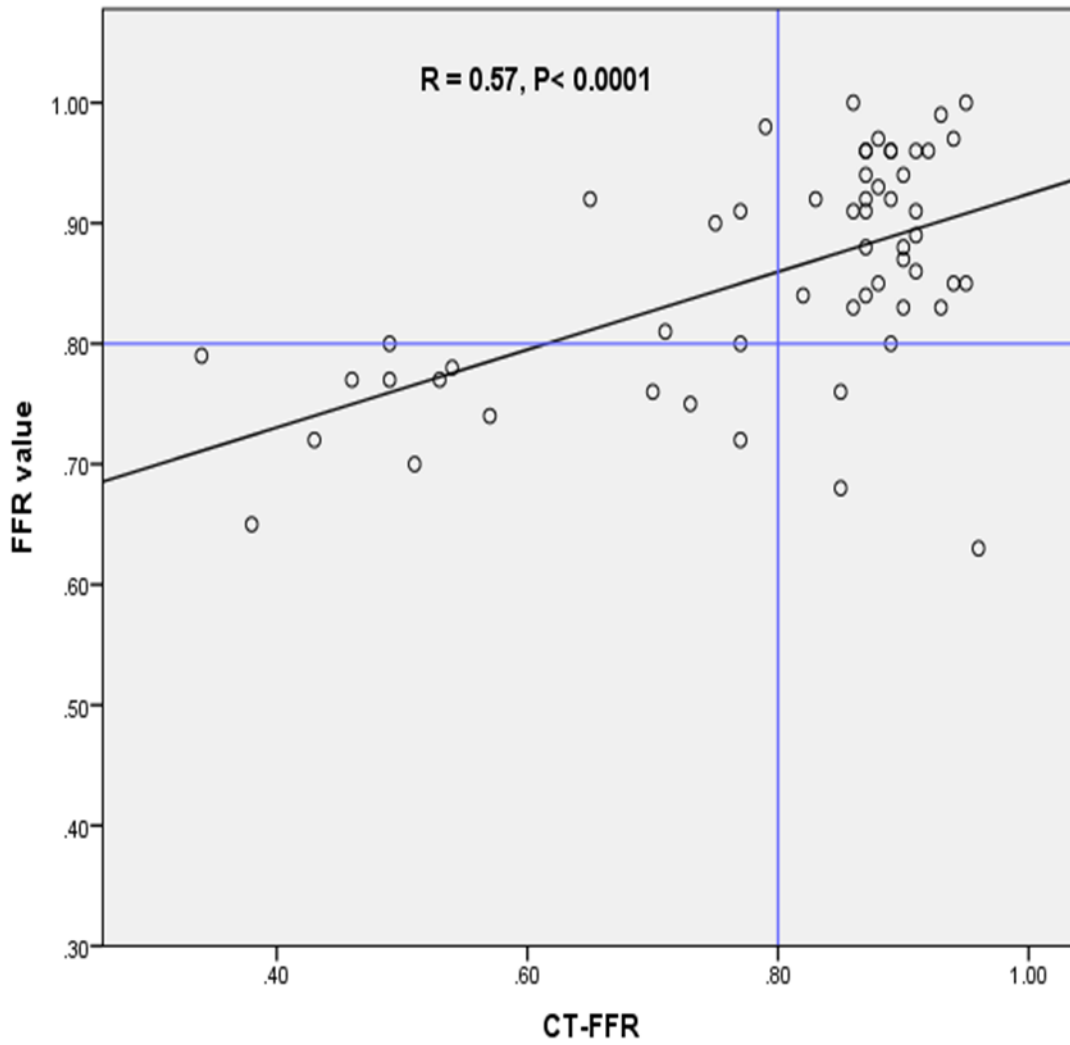




**Figure 4 – Receiver operating characteristics curves of CT-FFR in the derivation cohort and CTCA and CT-FFR in the validation cohort, in predicting FFR significant stenosis**

Abbreviations as per Figure 2

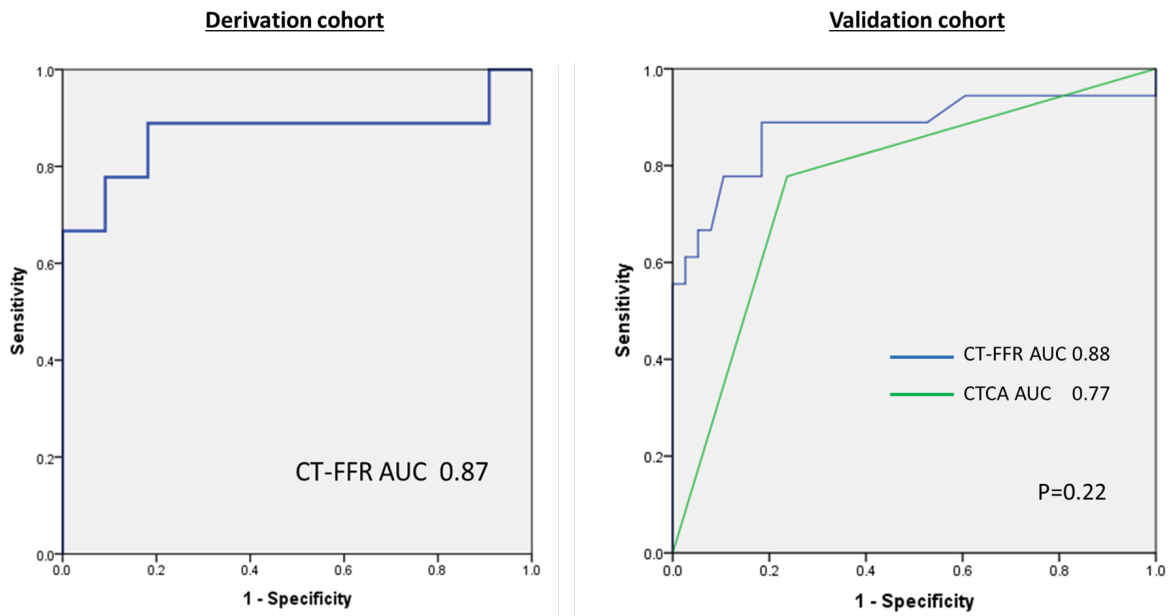


**Figure 6 Representative case example from study**

53 year old man with intermediate risk of coronary artery disease, presents with chest pains. CT coronary angiography demonstrated a moderate (51-70%) stenosis in the mid LAD (Panel A). The CT –FFR was 0.73 in the distal LAD (Panel B). Invasive coronary angiography again demonstrated a moderate stenosis in the mid LAD (Panel C), fractional flow reserve was 0.75 in the distal LAD.

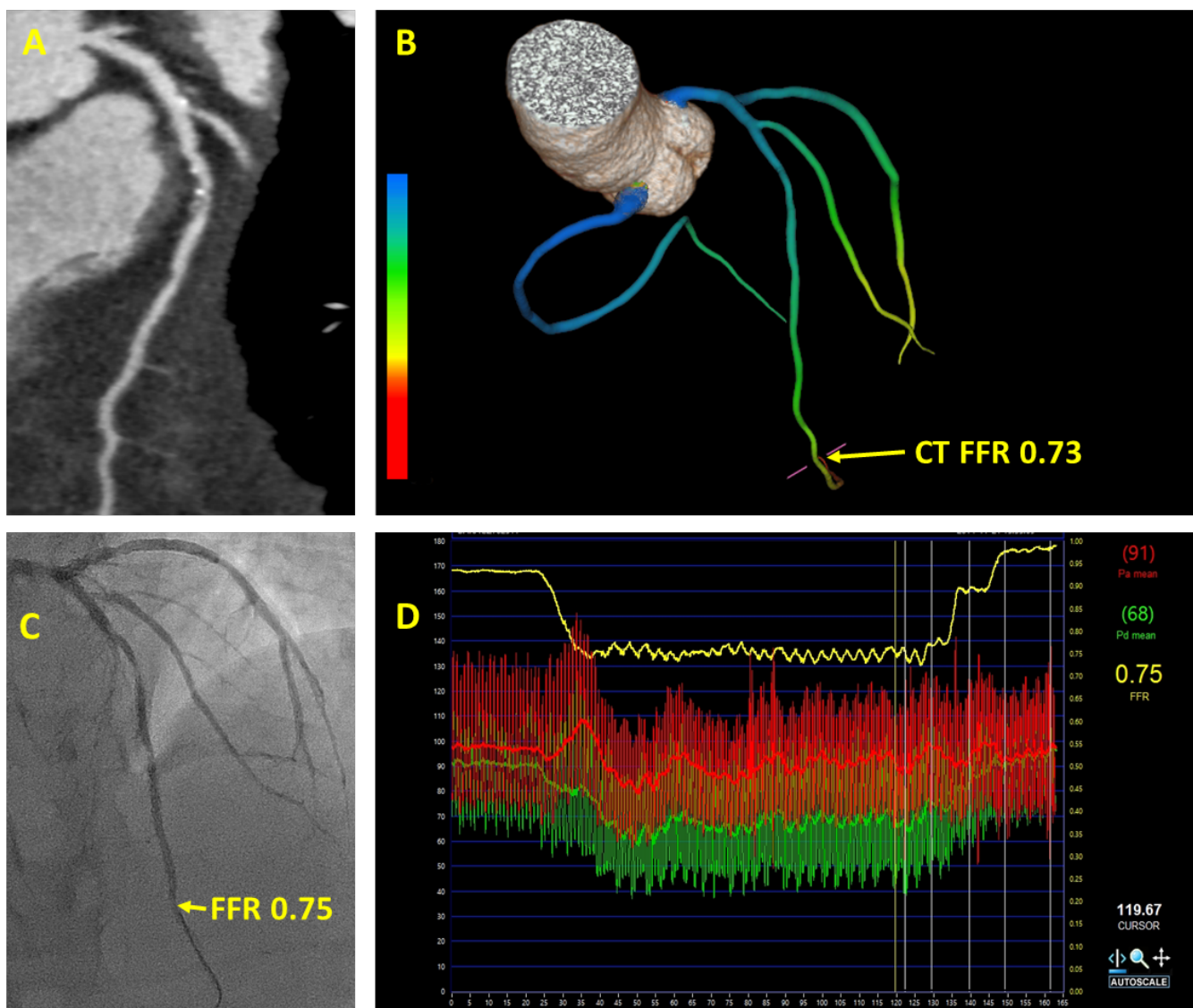


**Figure 6 Representative case example from study**

A 66 year old woman with intermediate risk of coronary artery disease, presents with atypical chest pains. CT coronary angiography demonstrated a moderate (51-70%) stenosis in the mid LAD after the 2<sup>nd</sup> diagonal bifurcation (Panel A). Invasive coronary angiography demonstrated the stenosis

was severe at 70% (Panel B). Fractional flow reserve in the distal LAD was 0.84 (Panel C). CT-FFR, performed blinded to the FFR result, was 0.82 (Panel D).

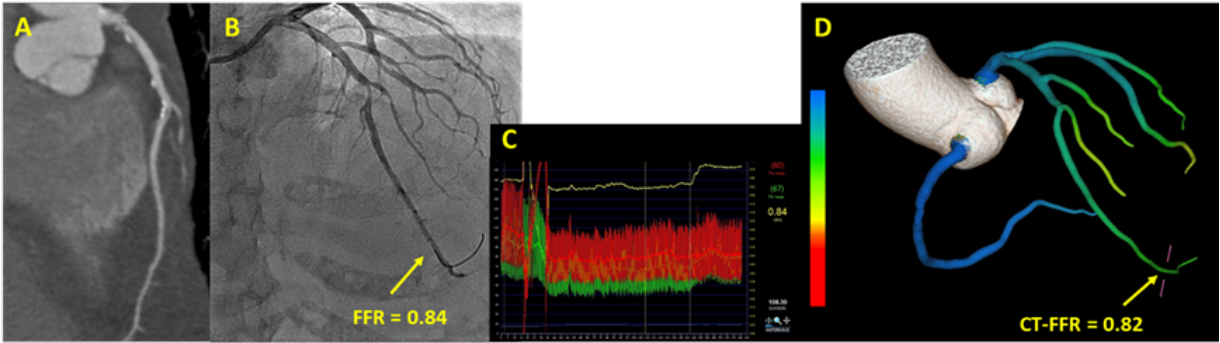


## Table legend

**Table 1- Patient Characteristics**

	<b>N = 30 Patients</b>
Age (years)	
Mean ± SD (N)	60.0±8.5(30)
Median	60
Range (Min, Max)	(43.0, 80.0)
Gender	
Male	70.0% (21/30)
Female	30.0% (9/30)
Diabetes mellitus	30.0% (9/30)
Hypertension*	73.3% (22/30)
Hyperlipidemia†	80.0% (24/30)
Smoking	
Former Smoker	33.3% (10/30)
Current Smoker	26.7% (8/30)
Never Smoked	40.0% (12/30)
Prior Myocardial Infarction	0.0% (0/30)
Angina Type*	
Typical	13.3% (4/30)

Atypical	66.7% (20/30)
Non cardiac chest pain	20.0% (6/30)
Updated Diamond-Forrester risk score, %	
Intermediate (20%-80%) pre-test risk	86.7%(30)
Body mass index	
Mean $\pm$ SD (N)	28.5 $\pm$ 4.6(30)
Median	29
Creatinine (mmol/L)	
Mean $\pm$ SD (N)	79.1 $\pm$ 16.2 (30)
Median	80.5

SD indicates standard deviation; \*Blood pressure >140/90 mmHg or treatment for hypertension.

†Total cholesterol >180 mg/dl or treatment for hypercholesterolemia.

**Table 2: Vessel characteristics**

Characteristics	N = 30 Patients N = 58 Vessels
Calcium Score (Agatston Units)	
Mean ± SD (N)	910.3±1075.6 (30)
Median	528
Patients with CTCA maximum stenosis >50%	50% (15/30)
Vessels with CTCA maximum stenosis >50%	43.1% (25/58)
Patients with QCA maximum stenosis >50%	53.3% (16/30)
Vessels with QCA maximum stenosis on >50%	29.3% (17/58)
Patients with CT-FFR ≤ 0.80	48.3% (14/29)
Vessels with CT-FFR ≤ 0.80	33.9% (19/56)
Patients with FFR ≤ 0.80	46.7% (14/30)
Vessels with FFR ≤ 0.80	33.0% (19/58)

Patients with FFR $\leq 0.80$ in $>1$ vessel	10% (3/30)

**Table 3: Scan characteristics**

<b>CT Scan acquisition characteristics</b>	<b>N = 30 Patients</b>
Heart Rate Prior to CTCA (bpm)	
Mean ± SD (N)	52.5±6.8(30)
Median	52.0
Nitrates Administered	100.0% (30/30)
Beta Blockers Administered	90.0% (27/30)
Radiation Calculated from DLP (mSv)	
Mean ± SD (N)	4.9±2.2(30)
Median	4.7
kV	
100	46.7% (14/30)
120	53.3% (16/30)
mA	
Mean ± SD (N)	630.3±157.8
Range (Min, Max)	(340, 820)
Single beat acquisition	100% (30/30)

**Table 4 – Per vessel diagnostic accuracy of CTCA, CT-FFR, quantitative and invasive coronary angiography compared with FFR.**

	CTCA ( $\geq 50\%$ )	CT-FFR ( $\leq 0.80$ )	QCA ( $\geq 50\%$ )	Visual ICA ( $\geq 50\%$ )
N	58	56	58	58
True positive	15	14	9	17
True negative	29	33	31	21
False positive	10	5	8	18
False negative	4	4	10	2
Accuracy (%)	77.6	83.9	69.0	65.5
Sensitivity (%)	78.9 (53.9-93.0)	77.8 (51.9-92.6)	47.4 (25.2-70.5)	89.5 (65.5-98.2)
Specificity (%)	74.3 (57.6-86.4)	86.8 (71.1-95.1)	79.5 (63.1-90.1)	53.8 (37.4-69.6)
PPV (%)	60.0 (38.9-78.2)	73.7 (48.6-89.9)	52.9 (28.5-76.1)	48.6 (31.7-65.7)
NPV (%)	87.9 (70.9-96.0)	89.2 (73.6-95.6)	75.6 (59.4-87.1)	91.3 (70.5-98.5)
AUC	0.77 (0.65-0.88)	0.88 (0.76-1.0)	0.67 (0.51-0.83)	0.82 (0.71-0.94)

**Table 5: Comparison of FFR<sub>CT</sub> and CT-FFR**

	HeartFlow FFR <sub>CT</sub>	Toshiba CT-FFR
<b>Scan characteristics</b>		
Scanner requirements	$\geq 64$ detector CT	320 detector CT
Scan acquisition	Prospective ECG gating	Prospective ECG gating
Phases required	One phase (typically 75% of R-R interval)	4 phases between 70-100% (typically 70%, 80%, 90%, 99% of R-R interval)
Requirements for nitrates and heart rate control	Compulsory	Compulsory
<b>CT Anatomical model</b>		
How is it generated?	Semi-automated using dedicated software, with manual adjustments.	Semi-automated using Sure Plaque software, with manual adjustments as required

<b>Mathematical Model</b>		
Derivation of boundary outlet conditions	<ol style="list-style-type: none"> <li>1) Boundary outlet pressure and resistance are derived from diameter of coronary outlets and myocardium subtended (allometric scaling laws)</li> <li>2) Assumptions are made regarding microvascular resistance – assumed to be 0.24 of microvascular resistance at rest.</li> </ol>	<ol style="list-style-type: none"> <li>1) Boundary outlet pressure is derived from the changes in luminal CSA, vessel stiffness vessel shape and flow at rate 0</li> <li>2) Pressure difference from aorta to coronary outlet determines outlet coronary flow.</li> <li>3) Assumption is made that resistance is constant such that pressure is proportional to flow.</li> </ol>
Derivation of boundary inlet conditions	<ol style="list-style-type: none"> <li>1) Brachial pressure is used to derive aortic pressure</li> <li>2) Total coronary inlet flow is proportional to the total amount of myocardium subtended</li> </ol>	<ol style="list-style-type: none"> <li>1) Common blood pressure is used to derive aortic pressure.</li> <li>2) Coronary inlet flow during diastole is proportional to the change in aortic volume at the same time.</li> </ol>
Fluid assumptions	Blood modelled as Newtonian fluid	Blood modelled as non-Newtonian fluid
<b>Numerical solution to account for fluid dynamics</b>		
How is computed?	<ol style="list-style-type: none"> <li>1) Using a finite element mesh model derived from CT data</li> <li>2) 3 Dimensional fluid model of coronary arteries generated to estimate flow and pressure at each pixel of coronary tree</li> </ol>	<ol style="list-style-type: none"> <li>1) Using a finite element mesh model derived from CT data</li> <li>2) Reduced order (one dimensional) fluid model of the coronary outlets generated to estimate flow and pressure at each luminal cross section of the coronary tree.</li> </ol>
<b>Practical considerations</b>		
Operator	Processed by technician at HeartFlow in California USA.	Feasible by radiographer / physician at point of care
Computational requirements	Parallel supercomputer required for computing the fluid analysis model	Standard desktop computer.
Time	1-4 hours	30 mins

## **Chapter 8: Conclusion**

In order to broaden the use of computed tomography coronary angiography (CTCA), comprehensive plaque assessment was carried out in this thesis and we note several positive outcomes.

We demonstrated that accurate and reproducible plaque quantification on CTCA was feasible and comparable to intravascular ultrasound. Appropriate window and level setting is the key which in turn is determined by vendor, contrast and acquisition protocols. Our results suggest that measurement of plaque changes in an individual patient on CTCA is feasible and comparable to IVUS. CTCA has the potential to become an alternative imaging tool to study plaque response to various therapies.

Although it is well known that high-risk plaques are associated with events, our inability to identify the plaques that are likely to rupture has limited our management options. We observed that patients with obstructive high-risk plaques appear to be at greatest risk and plaque volume (PV) and low attenuation plaque (LAP) are important determinants. Quantitative plaque measurement is time consuming but we have shown that it is feasible to derive the prognostic information by measuring LAP volume just at a single cross section at the site of maximum stenosis to identify the patients who are at the greatest risk of future events. This may pave the way to clinical trials in these vulnerable patients for targeted therapies.

Determination of functional significance of coronary stenosis on CTCA will make it a 'one stop shop' for the assessment of coronary artery disease. ASLA score was found to be the best predictor of ischaemia specific lesions among various CT indices. It has the potential to be applied at the time of reporting and at extremes of ASLA scores it is feasible to rule out or identify ischaemia specific lesions with high accuracy. CT fractional flow reserve (FFR) is an emerging tool that has

generated tremendous enthusiasm. In one of the first studies of its kind, we tested novel methods of CT FFR, which can be applied routinely and has the ability to identify functionally significant lesions with high accuracy. There is potential for these applications to reduce health care costs by reducing downstream testing for identification of ischaemic lesions.